

1. Iron

Michael D. Ward

CONTENTS

INTRODUCTION	1
1.1 Complexes with carbonyl or isonitrile ligands	2
1.1.1 Homoleptic carbonyl or isonitrile complexes	2
1.1.2 Complexes also containing Si, Ge, or Sn donor ligands	3
1.1.3 Complexes also containing N, P, As, Sb or Bi donor ligands	6
1.1.4 Complexes also containing S, Se or Te donor ligands	11
1.1.5 Complexes containing other transition metals	15
1.2 Complexes with hydrogen or hydride ligands	20
1.3 Complexes with nitrosyl ligands	22
1.4 Complexes with halide ligands	24
1.5 Complexes with cyanide or other pseudohalide ligands	25
1.5.1 Complexes with cyanide ligands	25
1.5.2 Complexes with other pseudohalide ligands	28
1.6 Complexes with N donor ligands	29
1.6.1 Complexes with N-heterocyclic ligands	29
1.6.2 Complexes with imines and oximes	36
1.6.3 Complexes with macrocyclic ligands	38
1.6.4 Miscellaneous N donor complexes	42
1.7 Complexes with tetrapyrrole macrocycles	42
1.7.1 Complexes with phthalocyanines	42
1.7.2 Complexes with porphyrins	45
1.7.2.1 Axially-ligated porphyrin complexes	46
1.7.2.2 Complexes with oxygen, peroxides and superoxides	55
1.7.2.3 Other porphyrin complexes	57
1.8 Complexes with O donor ligands	61
1.8.1 Complexes with carboxylic acids and derivatives	61
1.8.2 Complexes with other O donor ligands	63
1.9 Complexes with S donor ligands	68
1.10 Complexes with mixed-donor ligands	70
1.10.1 Complexes with mixed N,O donor sets	70
1.10.2 Complexes with mixed N,S donor sets	87
1.10.3 Complexes with other mixed-donor ligands	89
1.11 Iron-sulphur clusters	91
1.11.1 Iron-sulphur cubanes	91
1.11.2 Heterometallic cubanes	95
1.11.3 Other iron-sulphur clusters	97
1.12 Complexes exhibiting spin equilibria	99
REFERENCES	103

INTRODUCTION

This review covers the coordination chemistry of iron for 1990, and is the first since the 1981 review published in volume 67 of Coordination Chemistry Reviews. All work cited in Chemical Abstracts volumes 112 and 113 has been covered, which comprises publications from 1989 to late 1990 depending on the journal. In addition the following journals have been searched independently from the period January to December 1990: *J. Amer. Chem. Soc.*, *Inorg.Chem.*,

Angew. Chem., J. Chem. Soc., Dalton Trans., J. Chem. Soc., Chem. Commun., Inorg. Chim. Acta, Polyhedron, J. Organometal. Chem., Organometallics, Helvetica Chimica Acta, Bull. Chem. Soc. Jpn., Chemische Berichte, New J. Chem., Australian J. Chem. and Canadian J. Chem.

The main change in the layout compared to previous years is that there is no subdivision by oxidation state, only by ligand type. Many ligands have been used to prepare complexes in both the +2 and +3 oxidation states and the undesirable fragmentation of a single piece of work is thereby avoided. In all cases where the oxidation state is not obvious it is explicitly stated. As always the distinction between 'coordination' compounds and 'organometallic' compounds is rather difficult; as a general rule, any compounds containing a metal-carbon σ -bond (apart from carbonyl and isonitrile complexes, and a few alkyl and aryl porphyrin complexes) or a π -coordinated unsaturated hydrocarbon (including cyclopentadienyl derivatives) are outside the scope of this review. Such organometallic iron compounds are periodically reviewed in *J. Organometal. Chem.*. Within these limits this review aims to be comprehensive, and any omissions or errors are entirely the fault of the author.

1.1 COMPLEXES WITH CARBONYL OR ISONITRILE LIGANDS

1.1.1 Homoleptic carbonyl or isonitrile complexes

The fluxional and isomerisation processes of $\text{Fe}_3(\text{CO})_{12}$ and $\text{Fe}_3(\text{CO})_{12-n}\text{L}_n$, both in solution and the solid state, have been interpreted in terms of the ligand polyhedral model. It is suggested that the carbonyl scrambling patterns in these compounds may be accounted for by the M_3 triangle moving inside the ligand envelope, which may in turn undergo polyhedral rearrangements of a type normally associated with mononuclear coordination complexes [1]. Examination of the crystal packing in $\text{Fe}(\text{CO})_5$ and $\text{Fe}_2(\text{CO})_9$ show that each molecule is surrounded by a shell of twelve other molecules, with the close-packed cubooctahedral (ABC) and anti-cubooctahedral geometries (AB) respectively [2]. A revised MO treatment of the bonding in $\text{Fe}_2(\text{CO})_9$ explains the weakness of the Fe-Fe bond, due to antibonding interactions from participation of CO π^* orbitals in the bridge bonding network [3]. IR studies show that UV-induced decarbonylation of $\text{Fe}(\text{CO})_5$ in low-density polyethylene, polyvinyl chloride or polytetrafluoroethylene films at 12K generates $\text{Fe}(\text{CO})_3$ and $\text{Fe}(\text{CO})_4$, which may react with the polymeric medium or residual solvent molecules (CH_2Cl_2 , hexane, thf (thf = tetrahydrofuran)) to form a variety of adducts. The potential of polymer films for trapping and characterising unstable species is discussed [4]. Single-molecule isolation of $\text{Fe}(\text{CO})_5$ has been achieved by codeposition from the vapour phase with excess alkali halide vapour onto a cold substrate. The photochemistry of 'salted' $\text{Fe}(\text{CO})_5$ was compared to that of $\text{Fe}(\text{CO})_5$ adsorbed onto alkali halide films; photo-induced fragmentation, oxidation and reduction were observed [5]. $\text{Fe}(\text{CO})_5$ reacts with $\text{Fe}^{13}\text{CO}^+$ in the gas phase to give $[\text{Fe}_x(^{13}\text{CO})_r(\text{CO})_s]^+$ ($x = 1-3$; $r = 0,1$; $s = 4-8$). The kinetics of these reactions were studied by Fourier-Transform ICR mass spectrometry; ^{13}CO is lost in preference to ^{12}CO during cluster formation. The results are interpreted with reference to the non-fluxionality of $[\text{Fe}_x(\text{CO})_{r+s}]^+$ clusters [6]. The distribution of internal energy in $[\text{Fe}(\text{CO})_5]^+$

(generated by collision-induced dissociation using Ar gas) was determined as a function of collision energy and scattering angle [7]. The photoelectron/photoion coincidence spectra of $[\text{Fe}(\text{CO})_n]^+$ ($n = 0 - 5$), produced from photoionisation of $\text{Fe}(\text{CO})_5$, have been recorded. The ionisation energy of $\text{Fe}(\text{CO})_5$ and CO bond dissociation energies in $[(\text{CO})-\text{Fe}(\text{CO})_n]^+$ were determined from them [8].

The activation of CO in the water-gas shift reaction was modelled by CO activation in $\text{Fe}(\text{CO})_5$. Reaction of $\text{Fe}(\text{CO})_5$ with $[\text{Et}_4\text{N}][\text{OH}]$ in methanol at -78° yields $[\text{Fe}(\text{CO})_4(\text{CO}_2\text{H})]^-$ and $[\text{Fe}(\text{CO})_4(\text{CO}_2\text{Me})]^-$, both of which regenerate $\text{Fe}(\text{CO})_5$ on protonation with $\text{CF}_3\text{CO}_2\text{H}$. Their reactivity towards Et_3N and Li^+ is discussed [9]. There is a separate report of $\text{Fe}(\text{CO})_5$ reacting with OH^- to give $[\text{Fe}(\text{CO})_4(\text{CO}_2\text{H})]^-$ [10].

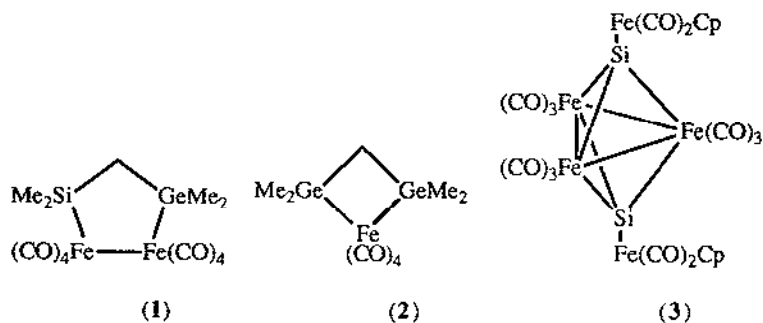
Photolysis of $\text{Fe}(\text{CO})_5$ adsorbed on hydrated alumina produces $[\text{HFe}_3(\text{CO})_{11}]^-$, $[\text{HFe}(\text{CO})_4]^-$ and alumina-bound $\text{Fe}(\text{CO})_4$, as determined by IR experiments involving deuterium exchange [11]. $\text{Fe}(\text{CO})_5$ is capable of catalytically carbonylating aryl iodides to benzophenones under phase-transfer conditions and 1 atmosphere pressure of CO; for example, o-iodotoluene was converted to 2,2'-dimethylbenzophenone in 47% isolated yield [12]. $\text{Fe}(\text{CO})_5$ adsorbed on NaY zeolite shows photoinduced catalytic activity for butene isomerisation fifteen times higher than when adsorbed on KY zeolite. This indicates that the cationic electrostatic field plays an important part in the catalytic process [13].

$\text{Fe}(\text{CO})_4\text{-xL}_{1+\text{x}}$ ($\text{L} = 1,3\text{-dimethyl-2-isocyanobenzene}$; $\text{x} = 0\text{-}4$) were prepared from $\text{Fe}(\text{CO})_5$ and L [14]. $\text{Fe}(\text{CNCF}_3)_5$ has been prepared and studied by NMR spectroscopy; it is non-rigid in solution even at -100°C . It decomposes at room temperature to $\text{Fe}_2(\text{CNCF}_3)_6(\mu\text{-CNCF}_3)_3$ [15]. New routes to $\text{Fe}_3(\text{CO})_{12-\text{x}}(\text{CNR})_{\text{x}}$ ($\text{R} = \text{tert-butyl, xylyl}$; $\text{x} = 1 - 3$) are described. $\text{Fe}_3(\text{CO})_{10}(\text{CN}^t\text{Bu})_2$ has been structurally characterised, and unexpectedly both isonitrile ligands are on the same Fe atom. $\text{Fe}_3(\text{CO})_{11}(\text{CN}^t\text{Bu})$ undergoes facile decarbonylation to give $\text{Fe}_3(\text{CO})_9(\mu_3\text{-}\eta^2\text{-CN}^t\text{Bu})$, which reacts further with two $^t\text{BuNC}$ to give $\text{Fe}_3(\text{CO})_9(\text{CN}^t\text{Bu})_3$ and with other Lewis bases L to give $\text{Fe}_3(\text{CO})_9(\text{CN}^t\text{Bu})\text{L}_2$ ($\text{L} = \text{CN-Xylyl, P(OEt)}_3, \text{PMe}_2\text{Ph}$) for which structures are proposed on the basis of IR spectra [16].

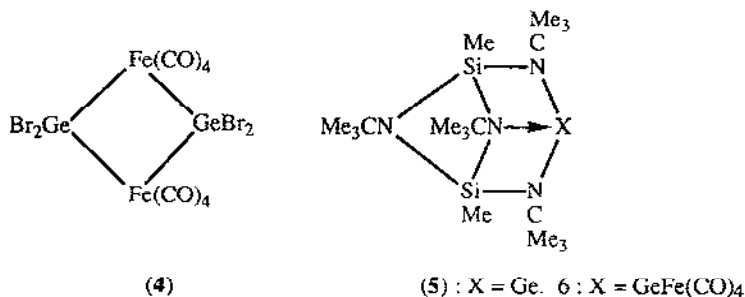
1.1.2 Complexes also containing Si, Ge or Sn donors

The pentacoordinate complexes $\text{Fe}(\text{CO})_3(\text{SiCl}_3)(\text{PPh}_3)$ and $\text{Fe}(\text{CO})_3(\text{SiCl}_3)(\text{P}(\text{OPh})_3)$ have been prepared and crystallographically characterised; both have near-trigonal bipyramidal geometries with the three CO ligands in the equatorial plane [17]. $\text{Me}_2\text{HSi-CH}_2\text{-GeMe}_2\text{H}$ reacts with $\text{Fe}(\text{CO})_5$ under UV irradiation to give the five-membered cyclic product (1) [18]. The 4-membered cyclic compound (2) reacts with aldehydes to give cyclic germanium oxides and iron carbonyls, and with quinones to give new germanium-containing heterocycles [19].

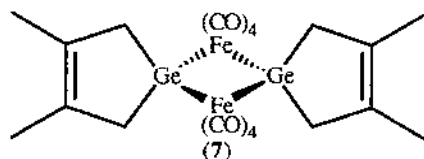
Reaction of RGeH_3 ($\text{R} = \text{Me, Et}$) with $\text{Fe}_3(\text{CO})_{12}$ at 50°C , or between RGeH_3 and $\text{Fe}(\text{CO})_5$ at 140°C , results in $\text{Fe}_3(\text{CO})_9(\mu_3\text{-GeR})_2$. Silanes give similar trigonal bipyramidal products but these were poorly characterised due to instability. The trigonal-bipyramidal $[\mu_3\text{-Si}\{\text{Fe}(\text{CO})_2\text{Cp}\}]_2\text{Fe}_3(\text{CO})_9$ ($\text{Cp} = \eta^5\text{-cyclopentadienyl}$) (3) was prepared from $\text{Fe}(\text{CO})_5$, SiH_4 and $[\text{Fe}(\text{CO})_2\text{Cp}]_2$ and has been crystallographically characterised [20].



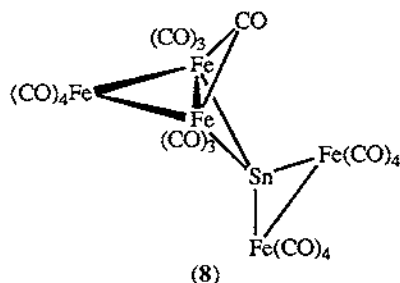
Reaction of $[(\text{CO})_4\text{FeGeBr}_2]_2$ (4) with $\text{Na}_2\text{Fe}(\text{CO})_4$ in diethyl ether/pyridine gives $[(\text{CO})_4\text{Fe}]_2\text{Ge}(\text{py})_2$ in good yield, with the two pyridines and two $\text{Fe}(\text{CO})_4$ units disposed in a



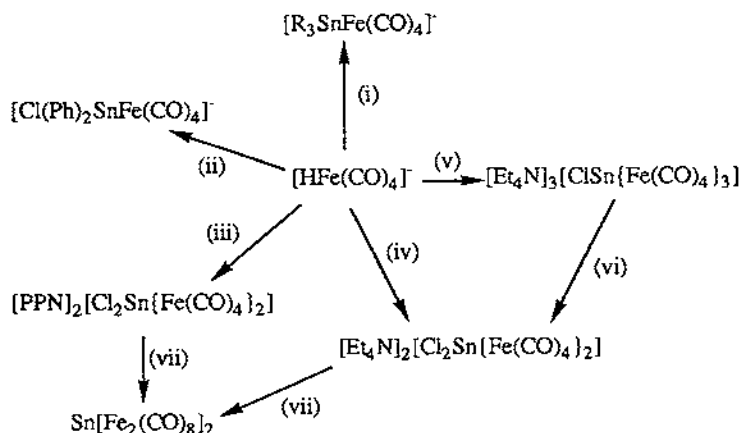
distorted tetrahedral array around the Ge atom [21]. Compound (5) reacts with $\text{Fe}_2(\text{CO})_9$ to give (6) [22]. Compound (7) has been crystallographically characterised; the cyclopentene rings are puckered [23].



$\text{Fe}_2(\text{CO})_9$ reacts with SnH_4 to give the known compound $\text{Sn}[\text{Fe}_2(\text{CO})_8]_2$ and a new compound $\text{SnFe}_5(\text{CO})_{19}$ (8). The crystal structure shows an Fe_3 triangle edge-bridged by an SnFe_2 triangle [24]. Reaction of $\text{Fe}(\text{CO})_5$ with $\text{N}(\text{SnMe}_3)_3$ gives $\text{cis-Fe}(\text{CO})_4(\text{SnMe}_3)_2$; the analogous reaction with $\text{Fe}(\text{CO})_4(\text{CS})$ gives mostly $\text{fac-Fe}(\text{CO})_3(\text{CS})(\text{SnMe}_3)_2$. ^{13}C , ^{17}O and ^{119}Sn NMR spectroscopic measurements were made to study the dynamic behaviour of these compounds [25].



Reactions of $[\text{Et}_4\text{N}]^+$ and $[(\text{Ph}_3\text{P})_2\text{N}]^+$ (PPN) salts of $[\text{HFe}(\text{CO})_4]^-$ with several tin halides have been studied; the results are summarised in scheme 1. The crystal structure of $[\text{Et}_4\text{N}]_2[\text{Cl}_2\text{Sn}\{\text{Fe}(\text{CO})_4\}_2]$ shows a tetrahedral arrangement of two chlorides and two $\text{Fe}(\text{CO})_4$ units around the Sn atom [26].



Scheme 1: Reactions of $[\text{HFe}(\text{CO})_4]^-$ with tin compounds.

(i) R_3SnCl ($\text{R} = \text{Ph}, p\text{-tolyl}$) (ii) Ph_2SnCl_2 (iii) SnCl_4 (iv) 0.5 equiv. SnCl_4
 (v) 0.33 equiv. SnCl_4 (vi) SnCl_4 (vii) Cu^+

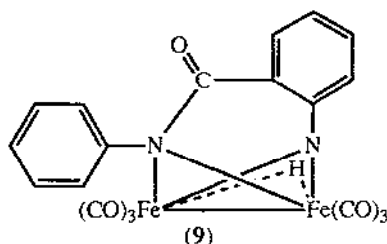
Three routes have been determined for the preparation of octahedral hydrido-stannyl complexes of iron. Firstly, a silyl group can be replaced by a stannane: thus $\text{mer}(\text{CO})_3(\text{PPh}_3)\text{Fe}(\text{H})\text{SiMe}_3$ and R_3SnH react to give $\text{mer}(\text{CO})_3(\text{PPh}_3)\text{Fe}(\text{H})\text{SnR}_3$, and $\text{cis}, \text{cis}(\text{CO})_2(\text{dppe})\text{Fe}(\text{H})\text{SiMe}_3$ ($\text{dppe} = 1,2\text{-bis(diphenylphosphino)ethane}$) reacts similarly to give $\text{cis}, \text{cis}(\text{CO})_2(\text{dppe})\text{Fe}(\text{H})\text{SnR}_3$. Secondly, R_3SnH adds to $\text{Fe}(\text{CO})_2[\text{P}(\text{O}^i\text{Pr})_3]_2$ to give $(\text{CO})_2[\text{P}(\text{O}^i\text{Pr})_3]_2\text{Fe}(\text{H})\text{SnR}_3$ (cis or trans isomer). Thirdly, $(\text{CO})_2\text{L}_2\text{Fe}(\text{H})\text{SnCl}_3$ ($\text{L}_2 = \text{dppe}, [\text{P}(\text{O}^i\text{Pr})_3]_2$) are prepared by reaction of the corresponding dihydride complexes $(\text{CO})_2\text{L}_2\text{Fe}(\text{H})_2$ with SnCl_4 . Deprotonation of these Sn-substituted hydride complexes with KH gives $\text{K}[(\text{CO})_3(\text{PPh}_3)\text{Fe}(\text{SnR}_3)]$ ($\text{R} = \text{Ph}, \text{Me}$) and $\text{K}[(\text{CO})_2\text{L}_2\text{Fe}(\text{SnR}_3)]$ ($\text{L}_2 = \text{dppe}, [\text{P}(\text{O}^i\text{Pr})_3]_2$). Reaction of $\text{K}[(\text{CO})_3(\text{PPh}_3)\text{Fe}(\text{SnR}_3)]$ with CH_3I gives the methyl-stannyl complexes $(\text{CO})_3(\text{SnR}_3)(\text{PPh}_3)\text{Fe}(\text{CH}_3)$, with $\text{R}'_3\text{SnCl}$ gives the bis-stannyl complexes

$(\text{CO})_3(\text{PPh}_3)\text{Fe}(\text{SnR}_3)(\text{SnR}'_3)$, and with Me_2SnCl_2 gives $\text{mer}-(\text{CO})_3(\text{PPh}_3)\text{Fe}(\text{SnMe}_2\text{Cl})_2$, whose crystal structure shows a roughly octahedral geometry around the Fe atom in which the two cis-stannyl ligands do not interact [27].

The reaction of $[\text{Et}_4\text{N}]_2[\text{Cl}_2\text{Sn}\{\text{Fe}(\text{CO})_4\}_2]$ with $\text{ClHgMo}(\text{CO})_3\text{Cp}$ gives the very unusual heptanuclear complex $[\text{Et}_4\text{N}]_2[\{(\text{CO})_4\text{FeSnCl}_2\text{Fe}(\text{CO})_4\}_2\text{Hg}]$, which has a 'linear' backbone, i.e. $(\text{CO})_4\text{Fe}-\text{SnCl}_2-\text{Fe}(\text{CO})_4-\text{Hg}-\text{Fe}(\text{CO})_4-\text{SnCl}_2-\text{Fe}(\text{CO})_4$. The crystal structure shows that the terminal Fe are square pyramidal, the internal Fe are octahedral, the Sn are tetrahedral and the Hg is linear [28].

1.1.3 Complexes also containing N, P, As, Sb or Bi donors

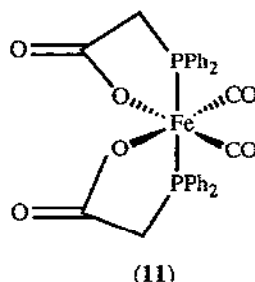
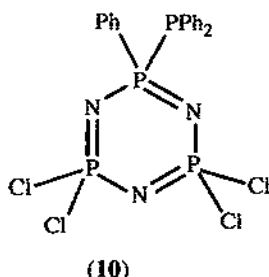
$\text{HFe}_4(\text{CO})_{12}\text{N}$ was used to prepare an iron-nitride film, by chemical vapour deposition at $160-180^\circ$ onto glass. Mössbauer spectroscopy, XPS and X-ray diffraction confirmed the presence of the $\gamma\text{-Fe}_4\text{N}$ phase [29]. $\text{Fe}_2(\text{CO})_6(\mu\text{-PhNC}(\text{O})\text{C}_6\text{H}_4\text{NH})$ (9) was prepared in very low yield from the photochemical reaction of $\text{Fe}(\text{CO})_5$ with azobenzene in toluene; the Fe-Fe bond is bridged by the anthranilic acid anilide, and there is a weak interaction between the amine hydrogen atom and both Fe atoms [30].



Reaction of α,β -unsaturated ketones with $\text{cis-Fe}(\text{phen})_2(\text{CN})_2$ (phen = 1,10-phenanthroline) or $\text{CpFe}(\text{dppe})(\text{CN})$ in the presence of $\text{Et}_2\text{O.HBF}_4$ gives complexes containing γ -oxo-isonitrile ligands by (effectively) Michael reaction of the cyanide ion with the unsaturated ketone. The products are $\text{cis-Fe}(\text{phen})_2(\text{CN-CR}_1\text{R}_2\text{-CHR}_3\text{-C}(\text{O})\text{-R}_4)_2$ (for $\text{R}_1 = \text{R}_2 = \text{Me}$, $\text{R}_3 = \text{H}$ and $\text{R}_4 = \text{CH:CM}_2$ the crystal structure has been determined and shows the expected octahedral N_4C_2 coordination environment) and $\text{Cp}(\text{dppe})\text{Fe}(\text{CN-CR}_1\text{R}_2\text{-CHR}_3\text{-C}(\text{O})\text{-R}_4)_2$ respectively. In both cases the carbonyl group could be reduced [31].

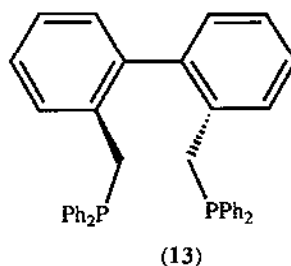
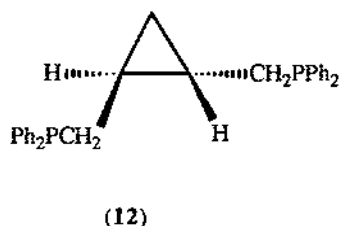
$\text{Fe}(\text{CO})_4\text{L}$ ($\text{L} = \text{PPh}_3$, AsPh_3 , SbPh_3 , PMe_2Ph , $\text{P}(\text{cyclohexyl})_3$, PBu_3 , $\text{P}(\text{OPh})_3$, $\text{P}(\text{OEt})_3$, $\text{P}(\text{OMe})_3$) have been prepared by reaction of $\text{Fe}(\text{CO})_5$ with L in the presence of various cobalt or iron catalysts [32]. 2-Pyridyldiphenylphosphine (pdpp) reacts with $\text{Fe}(\text{CO})_5$ and $\text{Fe}_2(\text{CO})_9$ to give $(\text{pdpp})\text{Fe}(\text{CO})_4$ in which pdpp ligates through the P atom [33]. Reaction of $[\text{Fe}(\text{CO})_3\text{L}(\text{H})\text{SiPh}_3]$ ($\text{L} = \text{PMe}_3$) with L' ($\text{L}' = \text{PPh}_3$, $\text{P}(\text{OPh})_3$, $\text{P}(\text{OEt})_3$, $\text{P}(\text{OCHMe}_2)_3$) in benzene yields the mixed disubstituted complexes $\text{Fe}(\text{CO})_3\text{LL}'$. If, however, $\text{L}' = \text{PMe}_2\text{Ph}$, PMePh_2 or PET_3 a mixture of $[\text{Fe}(\text{CO})_3\text{L}_2]$, $[\text{Fe}(\text{CO})_3\text{LL}']$ and $[\text{Fe}(\text{CO})_3\text{L}'_2]$ appears. $^{31}\text{P}\{^1\text{H}\}$ NMR shifts and $^2\text{J}_{\text{pp}}$ coupling constants correlate well with the ligand cone angles and pK_a values respectively [34]. $\text{Trans-Fe}(\text{CO})_2(\text{PMe}_3)_3$ was prepared by reaction of anhydrous FeCl_2 with PMe_3 and then CO_2 in the

presence of sodium sand [35]. The phosphinophosphazene $\text{N}_3\text{P}_3\text{Cl}_4\text{PhPPh}_2$ (**10**) reacts with $\text{Fe}_2(\text{CO})_9$ in toluene to give $(\text{10})\text{-Fe}(\text{CO})_4$ in which the phosphine P atom bonds to Fe [36].



The octahedral $\text{Fe}(\text{II})$ complex (**11**) has been prepared and structurally characterised; it is the first example of an iron carbonyl complex with two carboxylate ligands [37].

Nitrosylation of $\text{Fe}(\text{CO})_3\text{L}^1$ ($\text{L}^1 = \text{Ph}_2\text{P}(\text{CH}_2)_x\text{PPh}_2$, $x = 1, 2, 3$) and $\text{Fe}(\text{CO})_4\text{L}^2$ ($\text{L}^2 = \text{PPh}_3$, AsPh_3) gives the five coordinate products $[\text{Fe}(\text{CO})_2(\text{NO})\text{L}^1][\text{PF}_6]$ and $[\text{Fe}(\text{CO})_2(\text{NO})(\text{L}^2)_2][\text{PF}_6]$ respectively; their geometries were determined by spectroscopic methods [38]. The coordinating behaviour of the chelating diphosphines (**12**) and (**13**), whose bite angles were calculated to be greater than 120° , was examined. In $\text{Fe}(\text{CO})_3(\text{12})$ the bite angle is 123.9° , with the P atoms occupying equatorial sites in a distorted trigonal bipyramidal structure. The structure of $\text{Fe}(\text{CO})_3(\text{13})$ is better described as a square-based pyramid with a CO in the apical position; the bite angle is 152.0° [39].

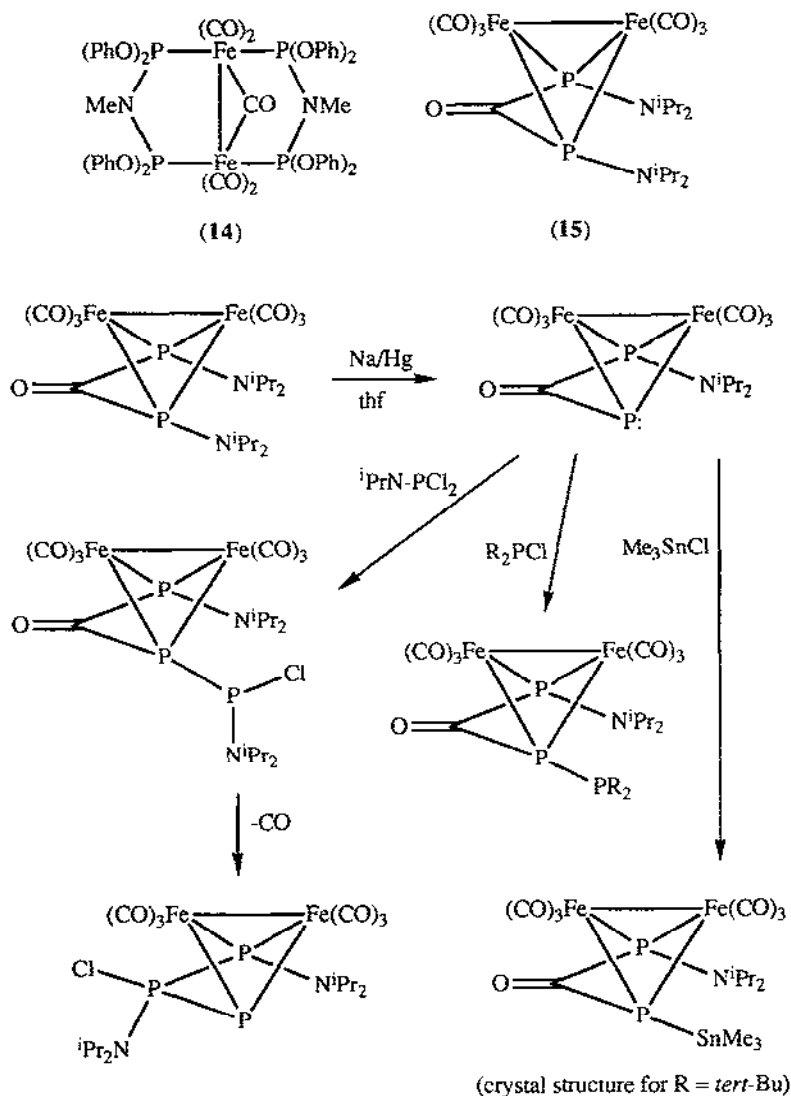


$\text{Fe}(\text{CO})_4(\eta^1\text{-dppf})$ and $\text{Fe}_2(\text{CO})_8(\mu\text{-dppf})$ ($\text{dppf} = 1,1'$ -bis(diphenylphosphino)ferrocene) were prepared by reaction of $\text{Fe}(\text{CO})_5$ with dppf in the presence of Me_3NO ; $\text{Fe}(\text{CO})_3(\eta^2\text{-dppf})$ may also be prepared under more vigorous conditions [40]. $\text{Fe}(\text{CO})_4(\eta^1\text{-dppf})$, with a 'dangling' ligand, is a good precursor for the buildup of polyheterometallic species such as $(\text{CO})_4\text{Fe}(\mu\text{-dppf})\text{L}$ ($\text{L} = \text{Cr}(\text{CO})_5$, $\text{Mo}(\text{CO})_5$, $\text{W}(\text{CO})_5$, $\text{Mn}_2(\text{CO})_9$) [40, 41].

The bidentate diphosphinoamines $\text{X}_2\text{PN}(\text{R})\text{PX}_2$ ($\text{L}; \text{R} = \text{Me}, \text{X} = \text{OPh}; \text{R} = \text{Ph}, \text{X} = \text{OPh}; \text{R} = i\text{Pr}, \text{X} = \text{Ph}$) react with $\text{Fe}(\text{CO})_5$ to give $\text{Fe}(\text{CO})_3\text{L}$ in which L chelates. However under UV irradiation in thf , L ($\text{R} = \text{Me}, \text{X} = \text{OPh}$) reacts with $\text{Fe}(\text{CO})_5$ to give the bimetallic $[\text{Fe}_2(\text{CO})_5\{\text{MeN}[\text{P}(\text{OPh})_2]_2\}_2]$ (**14**) instead [42].

$\text{NaFe}(\text{CO})_4$ reacts with sterically hindered R_2NPCl_2 ($\text{R}_2\text{N} =$ diisopropylamino, dicyclohexylamino, 2,2,6,6-tetramethylpiperidino) to give $(\text{R}_2\text{NP})_2\text{COFe}_2(\text{CO})_6$ (**15**), $\text{R} =$

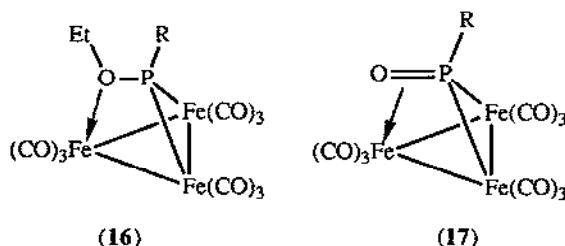
isopropyl in this example, by CO migration from Fe to P. The carbonyl group behaves in many respects like a conventional ketone; many previously-reported reactions of these compounds are discussed [43]. (15) may be reduced by Na/Hg amalgam in thf with P-N bond cleavage. This allows new complexes to be prepared by reactions at the bridging P atom; the reactions are outlined in scheme 2 [44].



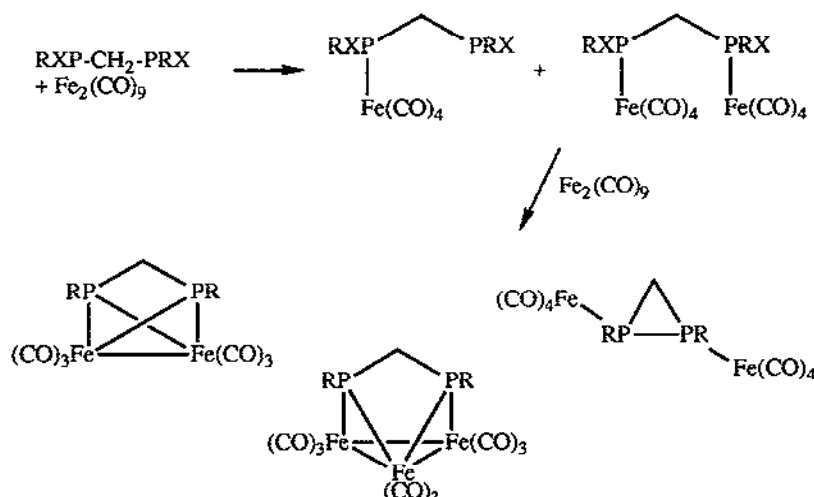
Scheme 2 : Further reactions of (15)

The solution structures of $[\text{Fe}_3(\text{CO})_{12-x}\{\text{P}(\text{OMe})_3\}_x]$ ($x = 0, 1, 2, 3$) have been examined by ^{31}P and ^{13}C NMR studies. The mechanisms of fluxionality are discussed and probable structures for various isomers are proposed. An X-ray crystal structure of $[\text{Fe}_3(\text{CO})_{10}\{\text{P}(\text{OMe})_3\}_2]$

shows it to have the P(OMe)_3 ligands forming a nearly linear P-Fe-Fe-P arrangement, with bridging carbonyls between the unique unsubstituted Fe and a substituted Fe [45]. $\text{Fe}_3(\text{CO})_{10}(\mu_3\text{-RP})$ ($\text{R} = \text{CHMe}_2, \text{CMe}_3$) react with KOCN followed by Et_3OBF_4 to give a variety of products. The major products (**16**) contain an RPOEt fragment which acts as a $\mu_3\text{-}\eta^2$ -ligand bridging an $\text{Fe}_3(\text{CO})_9\text{H}$ unit; (**17**) contains a $\mu_3\text{-}\eta^2\text{-RPO}$ ligand bridging an $\text{Fe}_3(\text{CO})_{10}$ triangle. Both products were characterised spectroscopically and crystallographically. In both cases, the OCN^- acts as an oxygen transfer reagent, and possible mechanisms for the reactions are discussed. Other by-products are $\text{Fe}_3(\text{CO})_9(\mu_3\text{-RP})(\mu\text{-H})_2$ and $\text{Fe}_4(\text{CO})_{12}(\mu_3\text{-RP})$ ($\text{R} = \text{CHMe}_2$ only) [46]. The crystal structure of this last complex $\text{Fe}_4(\text{CO})_{12}(\mu_3\text{-PCHMe}_2)$ has also been determined; it is a trigonal bipyramid, with the PCHMe_2 fragment in an equatorial position, and is described as a 'triple-decker' derivative of the 2π -ligand $\text{Fe}_2(\text{CO})_6(\mu\text{-PCHMe}_2)$ [47].



Reactions of $\text{RXP-CH}_2\text{-PRX}$ ($\text{X} = \text{halogen}$; $\text{R} = \text{Et}_2\text{N}, \text{Ph}_2\text{N}, 2,4,6\text{-trisubstituted phenyl}$) with $\text{Fe}_2(\text{CO})_9$ produce a variety of mono-, bi- and trinuclear complexes (scheme 3) [48].

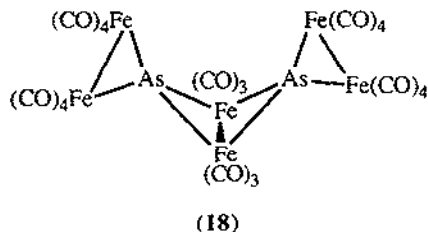


Scheme 3 : Iron carbonyl complexes based on $\text{RXP-CH}_2\text{-PRX}$

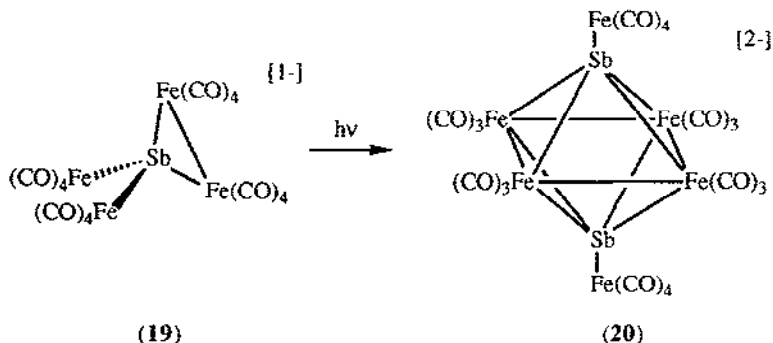
$[\text{Fe}_5\text{C}(\text{CO})_{12}(\text{PMe}_2\text{Ph})_3]$, an electron-rich derivative of $\text{Fe}_5\text{C}(\text{CO})_{15}$, was synthesised in an attempt to increase the reactivity of the carbido carbon. Its crystal structure shows that the square-

pyramidal Fe_5C core is retained. Two of the phosphines occupy trans axial sites on the basal plane; the third is also bound to a basal atom but in an equatorial position. The carbido carbon is 0.2\AA below the basal plane, which indicates partial localisation of the extra electron density in the cluster onto the C atom. The electrochemistry of this compound, and of $[\text{Fe}_5\text{C}(\text{CO})_{13}(\text{dmpe})]$ ($\text{dmpe} = 1,2\text{-bis-dimethylphosphinoethane}$) both show irreversible two-electron reductions [49].

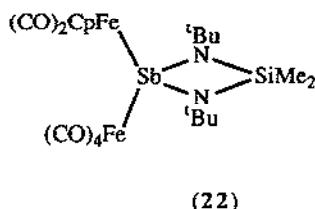
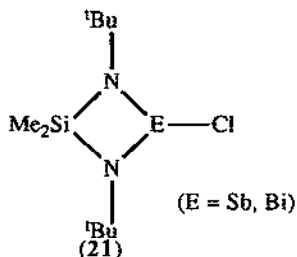
An improved synthesis of the known compound $\text{Fe}_3(\text{CO})_9(\mu_3\text{-As})_2$ is the reaction of AsH_3 with $\text{Fe}(\text{CO})_5$ at 110°C . By contrast the same reagents at 70°C give predominantly $[\text{Fe}_2(\text{CO})_8(\mu_4\text{-As})]_2[\text{Fe}_2(\text{CO})_6]$ (18) [50].



Oxidation of the cluster $[\text{R}_4\text{N}]_3[\text{SbFe}_4(\text{CO})_{16}]$ ($\text{R} = \text{Me}, \text{Et}$) with $[\text{Cu}(\text{MeCN})_4][\text{BF}_4]$ in acetonitrile gave the new compound $[\text{R}_4\text{N}][\text{SbFe}_4(\text{CO})_{16}]$ (19). The crystal structure shows that the central Sb atom is in a distorted tetrahedral environment, bound to two $\text{Fe}(\text{CO})_4$ units and an $\text{Fe}_2(\text{CO})_8$. 19 reduces back to the starting material with sodium amalgam. Photolysis of (19) ($\text{R} = \text{Et}$) with UV light gave $[\text{Et}_4\text{N}]_2[\text{Sb}_2\text{Fe}_6(\text{CO})_{20}]$ (20), which could also be prepared from $[\text{Et}_4\text{N}][\text{Fe}_4(\text{CO})_{13}]$ and SbCl_3 [51].

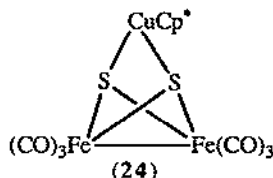
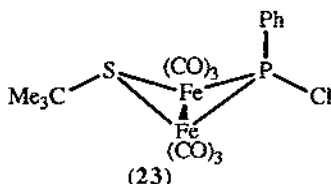


Reaction of $\text{Me}_2\text{Si}(\text{N}^i\text{Bu})_2\text{ECl}$ (21) ($\text{E} = \text{Sb}, \text{Bi}$) with $[\text{CpFe}(\text{CO})_2]^-$ gives the stibanes and bismuthanes $\text{Cp}(\text{CO})_2\text{Fe-E}(\text{N}^i\text{Bu})_2\text{SiMe}_2$. For $\text{E} = \text{Sb}$, further reaction with $\text{Fe}_2(\text{CO})_9$ yields $[\text{Fe}(\text{CO})_4][(\text{CO})_2\text{FeCp}]\text{Sb}(\text{N}^i\text{Bu})_2\text{SiMe}_2$ (22) by complexation of the Sb lone pair to iron; the crystal structure has been determined [52].



1.1.4 Complexes also containing S, Se or Te donors

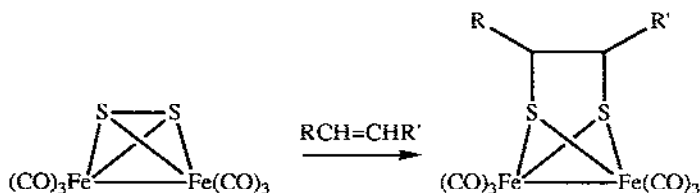
Reaction of $\text{Fe}_3(\text{CO})_{12}$, RSH ($\text{R} = \text{Et}, \text{CHMe}_2, \text{Bu}, \text{tBu}$) and Et_3N yields $[\text{Et}_3\text{NH}][(\mu\text{-CO})(\mu\text{-RS})\text{Fe}_2(\text{CO})_6]$, which reacts in turn with PhPCl_2 to give $(\mu\text{-PhPCl})(\mu\text{-RS})\text{Fe}_2(\text{CO})_6$ (23, $\text{R} = \text{tBu}$ in this example). The crystal structure ($\text{R} = \text{tBu}$) shows the core to be an Fe_2PS butterfly [53].



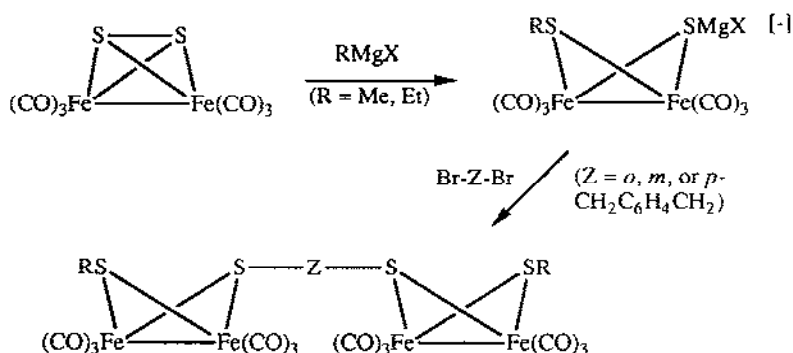
$\text{Fe}_2(\text{CO})_6(\text{S}_2)$ reacts with $\text{Et}_3\text{N} \cdot \text{HSnBr}_3$ in ethanol to give $[\{\text{Fe}(\text{CO})_3\}_2(\mu\text{-SSnBr}_3)_2]^{2-}$ and with SnCl_2 to give $[\text{Fe}(\text{CO})_3(\text{S})_2]_2\text{SnCl}_2$ [54]. $\text{Fe}_2(\text{CO})_6(\text{S}_2)$ also reacts with $(\text{thf})\text{CuCp}^*$ ($\text{Cp}^* = \eta^5\text{-pentamethylcyclopentadienyl}$) to give (24) by insertion into the S-S bond [55]. 1-Pentene, 2-pentene, 1,3-butadiene and 1,4-pentadiene insert into the S-S bond of $\text{Fe}_2(\text{CO})_6(\text{S}_2)$ in a [2+2] photochemical reaction (scheme 4) [56]; for the diene substrates, one double bond is unaffected, so the reaction with 1,3-butadiene gives the product depicted with $\text{R} = \text{H}$ and $\text{R}' = \text{-CH=CH}_2$. The cyclic alkenes cyclohexene, cyclooctene, cyclopentadiene, 1,4-cyclooctadiene and cycloheptatriene behave in the same way to produce $\text{Fe}_2(\text{CO})_6\text{L}$ ($\text{H}_2\text{L} = \text{cyclic 1,2-dithiol}$) [57]. The products were characterised by IR, ^1H and ^{13}C NMR spectroscopy, mass spectrometry and one crystal structure. $\text{Fe}_2(\text{CO})_6(\text{S}_2)$ also reacts with Grignard reagents to give anions, which react with *o*, *m* and *p*-dibromomethylbenzene to give bridged species containing two Fe_2S_2 butterfly units (scheme 5); the crystal structure of the metal-bridged complex has been determined [58].

Decarbonylation of $\text{Fe}(\text{CO})_5$ in the presence of $\text{Fe}_3(\text{CO})_9(\mu\text{-S})_2$ produces $\text{Fe}_4(\text{CO})_{10}(\mu\text{-CO})(\mu\text{-S})_2$. The crystal structure shows a planar array of four Fe atoms with one $\mu\text{-S}$ on each side of the plane. Differences in the bond lengths between this and $\text{Fe}_2\text{Co}_2(\text{CO})_{11}(\mu\text{-S})_2$ are rationalised by molecular orbital theory [59]. N,N' -thiobismorpholine (25) reacts with $\text{Fe}(\text{CO})_5$ under UV-irradiation in CH_3OH to give the known compound $\text{Fe}_3\text{S}_2(\text{CO})_9$ by desulphurisation. (25) also reacts with $\text{Fe}_2(\text{CO})_9$ to give the adduct $\text{Fe}(\text{CO})_4(25)$, whose Mössbauer spectrum indicates a trigonal bipyramidal structure with the S donor in an axial position. Reaction of (25) with $\text{Fe}_3(\text{CO})_{11}$ (*sic* - whether the author means $[\text{Fe}_3(\text{CO})_{11}]^{2-}$ or $\text{Fe}_3(\text{CO})_{12}$ is not clear) yields no

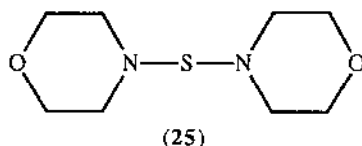
characterisable products; S-N bond cleavage occurs on attempted reaction with $[\text{CpFe}(\text{CO})_2(\text{thf})]$ [60].



Scheme 4 : Photochemical reaction of $\text{Fe}_2(\text{CO})_6(\text{S}_2)$ with alkenes



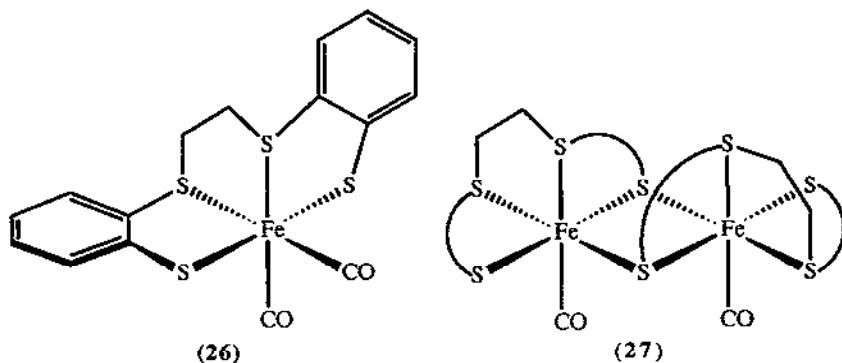
Scheme 5 : Formation of bridged di-butterfly clusters from $\text{Fe}_2(\text{CO})_6\text{S}_2$



Reaction of $\text{Fe}_2(\text{CO})_9$ or $\text{Fe}_3(\text{CO})_{12}$ with the dithiadiazole $(\text{PhCN}_2\text{S}_2)_2$ yields $\text{Fe}_2(\text{CO})_6(\text{PhCN}_2\text{S}_2)_2$; the crystal structure reveals an Fe_2S_2 core with the typical butterfly structure. Molecular orbital calculations suggest, and the crystal structure confirms, that the unpaired electron is in a ligand-centred antibonding orbital [61]. A new compound $[\text{Fe}(\text{CO})_3]_2(\mu\text{-SSCH}_2\text{S})$ was one of many products isolated from the reaction of $\text{Fe}_3(\text{CO})_{12}$ with styrene and elemental sulphur [62]. The bis-bridged complexes $\text{Fe}_2(\text{CO})_6(\mu\text{-RS})(\mu\text{-R'S})$ ($\text{R} = \text{PhCH}_2$, cyclohexyl, $\text{R}' = \text{CH}_2\text{CH}_2\text{CN}$; $\text{R} = \text{PhCH}_2$, Me, $\text{R}' = \text{CH}_2\text{COCH}_2\text{CH}_3$) were reacted with PPh_3 and AsPh_3 to give various products $\text{Fe}_2(\text{CO})_{6-x}\text{L}_x(\mu\text{-RS})(\mu\text{-R'S})$ ($\text{L} = \text{PPh}_3$, $x = 1, 2$; $\text{L} = \text{AsPh}_3$, $x = 1$); the products were spectroscopically characterised [63].

The crystal structure of $\text{FeCp}^*(\eta^1\text{-dtc})(\text{CO})_2$ (dtc = dithiocarbamate, S_2CNMe_2) confirms the unusual monodentate binding mode of the dtc ligand. Irradiation generates the chelate $\text{FeCp}^*(\eta^2\text{-dtc})(\text{CO})$; the reaction was followed by electronic spectroscopy. Further photolysis of the product with PPh_3 gives $\text{FeCp}^*(\eta^2\text{-dtc})(\text{PPh}_3)$ which was crystallographically characterised. Thermal and photochemical reaction pathways for these processes are compared [64]. Conversion

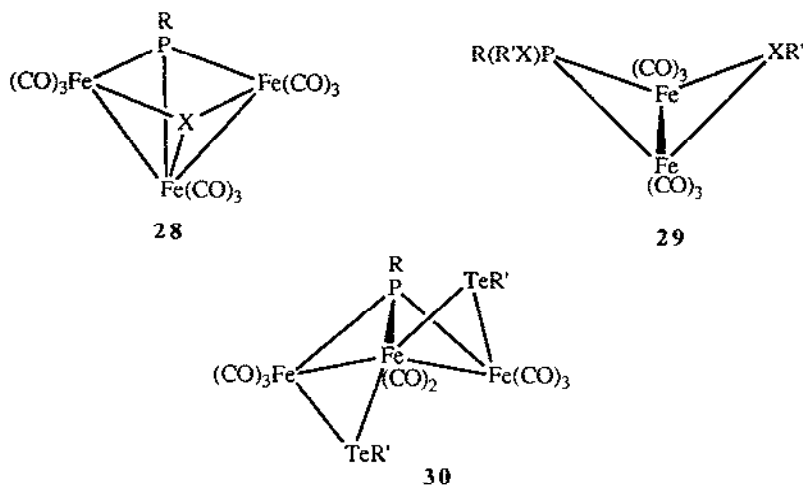
of the monodentate dtc complex to chelating bidentate complex can also be achieved by chemical oxidation or reduction and electrochemical reduction; the mechanisms for the different pathways are discussed [65].



Decarbonylation of $\text{Fe(CO)}_2\text{L}$ (26, $\text{H}_2\text{L} = 2,2'\text{-[ethanedithio]bis[benzenedithiol]}$) gives the dimer (27), in which the terminal thiolates now bridge the two metal centres (the aromatic rings have been replaced by curved lines for clarity). There are ten possible isomers of (27); the crystal structure of one enantiomeric pair has been determined. Each Fe atom is pseudo-octahedral. The steric environment of the binuclear site suggests that (27) may be a good model for oxidoreductase enzymes: one side is encumbered by the bulky sulphur ligand, whereas the other side is relatively unhindered, contains labile ligands, and may be capable of chiral discrimination [66, 67]. The reactivity of the binuclear chirotopic site was further studied. Reaction of (27) with $[\text{NO}]^+$ gives the complex cation in which one CO is replaced by a nitrosyl. With neutral NO, a three-electron donor, the only product is the mononuclear complex $\text{Fe(NO)}_2\text{L}$ in which L is tridentate to satisfy the 18-electron rule. Reaction with PMe_3 gives the mononuclear complex $\text{Fe(CO)(PMe}_3)_3\text{L}$. Reaction with MeLi under forcing conditions produces $[\text{Fe(C}_6\text{H}_4\text{S}_2)_2]_2^{2-}$, in which two planar $[\text{Fe(C}_6\text{H}_4\text{S}_2)_2]^-$ moieties are connected via thiolato bridges, yielding a binuclear complex with five coordinate Fe(III) centres. The complexes were examined by Mössbauer spectroscopy [67]. The tendency of the thiolate groups of (26) to act as bridges has been exploited in the synthesis of other binuclear and trinuclear compounds. Reaction of (26) with $\text{M(CO)}_5(\text{thf})$ ($\text{M} = \text{Cr, Mo, W}$) yields $[\text{Fe(CO)}_2(\mu\text{-L})\{\text{M(CO)}_5\}]$ and (for tungsten only) $[\text{Fe(CO)}_2(\mu\text{-L})\{\text{M(CO)}_5\}_2]$. The crystal structures show that the M(CO)_5 fragments coordinate to the terminal thiolato groups of (26) in an exo manner; NMR spectroscopy shows that the configuration is preserved in solution [68].

Face-capping S, Se and Te have been inserted into iron clusters. Treatment of $\text{Fe}_3(\text{CO})_{10}(\mu_3\text{-RP})$ ($\text{R} = \text{Me}_2\text{CH, Me}_3\text{C}$) with XCN^- ($\text{X} = \text{S, Se, Te}$) yields the addition products $[\text{Fe}_3(\text{CO})_{10}(\mu\text{-PR})(\text{XCN})]^-$, which react further with Et_3OBF_4 to give $[\text{Fe}_3(\text{CO})_9(\mu_3\text{-RP})(\mu_3\text{-X})]$ (28) in over 90% yield. The crystal structures of (28) ($\text{R} = \text{Me}_2\text{CH, X} = \text{Te}$; $\text{R} = \text{Me}_3\text{C, X} = \text{Se}$) reveal a near-planar metallaheterocyclobutadiene Fe_2PX unit, capped by Fe(CO)_3 . (28) are also obtainable directly from $\text{Fe}_3(\text{CO})_{10}(\mu_3\text{-RP})$ and R'XXR' ($\text{X} = \text{Se, Te}$) but in 60% yield and with

formation of appreciable amounts (30%) of the compounds $\text{Fe}_2(\text{CO})_6(\mu_2\text{-R}'\text{X})(\mu_2\text{-RPXR}')$ (29), $\text{R} = \text{Me}_2\text{CH}$, $\text{R}'\text{X} = \text{PhSe}$, mesityltelluroolato, which contain an Fe_2PX butterfly core. For the reaction of $\text{Fe}_3(\text{CO})_{10}(\mu_3\text{-RP})$ with $\text{R}'\text{TeTeR}'$ only, $\text{Fe}_3(\text{CO})_8(\mu_3\text{-RP})(\mu_2\text{-R}'\text{Te})_2$ (30, $\text{R} = \text{Me}_2\text{CH}$, $\text{R}' = \text{mesityl}$) is a third product. The core contains an Fe_3P butterfly with two $\mu_2\text{-TeR}'$ bridging Fe-Fe edges [69].



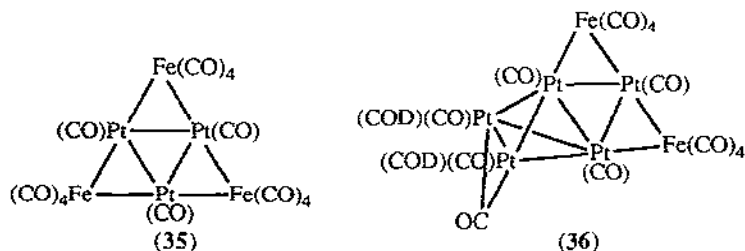
Several new syntheses of polynuclear tellurium-containing cluster compounds take advantage of the ease with which coordinatively unsaturated groups add across the reactive Te-Te bond of $\text{Fe}_2(\text{CO})_6(\mu_2\text{-Te}_2)$ (scheme 6). Thus CH_2 [70], $\text{M}(\text{PPh}_3)_2$ ($\text{M} = \text{Ni}, \text{Pd}, \text{Pt}$), $\text{Ti}(\text{C}_5\text{H}_5)_2$, R_2SnCl_2 ($\text{R} = \text{Me}, \text{Bu}$) and $\text{M}_3(\text{CO})_{11}$ ($\text{M} = \text{Ru}, \text{Os}$) [71, 72, 73] groups may be inserted directly into the Te-Te bond. The required $\text{Fe}_2(\text{CO})_6(\mu_2\text{-Te}_2)$ may be prepared directly, or generated in situ from $\text{Fe}_3\text{Te}_2(\text{CO})_9$ by addition of L (CO, PPh_3) followed by loss of $\text{Fe}(\text{CO})_3\text{L}$ in the presence of incoming metal fragments [71]. Alternatively, the Te-Te bond in $\text{Fe}_2(\text{CO})_6(\mu_2\text{-Te}_2)$ may be reduced first by LiEt_3BH to give the dianion depicted in scheme 6, which will react with a variety of mononuclear metal complexes to give the same products [72, 73].

Reaction of $\text{Fe}_2(\text{CO})_6(\mu_2\text{-Te}_2)$ with $\text{Ru}(\text{CO})_4(\text{C}_2\text{H}_4)$ (generated in situ from photolysis of $\text{Ru}_3(\text{CO})_{12}$ in the presence of C_2H_4) gives $\text{Fe}_2\text{Ru}(\text{CO})_9(\mu_3\text{-Te})_2$. The complex consists of a triangular Fe_2Ru core with a face-capping Te ligand on either side, and shows similar reactivity to $\text{Fe}_3(\text{CO})_9(\mu_3\text{-Te})_2$. It reacts further with $\text{Ru}(\text{CO})_4(\text{C}_2\text{H}_4)$ to give $\text{Fe}_2\text{Ru}_2(\text{CO})_{10}(\mu\text{-CO})(\mu_4\text{-Te})_2$, which has been structurally characterised. It contains a square-planar Fe_2Ru_2 core with a $\mu_4\text{-Te}$ cap on each face, and a bridging CO between the two adjacent Ru atoms. Simple electron-counting indicates that there are 7 skeletal electron pairs, which is consistent with the observed octahedral geometry [74, 75].

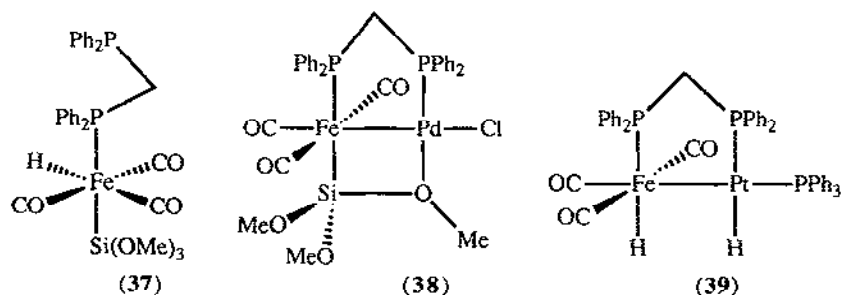
edge, and $\text{Fe}(\text{CO})_3$ and $\text{Au}(\text{PPh}_3)$ fragments in the apical positions. Preparations of $[\text{Fe}_2\text{Ir}_2\text{H}(\text{CO})_{12}]^-$ and $[\text{Fe}_3\text{Ir}(\text{CO})_{13}]^-$ are also described [84].

$[\text{FeRu}(\text{CO})_8]^{2-}$ was prepared by reaction of $\text{Ru}(\text{CO})_5$ with $[\text{Fe}(\text{CO})_4]^{2-}$, and isolated as the bis- $[\text{PPN}]^+$ salt. The crystal structure closely resembles that of $[\text{Ru}_2(\text{CO})_8]^{2-}$ but with disorder at the metal atom sites. For comparison purposes the structure of $[\text{PPN}]_2[\text{Fe}_2(\text{CO})_8] \cdot 2\text{MeCN}$ was also determined, and consists of two trigonal bipyramidal Fe centres in a staggered conformation joined at apical sites [85]. The crystal structure of $\text{Fe}_2\text{Os}(\text{CO})_{12}$ is very similar to that of $\text{Fe}_3(\text{CO})_{12}$, with two bridging carbonyl ligands along the Fe-Fe edge of the triangle [86].

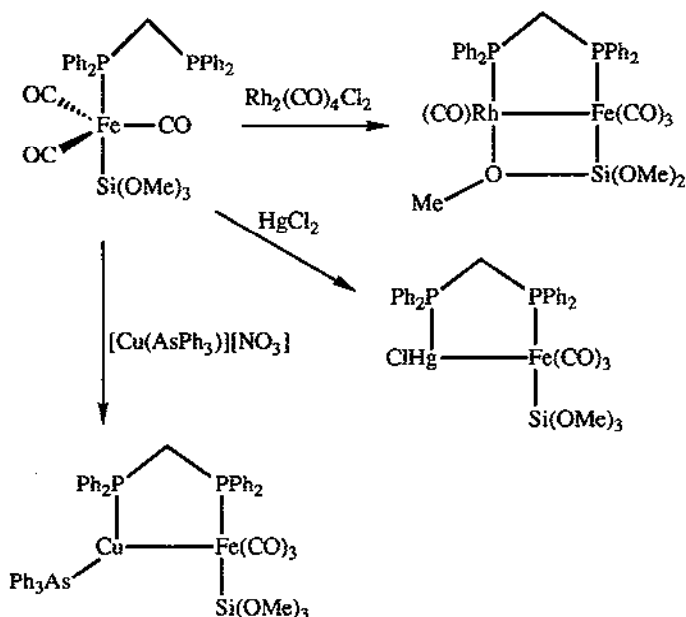
$\text{Fe}(\text{CO})_5$ reacts with $\text{Pt}(\text{COD})_2$ to yield $\text{Pt}_3\text{Fe}_3(\text{CO})_{15}$ (35), $\text{PtFe}_2(\text{CO})_8(\text{COD})$ and $\text{Pt}_5\text{Fe}_2(\text{CO})_{12}(\text{COD})_2$ (36). 35 is a raft in which $\text{Fe}(\text{CO})_4$ groups bridge each edge of the Pt_3 triangle. (36) contains a Pt_4 tetrahedron with a $\text{Pt}(\text{CO})$ bridge along one edge; each edge of the bridge is in turn bridged by $\text{Fe}(\text{CO})_4$ groups [87, 88]. $\text{Hg}_2\text{Fe}(\text{CO})_4\text{SO}_4$ and $\text{Hg}_2\text{Fe}(\text{CO})_4\text{LSO}_4$ (L = thiourea) were prepared and characterised by IR spectroscopy [89].



Reaction of $\text{trans-PdCl}_2(\text{PhCN})_2$ with (37), an octahedral complex with a monodentate dppm ligand, gives the binuclear complex (38) in which the trimethoxysilyl group exhibits a previously unseen $\eta^2\text{-}\mu_2\text{-SiO}$ coordination mode. The crystal structure shows octahedral geometry at the Fe centre and square-planar geometry at the Pd centre. In contrast, reaction of $\text{Pt}(\text{C}_2\text{H}_4)(\text{PPh}_3)_2$ with (37) gives (39) [90].

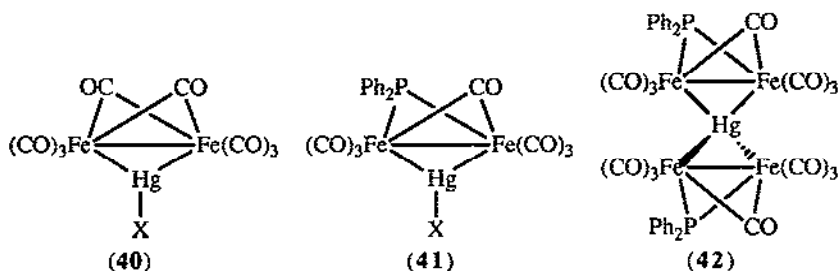


Scheme 8 outlines some reactions of $\text{Fe}(\text{CO})_3(\text{Si}(\text{OMe})_3)(\eta^1\text{-dppm})$ in the preparation of binuclear complexes. The Fe-Cu complex has been crystallographically characterised [91].



Scheme 8 : Reactions of $\text{Fe}(\text{CO})_3\text{Si}(\text{OMe})_3(\eta^1\text{-dppm})$

$[\text{Et}_4\text{N}][\text{HFe}(\text{CO})_4]$ reacts with MCl_2 ($\text{M} = \text{Zn}, \text{Cd}, \text{Hg}$) to give $[(\text{CO})_4\text{HFe-M-FeH}(\text{CO})_4]$, which all undergo proton abstraction with *n*-butyllithium to give $[(\text{CO})_4\text{Fe-M-Fe}(\text{CO})_4]^{2-}$, which were stabilised as the $[\text{PPN}]^+$ salts. For $\text{M} = \text{Hg}$ the crystal structure has been determined; the complex is almost linear (Fe-Hg-Fe angle = 178.7°). Each Fe atom displays trigonal bipyramidal geometry. The two sets of equatorial CO ligands are eclipsed, resulting in D_{3h} symmetry. The possible existence of two conformers for this anion and the presence of $\text{Hg}\cdots\text{CO}$ backbonding are discussed on the basis of qualitative MO theory. $[(\text{CO})_4\text{FeHgFe}(\text{CO})_4]^{2-}$ undergoes redistribution reactions with $[\text{M}(\text{CO})_3\text{Cp}]_2\text{Hg}$ ($\text{M} = \text{Mo}, \text{W}$) to give $[(\text{CO})_4\text{FeHgM}(\text{CO})_3\text{Cp}]^-$ [92].

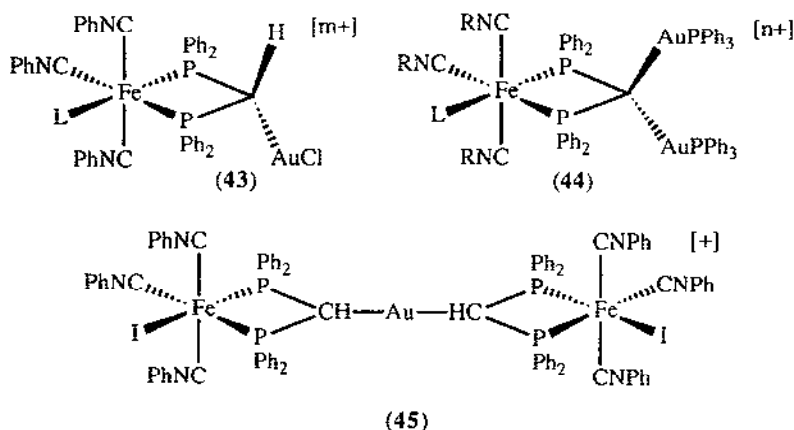


The 'spiked' triangular clusters $[\text{Fe}_2(\text{CO})_6(\mu\text{-CO})_2(\mu\text{-HgX})]^-$ (40), where $\text{X} = \text{Mo}(\text{CO})_3\text{Cp}$, $\text{W}(\text{CO})_3\text{Cp}$, $\text{Mn}(\text{CO})_5$, $\text{Co}(\text{CO})_4$ or $\text{Fe}(\text{CO})_2\text{Cp}$, are prepared by reaction of $[\text{Fe}_2(\text{CO})_8]^{2-}$ with HgXCl ; no ligand redistribution occurs. Similarly the reaction of $[\text{Fe}_2(\text{CO})_6(\mu\text{-$

$\text{CO}(\mu\text{-PPh}_2)]^-$ with HgXCl gives $[\text{Fe}_2(\text{CO})_6(\mu\text{-CO})(\mu\text{-PPh}_2)(\mu\text{-HgX})]$ (**41**), but this undergoes spontaneous ligand redistribution to HgX_2 and $[\text{Hg}\{\text{Fe}_2(\text{CO})_7(\mu\text{-PPh}_2)\}_2]$ (**42**) [93].

$[\text{Et}_4\text{N}][\text{HFe}(\text{CO})_4]$ also reacts with $\text{Au}(\text{PPh}_3)\text{Cl}$ to give $[\text{Et}_4\text{N}][\text{Fe}_2(\text{CO})_8(\mu\text{-AuPPh}_3)]$, which is the first example of an Fe_2Au cluster. The crystal structure has been determined. The complex is isoelectronic to $[\text{HFe}_2(\text{CO})_8]^-$, but with H^- replaced by an AuPPh_3 fragment [94]. The FeAu_2 clusters $[(\text{Ph}_3\text{P})\text{Au}]_2\text{Fe}(\text{CO})_3(\text{PR}_3)$ ($\text{R} = \text{OMe}, \text{OEt}, \text{OPh}, \text{Me}, \text{Ph}$) are produced in the reaction of $[\text{HFe}(\text{CO})_3(\text{PR}_3)]^-$ with $\text{Au}(\text{PPh}_3)\text{Cl}$. The crystal structure for $\text{R} = \text{EtO}$ was determined. The structural parameters for this compound are compared with other similar MAu_2 compounds [95].

Deprotonation of the methylene group in $[\text{FeL}(\text{dppm})(\text{CNPh})_3]^{n+}$ ($\text{L} = \text{PPh}_3, \text{PhNC}$, $n = 2$; $\text{L} = \text{Cl}, \text{I}$, $n = 1$) with KOH gives the corresponding bis-(diphenylphosphino)methanides $[\text{FeL}\{(\text{Ph}_2\text{P})_2\text{CH}\}(\text{CNPh})_3]^{(n-1)+}$. These react with $\text{Au}(\text{I})$ complexes to give new dimetallic and trimetallic species containing Au-C bonds. For example, $[\text{FeL}\{(\text{Ph}_2\text{P})_2\text{CH}(\text{AuCl})\}(\text{CNPh})_3]^{m+}$ (**43**: $\text{L} = \text{PPh}_3$, $m = 1$; $\text{L} = \text{Cl}$, $m = 0$) are prepared by reaction of the appropriate methanides with $\text{AuCl}(\text{tht})$ ($\text{tht} = \text{tetrahydrothiophene}$). Two methanide carbons may attach to one Au centre to give a 'linear' trinuclear complex, as in $[\text{FeL}\{(\text{PPh}_2)\text{CH}\}(\text{CNPh})_3]_2\text{Au}^+$ (**45**), or both methylene protons may be replaced by $\text{Au}(\text{PPh}_3)$ groups to give $[\text{FeL}\{(\text{PPh}_2)\text{C}(\text{AuPPh}_3)_2\}(\text{CNPh})_3]^{n+}$ (**44**: $\text{L} = \text{PhNC}$, $\text{R} = \text{Ph}$, $n = 2$; $\text{L} = \text{p-CN-C}_6\text{H}_4\text{Me}$, $\text{R} = \text{p-tolyl}$, $n = 2$; $\text{L} = \text{Cl}, \text{I}$, $\text{R} = \text{Ph}$, $n = 1$). For $\text{R} = \text{Ph}$ and $\text{L} = \text{Cl}$, (**44**) has been structurally characterised; the Fe is in a distorted octahedral environment with the isonitrile ligands meridional. The bridging carbon is distorted tetrahedral, and there is a close contact between the two Au atoms [96].



1.2 COMPLEXES WITH HYDROGEN OR HYDRIDE LIGANDS

$[\text{HFe}(\text{CO})_4]^-$ undergoes rapid axial/equatorial CO exchange in the solid state, observed by ^{13}C magic-angle-spinning NMR. This process is virtually independent of the counter cation, and is in contrast to the solid-state behaviour of $\text{Fe}(\text{CO})_5$ which shows no such fluxionality [97].

$\text{FeCl}_2(\text{depe})_2$ ($\text{depe} = 1,2\text{-bis-diethylphosphinoethane}$) reacts with NaBPh_4 and H_2 in ethanol or thf to give a mixture of $\text{trans-FeHCl}(\text{depe})_2$, $[\text{FeCl}(\eta^2\text{-H}_2)(\text{depe})_2]^+$ and trans-

$[\text{Fe}(\text{H})(\eta^2\text{-H}_2)(\text{depe})_2]^+$; in the presence of NaOEt or NEt_3 , $\text{trans-}[\text{Fe}(\text{H})(\eta^2\text{-H}_2)(\text{depe})_2]^+$ is the major product. Also the known complex $\text{Fe}(\text{H})_2(\text{depe})_2$, which is difficult to prepare by other routes, may be readily prepared from $\text{cis-FeCl}_2(\text{depe})_2$ by reaction with H_2 and NaOEt or NaOCMe_3 . The proposed mechanism for these reactions involves heterolytic cleavage of η^2 -coordinated dihydrogen [98]. $\text{FeCl}_2(\text{dmpe})_2$ reacts with NaBH_4 in ethanol to give $[\text{Fe}(\text{H})(\text{H}_2)(\text{dmpe})_2]^+$ in a similar reaction to that just described for the *depe* analogue. The $\eta^2\text{-H}_2$ ligand is labile and may be displaced by N_2 , CO , MeNC or C_2H_4 ; $[\text{Fe}(\text{H})(\text{N}_2)(\text{dmpe})_2]^+$ has been crystallographically characterised and has a linear, end-on N_2 ligand. Reaction of $[\text{Fe}(\text{H})(\text{H}_2)(\text{dmpe})_2]^+$ with CO_2 or CS_2 results both in displacement of H_2 and insertion of the substrate into the Fe-H bond to give $[\text{Fe}(\text{dmpe})_2\text{X}_2]^+$ where X_2 is a chelating formate or dithioformate ligand [99].

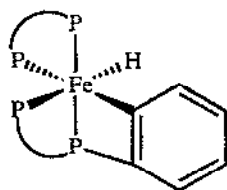
The influence of the phosphite ligand and the metal ion on the properties of the known complexes $[\text{FeH}(\eta^2\text{-H}_2)\text{L}_4]^+$ ($\text{L} = \text{PhP}(\text{OEt})_2$, $\text{P}(\text{OEt})_3$, $\text{P}(\text{OMe})_3$) are discussed [100]. The dihydride $\text{Fe}(\text{H})_2(\text{PP}_3)$ ($\text{PP}_3 = \text{P}(\text{CH}_2\text{CH}_2\text{CH}_2\text{PMe}_2)_3$, a tetradentate tripodal ligand which constrains the two hydrides to be *cis*) protonates to form a trihydride; in the D-exchanged isotopomers HD_2 and H_2D low-temperature NMR studies revealed one classically-bound hydride and one $\eta^2\text{-H}_2$ ligand [101].

Such 'classical' and 'non-classical' modes of hydrogen coordination may be distinguished electrochemically. $\text{Fe}(\text{H})_2(\text{PP}_3')$ ($\text{PP}_3' = \text{P}(\text{CH}_2\text{CH}_2\text{PPh}_2)_3$, a tripodal tetradentate ligand) was proven by NMR studies on it and its deuterated isotopomers to behave like a classical *cis*-dihydride. It may be oxidised electrochemically to the mono- and di-cation without loss of H^+ . This is in contrast to the behaviour of the $\eta^2\text{-H}_2$ complexes $[(\text{PP}_3')\text{M}(\text{H}_2)]^+$ ($\text{M} = \text{Co}, \text{Rh}$) which deprotonate when electrochemically oxidised. $[\text{Fe}(\text{PP}_3')\text{H}]^+$ was also prepared; it undergoes two metal-centred reductions. The first reduction compound $[\text{Fe}^{\text{I}}(\text{H})(\text{PP}_3')]$ was examined by X-band ESR spectroscopy [102]. $[\text{Fe}(\text{PP}_3')(\text{H})_2]$ reacts with $\text{Au}(\text{PPh}_3)\text{Cl}$ or $[\text{Au}(\text{PPh}_3)]^+$ to give the hydrido-bridged binuclear species $[(\text{PP}_3')\text{Fe}(\text{H})(\mu\text{-H})\text{Au}(\text{PPh}_3)]^+$. It is thought to contain an Fe-Au bond with a $\mu_2\text{-H}$ bridge [103].

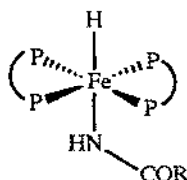
The structure of *cis,mer-Fe*(H) $_2$ ($\eta^2\text{-H}_2$)(PEtPh_2) $_3$ has been determined by neutron diffraction. The unusual orientation of the H-H bond (staggered with respect to the *cis* Fe-P and Fe-H axes) is rationalised by extended Hückel calculations, which reveal a stabilising overlap between the filled $\sigma_{\text{Fe-H}}$ and the empty $\sigma^*_{\text{H-H}}$ orbitals. This nascent bond formation also explains the H^+/H_2 fluxionality of the complex [104]. Neutron-scattering experiments and high-resolution neutron spectroscopy were also used to determine the behaviour of the $\text{Fe}(\text{H}_2)\text{H}$ fragment in *trans-Fe*(H)($\eta^2\text{-H}_2$)(*dppe*)[BF_4]. The results suggest a planar rotation of the $\eta^2\text{-H}_2$ ligand with one angular degree of freedom; steric and electronic contributions to the rotational barrier are discussed [105].

The cyclometallated *dppe* complex (46) and *cis-Fe*H $_2$ (*dppm*) $_2$ both activate the N-H bonds of amides, to give *trans* products of the type (47) ($\text{R} = \text{CF}_3$, C_6F_5 , CH_3 and others). The reaction rates and product stability depend on the natures of the amide and phosphine ligands [106]. $[\text{Fe}^{\text{III}}(\text{dmpe})_2\text{Cl}_2][\text{FeCl}_4]$ was prepared by photochemical oxidation of $\text{Fe}(\text{dmpe})_2\text{Cl}_2$ and

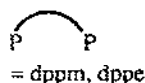
crystallographically characterised. The cation has an octahedral geometry with the two chloride ligands *trans* to one another [107].



(46)



(47)



$\text{H}_2\text{Fe}(\text{CO})_2[\text{P}(\text{OR})_3]_2$ ($\text{R} = \text{Me}, \text{Et}, \text{Ph}$) are formed in high yield from the reaction of $\text{K}[\text{HFe}(\text{CO})_4]$ with $\text{P}(\text{OR})_3$ in aqueous thf, and have a *cis*-dihydrido-*trans*-diphosphite disposition of ligands [108].

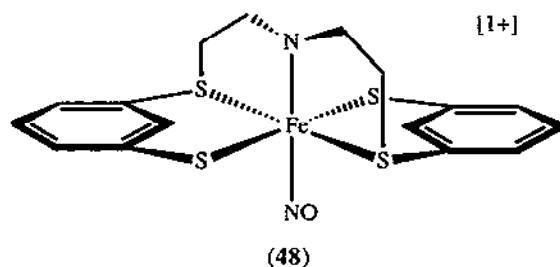
The hydrido-bridged heterobinuclear complex $[(\text{CO})_3\text{Fe}(\mu\text{-H})(\mu\text{-PCy}_2)\text{Pt}(\text{PEt}_3)_2]$ ($\text{Cy} = \text{cyclohexyl}$) was prepared by reaction of $[\text{Fe}(\text{CO})_4(\text{PCy}_2)]^-$ with *trans*- $\text{PtCl}(\text{H})(\text{PEt}_3)_2$. Protonation with $\text{HBF}_4 \cdot \text{Et}_2\text{O}$ gives the stable dihydrido-bridged complex $[(\text{CO})_3\text{Fe}(\mu\text{-H})_2(\mu\text{-PCy}_2)\text{Pt}(\text{PEt}_3)_2][\text{BF}_4]$ which has been fully characterised by ^{31}P and ^1H NMR spectroscopy and IR spectroscopy. With HCl by contrast, coordination of the anion causes elimination of H_2 after protonation to give $[(\text{CO})_3\text{ClFe}(\mu\text{-PCy}_2)\text{Pt}(\text{PEt}_3)_2]$, which has also been fully characterised by ^{31}P and ^1H NMR spectroscopy, IR spectroscopy, and an X-ray structural analysis [109].

1.3 COMPLEXES WITH NITROSYL LIGANDS

Three complexes containing the $\text{Fe}(\text{NO})_2^+$ moiety were prepared from $[\text{Fe}(\text{H}_2\text{O})_6]^{2+}$. The binuclear complexes $[\text{Fe}(\text{NO})_2\text{L}]_2$ ($\text{LH} = \text{benzyl mercaptan}, 2\text{-mercaptoethanol}$; both bridge the two Fe centres) show two reversible reductions; the mononuclear $\text{Fe}(\text{NO})_2\text{L}'$ ($\text{L}' = 2\text{-aminobenzenethiol}$) shows only one reduction and electrochemical behaviour consistent with electropolymerisation [110]. Sixteen complexes $\text{LFe}(\text{NO})_2$ ($\text{LH} = \text{a } 1,2\text{-diimine}$), all also containing the $\text{Fe}(\text{NO})_2^+$ moiety, were prepared. All are intensely coloured and strongly solvatochromic. All show at least one reversible reduction, and a reversible oxidation. The complexes were studied by NMR, UV-visible and ESR spectroscopy. The crystal structure of $\text{Fe}(\text{NO})_2(\text{tBuN:CHCH:NtBu})$ was determined, and shows a roughly tetrahedral coordination around the Fe centre. An MO description of the bonding in these complexes is discussed [111].

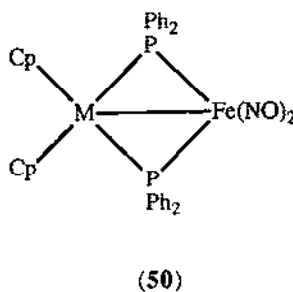
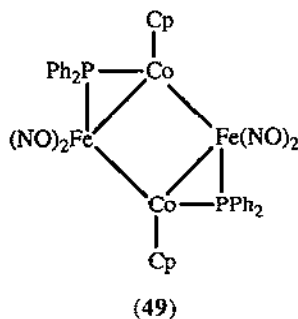
$[\text{Fe}(\text{NO})_2\text{Cl}]_2$ with one equivalent of dppe gives $[\text{Fe}(\text{NO})_2\text{Cl}]_2(\mu\text{-dppe})$, the first structurally characterised binuclear complex with dppe as the single bridge between two non-bonded metal centres. Both metal atoms are in a near-tetrahedral environment. Reaction with a second equivalent of dppe gives $\text{Fe}(\text{NO})_2(\text{dppe})$, again with a tetrahedral coordination environment for the Fe atom [112]. $[\text{Fe}(\text{CO})(\text{NO})(\text{CH}_3\text{CN})(\text{PPh}_3)_2][\text{BF}_4] \cdot \text{CH}_2\text{Cl}_2$ has a roughly trigonal bipyramidal coordination environment around the Fe atom, with the two PPh_3 in apical positions and CO , NO and CH_3CN disordered in the trigonal plane. Comparison of the structure with $\text{Fe}(\text{CO})(\text{NO})(\text{H})(\text{PPh}_3)_2$ shows that formal substitution of H^+ for CH_3CN causes several geometric

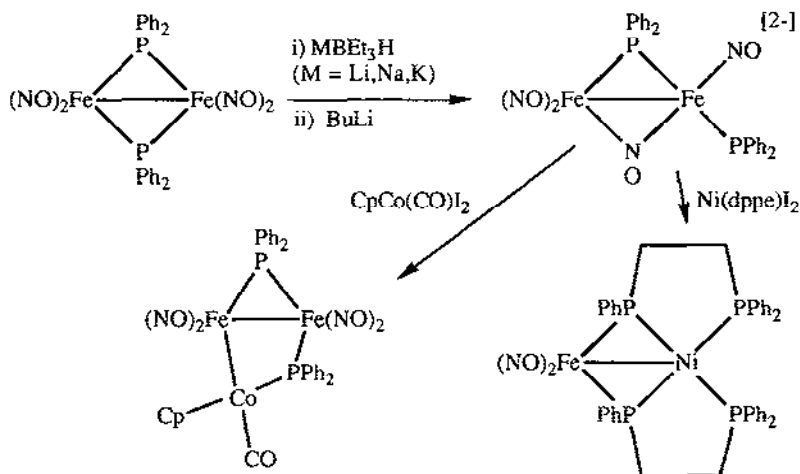
changes which are explained in terms of electron-pair repulsions [113]. $[\text{Fe}(\text{NO})\text{L}][\text{BF}_4]$ (48), $\text{H}_2\text{L} = \text{bis}\{2\text{-[2-mercaptophenylthio]-ethyl}\}$ amine, undergoes a primarily ligand-centred one-electron reduction by N_2H_4 or azide ion. The resultant nineteen-electron species $\text{Fe}(\text{NO})\text{L}$ has a strongly bent Fe-NO group and weakened Fe-L bonds [114].



$\text{Fe}(\text{NO})_2(\text{PPh}_2\text{H})_2$ has been shown to be a useful starting material for the preparation of new polynuclear phosphido-bridged complexes. It can be doubly deprotonated with butyllithium to give $[\text{Fe}(\text{NO})_2(\text{PPh}_2)_2]^{2-}$, which reacts with cobaltocene to give (49) and with CpMCl_2 ($\text{M} = \text{Ti}, \text{Zr}$) to give (50) [115]. $\text{Fe}_2(\text{NO})_4(\mu\text{-PPh}_2)_2$ has also been used in a similar way. Reaction with a source of hydride causes Fe-P bond cleavage and rearrangement to give a monoanionic complex with a terminal phosphine; deprotonation then gives the dianion $[\text{Fe}_2(\text{NO})_3(\mu\text{-NO})(\text{PPh}_2)(\mu\text{-PPh}_2)]^{2-}$, whose reactions are summarised in scheme 9 [116].

The iron-nitrosyl heteropolytungstates $[\text{PW}_{11}\text{Fe}(\text{NO})\text{O}_{39}]^{5-}$, $[\text{P}_2\text{W}_{17}\text{Fe}(\text{NO})\text{O}_{61}]^{8-}$, $[\text{SiW}_{11}\text{Fe}(\text{NO})\text{O}_{39}]^{6-}$ and $[(\text{PW}_9\text{O}_{34})_2(\text{Fe}(\text{NO}))_3]^{12-}$ were prepared and characterised [117]. The crystal structure of $[\text{Ph}_4\text{As}][\text{Fe}_4\text{Se}_3(\text{NO})_7]^-$ has been determined, and consists of a flattened Fe_4 tetrahedron, with the three equivalent faces each capped by Se. The apical Fe carries a single nitrosyl ligand and the others carry two each [118]. $\text{Fe}(\text{NO})_2\text{XL}$ and $\text{Fe}(\text{NO})\text{X}_2\text{L}$ ($\text{X} = \text{Cl}, \text{I}; \text{L} = \text{HMPA}, \text{dppc}, \text{PPh}_3$) react with molecular O_2 to yield nitrate complexes. These transfer oxygen to a variety of substrates; the reactivity is dependent on the nature of the phosphorus ligand [119].





Scheme 9 : Polynuclear complexes prepared from $\text{Fe}_2(\text{NO})_4(\mu\text{-PPh}_2)_2$

1.4 COMPLEXES WITH HALIDE LIGANDS

NaFeF_3 was prepared and has a perovskite structure isotypic to GdFeO_3 [120]; similarly CsFeF_3 is structurally isotypic to BaTiO_3 [121]. The pentafluoroferrate(III) compounds K_2FeF_5 [122], BaFeF_5 [123], Rb_2FeF_5 [124] and $(\text{CH}_3\text{NH}_3)_2\text{FeF}_5$ [124] have been structurally characterised, and all contain chain structures of linked FeF_6 octahedra: by contrast the hydrated $\text{MnFeF}_5 \cdot 7\text{H}_2\text{O}$ contains discrete $[\text{FeF}_6]^{3-}$ and $[\text{FeF}_4(\text{H}_2\text{O})_2]^-$ anions cubically arranged around the $[\text{Mn}(\text{H}_2\text{O})_6]^{2+}$ cations [125]. $\text{CuFe}_2\text{F}_8 \cdot 2\text{H}_2\text{O}$ consists of infinite sheets of corner-shared FeF_6 octahedra linked by Cu polyhedra [126]. The structure $\text{NaPbFe}_2\text{F}_9$ is compared to that of $\text{Fe}_3\text{F}_8 \cdot 2\text{H}_2\text{O}$ [127].

$\text{FeCl}_3 \cdot \text{thf}$ has been prepared and found by X-ray analysis to have a tetrahedral stereochemistry [128]. Anhydrous FeCl_3 may be prepared by dehydration of the hydrated salt with Me_3SiCl [129]. Detailed variable-energy photoelectron spectroscopic studies have been carried out on $[\text{FeCl}_4]^{2-}$ and $[\text{FeCl}_4]^-$, yielding information on their electronic structure and orbital energy levels. The relevance of these results to the solution redox chemistry of these species is discussed [130, 131].

$[\text{4-Cl-pyH}][\text{FeCl}_4]_2\text{Cl}$ (4-Cl-py = 4-chloropyridine) contains a cubic array of slightly distorted $[\text{FeCl}_4]^-$ tetrahedra, in which the $S = 5/2$ centres undergo antiferromagnetic couplings along all directions at 2.73K. The 4-bromopyridinium analogue behaves similarly [132], as do $[\text{4-Cl-pyH}][\text{FeBr}_4]_2\text{Br}$ (which contains $[\text{FeBr}_4]^-$ tetrahedra) and $[\text{4-Cl-pyH}][\text{Fe}_2\text{Cl}_{1.3}\text{Br}_{7.7}]$ (which contains mixed-ligand $[\text{Fe}(\text{halide})_4]^-$ tetrahedra) [133]. Antiferromagnetic ordering is also observed at 1.3K in $[\text{Me}_3\text{NH}][\text{FeBr}_2(\text{H}_2\text{O})_2]\text{Br}$, which contains chains of Br_2 -bridged iron(II) centres, each in a *trans*- $\text{Fe}(\text{H}_2\text{O})_2\text{Br}_4$ distorted octahedral environment [134].

FeI_3 was prepared by photochemical oxidation of $\text{Fe(CO)}_4\text{I}_2$ under argon in hexane; it reacts with iodide ion to give $[\text{FeI}_4]^-$, and with RCl ($\text{R} = \text{Me}_3\text{C}$, 1-adamantyl, 2-norbornyl) to give

FeCl_3 . FeI_3 exists in solution as a μ -iodo dimer, and in the solid state as a polymeric structure containing I-bridged tetrahedral FeI_4 centres. It decomposes to FeI_2 and I_2 when exposed to water or light [135].

1.5 COMPLEXES WITH CYANIDE OR OTHER PSEUDOHALIDE LIGANDS

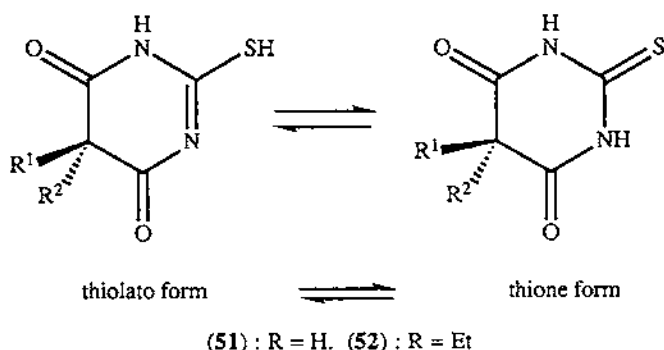
1.5.1 Complexes with cyanide ligands

A wide variety of pentacyanoferrate(II) complexes, of general formula $[\text{Fe}(\text{CN})_5\text{L}]^n$ ($n = 3$ for neutral L, $n = 2$ for cationic L, etc.) have been examined; some results are summarised in Table 1 [136 - 151]. Reaction of $\text{Na}_3[\text{Fe}^{\text{II}}(\text{CN})_5\text{NH}_3]$ with 2-pyridinealdoxime (L) gave the cyano-bridged binuclear complex $\text{Na}_5[(\text{CN})_5\text{Fe}^{\text{II}}(\text{CN})\text{Fe}^{\text{II}}(\text{CN})_3\text{L}]\cdot 8\text{H}_2\text{O}$, in which L acts as a bidentate ligand to one Fe [152]; this is in direct contrast to the mononuclear complex with 4-pyridinealdoxime [142].

The complexes $\{\text{Ru}(\text{bpz})_3[\text{Fe}^{\text{II}}(\text{CN})_5]_n\}^{2-3n}$ ($n = 1-6$; bpz = bipyrazine) were surface-attached to various electrode surfaces. Under illumination the electrodes yield a photocurrent, which is explained in terms of charge-transfer quenching of the $\text{Ru}(\text{II})$ -bpz excited state by the pendant pentacyanoferrate groups [153].

The redox potentials of nine $[\text{Fe}(\text{CN})_5\text{L}]^{2-/3-}$ couples have been measured (L = AsPh_3 , SbPh_3 , various phenyl-substituted PPh_3 derivatives). For the phosphines, the redox potentials are sensitive to the inductive effects of substituents on the phenyl rings [154]. The kinetics of electron-transfer between $[\text{Fe}(\text{CN})_6]^{4-}$ and $[\text{Fe}(\text{CN})_6]^{3-}$ [155], $\text{Cr}(\text{III})$ [156] and $[\text{Co}(\text{NH}_3)_4(\text{NH}_2\text{R})\text{X}]^{(3-n)+}$ ($\text{X} = \text{N}_3^-$, $\text{R} = \text{H}$; $\text{X} = \text{Cl}^-$, $\text{R} = \text{H}$, CH_3 , *iso*- C_4H_9) [157] have been examined and thermodynamic activation parameters evaluated for each. ^{13}C and ^{14}N NMR studies on $\text{K}_4[\text{Fe}(\text{CN})_6]\cdot 3\text{H}_2\text{O}$ have shown that the NMR shifts can be used to deduce the coordination environment of the metal ion [158]. IR and Mössbauer studies were undertaken to determine the electronic state of the iron complexes $[\text{Fe}(\text{CN})_6]^{n-}$ ($n = 3, 4$) and $[\text{Fe}^{\text{II}}(\text{CN})_5\text{NO}]^{2-}$ when incorporated into hydrotalcite-like materials $\text{Mg}_6\text{Al}_2(\text{OH})_{16}(\text{NO}_3)_2\cdot 4\text{H}_2\text{O}$ by anion-exchange [159].

Sodium nitroprusside $\text{Na}_2[\text{Fe}^{\text{II}}(\text{CN})_5(\text{NO})]$ is a potent vasodilator which is used in conjunction with anaesthetics such as thiopental. The interactions between $\text{Na}_2[\text{Fe}(\text{CN})_5(\text{NO})]$ and



the thiopental analogues thiobarbituric acid (51) and diethylthiobarbituric acid (52) were accordingly studied. The thiobarbiturates act as thiones at physiological pH, forming simple adducts with nitroprusside in which the S atom ligates to the Fe(II) centre in a manner analogous to thiourea [160].

The reactions of nitroprusside with pyrimidines, purines, nucleosides and 5'-nucleotides were studied spectrophotometrically; in particular, the effects of illumination, ligand concentration, temperature and pH were examined. The observed reactions could be accounted for by decomposition of the nitroprusside anion to $[\text{Fe}(\text{CN})_5(\text{H}_2\text{O})]^{n-}$ ($n = 2, 3$), which then undergo further substitution reactions with the other ligands [161].

Three new mixed-metal polymeric compounds have been reported, all consisting of infinite three-dimensional networks containing $\text{Fe}(\text{CN})_6$ units linked to main-group metal cations by cyanide bridges. In $[(\text{G}^{2+})_{0.5}(\text{Me}_3\text{Sn})_3\text{Fe}^{\text{II}}(\text{CN})_6]_{\infty}$ (G^{2+} = methyl or benzyl viologen) and $[(\text{G}^{+})_1(\text{Me}_3\text{Sn})_3\text{Fe}^{\text{II}}(\text{CN})_6]_{\infty}$, the cationic guests (G^{2+} or G^{+}) are encapsulated in the cavities formed by the network of $\text{Fe}(\text{CN})_6$ and Me_3Sn units. The charge-transfer spectra of these compounds were recorded [162]. $[(\text{Me}_3\text{Sn})_2(\text{Me}_3\text{Sb})\text{Fe}^{\text{II}}(\text{CN})_6]_{\infty}$ was prepared by coprecipitation of Me_3SnCl , Me_3SbBr_2 and $\text{K}_4[\text{Fe}(\text{CN})_6]$ from water, or by ion-exchange of the known polymers $[\text{A}(\text{Me}_3\text{Sn})_3\text{Fe}(\text{CN})_6]_{\infty}$ ($\text{A} = \text{Et}_4\text{N}^+$, $[(\eta^5\text{-C}_5\text{H}_5)_2\text{Co}]^+$, Me_3Sn^+ , NH_4^+) with Me_3SbBr_2 . The IR spectra suggest a statistical distribution of $\text{Fe}(\text{CN-Sn})_{6-x}(\text{CN-Sb})_x$ building blocks ($x = 0 - 6$) in the three-dimensional network [163]. $[(\text{Me}_3\text{Sn})_4\text{Fe}^{\text{II}}(\text{CN})_6 \cdot 2\text{H}_2\text{O} \cdot \text{dioxane}]_{\infty}$, crystallised from H_2O -dioxane solutions of Me_3SnCl and $\text{K}_4\text{Fe}(\text{CN})_6$, consists of a three-dimensional network of two non-linear chains $[\text{Sn-NC-Fe-CN-Sn-NC-Fe-CN}]_{\infty}$ and $[\text{Sn}(\text{OH}_2)\text{-O}(\text{C}_2\text{H}_4)_2\text{O}(\text{H}_2\text{O})\text{Sn-NC-Fe-CN}]_{\infty}$ ($\text{O}(\text{C}_2\text{H}_4)_2\text{O}$ = dioxane) which are linked at their joint, octahedrally coordinated Fe atoms [164].

The redox reaction of $[\text{Pt}(\text{NH}_3)_4](\text{NO}_3)_2$ with $\text{K}_3\text{Fe}(\text{CN})_6$ in water yields the trinuclear, cyano-bridged complex $[\text{Pt}(\text{NH}_3)_4]_2[(\text{NC})_5\text{Fe}(\text{CN})\text{Pt}(\text{NH}_3)_4(\text{NC})\text{Fe}(\text{CN})_5] \cdot 9\text{H}_2\text{O}$ containing two Fe(II) and one Pt(IV) centres, all octahedrally coordinated. Each complex anion H-bonds to two cations via a terminal cyanide ligand from each iron. The electronic spectrum shows an Fe(II)-Pt(IV) inter-valence charge transfer band at 470nm; excitation at this wavelength causes electron transfer from Fe(II) to Pt(IV), regenerating $[\text{Pt}(\text{NH}_3)_4]^{2+}$ and $2[\text{Fe}(\text{CN})_6]^{3-}$ [165].

Vanadium hexacyanoferrate (VHCF) is an electrochromic material similar in structure to Prussian blue. Electrochemical and spectroelectrochemical studies of VHCF films show that the electrochromic reaction is due only to redox processes at the Fe centres rather than the V(IV) centres [166].

Detailed ^1H and ^{13}C NMR studies on the low-spin complexes $[\text{Fe}^{\text{III}}(\text{CN})_4(\text{en})]^-$ and $[\text{Fe}^{\text{III}}(\text{CN})_4(\text{Me}_2\text{en})]^-$ ($\text{en} = 1,2\text{-ethanediamine}$, $\text{Me}_2\text{en} = \text{N,N'-dimethyl-1,2-ethanediamine}$) between 185 and 323K showed that the complexes have non-Curie magnetic behaviour. The ESR spectrum of $[\text{Fe}(\text{CN})_4(\text{en})]^-$ at 4K in conjunction with the NMR data allowed determination of the Fermi contact shifts δ^{con} , the dipolar shifts δ^{dp} , and the g-values and spin-orbit coupling constant for the complex [167]. The chair-to-chair interconversion of the six-membered chelate ring in $[\text{Fe}(\text{CN})_4(\text{pn})]^-$ ($\text{pn} = 1,3\text{-propanediamine}$) could be studied by ^1H NMR of the paramagnetic

Table 1: Summary of complexes $[\text{Fe}^{\text{II}}(\text{CN})_5\text{L}]^n$

<u>Nature of L</u>	<u>Studies performed</u>	<u>ref</u>
Various	FAB Mass Spectrometry used to study ligand-removal and redox reactions	[136]
N-heterocycle	Theoretical studies on MLCT interactions	[137]
2-aminopyrazine	Formation kinetics; presence of linkage isomers; kinetics of isomer interconversion	[138]
NH_3 , pyridine, $[\text{N}_2\text{H}_5]^+$, $[\text{H}_2\text{NCH}_2\text{CH}_2\text{NH}_3]^+$	Kinetics of reaction with cyanide in the solid state; Mössbauer spectroscopy (for $\text{L} = \text{NH}_3$)	[139]
Neutral, protonated & N-methylated 4,4'-bipyridine; 1-(4-pyridyl)-pyridinium; 1,2-bis(4-pyridyl)-ethane; 1,2-bis(4-pyridyl)ethene	Kinetic and spectroscopic studies on complex formation; pH dependency of kinetic behaviour; relation of kinetics to size and nature of L	[140]
Aniline	Preparation, kinetics of formation and oxidation by $[\text{Fe}(\text{CN})_6]^{3-}$, spectroscopic properties	[141]
4-pyridinealdoxime	Preparation, kinetics of formation and substitution by CN^- , spectroscopic properties	[142]
NO^+ , N_2H_5^+ , NH_3 , H_2O , $[\text{H}_2\text{NCH}_2\text{CH}_2\text{NH}_3]^+$, pyridine	Thermal decomposition behaviour studied by gas chromatography, Mössbauer and IR spectroscopy	[143]
Adenosine, 1-methyladenosine, tubercidin, 2-amino-pyridine, 3-aminopyridine	Preparation, MLCT spectrum, kinetics of formation/dissociation, reversible electrochemical oxidations	[144]
CO	Formation by nucleophilic substitution in gaseous plasma	[145]
Azoles, benzazoles	Relationship between ligand pK_a and oxidation potential of complex	[146]
3-pyrazinecarboxylate	Kinetics of formation in various solvents	[147]

complex, since the two forms have large differences in chemical shift values; the activation parameters for the interconversion were deduced and compared to those of $[\text{Fe}(\text{CN})_4(\text{en})]^-$ [168].

Thermal and photochemical substitution of the NO_2^- ligand in $\text{K}_3[\text{Fe}^{(\text{III})}(\text{CN})_5(\text{NO}_2)]$ have been examined [169]. The kinetics of the reactions between $[\text{Fe}^{(\text{III})}(\text{CN})_5\text{OH}]^{3-}$ and CN^- , and between $[\text{Fe}(\text{CN})_6]^{3-}$ and triethylenetriaminehexaacetic acid were examined at a variety of pH values, and their respective activation parameters determined [170]. The kinetics of oxidation of lysine, arginine and histidine by alkaline $[\text{Fe}(\text{CN})_6]^{3-}$ were examined; the reactions are first-order in substrate and oxidant. The amino acids are oxidised to α -keto acids in two steps, via an imino-acid intermediate [171]. A series of complexes $[\text{Fe}(\text{CN})_5\text{L}]^{n-}$ ($n = 2, 3$; L = glycine, imidazole, triglycine, histidine) have been examined as possible models for peroxidase and catalase enzymes. The kinetics of H_2O_2 decomposition catalysed by these complexes was examined over a wide pH range and conforms to the Michaelis-Menten-type kinetics characteristic of enzymes [172].

Detailed ESR studies on $[\text{Fe}(\text{CN})_6]^{3-}$ in a KCl lattice showed that there are two principal Fe(III) environments, which correspond to different configurations of the charge-compensating cations in the lattice. Both centres are very anisotropic; the g-values, ligand-field splittings and orbital reduction factors were obtained for each. In addition the ^{13}C and ^{14}N coupling tensors were determined [173]. Charge-density measurements by X-ray diffraction of $\text{Cs}_2\text{K}[\text{Fe}(\text{CN})_6]$ yielded detailed information on the bonding in the $[\text{Fe}(\text{CN})_6]^{3-}$ fragment and the degrees of σ -donor and π -acceptor behaviour. The results were confirmed by ESR spectroscopy and neutron diffraction studies [174]. The crystal structure of $\text{Bi}[\text{Fe}^{(\text{III})}(\text{CN})_6] \cdot 4\text{H}_2\text{O}$ has been determined [175].

1.5.2 Complexes with other pseudohalide ligands

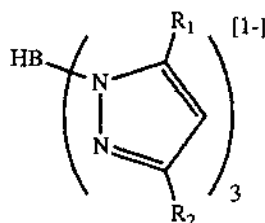
Buff's 'ferrocyanethyl', first made in 1854 by reaction of gaseous HCl with $\text{H}_4[\text{Fe}(\text{CN})_6]$ in ethanol, has been crystallographically characterised. It is a homoleptic hydrogen isocyanide complex, with an octahedral $[\text{Fe}(\text{CNH})_6]^{2+}$ core stabilised by very strong hydrogen-bonds between each isocyanide H-atom and an ethanol molecule in the second co-ordination sphere [176]. $\text{M}_2[\text{Fe}^{(\text{II})}\text{X}_4\text{L}]$ ($\text{M} = \text{K}, \text{Na}$; $\text{X} = \text{OCN}, \text{SCN}, \text{N}_3$; L = pyridine-N-oxide, 4-picoline-N-oxide or L-ascorbic acid) were prepared and characterised. They are all 1:2 electrolytes and probably have a square-pyramidal geometry [177].

A positive kinetic salt effect was observed in the reaction between Fe(III) and SCN^- ions in a variety of electrolyte solutions at different concentrations; it is ascribed to ion-solvent interactions [178]. The reaction of Fe(II) at an Hg electrode was studied in solutions containing SeCN^- [179].

1.6 COMPLEXES WITH N-DONOR LIGANDS

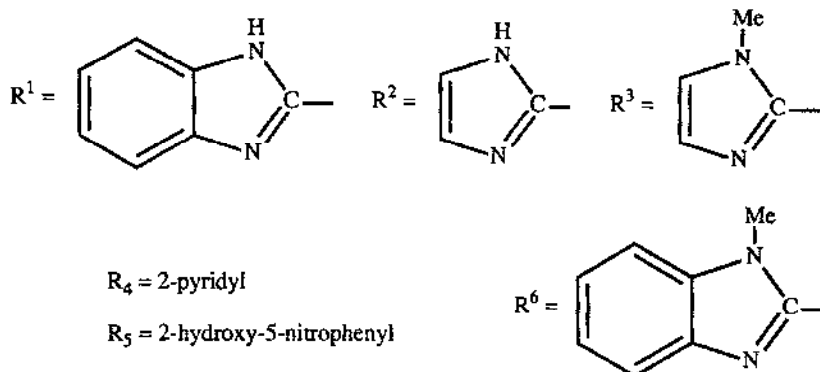
1.6.1 Complexes with N-heterocyclic ligands

The trispyrazolylborate ligands (53-57) are finding increasing use as face-capping analogues of cyclopentadienyl. The sterically congested complex $\text{Fe}^{\text{II}}(\text{53})_2$ has been prepared and structurally characterised. Each ligand caps one face of an essentially octahedral complex; the bulky phenyl groups result in longer Fe-N bonds than are found for less substituted ligands such as 55, which results in a relatively high $\text{Fe}^{\text{II}}/\text{Fe}^{\text{III}}$ oxidation potential. The magnetic behaviour is consistent with a high-spin d^6 configuration [180]. $\text{Fe}^{\text{III}}(\text{54})\text{Cl}$ has a distorted tetrahedral coordination geometry, and reacts with AgBF_4 to give $\text{Fe}^{\text{III}}(\text{54})\text{F}$ [181]. $[\text{Fe}^{\text{III}}(\text{55})\text{Cl}_3]^-$ and $[\text{Fe}^{\text{III}}(\text{56})\text{Cl}_3]^-$ have been prepared; X-ray analysis of the former shows the expected half-



- (24) $R_1 = \text{H}; R_2 = \text{C}_6\text{H}_5$
 (25) $R_1 = \text{H}; R_2 = \text{tert-Butyl}$
 (26) $R_1 = R_2 = \text{H}$
 (27) $R_1 = R_2 = \text{Me}$
 (28) $R_1 = R_2 = \text{iso-Propyl}$

(53): $R_1 = \text{H}, R_2 = \text{C}_6\text{H}_5$. (54): $R_1 = \text{H}, R_2 = \text{tert-butyl}$. (55): $R_1 = R_2 = \text{H}$
 (56): $R_1 = R_2 = \text{Me}$. (57): $R_1 = R_2 = \text{iso-propyl}$



$(R^1\text{CH}_2)_2\text{NR} = (58) (R = \text{H}), (59) (R = \text{CH}_3); (R^6\text{CH}_2)_2\text{NMe} = (60);$
 $(R^1\text{CH}_2)_2\text{NCH}_2\text{CH}_2\text{N}(\text{CH}_2\text{R}^1)_2 = (61); (R^2)_3\text{P} = (62); (R^3)_3\text{P} = (63); (R^1\text{CH}_2)_3\text{N} = (64);$
 $(R^1\text{CH}_2)_2\text{NCH}_2\text{R}^4 = (65); (R^4\text{CH}_2)_2\text{NCH}_2\text{R}^5 = \text{H}, (66); (R^4\text{CH}_2)_3\text{N} = (67);$
 $(R^2)_2 = 2,2'\text{-biimidazole}, (68); (R^1)_2 = 2,2'\text{-bibenzimidazole}, (69); R^2\text{CH}_2\text{R}^2 = (70);$
 $R^2\text{COR}^2 = (71)$

sandwich octahedral structure, and the latter reacts with NaN_3 to give $[\text{Fe}^{\text{III}}(\text{56})(\text{N}_3)_3]^-$ which has a similar coordination geometry [182]. Five coordinate $\text{Fe}^{\text{II}}(\text{57})(\text{PhCO}_2)$ reacts with CH_3CN to

give an octahedral adduct in which the benzoate coordinates in a bidentate manner. It also reversibly binds dioxygen in toluene at -20°C ; the Raman spectrum of the oxygen adduct indicates a μ -peroxo-bridged bis-Fe(III) species. However it does not bind CO and thus mimics in part the behaviour of some iron-containing oxygen transport proteins [183].

The highly asymmetric complex $[\text{Fe}^{\text{III}}(\mathbf{61})\text{OFe}^{\text{III}}\text{Cl}_3]^+$, in which (**61**) acts as a pentadentate ligand with one non-coordinated imidazole, shows much stronger antiferromagnetic coupling than is normally seen for a singly-bridged μ -oxo species. Analysis of orbital interactions shows that the large coupling may be explained by the low symmetry of the complex [184].

In the octahedral complex $\text{Fe}(\mathbf{59})\text{Cl}_3$ the tridentate ligand coordinates meridionally. In the presence of pivalate by contrast, (**58**) (which differs only by the absence of a methyl group) reacts with Fe(III) to give the symmetrical dimer $[\text{Fe}_2(\mathbf{58})_2(\mu\text{-O})(\mu\text{-}^i\text{BuCO}_2)_2][\text{ClO}_4]_2$ in which (**58**) acts as a face-capping ligand. This is one of many examples of binuclear Fe(III) complexes containing μ -oxo and μ -carboxylato bridges, which are currently under intense examination as possible models for the active sites of many non-heme iron proteins. Each Fe(III) centre is in a roughly octahedral environment, with the ligand (**58**) folded up to bind in a face-capping manner, and the other three coordination sites occupied by the oxo and two carboxylato bridges. The complex shows antiferromagnetic coupling between the high-spin Fe(III) centres, which is a typical feature of the Fe(III)-O-Fe(III) core unit [185, 186]. Ligand (**60**), which is methylated on the benzimidazole groups, also acts as a tridentate face-capping ligand and supports the same binuclear structures. A series of complexes $[\text{Fe}_2(\mathbf{60})_2(\mu\text{-O})(\mu\text{-RCO}_2)_2][\text{ClO}_4]_2$ were prepared with various bridging carboxylates by a simple carboxylate exchange process, and their electronic and IR spectra reported [186]. The similar complexes $[\text{L}_2\text{Fe}^{\text{III}}_2(\mu\text{-O})(\mu\text{-OAc})]^{n+}$ (L = (**64**), $n = 3$; L = (**65**), $n = 3$; L = (**66**), $n = 1$; OAc = acetate) were prepared and show typical antiferromagnetic behaviour; some cyclic voltammetry studies were also performed [187].

The tris-imidazol-2-yl phosphines (**62**) and (**63**) act as terdentate face-capping N-donor ligands to Fe(III) with no coordination through the P atom, and can support binuclear oxo- or hydroxo-bridged Fe(III) cores, although (**63**) results in more stable and easily isolable products. $[\text{Fe}_2(\mathbf{63})_2\text{O}(\text{OAc})_2][\text{ClO}_4]_2$ has been prepared and structurally characterised (as its acetone/trile/ethanol solvate); the structure is typical. $[\text{Fe}_2(\mathbf{63})\text{O}(\text{EtCO}_2)_2][\text{PF}_6]_2$ was also prepared and exhibits antiferromagnetic coupling. The hydroxo-bridged complexes $[\text{Fe}_2(\mathbf{63})(\text{OH})(\text{RCO}_2)_2]^{3+}$ (R = methyl, ethyl) also show antiferromagnetic coupling but it is much weaker. The electronic and Mössbauer spectra suggest that protonation of the oxo-bridge results in lengthening of the Fe-O_{oxo} bonds and concomitant shortening of the *trans* Fe-N bonds. These results confirm earlier interpretations of NMR data for the complexes [188].

$[\text{Fe}^{\text{III}}_2(\mathbf{67})_2(\mu\text{-O})(\mu\text{-L})][\text{ClO}_4]_3$ ((**67**) = tris(2-pyridylmethyl)amine, a tetradentate tripodal ligand, L = acetate, benzoate, diphenylphosphate) have all been structurally characterised. Since the capping ligand (**67**) is tetradentate, only one bridging ligand in addition to the μ -oxo group is necessary to complete the coordination spheres of the Fe(III) centres. The orientation of (**67**) is different at each end of the complex, which means that the two Fe(III) sites are inequivalent, unlike the majority of these binuclear complexes; on one Fe the amine N atom is *trans* to the oxo bridge, while at the other end a pyridine ligand is *trans* to the oxo bridge. This inequivalence is

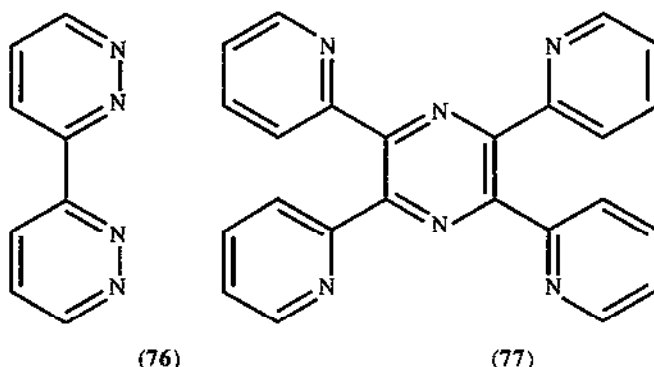
retained in solution. The electronic, magnetic and Mössbauer properties of these complexes are very similar to those of $(\mu\text{-oxo})\text{diiron(III)}$ proteins, as well as those of the triply-bridged $(\mu\text{-oxo})(\mu\text{-carboxylato})_2$ dimers, which shows that these properties are not significantly affected by the number of carboxylate bridges and the inequivalence of the Fe(III) sites [189]. The relationship between spectroscopic and magnetic behaviour, and the geometry of the Fe(III)-O-Fe(III) core, was studied systematically for the series of complexes $[\text{Fe(III)}_2(67)_2(\mu\text{-O})(\mu\text{-L})]^{n+}$ (L = carbonate, hydrogen maleate, diphenylphosphate, diphenylphosphinate, maleate, phthalate, all of which act as bridging ligands). In particular, the complexes with L = carbonate, hydrogen maleate and phthalate were structurally characterised and reveal a steady increase in Fe-O-Fe angle and Fe-Fe distance, due to the increasing bites of the bridging ligands. Magnetic moment measurements showed no apparent correlation in this instance between the magnitude of the coupling constant J and the structural parameters; however electronic spectra showed a steady blue-shift of the absorption features with increasing Fe-O-Fe angle [190].

The tridentate face-capping ligand hydro-trispyrazolylborate (55) has also been used to prepare similar complexes, but with phosphate and phosphinate bridges between the Fe(III) centres. This is to model the possible behaviour of enzymes such as purple acid phosphatase and ribonucleotide reductase, where binding of a phosphate group to the Fe(III)-O-Fe(III) core is thought to occur. $[\text{Fe(III)}_2(55)_2(\mu\text{-O})(\mu\text{-L})_2]$ (L = diphenylphosphate, diphenylphosphinate) were easily prepared by displacement of acetate by the appropriate acid from the parent complex $[\text{Fe(III)}_2(55)_2(\mu\text{-O})(\mu\text{-OAc})_2]$. The crystal structures are similar to those already described, but the Fe-O bond lengths are longer than in the analogous dicarboxylato-bridged complexes, so the anti-ferromagnetic exchange is weaker. The Mössbauer and electronic spectral parameters for the complexes resemble those of the dicarboxylato-bridged complexes, but are different from those of purple acid phosphatase, which suggests that the enzymes may not have phosphate bound at the core after all [191].

$[\text{Fe(III)}\text{LX}_2]^+$ (L = (64), (67), N,N'-bis(2-pyridylmethyl)glycine; X = Cl, Br) are capable of C-H bond activation in alkanes and thus catalysing alkane oxidation. Thus, cyclohexane reacts with $[\text{Fe(67)Cl}_2]^+$ and $^t\text{Bu-OOH}$ to give cyclohexanol, cyclohexanone, chlorocyclohexane and $^t\text{Bu-peroxocyclohexane}$. C-H bond cleavage is at least partially rate-determining; an Fe(V)=O or Fe(IV)=O species may be involved, as in heme oxidations [192].

2,2'-bibenzimidazole (69) forms a high-spin octahedral complex $[\text{Fe(69)}_3]^{2+}$ with Fe(II). It also forms $\text{Fe(69)}_2\text{Cl}_2$ and $\text{Fe(69)}_2(\text{HCO}_2)_2$, which are thought to be *cis* on the basis of steric hindrance considerations and Mössbauer spectroscopy. By contrast the complexes $\text{Fe(68)}_2\text{Cl}_2$ and $\text{Fe(68)}_2(\text{HCO}_2)_2$, with the smaller ligand 2,2'-biimidazole, are thought to have *trans* structures. $\text{Fe(68)}_2(\text{OAc})_2$ consists of a mixture of *cis* and *trans* isomers, and is spectroscopically the most similar to the iron(II) sites in photosystem II. The relationship between distortions in coordination environment and Mössbauer spectra are discussed [193].

The colourless, high-spin iron(II) complex $[\text{Fe(70)}_3]^{2+}$ oxidises in methanol or ethanol solutions in air to give $[\text{Fe(II)(71)}_3]^{2+}$, in which the $-\text{CH}_2-$ group of each ligand is oxidised to a ketone. The mechanism, and the catalytic role of the iron centre, are discussed [194].



$[\text{Fe}^{\text{II}}(\text{76})_3][\text{Fe}^{\text{II}}\text{Cl}_4]$ and $[\text{Fe}^{\text{II}}(\text{76})_3][\text{Fe}^{\text{III}}\text{Cl}_4]_2$ were also prepared and contain low-spin cations and high-spin anions. All of these complexes were characterised by magnetic and Mössbauer measurements. The crystal structure of $[\text{Fe}(\text{76})_3][\text{ClO}_4]_2$ was determined, and is notable for the particularly short Fe-N distances. These are ascribed to both the strong ligand field, and the absence of steric effects from H_5 protons [200].

The 'host' complex $\text{trans-}[\text{Fe}^{\text{II}}\text{L}_4(\text{SCN})_2]$ (L = 4-methylpyridine) is zeolite-like, in that the crystals contain a network of three-dimensional cavities which accommodate 'guest' molecules such as benzene or xylenes [201]. Tetrakis(2-pyridyl)-1,4-diazine (77, a potentially binucleating ligand with two terdentate binding pockets) has been used to prepare mono- and binuclear complexes with $\text{Fe}(\text{II})$. Both $[\text{Fe}(\text{CN})_3(\text{77})]^-$ and $[\{\text{Fe}(\text{CN})_3\}_2(\text{77})]^{2-}$ show intense solvent-dependent MLCT transitions in the visible region, and ligand-based $\pi-\pi^*$ transitions in the UV region; they have one and two reversible $\text{Fe}(\text{II})/\text{Fe}(\text{III})$ oxidations respectively. Despite the 0.25V difference between the oxidation potentials in the binuclear complex, no inter-valence transition band was observed for the mixed-valence species [202].

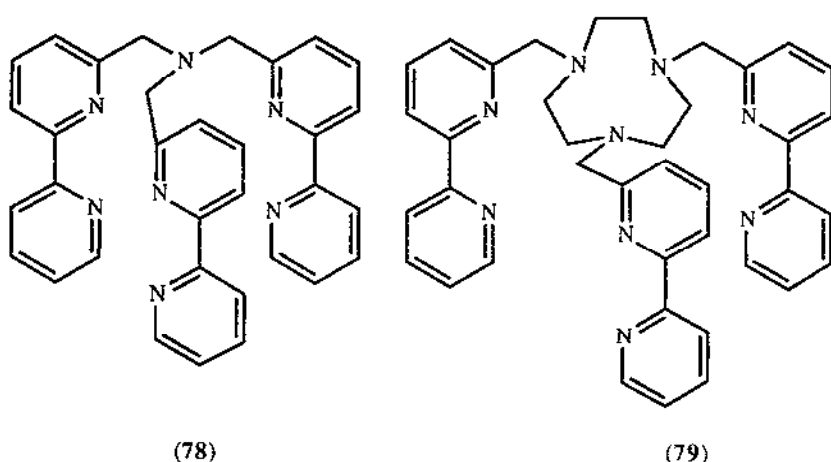
A resonance Raman study on $[\text{Fe}(\text{bipy})_3]^{2+}$ (bipy = 2,2'-bipyridine) under excitation into two different $d-\pi^*$ bands was performed to examine the skeletal vibrations of the bipy ligands. The results are consistent with the coefficients and phase relations for the ligand LUMO that have been calculated by extended Hückel theory, and are also consistent with similar spectral assignments for $[\text{Ru}(\text{bipy})_3]^{2+}$ and $[\text{Os}(\text{bipy})_3]^{2+}$. The band intensities were found to be very dependent on the excitation wavelength [203].

The kinetics and mechanism of the oxidation of $[\text{FeL}_3]^{2+}$ (L = phen, bipy) with $\text{S}_2\text{O}_8^{2-}$ have been examined; two different mechanisms occur, both being dissociative and oxidative [204]. The kinetics of ligand substitution of $[\text{Fe}(\text{phen})_3]^{3+}$ by EDTA (H_4EDTA = ethylenediamine- $\text{N},\text{N},\text{N}',\text{N}'$ -tetraacetic acid) have also been studied with a rotating disc electrode [205]. The kinetics of aquation of $[\text{Fe}(\text{Br-phen})_3]^{2+}$ (Br-phen = 5-Bromo-1,10-phenanthroline) have been determined as a function of both temperature and pressure, yielding activation parameters. The isochoric, isobaric and isothermal activation parameters are compared [206]. The intercalation of $[\text{Fe}(\text{bipy})_3]^{2+}$ and $[\text{Fe}(\text{phen})_3]^{2+}$ into montmorillonite clay was examined by electronic spectroscopy [207].

A new series of ligands has been prepared by per-alkylation of various macrocyclic and open-chain amines (NH_3 , ethylene diamine, 1,4,7-triazacyclononane [=tacn], cyclam, hexaaza-18-

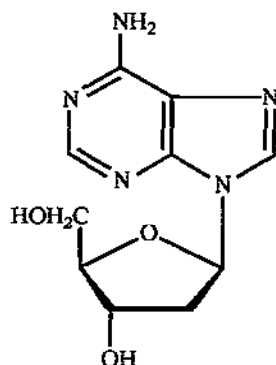
crown-6) with 2-bromomethylbipyridine. Thus, ammonia reacts to give the tripodal ligand (78) and tacn gives (79); several metal complexes have been prepared and characterised by electrochemistry and electronic spectroscopy. $[\text{Fe}(\text{78})]^{2+}$ is an analogue of $[\text{Fe}(\text{bipy})_3]^{2+}$ with higher kinetic stability since ligand dissociation is much harder. Unlike $[\text{Fe}(\text{bipy})_3]^{2+}$, it undergoes a reversible one-electron at a low potential, which is ascribed to the weak coordination of the apical N-atom. Other ligands give polynuclear complexes of varying stoichiometries; for example $\text{R}_2\text{NCH}_2\text{CH}_2\text{NR}_2$ ($\text{R} = -\text{CH}_2\text{-2-bipyridyl}$) forms $[\text{Fe}_4\text{L}_3][\text{SO}_4]_4$ [208].

Reactions of the hydroxyl radical (generated by pulse radiolysis of an N_2O -saturated aqueous solution) with $[\text{Fe}(\text{bipy})_3]^{2+}$, $[\text{Fe}(\text{bipy})_2(\text{CN})_2]$, $[\text{Fe}(\text{bipy})_2(\text{CN})_4]^{2-}$, $[\text{Fe}(\text{CN})_6]^{4-}$ and $[\text{Fe}(4,4'\text{-Me}_2\text{bipy})_3]^{2+}$ have been examined by time-resolved electronic spectroscopy and conductivity measurements. For $[\text{Fe}(\text{bipy})_3]^{2+}$ the first step involves addition of OH^\bullet to give a ligand-centred radical; $[\text{Fe}(\text{CN})_6]^{4-}$ by contrast undergoes an electron transfer reaction to give $[\text{Fe}(\text{CN})_6]^{3-}$ and OH^\bullet . The mixed cyanide-bipyridine complexes react by both mechanisms simultaneously [209].

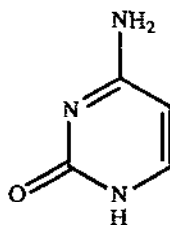


Excitation of $[\text{Fe}(\text{II})\text{L}(\text{CN})_4]^{2-}$ ($\text{L} = \text{bipy}, 4,4'\text{-dimethylbipy}$) with 266nm light produces the oxidised species $[\text{Fe}(\text{III})\text{L}(\text{CN})_4]^-$ and a solvated electron, e_{aq}^- , which has a characteristic absorption at 600nm. A second reaction between e_{aq}^- and the starting material $[\text{FeL}(\text{CN})_4]^{2-}$ causes a ligand-centred reduction of the complex, giving $[\text{FeL}(\text{CN})_4]^{3-}$. Spectrophotometric studies showed that $[\text{FeL}(\text{CN})_4]^{3-}$ appears at the same rate as e_{aq}^- disappears. The pH dependence of e_{aq}^- formation in the initial step was examined [210].

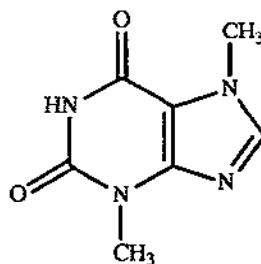
$\text{Fe}(\text{phen})_2(\text{CN})_2$ is very solvatochromic, due to differing degrees of interaction of the externally-directed N lone pairs with different solvents; hence it is an excellent indicator of solvent polarity. There is a good correlation between λ_{max} for the complex in different solvents with the solvent acceptor number [211].



(80), 2'-Deoxyadenosine

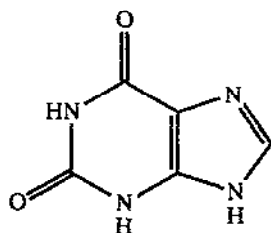


(81), Cytosine

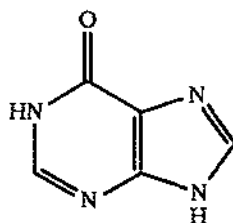


(82), Theobromine

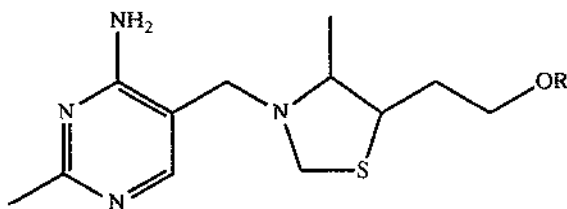
The interactions of metal ions with biomolecules such as nucleotides and vitamins are currently receiving much attention. $[\text{Fe}(\text{III})_2(\text{80})_3][\text{ClO}_4]_6 \cdot 4\text{H}_2\text{O}$, $[\text{Fe}(\text{III})(\text{80})_2][\text{ClO}_4]_3 \cdot 2\text{H}_2\text{O}$ and $[\text{Fe}(\text{II})(\text{80})_2]\text{Cl}_3$ were prepared and have normal magnetic moments at room temperature. They are thought to be six-coordinate linear polymers, in which the 2'-deoxyadenosine behaves both as a terminal monodentate ligand (through N7) and a bidentate bridging ligand (through N1 and N7) [212,213]. In $[\text{Fe}(\text{II})(\text{81})_4][\text{SO}_4]$ the cytosine is a monodentate N-donor [214]. $\text{Fe}(\text{82})_2\text{X}_3 \cdot \text{H}_2\text{O}$ has an octahedral geometry in which two theobromine ligands act as monodentate N-donors [215]. In the complexes $\text{Fe}(\text{III})(\text{HL})_3\text{LX}_2$ ($\text{HL} = (\text{83}), (\text{84})$) both xanthine and hypoxanthine are monodentate, via one of the imidazole nitrogen atoms. Spectroscopic characterisation suggests a *cis*- FeN_4X_2 arrangement of ligands [216]. Pseudo-tetrahedral $\text{Fe}(\text{MPP})_2\text{X}_2$ ($\text{MPP} = 3\text{-methyl-5-phenylpyrazole}$; $\text{X} = \text{Cl}, \text{Br}$) contains, by analogy with the $\text{Co}(\text{II})$ and $\text{Zn}(\text{II})$ complexes which were structurally characterised, monodentate MPP ligands [217]. Tetrahydrothiamine (85) forms the complex $\text{Fe}(\text{III})(\text{85})(\text{H}_2\text{O})\text{Cl}_3$ with $\text{Fe}(\text{III})$ in which (85) acts as a monodentate N-donor, but through which nitrogen atom is unclear; its phosphate esters behave similarly [218].



(83), Xanthine



(84), Hypoxanthine



(85), Tetrahydrothiamine: R = H. Phosphate esters: R = PO_3H_2 , $\text{P}_2\text{O}_6\text{H}$

Deuteration of 8-aminoquinoline (AQ) at the amino position has helped to elucidate the IR spectra, and hence determine the geometries, of its complexes. $[\text{Fe}(\text{AQ})_3][\text{ClO}_4]_2$ was prepared and deduced to be the *fac* isomer on the basis of the IR spectrum [219]. Similarly the spectrum of $\text{Fe}(\text{AQ})_2(\text{H}_2\text{O})_2\text{Cl}_2$ was fully assigned, and the structure of the complex determined to be *trans*- $[\text{Fe}(\text{AQ})_2(\text{H}_2\text{O})_2]\text{Cl}_2$ [220]. $[\text{Hg}_3\text{Fe}(\text{III})\text{L}_6][\text{NO}_3]_3$ (HL = 2-pyridone) was prepared, in which L is a bidentate bridge with coordination to Hg through the O atom and to Fe through the N atom. The crystal structure of octahedral $[\text{Fe}(\text{HL})_6][\text{NO}_3]_3$ was also determined [221].

The electron transfer reaction between Fe(III) and NADH is known to produce a transient blue intermediate, due to formation of Fe(III)-NADH π -complexes. A similar blue species was observed during the reaction between Fe(III) and 9,10-dihydro-10-methylacridine (an analogue of NADH but without the amide group) and is also ascribed to formation of a π -complex [222].

1.6.2 Complexes with imines and oximes

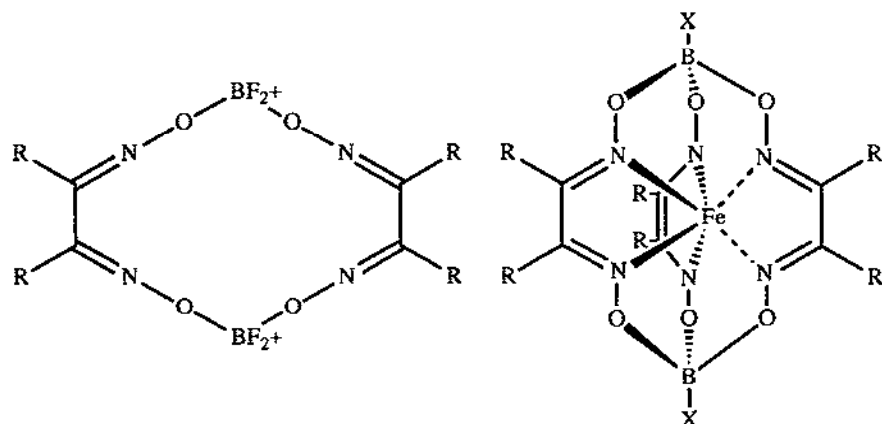
Electronic spectra of $\text{Fe}(\text{II})(\text{Hdmg})_2\text{L}_2$ (H_2dmg = dimethylgloxime; L = N-heterocycle) have been compared with the spectra of analogous $[\text{Fe}(\text{II})(\text{CN})_5\text{L}]^{3-}$ complexes; the energies of the MLCT bands correlate with the electronic properties of L and the Fe(II)/Fe(III) redox couples of the complexes [223]. The kinetics of formation of $\text{Fe}(\text{Hdmg})_2$, and of its subsequent reduction to $[\text{Fe}(\text{Hdmg})_2]^-$, have been studied by stopped-flow spectrophotometry [224].

The mixed-metal complexes $\text{Fe}(\text{II})_2\text{Sn}(\text{Hchd})_6\text{Cl}_2(\text{H}_2\text{O})_5$, $\text{Fe}(\text{II})_2\text{Sb}(\text{Hchd})_6\text{Cl}(\text{H}_2\text{O})_5$ and $\text{Fe}(\text{II})_2\text{Bi}(\text{Hchd})_6\text{Cl}(\text{H}_2\text{O})_4$ (H_2chd = 1,2-cyclohexanedionedioxime) were prepared and characterised by IR and Mössbauer spectra, thermogravimetric analysis and magnetic susceptibility measurements, and all contain a low-spin $\text{Fe}(\text{II})\text{N}_6$ core [225]. $[\text{Fe}(\text{III})(\text{Hbd})_2\text{L}_2]\text{Cl}_n/2\text{Cl}_2$ (L = pyridine and derivatives; H_2bd = α -benzildioxime) was shown by potentiometric titration to contain zero-valent chlorine. Confirmatory evidence was provided by the preparation of $[\text{Fe}(\text{III})(\text{Hbd})_2\text{L}]_3$ and $[\text{Fe}(\text{III})(\text{Hfd})_2(\text{py})]_3 \cdot 1/2\text{I}_2$ (H_2fd = α -furildioxime; py = pyridine) [226]. Rate constants and activation volumes for the alkaline hydrolysis of $[\text{Fe}(\text{gmi})_3]^{2+}$ (gmi = gloxal-bismethylimine, 2,5-diaza-2,4-hexadiene) were determined in water/*tert*-butanol mixtures. From the dependence of these parameters on the solvent composition, the change in affinities of the complex for the solvent components between the initial and transition states, and the degree of preferential solvation, were determined [227].

The low-spin Fe(II) complexes *trans*- $\text{FeQ}(\text{MeCN})_2$ (Q = (86), (87), (88)), have been prepared by reaction of the parent Fe(oximate)₂ complexes with BF_3 . The axial ligands could be

substituted to give *trans*-FeQLL' (L,L' = 1-methylimidazole, pyridine, PBU₃, CO, P(Obu)₃, Me₃CNC). Their MLCT spectra and rate constants for axial ligation are similar to the parent Fe(dioxH)₂LL' (dioxH₂ = dimethylglyoxime, naphthoquinine dioxime, benzoquinine dioxime) complexes; however the Fe(II)/Fe(III) oxidation potential is 500mV greater. The kinetic data for the MeCN derivatives in MeCN and toluene are compared with other FeN₄ complexes [228].

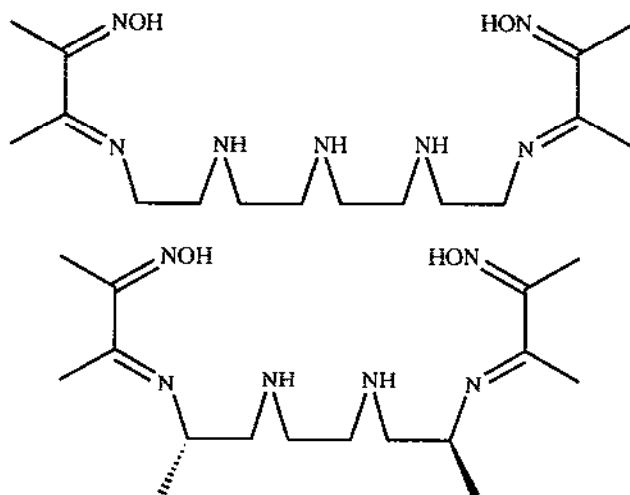
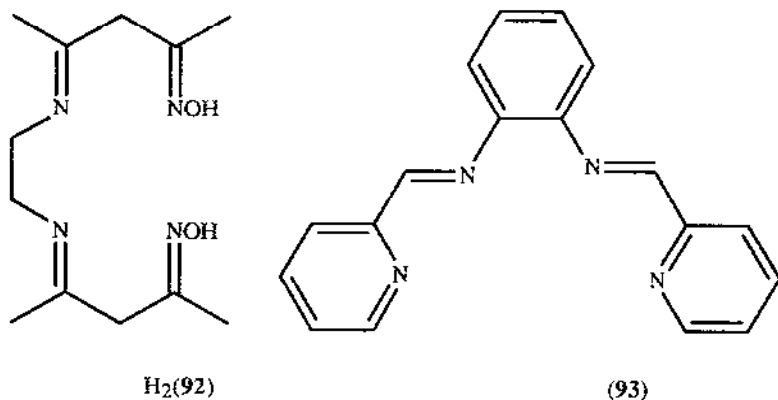
The structures of the clathrochelate complexes Fe(II)(89) (R = OH, F, alkyl, alkoxy; X = F, OH, OMe, OEt, OBu, OPh) were deduced by Mössbauer spectroscopy and one crystal structure. The complexes were characterised by ¹H, ¹³C and ¹¹B NMR spectroscopy, and IR and UV-visible spectroscopy. The coordination geometry around the iron is a distorted trigonal prism, with distortion angles of 20 - 30°. The closure of the macrobicycles by the capping boron atoms results in a change of various physical properties ascribable to the macrocyclic effect; these include a decrease in the Mössbauer isomer shift, increased Debye temperature, and increased extinction coefficients and narrower linewidths for the MLCT transitions [229].



(RC=NOH)₂ = dimethylglyoxime, (86)
 (RC=NOH)₂ = benzoquinone dioxime, (87)
 (RC=NOH)₂ = naphthoquinone dioxime, (88)

Fe(89)

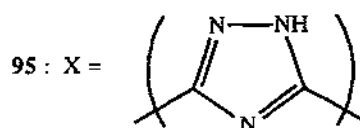
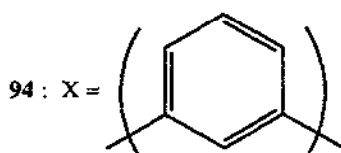
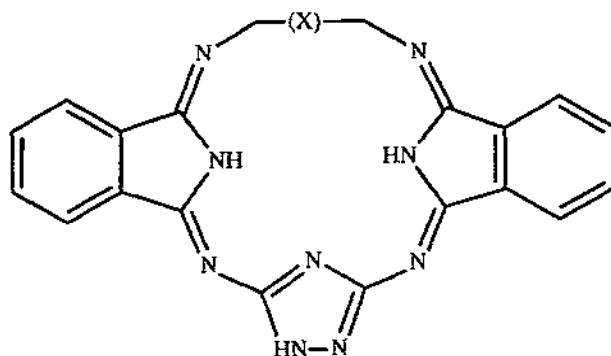
The redox reactions of Fe(II)(90) with [Co(III)(EDTA)]⁻ and [Co(III)(phen)₃]³⁺, and between [Fe(III)(90)]⁺ and [Co(II)(phen)₃]²⁺, were studied at various pH values and with constant ionic strength; the second-order kinetics are discussed in some detail. The possibility of stereoselectivity in such electron-transfer reactions was investigated, by reacting the chiral complexes [Fe(91)]ⁿ⁺ (n = 0,1) with racemic [Co(phen)₃]^{m+} (m = 3,2). Selectivities of between 2% and 11% were found; the behaviour of these chiral iron complexes is compared with that of the isostructural Ni(III) and Ni(IV) complexes [230].

 $H_2(90)$ (top) and $H_2(91)$  $H_2(92)$ (93)

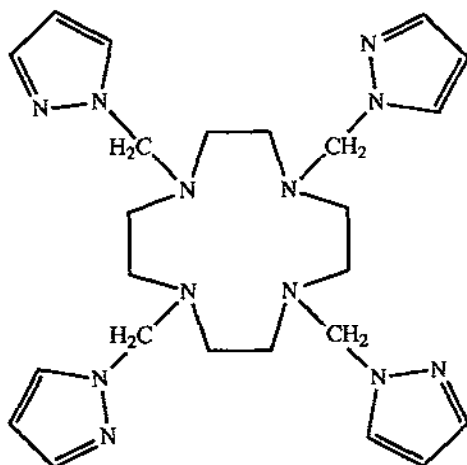
The octahedral Fe(III) complex $Fe(92)Cl \cdot H_2O$ was prepared and spectroscopically characterised [231]. A series of Fe(III) Schiff-base chelates was prepared from 2-pyridine-carboxaldehyde and *o*-, *m*-, or *p*-(H_2N) $_2C_6H_4$ in the presence of $FeCl_3$ (e.g. $[Fe(93)Cl_2]^+$); they were found to catalyse the epoxidation of alkenes by $PhIO$ [232].

1.6.3 Complexes with macrocyclic ligands

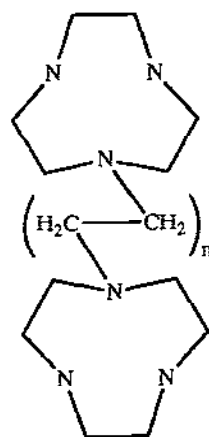
The macrocycles (94) and (95) have been prepared and their Fe(II) complexes characterised by IR and UV spectroscopy [233, 234].



Reaction of 1-hydroxymethylpyrazole with 1,4,7,10-tetraazacyclododecane gave the potentially octadentate ligand **96**, which reacts with FeCl_2 to give $\text{Fe}(\mathbf{96})\text{Cl}_2$. Spectroscopic characterisation suggests an FeN_6 coordination sphere in which two of the pyrazolyl ligands are uncoordinated [235]. The polyazamacrocycles 1,4,7,10-tetraaza-18-crown-6, pentaaza-15-crown-5 and hexaaza-18-crown-6, with ethyl or hydrogen substituents on the N-atoms, were prepared and covalently bound to silica gel via one of the N-atoms. The bound ligands have strong, selective



(96)

(97) ($n = 1$); (98) ($n = 2$)

interactions with soft heavy-metal cations and protons; these interactions are similar to those of the unbound macrocycles. The silica-bound ligands can separate part-per-billion quantities of heavy-metal cations from large excesses of alkali and alkaline earth cations in water [236].

1,4,7-Triazacyclononane (tacn) and its derivatives are popular as tridentate face-capping ligands, in the same way as the trispyrazolylborate ligands mentioned earlier. The complexes $[(\text{tacn})_2\text{Fe}(\text{III})_2(\mu\text{-O})(\mu\text{-SO}_4)_2]$, $\{(\text{tacn})_2\text{Fe}(\text{III})_2(\mu\text{-O})(\mu\text{-SO}_3)_2\}$ and $\{(\text{tacn})_2\text{Fe}(\text{III})_2(\mu\text{-O})(\mu\text{-SeO}_3)_2\}$ are sulphato-, sulphito- and selenito-bridged analogues of the $(\mu\text{-O})(\mu\text{-carboxylato})_2$ -bridged binuclear Fe(III) complexes used as enzyme active site models. All three complexes have been structurally characterised, and all show strong antiferromagnetic couplings. The tris-sulphato bridged complex $[(\text{tacn})_2\text{Fe}(\text{III})_2(\mu\text{-SO}_4)_3]$ has also been prepared; the antiferromagnetic exchange is very weak, as would be expected in the absence of a μ -oxo bridge [237].

The heterobinuclear complex $[(\text{tacn})\text{Fe}(\text{III})(\mu\text{-O})(\mu\text{-OAc})_2\text{Ru}(\text{Me}_3\text{tacn})][\text{PF}_6]$ ($\text{Me}_3\text{tacn} = \text{N},\text{N},\text{N}'$ -trimethyl-1,4,7-triazacyclononane) was prepared from $\text{Fe}(\text{tacn})\text{Cl}_3$, $\text{Ru}(\text{Me}_3\text{tacn})\text{Cl}_3$ and sodium acetate in methanol, and has been structurally characterised. Magnetic susceptibility measurements show an $S = 2$ ground state, which is consistent both with an Fe(IV)-Ru(II) formulation and a strongly antiferromagnetically coupled Fe(III)-Ru(III) formulation. However the electronic, ESR and Mössbauer spectra unequivocally support the latter formulation [238].

The low-spin Fe(III) complex $[\text{Fe}(\mathbf{97})]\text{Br}_3 \cdot 4\text{H}_2\text{O}$ has been structurally characterised. The Fe centre is in a distorted trigonal prismatic N_6 environment [239]. By contrast the ligand (**98**), with a four-carbon chain between the two face-capping macrocycles, forms $[\text{Fe}(\text{III})_4(\mathbf{98})_2\text{O}_2(\text{OAc})_4][\text{PF}_6]_4$ and the solvated analogue $\{[\text{Fe}(\text{III})_4(\mathbf{98})_2\text{O}_2(\text{OAc})_4][\text{PF}_6]_4 \cdot 2\text{MeCN}\}$, both of which have the structure depicted in Figure 1 [240].

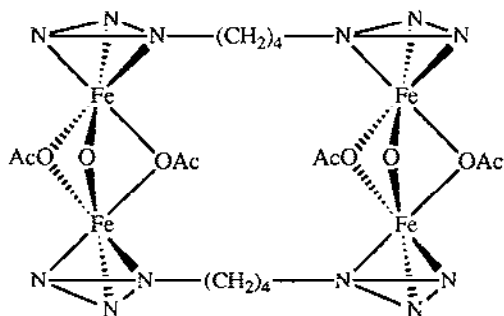
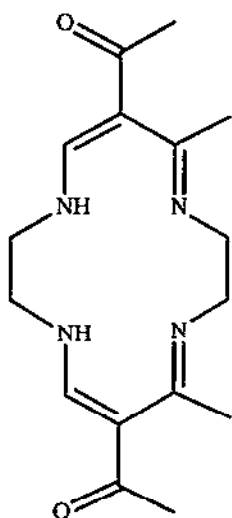
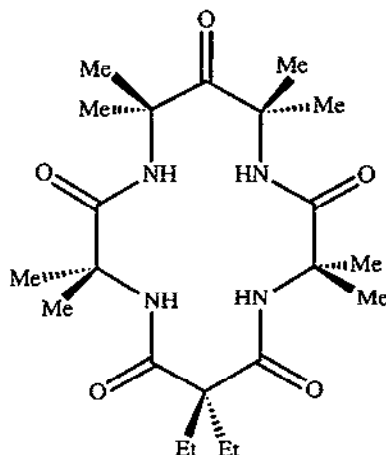


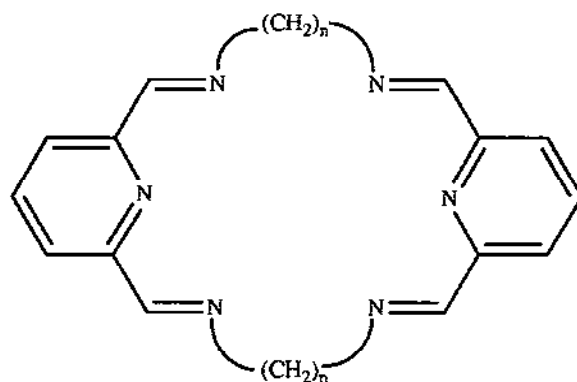
Figure 1 : Schematic diagram of $[\text{Fe}(\text{III})_4(\mathbf{98})_2\text{O}_2(\text{OAc})_4][\text{PF}_6]_4$

$[\text{Fe}(\text{III})(\mathbf{99})]^+$, which has a hemine-like coordination environment, tends to form neutral, covalent monoadducts $\text{Fe}(\mathbf{99})\text{X}$ by axial ligation of X^- ($\text{X} = \text{F}, \text{Cl}, \text{Br}, \text{I}, \text{NCS}$). With a variety of other neutral or anionic ligands, octahedral low-spin diadducts are preferred. This behaviour was examined in H_2O and CHCl_3 [241]. $[\text{Fe}(\mathbf{100})\text{Cl}]^+$ contains iron in the 4+ oxidation state. It has a

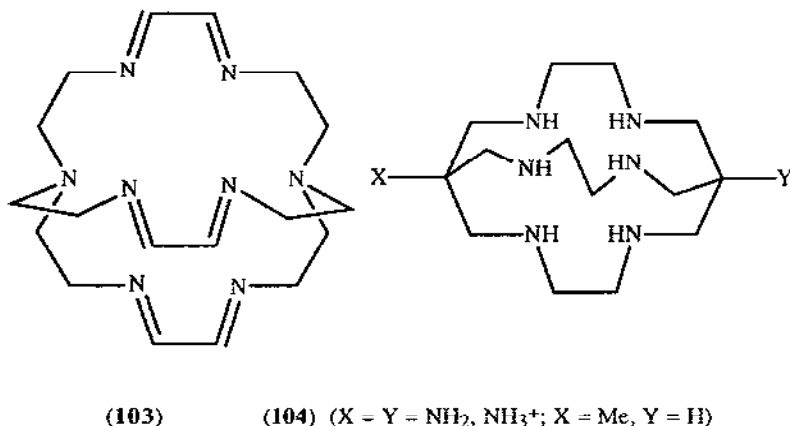
square pyramidal structure, with the Fe(IV) centre slightly above the plane of the four amide nitrogen atoms. Mössbauer spectroscopy confirmed the oxidation state, and the complex shows an irreversible Fe(IV)-Fe(III) reduction at a low potential [242].

H₂(99)H₄(100)

The macrocycles **101** and **102** were used to prepare binuclear, thiocyanato-bridged complexes of some first-row transition-metal ions including Fe(II). The thiocyanate adopts the unusual $\eta^1\text{-}\mu_2\text{-N}$ bridging mode. Magnetic susceptibility measurements suggest that the thiocyanate bridge is poor at mediating magnetic exchange processes [243].

(101) ($n = 3$); (102) ($n = 4$)

The sepulchrate (**103**) was prepared by [2+3] condensation of tris(2-ethylamino)amine with glyoxal using a group IIa template ion. The Fe(II) complex is diamagnetic [244]. Complexes of a series of first-row transition metal ions with electronic configurations from $3d^1$ to $3d^{10}$ with the sepulchrates (**104**) were examined magnetically. The Fe(III) complexes are low-spin, whereas the Fe(II) complexes are either low or high-spin depending on the ligand apical substituent; they should thus be good systems for studying spin-equilibria [245].



1.6.4 Miscellaneous N-donor complexes

An unusual 2-coordinate Fe(II) complex $\text{Fe}[\text{N}(\text{Mes})(\text{B}[\text{Mes}]_2)]_2$ ($\text{Mes} = 2,4,6$ -trimethylphenyl) has been prepared, in which the borylamide ligand is highly sterically hindered. The N-Fe-N angle is 166.6° ; the deviation from linearity is attributed to the tendency of the electron-deficient metal centre to seek electron density from the aromatic ligand substituents. The complex was further characterised by electronic and NMR spectroscopy, and magnetic moment measurements [246]. Table 2 summarises the remaining complexes with N-donor ligands.

1.7 COMPLEXES OF TETRAPYRROLE MACROCYCLES

1.7.1 Phthalocyanines

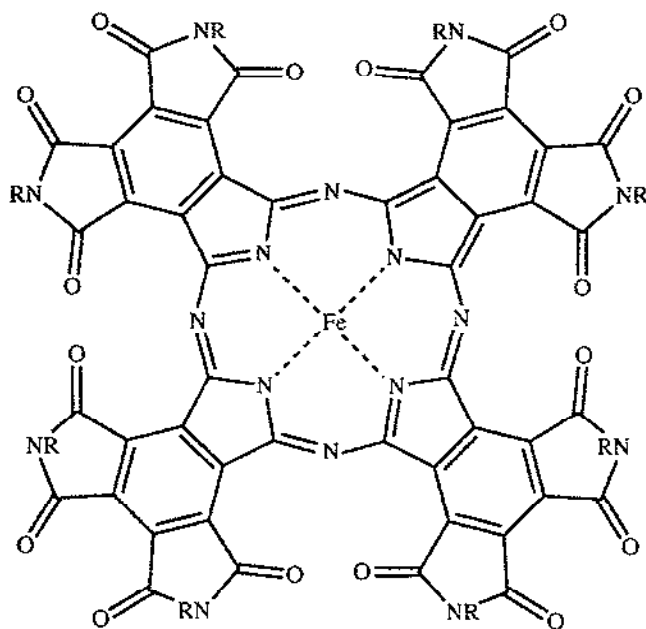
Three polymeric Fe(II) phthalocyanine (FePc) complexes were prepared by reaction of FePc with the bridging ligands 4,4'-bipyridine, *trans*-1,2-bis-(4-pyridyl)ethene and 1,2-bis-(4-pyridyl)ethane. Their IR and electronic spectra are discussed in comparison to FePc and FePcL_2 ($\text{L} = \text{pyridine}, 4\text{-cyanopyridine}$) and are shown to depend on the degree of π back-donation [254]. Similarly, FePc was polymerised by reaction with pyrazine, 4,4'-bipyridine, *trans*-1,2-bis-(4-pyridyl)ethene, 1,2-bis-(4-pyridyl)ethane and 1,3-bis-(4-pyridyl)propane in a separate study;

magnetic, electrical conductivity and compressibility studies were performed and the crystal-field splitting parameters determined [255]. Since many such polymeric complexes are insoluble in organic solvents, new FePc derivatives containing a *tert*-butyl or two 2-ethyl-*n*-hexyl groups on each phenyl ring have been prepared. These may be converted to the normal polymers with a variety of bridging ligands, but are soluble in organic solvents. The polymeric structures were confirmed by Mössbauer and NMR spectroscopy and thermogravimetric analysis [256]. FePc reacts with imidazole in two consecutive first-order processes to give the octahedral bis-axially coordinated adduct [257].

Table 2 : Complexes with N-donor ligands (N = oxidation state of Fe)

<u>N</u>	<u>Ligand</u>	<u>Studies performed</u>	<u>Ref</u>
3	2-acetylpyridine hydrazone	IR, proton NMR, ESR, X-ray powder diffraction, conductivity	[247]
3	2-acetylpyridine thiosemicarbazone	Spectroscopic & thermal properties; antifungal activity	[248]
2	Diiminosuccinonitrile	Reaction of unstable iron(II) complex with ether; crystal structure of product	[249]
2, 3	Schiff bases formed from isatin and amino acids	IR and electronic spectra, magnetic moments	[250]
3	3,4-diaminobenzene sulphonic acid	Electronic spectra, stability constant measurements	[251]
2	Polyaminoamides, from condensation of EDTA with $\text{H}_2\text{NCH}_2\text{CH}_2\text{NH}_2$ and $\text{H}_2\text{NCH}_2\text{CH}_2\text{NHCH}_2\text{CH}_2\text{NH}_2$	Oxidation kinetics	[252]
2	Ethylene diamine	Formation kinetics	[253]

The perchlorinated complex $\text{Fe}(\text{III})\text{L}$ (H_2L = hexadecachlorophthalocyanine) was prepared from tetrachlorophthalic acid and urea in a template reaction with FeCl_2 . Its magnetic properties are similar to those of unsubstituted FePc . The electrochemistry at a highly-oriented pyrolytic graphite electrode shows a metal-centred oxidation, and a pH-dependent reduction which is thought to be ligand-centred. The IR spectra, electronic spectra, spectroelectrochemistry and electrocatalytic oxygen-reduction behaviour are discussed [258]. The $\text{Fe}(\text{III})$ complex of a tetrasulphonated phthalocyanine can displace the heme group from the active site of horseradish peroxidase; the process was monitored by electronic spectroscopy. Circular dichroism spectroscopy shows that the helical content of the protein remains much the same; i.e. the structure of the enzyme is preserved. The $\text{Fe}(\text{II})$ form, produced by reduction of $\text{Fe}(\text{III})$ by dithionite, reversibly binds O_2 but in other respects has minimal enzymic activity [259].

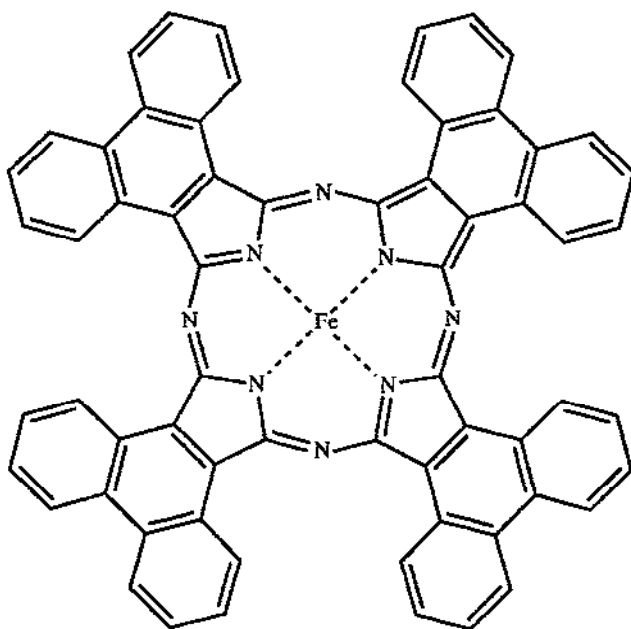


$\text{R} = \text{H}$, $\text{Fe}(\text{105})$; $\text{R} = \text{C}_{10}\text{H}_{21}$, $\text{Fe}(\text{106})$

$\text{Fe}(\text{105})$ and $\text{Fe}(\text{106})$ have unusual electronic spectra, showing strong hypochromism in the Q-band region compared to FePc . $\text{Fe}(\text{106})$ is capable of 4-electron reduction of O_2 to water in neutral and alkaline media [260].

FePc may be doubly oxidised to FePcCl_2 , in which the $\text{Fe}(\text{II})$ is oxidised to $\text{Fe}(\text{III})$ and the Pc dianion is oxidised to a radical monoanion. The crystal structure is similar to the parent FePc , but with a slightly shrunken N_4 square core and shorter $\text{Fe}-\text{Cl}$ bonds than for $\text{Fe}(\text{II})$ analogues

[261]. Mössbauer spectroscopy was used to study the synthesis of FePc within NaY zeolite [262].



Fe(107)

The iron(II) complex of 9,10-phenanthrophenocyanine, Fe(107), was prepared by a template reaction of 9,10-dicyanophenanthrene with $\text{Fe}(\text{CO})_5$ in 1-chloronaphthalene. It has similar spectroscopic and electrochemical properties to the analogous 1,2-naphthalocyanine and Pc complexes, and reacts with isocyanides RNC ($\text{R} = \text{CMe}_3$, cyclohexyl, PhCH_2 , Me_2Ph) to form axially substituted diadducts. Fe(107) also reacts with 1,4-diisocyanobenzene to give a linear polymer [263].

Fe(II) complexes of a series of fourteen Pc derivatives containing various electron-releasing substituents were studied by Mössbauer spectroscopy. The δ and ΔE_Q values were used to determine σ - and π - bonding parameters for each complex, which correlate well with the the sum of the Hammett σ -values of the substituents on the Pc backbone [264].

1.7.2 Porphyrins

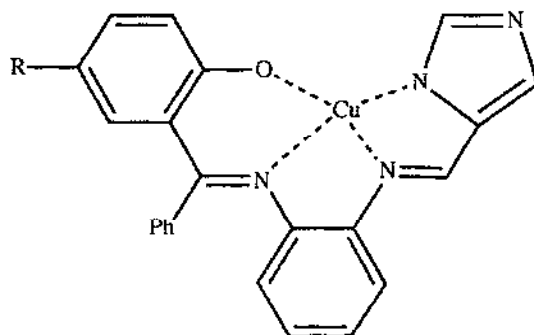
The interest in iron porphyrin complexes continues unabated, principally as models for heme proteins. For convenience this section is split into three parts: studies on complexes where the presence or behaviour of axial ancillary ligands is of particular interest; oxygen, peroxide and

superoxide complexes as enzyme models; and 'miscellaneous', which covers spectroscopic and magnetic studies, catalytic activity, and a few unusual new compounds.

1.7.2.1 Axially ligated porphyrin complexes

The study of the behaviour and effects of ancillary axial ligands in iron porphyrin complexes is crucial to understanding how heme proteins work, since wide variations in the biological roles of different heme proteins are intimately associated with changes in axial ligation at the heme site.

The novel trinuclear complex [(108)-Fe(TPP)-(108)]⁺, in which an Fe(III)-TPP core (TPP = *meso*-tetraphenylporphyrin) core is bis-axially coordinated to two Cu(II) complexes *via* imidazole bridges, has been structurally characterised and examined by magnetic susceptibility and Mössbauer measurements. The analogous Cu(II)-Fe(II)-Cu(II) and Ni(II)-Fe(III)-Ni(II) complexes have also been prepared, in order to study the behaviour of the bis-Cu(II) and the Fe(III) paramagnetic systems in isolation. In the former, where the Fe(II) centre is diamagnetic, there is antiferromagnetic coupling between the two Cu(II) centres below 20K. In the latter, where the Ni(II) centres are diamagnetic, the magnetic and Mössbauer properties are consistent with an S=1/2 Fe(III) centre. The parent Cu(II)-Fe(III)-Cu(II) complex has a susceptibility at 300K which is the sum of the two analogues, but shows ferromagnetic Fe-Cu coupling at lower temperatures [265].



(108) : R = Cl. (109) : R = H

The 'capping' of a porphyrin (Figure 2; the phenyl rings are in the *meso* positions) prevents dimerisation at the capped face whilst allowing a substrate to bind within the cavity formed by the blocking group. The effects of the capping benzene ring on axial ligation were examined. It was found that the rigid *meso*-phenyl groups also obstruct the face opposite the cap, so that axial ligation at both sites is hindered; for example, [Fe(II)(cap)(amine)₂] complexes could only be formed with small, flexible amine ligands, and [Fe(cap)Cl] would not easily bind axial imidazole ligands. [Fe(III)(cap)][ClO₄], having only a weakly coordinating anion, reacts with one equivalent of the Cu(II) complex (109) to give an adduct which is proposed as a model for the imidazole-bridged Fe-Cu site of cytochrome c oxidase [266].

$\text{Fe(II)}(\text{TPP})\text{L}$ ($\text{L} = 1\text{-vinyl}, 1\text{-benzyl}, 1\text{-methyl}, 1\text{-acetyl}$ or $1\text{-trimethylsilylimidazole}$) were prepared and characterised by Mössbauer and electronic spectroscopy. For $\text{L} = 1\text{-vinylimidazole}$ and 1-benzylimidazole the crystal structures of the adducts have been determined. Both complexes have crystallographic inversion centres at the Fe(II) , which means that the two bound imidazoles must be parallel. Comparison of these two structures with several analogous Fe(III) complexes shows similar trends in the orientation of the axial L groups; a possible electronic reason for this

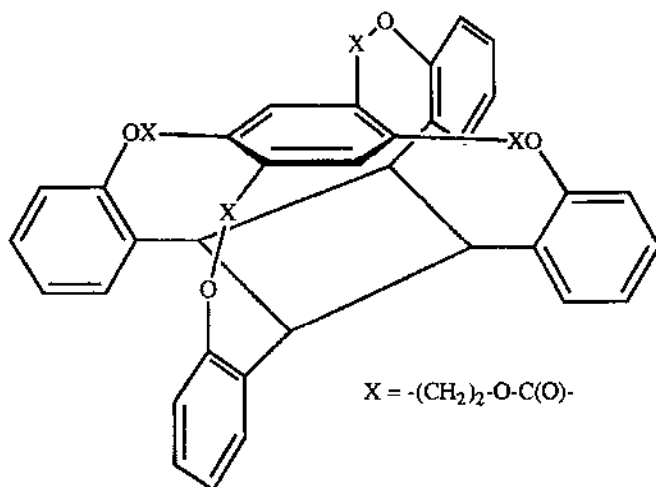
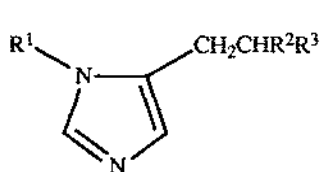


Figure 2 : Schematic diagram of the 'capped' porphyrin complex $\text{Fe}(\text{cap})$

behaviour is discussed [267]. In contrast, Mössbauer spectroscopic studies showed that two equivalents of the histidine derivatives (110)-(113) bind to the Fe(III) complex of protoporphyrin IX (PPIX) such that the imidazole rings are *not* parallel. Cytochrome b is known to contain two axial histidine residues at the heme site so these complexes were studied as possible models. The axial ligands bind as sterically hindered imidazoles, with weak Fe-N bonds; the Mössbauer parameters for these complexes are similar to those for the low-spin Fe(III) cytochromes. The imidazole plane orientations are thought to be influenced by the steric strain introduced by the histidine side-chains, and by electrostatic interactions between charged side-chain groups and the pendant propionate groups on the porphyrin skeleton [268, 269]. The Mössbauer properties of the complex with (110) as axial ligands were shown to be sensitive to intermolecular H-bonding between the amino side-chain and the imidazole NH , which affects the ligand's electronic properties [269].

The crystal structure of $[\text{Fe(III)}(\text{TPP})(\text{MeIm})_2][\text{ClO}_4]$ ($\text{MeIm} = 1\text{-methylimidazole}$) shows that the axial imidazoles are nearly (but not quite) coplanar. This is quite unusual since axial imidazoles are often precisely parallel due to crystallographically imposed inversion symmetry (as in ref. 267). There is a rhombic distortion of the FeN_4 core, resulting in a characteristic ESR spectrum from which crystal field parameters could be determined [270].



110 : $R^1 = H, R^2 = NH_2, R^3 = CO_2H$ (Histidine)

111 : $R^1 = H, R^2 = NHC(O)Me, R^3 = CO_2H$
(N-acetylhistidine)

112 : $R^1 = R^3 = H, R^2 = NH_2$ (Histamine)

113 : $R^1 = Me, R^2 = CH_2OH, R^3 = CH(Et)CO_2H$
(Pilocarpate)

(PPIX)Fe(thf)₂ is a rare example of a high-spin octahedral Fe(II) porphyrin complex, with the Fe(II) probably in the N₄ plane (in high-spin complexes the Fe is normally slightly out of the plane). The Mössbauer spectrum of the complex in frozen solution is very similar to that of the TPP analogue, which is also high-spin. The quadrupole splitting values are affected by the porphyrin basicity [271].

The axial ligation of [(X₄TPP)FeCl] (X₄TPPH₂ = *meso*-tetrakis[4-X-phenyl]porphyrin; X = Cl, H, Me, OMe) by imidazole, 2-methylimidazole and 2-ethyl-4-methylimidazole was studied kinetically as a function of temperature. Imidazole and 2-methylimidazole bind twice to give six coordinate complexes; the 4-ethyl-2-methylimidazole binds only once to give a five coordinate complex. Electron-donating *para* substituents on the phenyl rings increase electron density at the pyrrole nitrogen atoms, and so slow down adduct formation. Mechanisms for these processes are proposed based on the kinetic measurements [272].

In an effort to quantify σ - and π -bonding effects in axial ligand binding to Fe-porphyrin complexes, the binding constants between (PPIX)Fe(II) and various substituted pyridines and imidazoles were determined by spectrophotometric titration. Mössbauer spectroscopy was also employed. Both techniques show that bis-axial, octahedral low-spin complexes are formed by all ligands with the exception of pyridine-N-oxide. The binding constants increase linearly with the ligand pK_a, and are also related to the Mössbauer quadrupole splitting values [273].

The five co-ordinate 2-methylimidazolato and six co-ordinate (imidazole)(imidazolato) adducts of the 'picket-fence' Fe(II) complex of *meso*-tetrakis(*o*-pivalamidophenyl)porphyrin have been prepared and structurally characterised. In the monosubstituted complex, the 2-methylimidazole lies within the picket-fence cavity and the Fe(II) centre is high-spin. In the six co-ordinate disubstituted complex it is probable that the deprotonated imidazolato resides within the cavity, and that the Fe(II) centre is low-spin [274]. The Fe(III) complex of the same picket-fence porphyrin was reacted with nitrite to give low-spin [Fe(NO₂)₂L]⁺, whose structure has been determined. One nitrite is N-bound within the picket-fence cavity; the other is on the open face of the complex, and is shielded by formation of a tight ion-pair with the bulky cation [K(18-crown-6)(H₂O)]⁺. The complex was also studied by IR, NMR, ESR and electronic spectroscopy. The intermediate mono-nitro complex is high-spin; the association constants for the formation of the mono and bis-nitro complexes are reported as a function of the cation [275]. This behaviour is in direct contrast to that observed when nitrite reacts with the Fe(III) complexes of the 'unhindered' porphyrins TPP, OEP (H₂OEP = octaethylporphyrin) and TTP (H₂TTP = *meso*-tetrakis[*p*-tolyl]porphyrin). In these cases the initial nitro complexes react further with nitrite in solution by an oxygen-transfer reaction, to give nitrosyl complexes as the ultimate products [276]. This secondary

reaction is prevented in the previous example by the picket-fence barrier on one face of the complex and ion-pairing with the bulky cation on the other.

The Fe(II) complex of *meso*-tetrakis-(2,6-bis-pivaloyloxyphenyl)porphyrin is a bis-fenced complex with four pivaloyloxy groups protecting each face. Axial ligation of various imidazoles is considerably depressed compared to Fe(TPP); the mono-substituted complex binds oxygen reversibly at 25°C [277]. Replacement of one bulky pivaloyloxy group by a hydroxy group reduces the steric hindrance at one face sufficiently to allow easy formation of a 1,2-dimethylimidazole complex, which also forms a dioxygen complex at 25°C [278].

The series of Fe(II) basket-handle porphyrin complexes depicted in Figure 3 was used to investigate the effects of steric hindrance on CO and O₂ binding to heme models. The basket-handle is constrained to lie centrally across the porphyrin face by the bulky pivalamido groups. With the free face of the complex occupied by an axial 1-methylimidazole ligand, the binding of CO and O₂ to the hindered face was made successively more difficult by decreasing the length of the basket-handle. It was found that the free energy changes (ΔG) are nearly identical for CO and O₂, so no steric discrimination occurs, but the relative contributions of ΔH and ΔS associated with the ligand binding are very different for the two substrates. The reaction profiles and kinetics are discussed in detail [279]. A similar attempt to produce a heme model capable of discrimination between CO and O₂ was made by using the cross-strapped Fe(II) porphyrin complexes depicted in figure 4. The shorter C₇ chain is 'crushed' under the longer C₁₄ or C₁₈ chain. With the free face

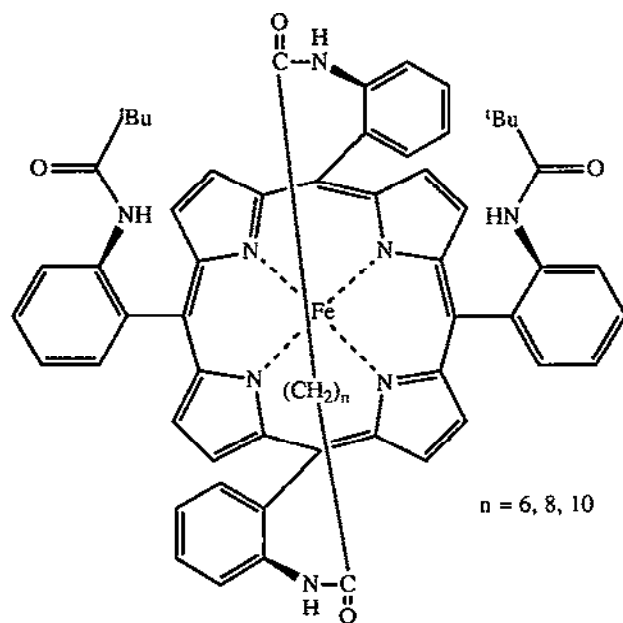


Figure 3 : A series of basket-handle porphyrins with sterically hindered faces

occupied by 1,2-dimethylimidazole, the complexes bind O_2 and CO reversibly at $20^\circ C$; the adducts have been spectroscopically characterised. The binding affinities are discussed in terms of the polar effect of the amide groups, H-bonding of the amide groups to O_2 and the steric effects of cavity size [280].

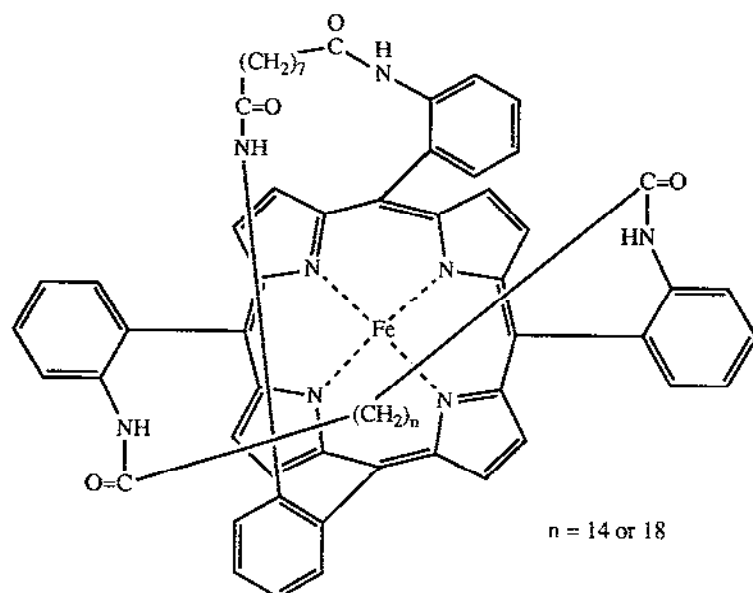


Figure 4 : Cross-strapped Fe(II)-porphyrin complexes as heme models

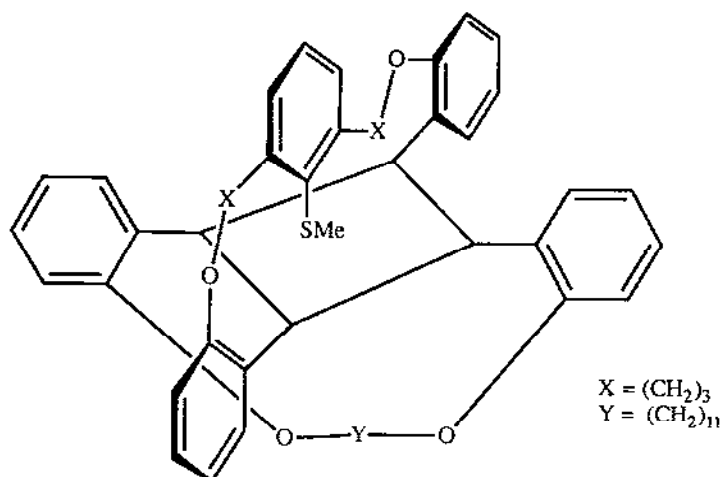


Figure 5 : A Bis-basket-handled porphyrin as a cytochrome c model

Two *bis*-basket-handle Fe(III) porphyrin complexes have been prepared, similar to those in Figure 3 but with a handle across each face of the complex. The handles consist of saturated C₁₂ chains, anchored at the ortho positions of the *meso*-phenyl rings by etheric or amide linkages. Their conversion to mono- and di-hydroxy derivatives in DMSO/water was studied by potentiometric and spectrophotometric methods, and the stability constants of the resulting complexes determined. Kinetic and thermodynamic factors affecting the formation of these hydroxo complexes are discussed [281]. A similar *bis*-basket-handled porphyrin (Figure 5) was prepared as a model for cytochrome c; the -SMe group held in place by one of the handles overcomes the normally poor binding of thioethers to iron. The enforced coordination of the axial SMe group and the hydrophobic environment of the imidazole are both characteristics of cytochrome c, and consequently the Fe(II) and Fe(III) complexes show spectroscopic and electrochemical properties similar to those of the native protein [282].

The Fe(III) complex of an N-methylated porphyrin, [Fe(NTTP)Cl]⁺ (NTTP = N-methyl-tetratolylporphyrin), has been structurally characterised. The Fe(III) has approximately square-pyramidal geometry, with the chloride at the unique apex. The N-methyl group is directed to the face opposite the chloride; as a result of the asymmetry induced by this group the macrocyclic core is considerably distorted from planarity. Several six-coordinate, low-spin complexes with strong-field ligands (cyanide, imidazole, substituted imidazoles) have been spectroscopically characterised. This indicates that the sterically hindering methyl group does not prevent addition of axial ligands on the same face of the complex; however the rotation of imidazoles about the Fe-N bond is prevented, which renders all of their ring protons inequivalent by NMR spectroscopy. Various synthetic procedures are described [283]. The asymmetric dimer [(NTTP)Fe(III)-O-Fe(III)(TPP)]⁺ (NTTP = N-methyl-tetraphenylporphyrin), has also been structurally characterised. The Fe(III) in the methylated porphyrin is again in a distorted square pyramidal environment; the coordination environment of the other Fe(III) is normal. The Fe-O-Fe linkage is bent, with an angle of 165.4° [284].

The orientation and axial rotation of axial ligands has significant effects on the NMR spectra of heme proteins. These effects have been studied in the Fe(III) complexes of Am-TPP, a derivative of TPP in which one phenyl ring has a bulky dialkylamido substituent at the ortho position to hinder partially one face of the complex. The substituents used are R-C(O)- (R = NMe₂, 3-azabicyclo-[3.2.2]nonane). In the low-spin complexes [Fe(III)(Am-TPP)(NMeIm)₂]⁺, the dialkylamide group prevents one of the axial N-methylimidazole ligands from rotating freely and locks it into one orientation at low temperatures. The NMR spectra show a novel pattern for the pyrrole protons and an unusually large spread of signals [285].

Fe(III) complexes of TTP with axial 1-adamantyl, 4-camphane and *tert*-butyl ligands were prepared and characterised by NMR spectroscopy. The paramagnetic NMR spectral patterns are compared with those of similar complexes containing axial aliphatic amines. Reaction with O₂ in toluene at -70°C gives a mixture of three products; (TTP)Fe(III)OH, (TTP)Fe(III)OFe(III)(TTP) and the alkyl peroxy complexes (TTP)Fe(III)(OOR). These last complexes are of interest with regard to the mode of action of peroxidases, lipoygenases and other enzymes in which Fe-catalysed O-O cleavage occurs. The absence of an α-hydrogen atom on the tertiary alkyl groups prevents thermal

decomposition to $(TTP)Fe(III)OH$ and $R_2C=O$, allowing the peroxo complexes to be detected by NMR. Treatment of $(TTP)Fe(III)(OOR)$ ($R = 4\text{-camphyl}$) with pyridine at $-70^\circ C$ gives $(TTP)Fe(IV)=O$ by homolysis of the O-O bond [286]. $Fe(III)$ complexes of protoporphyrin IX dimethylester and various *meso*-tetra-arylporphyrins with axial nitrophenoxide or nitrothiophenoxide substituents have also been examined by NMR spectroscopy, in order to identify specific features of the spectra which may help in assigning the spectra of other heme proteins and model systems. ArS^- and ArO^- coordination were studied since some mutant hemoglobins have axial tyrosinate ligands at the heme site. The change from ArS^- to ArO^- coordination gives different spectral characteristics for both the axial ligands and the substituents on the porphyrin skeleton; the axial ligand resonances were assigned fully. The relaxation of the aryl protons in the complexes of tetraarylporphyrins does not follow the simple r^{-6} fall-off expected for the effect of the paramagnetic centre, so other ligand-centred relaxation processes must be occurring. On the basis of these results, some low-field resonances in the spectra of mutant hemoglobins have been assigned [287].

The $Fe(IV)=O$ intermediate in various heme protein catalytic cycles is thought to be stabilised by axial anionic ligands. Accordingly the reactions of $[Fe(III)(OEP)(OMe)]$ with phenols, thiols and carboxylic acids were monitored spectrophotometrically. It was found that increased acidity of the substrates ROH and RSH correlates with a higher stability constant for the adduct. The high-spin five coordinate products were studied by resonance Raman spectroscopy; the porphyrin-Fe CT band maxima are a linear function of ligand pKa. The electronic spectra show a hypsochromic shift with increasing ligand pKa [288].

The reaction of O_2 with $Fe(III)$ complexes of TTP containing axially coordinated aryl groups has been studied by 1H NMR and ESR spectroscopy. Reaction of $Fe(TTP)(p\text{-}C_6H_4CH_3)$ with O_2 in toluene at room temperature produces principally the phenoxide complex, whereas at $-60^\circ C$ in chloroform no phenoxide formation is detected. Instead the main products are $[Fe(IV)(TTP)(p\text{-}C_6H_4CH_3)]^+$ and $Fe(III)(TTP)Cl$; on warming, the $Fe(IV)$ -aryl complex converts to the $Fe(III)$ -N-arylporphyrin complex. Mechanisms for these reactions are suggested [289]. The syntheses of the first alkyl and aryl-bridged binuclear $Fe(III)$ porphyrin complexes are described; these are of interest since σ -bonded alkyl and aryl porphyrin complexes are possible intermediates in the catalytic cycle of cytochrome P450. For example, $Fe(III)(TPP)Cl$ reacts with half an equivalent of 1,4-dilithiobutane or 1,4-dilithiobenzene to give the corresponding bridged dimers which were detected by NMR spectroscopy. Both of these react with O_2 at room temperature to give binuclear μ -oxo-bridged $Fe(III)$ complexes. By contrast the analogous dimeric complex with *meso*-tetrakis-(pentafluorophenyl)porphyrin $(F_{20}TPP)Fe-C_6H_4-Fe(F_{20}TPP)$ is stable to both CO and O_2 at room temperature [290].

An NMR spectroscopic study on the synthesis and reactivity of σ -alkyl $Fe(II)$ -porphyrin complexes has been carried out. Reaction of $(TPP)Fe(III)Cl$ with $LiHBEt_3$ in CH_2Cl_2 yields $(TPP)Fe(III)Et$; reduction to $\{(TPP)Fe(II)Et\}^-$ may be accomplished, with concomitant rapid electron exchange between the $Fe(II)$ and $Fe(III)$ alkyl complexes. The (paramagnetic) $\{(TPP)Fe(II)Et\}^-$ is reoxidised by O_2 [291]. CO inserts into the Fe-C bond of σ -alkyl porphyrin complexes, which were in turn produced from the reaction of electrochemically generated $Fe(0)$ and $Fe(I)$ complexes

Table 3 : Summary of some axially ligated iron-porphyrin complexes (N = iron oxidation state)

N	Porphyrin ligand	Studies performed	Ref
3	Various	Monomeric monohydroxo-iron(III) complexes of 'fenced' porphyrins detected by Mössbauer spectroscopy; the fences prevent the expected formation of oxo-bridged dimeric species	[293]
3	TPP	Formation of the low-spin ammonia adduct $[\text{Fe}(\text{TPP})(\text{NH}_3)_2]^+$ in non-aqueous solution; characterisation by electronic, NMR, ESR and Mössbauer spectroscopy	[294]
3	Pheophytin a, pheophytin b	Autoreduction of FeLCl to $\text{FeL}(\text{py})_2$ in the presence of pyridine and derivatives. Donor and acceptor properties of the axial ligands examined by Mössbauer spectroscopy	[295]
2,3	TPP, TMP, OEP	Intermolecular nitrosyl transfer between neutral and oxidised Fe and Co metalloporphyrin complexes followed by spectroelectrochemistry	[296]
2	<i>meso</i> -tetrakis- $\{o\}$ -[4-dimethylaminobutylamido-phenyl]triphenylporphyrin	Formation of $\text{FeL}(\text{CO})$ and $[\text{FeL}(\text{NO})]^+$; characterisation by electronic, MCD and ESR spectroscopy and cyclic voltammetry. The nitrosyl ligand weakens the <i>trans</i> bond between the $\text{Fe}(\text{II})$ and the coordinated amino group of the 'tail'	[297]
3	<i>meso</i> -tetrakis $\{o\}$ -[1-diethylamino]butylamido-phenyl]porphyrin	Electrochemical behaviour of $\text{Fe}(\text{III})$ complex; the coordinated terminal base in the 'tail' stabilises $\text{Fe}(\text{II})$. Solvent effects on redox properties	[298]
3	<i>meso</i> -tetrakis[2-(N-methyl)pyridyl]porphyrin	Formation of mono- and bis-hydroxo complexes; measurement of Fe-OH vibration frequencies, transition pH values, Fe-OH force constants. Resonance Raman, NMR, ESR spectroscopy	[299]
3	Protoporphyrin IX	Kinetics of axial addition of cyanide and imidazole with variation of temperature and pressure	[300]
3	TPP, TMP	Lability of various substituted imidazoles as a function of steric repulsion with the porphyrin ring; surprisingly, in all cases dissociation from $\text{Fe}(\text{TPP})$ is faster than from $\text{Fe}(\text{TMP})$	[301]
3	<i>meso</i> -tetrakis[2,4,6-trialkylphenyl]porphyrin	Thermodynamics of formation of axially substituted imidazole complexes; evidence for an attractive interaction between the <i>o</i> -alkyl substituents of the <i>meso</i> -phenyl rings and imidazole	[302]

Table 3 continued: Summary of some axially ligated iron-porphyrin complexes (N = iron oxidation state)

3	TPP	Reaction of Fe(TPP)Cl with various imidazoles to give [Fe(TPP)(Im) ₂ Cl]; enhancement of chloride dissociation rate in Fe(TPP)(Im)Cl due to steric strain caused by the <i>trans</i> -imidazole	[303]
3	TPP	Crystal structure of the bis-imidazole complex	[304]
3	Protoporphyrin IX	Mössbauer studies on bis-axial complexes with substituted imidazoles as cytochrome b models	[305]
3	Octaethylporphyrin	Crystal structure of Fe(OEP)(CH ₃ O) reveals weak dimeric interactions between porphyrin rings	[306]
3	<i>meso</i> -tetrakis[3,4,5-trimethoxyphenyl]porphyrin	Crystal structure of FeLCl - square pyramidal Fe(III) sitting slightly above N ₄ plane	[307]
2,3	<i>meso</i> -tetrakis[2,4,6-trimethoxyphenyl]porphyrin	Mössbauer studies on bis-axial pyridine and piperidine adducts of Fe(II) complex; mono-axial adducts of Fe(III) complex with iodide, bromide, chloride, hydroxide and azide	[308]
3	TMP	Formation and electronic spectroscopy of unusually stable sulphur adducts Fe(TMP)L ₁ L ₂ and Fe(TMP)L ₁ (HL ₁ = ethyl-3-mercaptopropionate, L ₂ = Lewis base)	[309]
3	TPP	Preparation of Fe(TPP)(NS), Fe(TPP)(SO ₂), Fe(TPP)(C ₅ H ₅) and Fe(TPP)(C ₅ H ₅)(NO); characterisation by IR and electronic spectroscopy	[310]
3	TPP	Crystal structure of [Fe(TPP)(Me ₂ PPh)]ClO ₄ , containing low-spin Fe(III)	[311]
2	TPP	Preparation and spin-states of Fe(TPP)(MeNC) _x (x = 1,2); adduct with dioxygen (for x = 1)	[312]
3	TPP	Kinetics and suggested mechanism of conversion of [(TPP)Fe] ₂ O to Fe(TPP)Cl	[313]
3	TPP	Oxidative cleavage of [(TPP)Fe] ₂ O with fluoride to give [Fe(TPP)F ₂] ⁺ ; electrochemistry and electrocatalytic oxidation of cyclohexane	[314]
3	<i>meso</i> -tetrakis[<i>p</i> -trimethylammonio-phenyl]porphyrin	Spectroscopic and magnetic studies on FeLi; pH dependent dimerisation. Kinetics of reaction between dimeric complex and axial ligands (imidazole, 1-methylimidazole, pyridine, histidine)	[315]

with alkyl halides. For example, reduction of $(\text{OEP})\text{Fe}(\text{III})\text{Cl}$ to $\text{Fe}(\text{I})$ at -1.6V in the presence of EtBr gives $[(\text{OEP})\text{Fe}(\text{II})\text{Et}]^+$. Oxidation of this to $\text{Fe}(\text{III})$ under CO gives $[(\text{OEP})\text{Fe}(\text{III})(\text{COEt})]$. Decomposition of the products is enhanced by the binding of CO to the resulting $\text{Fe}(\text{II})$ complex. Similar CO insertion does not occur in σ -aryl complexes [292].

Other work on axially-ligated iron-porphyrin complexes is summarised in Table 3 [293 - 316].

1.7.2.2 Complexes with oxygen, peroxides and superoxides

A model for cytochrome P_{450} is provided by the $\text{Fe}(\text{II})$ complex of a porphyrin which has three 'picket-fence' type *o*-pivalamidophenyl groups in *meso* positions, and a flexible 'tail' with a terminal thiolate ligand at the fourth *meso* position. The $\text{Fe}(\text{II})$ is in a six co-ordinate environment, with the thiolate 'tail' and a molecule of methanol in the axial positions. The presence of the thiolate ligand makes the complex a very efficient catalyst for O-O bond cleavage of hydroperoxides [317].

The $\text{Fe}(\text{III})$ complex of mesoporphyrin (IX) - mesoferriheme - has been examined as a peroxidase model. Two-electron oxidants such as hypochlorite react with two equivalents of mesoferriheme; this is a two-electron oxidation of a monomeric heme to give an $\text{Fe}(\text{V})\text{O}$ intermediate, followed by a rapid reaction with a second heme equivalent to give the dimeric product $\text{Fe}(\text{IV})\text{-O-Fe}(\text{IV})$. A competing side-reaction is oxidative degradation of the intermediate. The effects of various substituents on the porphyrin ring, which increase the tendency to dimerisation and therefore prevent degradation, are discussed. The $\text{Fe}(\text{IV})\text{-O-Fe}(\text{IV})$ dimer oxidises phenol in two distinct one-electron reactions, regenerating mesoferriheme [318]. Deuterioferriheme is also a good model for peroxidases. The $\text{Fe}(\text{IV})$ -oxo dimer intermediate (which is the species actually responsible for substrate oxidation) has been observed to decay slowly back to the starting $\text{Fe}(\text{III})$ complex even in the absence of substrates, although the reducing agent responsible for this is unknown. This regeneration of the starting complex has been examined by observing the recovery of optical density using stopped-flow spectrophotometry. Two parallel mechanisms appear to be operative. In the presence of excess initial oxidant (OCl^- , ClO_2^- , peroxyacids) some porphyrin ring degradation occurs [319].

The compounds $[\text{Bu}_4\text{N}][\{\text{Fe}(\text{p-Cl}_4\text{TPP})\}_2\{\text{Cu}(\text{MNT})_2\}_2] \cdot n\text{C}_6\text{H}_6$ ($n = 1, 2, 3$; $\text{p-Cl}_4\text{TPP}$ = *meso*-tetrakis[*p*-chlorophenyl]porphyrin; MNTH_2 = *cis*-1,2-dicyanoethylenedithiol) are proposed as models for the active site of cytochrome *c* oxidase, since they contain sulphur-bridged $\text{Fe}(\text{III})(\text{porphyrin})\text{-Cu}(\text{II})$ linkages; they differ only in the number of benzene solvent molecules, and all have similar crystal structures. All contain a neutral trinuclear $\text{Fe}(\text{III})\text{-Cu}(\text{II})\text{-Fe}(\text{III})$ unit, in which a pair of $\text{Fe}(\text{III})$ porphyrin fragments sandwich a $[\text{Cu}(\text{II})(\text{MNT})_2]^{2-}$ anion via a sulphur atom from each MNT ligand. The charge is balanced by the anion $[\text{Cu}(\text{III})(\text{MNT})_2]^+$, which is weakly associated with the trinuclear sandwich. Magnetic susceptibility measurements and Mössbauer and ESR spectra indicate that the $\text{Fe}(\text{III})$ centres are in a spin state intermediate between $S = 3/2$ and $S = 5/2$. The very weak ESR spectra (only 5% of the 'expected' intensity) supports their validity as models for cytochrome *c* oxidase, which is ESR silent [320].

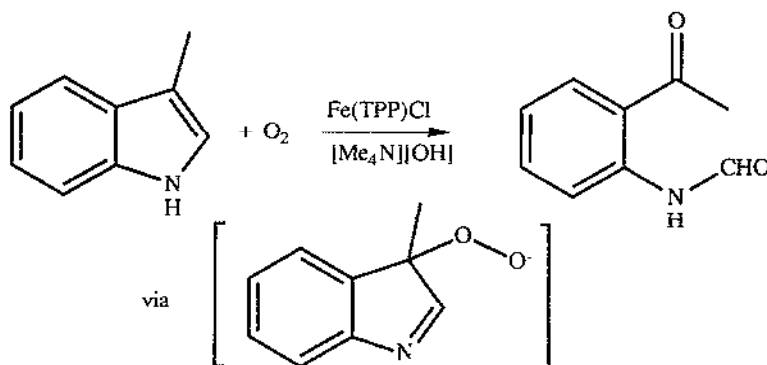
The reaction of H_2O_2 with *meso*-tetrakis(2,6-dichloro-3-sulphonatophenyl)-porphinatoiron(III) was studied in H_2O and D_2O over a wide range of pH/pD values. Three different reaction pathways occur depending on the pH; measurements of the kinetic isotope effect were used to help establish the mechanistic details [321]. Reactions of the same complex with alkyl and acyl hydroperoxides were also studied, and detailed mechanisms proposed [322].

Cleavage of the O-O bond at the active site of cytochrome P450 is known to require acid catalysis. To determine the feasibility of water or alcohols participating in this process, solvent polarity, acidity and isotope effects in reactions of various Fe(III) porphyrins with H_2O_2 , $t\text{BuOOH}$ and peroxy-acids were examined. The observed effects of these parameters on the reactions of hydroperoxides and peroxy-acids with Fe(III)-porphyrin complexes, all of which involve O-O heterolytic cleavage, are similar to those observed for naturally occurring systems. The results suggest that water may participate in acid catalysis at the active site of cytochrome P450 [323].

Electrochemistry, electronic spectroscopy and magnetic moment measurements of the superoxide complex $[\text{Fe}(\text{II})(\text{OCP})(\text{O}_2)]^-$ (OCP = *meso*-tetrakis[2,6-dichlorophenyl]porphyrin) established that the electrochemical activity is centred on the $[\text{O}_2]^-$ ligand rather than the metal. The complex has a covalent bond between the superoxide radical anion and an unpaired d-electron on the Fe(II). Similar conclusions were drawn for the O_2 and OH^- complexes [324].

The resonance Raman (RR) spectra of $(\text{P})\text{Fe}(\text{III})\text{-O-O-Fe}(\text{III})(\text{P})$ (P = TPP, OEP and other substituted porphyrins) were recorded at -80°C ; on warming to -40°C complete conversion to the ferryl complexes $(\text{P})\text{Fe}(\text{IV})=\text{O}$ occurs [325]. A similar study was carried out on the complexes $\text{Fe}(\text{TMP})\text{O}_2$, $(\text{TMP})\text{Fe-O-O-Fe}(\text{TMP})$ and $(\text{TMP})\text{Fe}=\text{O}$ (H_2TMP = *meso*-tetrakis[2,4,6-trimethylphenyl]porphyrin), which are formed as intermediates during the autoxidation of $\text{Fe}(\text{TMP})$ to $\text{Fe}(\text{TMP})\text{OH}$; their RR and electronic spectra were recorded at -80°C [326].

Reaction of $\text{Fe}(\text{III})(\text{TPP})\text{Cl}$ with H_2O_2 in alkaline media produces $[\text{Fe}(\text{III})(\text{TPP})(\text{OH})(\text{OOH})]^-$ whose spectroscopic properties are similar to those of a horseradish peroxidase [327]. Similarly reaction of $\text{Fe}(\text{III})(\text{OEP})(\text{O}_2)(\text{py})$ with ascorbate produces $[\text{Fe}(\text{III})(\text{OEP})(\text{OH})(\text{OOH})]^-$. The complex was characterised by electronic and ESR spectroscopy, and should be a practical model for an intermediate heme-hydroperoxide complex of cytochrome P450 [328].



Scheme 10 : Oxidation of skatole by $\text{Fe}(\text{TPP})\text{Cl}$

The oxygenation of 3-methylindole (skatole) to *o*-formamidoacetophenone by Fe(TPP)Cl in the presence of tetramethylammonium hydroxide and O₂ (scheme 10) parallels the catalytic activity of tryptophan dioxygenase. Study of the reaction by ESR and electronic spectroscopy at -78°C allowed detection of the intermediate species [Fe(III)(TPP)(OMe)(OO-skatole)]⁻ and [Fe(III)(TPP)(OO-skatole)₂]⁻. A mechanism for the reaction is proposed [329].

Reduction of the Fe(III) complex of the picket-fence porphyrin *meso*-tetrakis(*o*-pivalamidophenyl)porphyrin, FeLCl, by Zn amalgam gives Fe(II)L (in PhMe or CH₂Cl₂) or Fe(II)L(thf)₂ (in thf). FeL reacts with O₂ in PhMe or CH₂Cl₂ to give the five coordinate adduct FeL(O₂), and similarly FeL(thf)₂ reacts with O₂ in thf to give the six coordinate FeL(O₂)(thf); in both of these the O₂ is bound end-on. Both of the dioxygen adducts were further reduced by Na[AlH₂(OCH₂CH₂OMe)₂] to give the peroxoiron complex [Fe(III)L(O₂)]⁻, in which the O₂²⁻ is now bound side-on to the Fe(III). Protonation of this species with HBF₄·Et₂O is solvent-dependent. In thf the product is LFe(IV)O, but in toluene/CH₂Cl₂ the product is the π -radical Fe(IV)=O species [LFeO]⁺ which is unstable and shows weak spin-pairing between the Fe(IV) and the ligand radical monoanion. [LFeO]⁺ could also be prepared by direct oxidation of FeLCl with *m*-chloroperoxybenzoic acid. The catalytic and spectroscopic properties of [LFeO]⁺ and LFeO are discussed [330] (see also ref. 350 for a similar example). A bis-fenced analogue *meso*-tetrakis-(2,6-dipivaloyl-oxyphenyl)porphyrinatoiron(II) has both faces 'protected' by picket-fence pivaloyl groups, which are joined to the *meso*-phenyl rings by ester linkages. The complex stably and reversibly binds O₂ in toluene at 25°C; the bulky substituents prevent formation of μ -oxo dimers at either face. A kinetic study of O₂ association and dissociation showed that the affinities of the hindered axial sites for O₂ and imidazole are similar to those of heme proteins [331].

The Fe(III) complex of *meso*-tetrakis-(*N*-methyl-4-pyridyl)porphyrin was electrochemically oxidised to the Fe(IV)=O species. The process was followed by electronic spectroscopy in an OTTLE cell at low pH [332]. The Fe(III) complex of TMP-*N*-oxide undergoes a double protonation of the oxygen atom followed by H₂O elimination to give [Fe(III)(TMP)]²⁺, which is isoelectronic with Fe(IV)=O species. Such a dication has been suggested as an intermediate in the reaction of H₂O₂ with horseradish peroxidase [333].

The membrane-spanning porphyrinatoiron(II) complex FeL (L = *meso*-tetrakis[2',6'-di(20"-hydroxy-2",2"-dimethylcosanoyloxy)phenyl]porphyrin) was prepared as a model for membrane-intrinsic proteins and characterised in a liposomal bilayer. The complex with 1-dodecylimidazole embedded in a phospholipid bilayer forms an adduct with O₂ at 25°C in water [334].

1.7.2.3 Other porphyrin complexes

A series of porphyrins containing three 4-pyridyl groups and a 4-nitrophenyl, 4-aminophenyl or 4-hydroxyphenyl in the *meso* positions have been prepared, and various transition-metal complexes (including Fe(II)) prepared which have moderate cytotoxic activity against leukaemia cells, possibly due to the generation of reactive oxygen species. The cytotoxicity is increased by methylation of the pyridyl groups. The external functional groups function as 'handles'

which should allow covalent attachment of the complexes to other molecules for targeting specific nucleic acid sequences [335].

The 'ruffling' of a porphyrin ring which occurs in many natural and synthetic heme complexes - especially sterically hindered ones - is of great structural interest but very hard to detect by conventional spectroscopic means. However ^{57}Fe NMR showed that the Fe chemical shift in a variety of Fe(II) porphyrin complexes is very sensitive to these slight distortions in the pyridine core geometry, due to d-orbital perturbations, and is therefore a useful structural probe [336]. In a similar vein, MCD spectra were found to be much more sensitive than electronic spectra to variations of the phenyl substituents in Fe(II) complexes of various *meso*-tetrakis-(*p*-substituted phenyl)porphyrins [337].

The charge distribution in Fe(II)(TPP) was derived from a detailed X-ray diffraction study. Deformation density maps indicate preferential occupancy of the d_{z^2} and d_{xy} orbitals, agreeing with previous MO calculations, and are therefore consistent with the observed $S = 3/2$ ($^3A_{2g}$) ground state. By contrast, FePc has a 3E_g ground state due to axial intermolecular Fe-N interactions [338].

The epoxidation of 1-alkenes, 1,1-disubstituted alkenes and styrenes by Fe(OCP)Cl results, as a side reaction, in the irreversible formation of N-alkyl complexes, and thus models the suicide inactivation of cytochrome P450. The partition numbers for various substrates (i.e. the number of successful catalyst turnovers per suicide event) were calculated, and resemble the results for cytochrome P450; they are very sensitive to the nature of the substrate alkene [339]. These partition numbers were further studied as a function of steric and electronic properties of some substituted styrenes and of different aryl substituents on the porphyrin. The transition state geometries for epoxidation and N-alkylation are different and might be expected to be sensitive to the nature of the 2,6 substituents on the *meso*-phenyl rings, since it is groups in these positions which cause steric hindrance over the porphyrin faces. It was found that the partition numbers are only slightly sensitive to the steric nature of the porphyrin, and insensitive to the electronic properties of the porphyrin and the olefin substrate. The N-alkyl porphyrins isolated in three model systems show the same regiochemical behaviour as the N-alkyl derivatives of cytochrome P450. On the basis of these findings possible mechanisms for the two competing processes are discussed [340].

Fe(III)(p-Cl₄TPP)Cl reacts with PhCH₂CHN₂ at -30°C to give a bridged carbene complex with a PhCH₂CH moiety inserted into the Fe(III)-N bond. This compound is spectroscopically similar to a previously reported Fe(III) porphyrin complex with a vinylidene C=CAr₂ fragment inserted into the Fe-N bond; both have $S = 3/2$. On chemical or electrochemical reduction, the bridged carbene complex gives a diamagnetic carbene complex (p-Cl₄TPP)Fe(II)(CHCH₂Ph) with an Fe=C bond. By contrast oxidation of the initial bridged carbene breaks the Fe-C bond to give a CH=CHPh group attached to the N atom (an N-vinyl complex) with the double bond in the E configuration. The formation of the bridged carbene and its oxidative transformation to the N-vinyl derivative provide the first model for formation of N-vinyl-heme during the cytochrome P450 metabolism of PhCH₂CHN₂. Possible mechanisms for the conversion are discussed; the complexes are characterised by electrochemistry and NMR spectroscopy [341].

Table 4 : Miscellaneous studies on iron-porphyrin complexes ($\underline{\text{N}}$ = iron oxidation state)

<u>N</u>	<u>Porphyrin ligand</u>	<u>Studies performed</u>	<u>Ref</u>
3	TPP	Aerobic oxidation of SO_2 to SO_4^{2-} promoted by $[\text{Fe}(\text{TPP})]_2\text{O}$	[345]
3	Mesoporphyrin IX	$[\text{Fe}(\text{III})\text{L}]^+$ shows greatly enhanced peroxidase activity when complexed to monoclonal antibodies	[346]
3	Various	$\text{Fe}(\text{III})$ -porphyrin complexes catalyse regioselective α -tosylation of alkanes by PhI:NTs ; effect of <i>meso</i> substituents on regioselectivity	[347]
3	<i>meso</i> -tetrakis[2,6-difluorophenyl]porphyrin	Electrocatalytic hydroxylation of cyclohexane to cyclohexanol by $[\text{FeL}\text{F}_2]^-$: Oxidation of $[\text{FeL}\text{F}_2]^-$ to a red $\text{Fe}(\text{V})$ derivative, characterised by UV/vis, ESR, NMR, magnetic moment	[348]
3	<i>meso</i> -tetrakis[4-pivaloylaminophenyl]porphyrin	X-ray structure of 'picket-fence' porphyrin $[\text{FeL}(\text{OSO}_2\text{CF}_3)(\text{H}_2\text{O})]$; Mossbauer, NMR, UV-vis and detailed ESR characterisation; mix of $S = 3/2$ and $S = 5/2$ states	[349]
3	<i>meso</i> -tetrakis[2,6-dichlorophenyl]porphyrin	Oxidation of $\text{FeL}(\text{CF}_3\text{SO}_3)$ to $\text{Fe}(\text{O})\text{L}(\text{CF}_3\text{SO}_3)$, an oxoferryl porphyrin radical. Weak ferromagnetic coupling between metal and radical cation spins, in contrast to TMP analogue	[350]
3	TTP	^1H NMR studies on the hydroquinone-bridged dimers $(\text{TTP})\text{Fe}(\text{1.4-OC}_6\text{R}_4\text{O})\text{Fe}(\text{TTP})$ ($\text{R} = \text{H}$, Cl , CH_3 , CN , OCH_3); the spectra resemble those of high-spin ($S = 5/2$) monomers	[351]
2	Various	Mild and efficient method of inserting iron into porphyrins, including picket-fence and basket-handle porphyrins. ^{57}Fe -enriched iron may be used	[352]
2	TPP	Reaction of $(\text{TPP})\text{Fe}(\text{:CCl}_2)$ with $\text{Na}[\text{Re}(\text{CO})_5]$ gave the μ_2 -carbido complex $[(\text{TPP})\text{Fe}=\text{C}=\text{Re}(\text{CO})_4\text{Re}(\text{CO})_5]$, whose crystal structure was determined	[353]
3	<i>meso</i> -tetrakis[2,6-dichlorophenyl]porphyrin; <i>meso</i> -tetrakis[perchlorophenyl] porphyrin; TPP	Reaction of FeLCl with Cl_2 gas and FeCl_3 gave the respective <i>meso</i> -substituted octachloroporphyrins. $\text{Fe}(\text{TPP})\text{Cl}$ underwent macrocycle decomposition under the same conditions, and could only be partially chlorinated by <i>N</i> -chlorosuccinimide. The effects of chlorination on redox potentials were studied.	[354]

Table 4 continued : Miscellaneous studies on iron-porphyrin complexes (N = iron oxidation state)

2,3	Various	Effect of pyrolysis temperature on O ₂ reduction activity of Fe-porphyrins deposited on carbon	[355]
2	<i>meso</i> -tetrakis[4-sulphonatophenyl]porphyrin	FeL adsorbed onto Ag electrode and its O ₂ reduction behaviour examined. Raman spectra assigned by comparison with [Fe(TPP) ₂ O] - spectra insensitive to applied potential	[356]
3	Protoporphyrin IX	Mossbauer studies show that (PPIX)Fe-O-Fe(PPIX) forms molecular π -complexes with histidine, N- α -acetylhistidine and histamine, via a charge-transfer interaction between the parallel imidazole and pyrrole rings. The complexes are stabilised by H-bonding	[357]
3	TPP	Proton NMR studies show that Fe(TPP)Cl forms complexes with aromatic nitro-compounds, in which the aromatic rings are located directly over the metal ion	[358]
3	<i>meso</i> -tetrakis[4-pyridyl]-porphyrin	FeL(OAc) reacts with 4 equivalents of Ru(HL')(H ₂ O) (HL' = EDTA) to give a pentanuclear complex in which each pyridyl residue on the porphyrin is attached to a Ru(HL') fragment; electrochemistry and O ₂ reduction activity are described	[359]
3	Various	Theoretical study of porphyrin-Fe charge-transfer bands in low-spin Fe(III) heme proteins and model complexes; determination of axial ligand orientations in bis-histidine coordinated hemes	[360]
3	Protoporphyrin(IX) dimethyl ester	Cyclic voltammetry of FeLCl at a microelectrode using extreme scan rates between -100°C and 100°C. Detailed mechanism of redox processes	[361]
3	Various	Autoreduction of Fe(III)-porphyrin complexes by cyanide ion in DMSO examined by electronic spectroscopy. Reactions are first order in cyanide	[362]
3	Protoporphyrin IX	NMR studies on monodispersed [FeL(CN) ₂] ⁻ and [FeL(py)(CN)] (py = pyridine) encapsulated in aqueous detergent micelles; effects of hydrophobic interactions and micelle size on the spectra	[363]
2	Protoporphyrin IX	NMR and electronic spectral studies on high-spin (S = 2), six co-ordinate [FeL(THF) ₂] encapsulated in aqueous detergent micelles; comparison with a five co-ordinate analogue	[364]

$\text{Fe}(\text{F}_{20}\text{TPP})\text{Cl}$ oxidises aldehydes to carboxylic acids in the presence of MCPBA by a hydrogen-atom transfer mechanism involving an $\text{Fe}(\text{IV})=\text{O}$ intermediate [342]. $\text{Fe}(\text{pfpp})\text{Cl}$ also performs benzylic oxidations of substituted benzenes and silanes in the presence of iodosylbenzene. Again, the mechanism probably involves hydrogen-atom transfer rather than electron transfer [343].

Weak antiferromagnetic coupling has been observed between $\text{Fe}(\text{III})$ and the oxidised ligand radical monoanions in the six-coordinate complexes $[(\text{OEP})\text{Fe}][\text{ClO}_4]_2$ and $[(\text{OEC})\text{Fe}][\text{ClO}_4]_2$ (OEC = octaethylchlorin). In the five-coordinate complexes $[(\text{OEP})\text{FeCl}][\text{SbCl}_6]$, $[(\text{OEC})\text{FeCl}][\text{SbCl}_6]$ and $[(\text{TPC})\text{FeCl}][\text{SbCl}_6]$ (TPC = tetraphenylchlorin) the coupling is rather stronger. All five complexes have an $S = 2$ ground-state, from antiferromagnetic coupling of $S = 5/2$ ($\text{Fe}(\text{III})$) and $S = 1/2$ (ligand radical). The difference in the values of J for the five- and six-coordinate complexes is due to the different symmetries of the ligand radical orbitals. The relevance of these results to the magnetic properties of horseradish peroxidase and myeloperoxidase compound I are discussed [344].

The remaining reported complexes are summarised in Table 4 [345 - 364].

1.8 COMPLEXES WITH O DONOR LIGANDS

1.8.1 Complexes with carboxylic acids and derivatives

Basic iron(III) acetate has long been known to contain the trinuclear, oxo-bridged cation $[\text{Fe}_3\text{O}(\text{OAc})_6(\text{H}_2\text{O})_3]^+$. The mixed-metal analogues $[\text{Fe}(\text{III})_2\text{M}(\text{II})\text{O}(\text{OAc})_6(\text{H}_2\text{O})_3] \cdot n\text{H}_2\text{O}$ ($\text{M} = \text{Mn}, \text{Fe}, \text{Co}, \text{Ni}, \text{Zn}$) have been prepared [365]. The mixed-valence complex $[\text{Fe}(\text{III})_2\text{Fe}(\text{II})(\text{Cl}_3\text{CCO}_2)_6(\text{CH}_3\text{OH})_3](\text{H}_2\text{O})_{1.5}$ has a dynamic temperature-dependent structure, involving electron motion at the three Fe centres and disorder of the H_2O molecules and CCl_3 groups [366]. The monochloroacetate analogue of iron(III) acetate $[\text{Fe}_3\text{O}(\text{CH}_2\text{ClCO}_2)_6(\text{H}_2\text{O})_3][\text{NO}_3]$ reacts with $\text{Fe}(\text{NO}_3)_3 \cdot \text{H}_2\text{O}$ in methanol to give the unusual decamer $[\text{Fe}(\text{OMe})_2(\text{CH}_2\text{ClCO}_2)]_{10}$, containing a planar, cyclic array of ten Fe atoms, each joined to its neighbour by two methoxide bridges and a carboxylate bridge [367]. A trinuclear, oxo-bridged complex is formed from the reaction of $\text{Fe}(\text{NO}_3)_3$ with *o*-phthalic acid. Mössbauer and magnetic susceptibility measurements indicate distorted octahedral high-spin $\text{Fe}(\text{III})$ centres [368].

Carbohydrate moieties in glycoproteins are involved in various biological regulative mechanisms which may involve metal ion complexation. Accordingly complexes of $\text{Fe}(\text{III})$ with the glucopyranosyl ester of glycine were prepared, and the structural effects of adding protecting groups (acetyl on the sugar hydroxyls, amide on the amino group) were examined. The core structure of the complex of the 'unprotected' ligand is similar to that of basic iron acetate; structures of the other complexes are proposed on the basis of elemental analyses [369].

Reaction of the Lewis acid FeCl_3 with $\text{Br}_3\text{CO}_2\text{H}$ (HA) gave FeClA_2 , which was spectroscopically characterised, and shown to retain Lewis acid character by forming an adduct with pyridine [370]. A detailed X-band and Q-band ESR study was performed on a series of tris-

chelate complexes of oxalate, malonate, α -ketovalerate, α -hydroxybutyrate and acetylacetonate to give a fingerprint library of spectra of octahedrally distorted, $S = 5/2$ " FeO_6 " complexes. The spectra are very sensitive to the counterion, lattice solvent molecules and lattice distortions [371]. Complexes of bromomalonaldehyde (HBM) were prepared for comparison with complexes of nitromalonaldehyde, which has similar steric properties but is more electron-withdrawing. $\text{Fe}^{(\text{II})}(\text{BM})_2(\text{H}_2\text{O})_2$ was prepared, and is readily dehydrated to $\text{Fe}^{(\text{II})}(\text{BM})_2$. The magnetic properties of $\text{Fe}(\text{BM})_2$ in the solid state indicate an octahedral geometry, which could only be attained in a polymeric structure with oxygen bridges; this is similar to the behaviour of $\text{Fe}(\text{acac})_2$. $\text{Fe}(\text{BM})_2$ readily reacts with water, pyridine and other Lewis bases to give $\text{Fe}(\text{BM})_2\text{L}_2$. $[\text{AsPh}_4][\text{Fe}(\text{BM})_3]$ was also prepared, and is a 1:1 electrolyte with a high-spin $\text{Fe}(\text{III})$ centre [372]. An electrochemical synthesis of $\text{K}_3[\text{Fe}^{(\text{III})}(\text{C}_2\text{O}_4)_3] \cdot 3\text{H}_2\text{O}$ using a sacrificial Fe electrode in oxalic acid solution is described [373]. The compositions, stabilities and distributions of dimeric, mixed-valence $\text{Fe}(\text{II})/\text{Fe}(\text{III})$ complexes of *d*- and *dl*-tartrate were determined as a function of pH. The influence of the degree of protonation on dimer complex structure and properties is discussed. The magnetic, optical and redox properties of the mixed-valence complexes are non-additive [374].

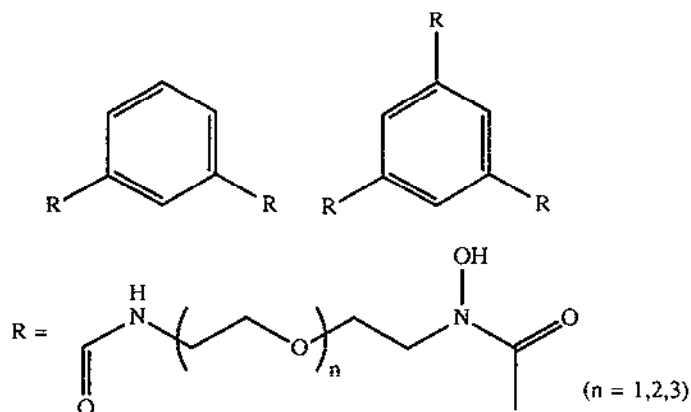
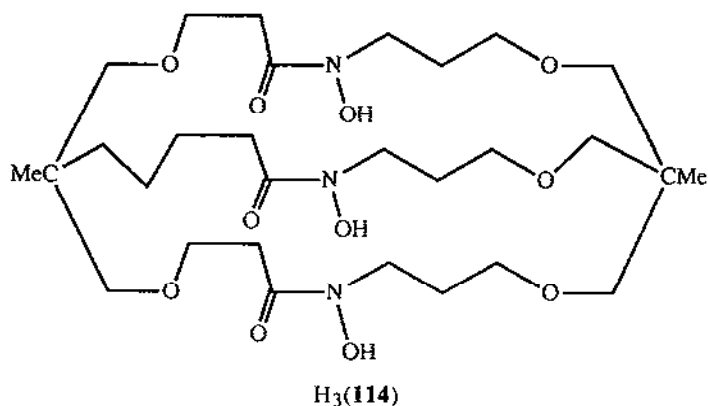
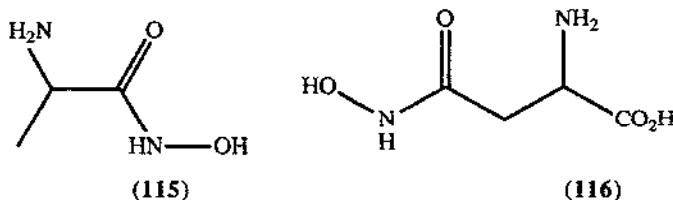


Figure 6 : A series of synthetic siderophores



The series of compounds in figure 6, all of which contain poly-oxyethylene chains with terminal hydroxamic acid groups, were prepared as iron(III) sequestering agents. The tris-hydroxamic acids form more stable complexes with Fe(III) than the bis-acids, although the latter transported Fe(III) more quickly in experiments using an $\text{H}_2\text{O}-\text{CHCl}_3/\text{CCl}_4$ [375]. The siderophore cryptand H_3 (114) contains three hydroxamic acid groups, which in the complex Fe(114) are all directed into the cavity, conferring an octahedral FeO_6 geometry on the metal ion. The nature and pH dependence of the electronic spectrum are very similar to those of desferrioxamine B, a natural siderophore [376].

Complexation of Fe(III) with *l*- α -alaninehydroxamic acid (115) [377] and *dl*-aspartic acid- β -hydroxamic acid (116) [378] has been investigated by spectrophotometric methods as a function of pH and of metal/ligand ratio. Ligand (115) coordinates via the hydroxamate oxygen atoms only, and (116) is thought to act as a tridentate ligand via the hydroxamate oxygens and the carboxylate. This is in contrast to the behaviour of these ligands with other transition-metal ions, where mixed N-O coordination occurs.



The polymeric complexes $(\text{Fe}(\text{II})\text{L}_2 \cdot 2\text{H}_2\text{O})_n$ (L = salicyl-, 5-chlorosalicyl-, 3,5-dichlorosalicyl- and benzo-hydroxamic acid) were prepared, and characterised by elemental analysis and electronic spectroscopy. The effects of the ligand substituents on the Mössbauer parameters are discussed [379]. The mononuclear complexes FeL_2 (L = benzo-, salicyl-, 5-bromosalicyl- and 3,5-dibromosalicylhydroxamic acid) have also been prepared and characterised; the ligands are tridentate [380].

An attempt to resolve a series of tris-hydroxamate complexes of Fe(III) into their geometrical and diastereoisomers was complicated by their kinetic lability [381]. The Fe(II) complexes of α - and β naphthalenesulfinic acids ($\text{R SO}_2\text{H}$) were prepared; their IR spectra indicate bidentate O,O' coordination [382].

1.8.2 Complexes with other O donor ligands

9,10-Phenanthrenequinone (117) reacts with $[\text{Li}(\text{TMEDA})][\text{Fe}(\text{Cp})(\text{COD})]$ (TMEDA = N,N,N',N'-tetramethylethylenediamine) to give $[\text{Li}(\text{TMEDA})]_2[\text{Fe}(\text{cat})_2]$, where H_2cat is the doubly reduced catechol form of (117). By contrast, direct reaction of (117) with FeCl_2 in TMEDA gives $[(\text{TMEDA})\text{Fe}(\text{cat})(\text{SQ})]$ where SQ is the once-reduced semiquinone form of (117). The complexes were characterised by magnetic measurements, electronic, IR and ESR spectroscopy [383].

The bimetallic chain compound depicted in figure 7, in which each Fe(II) is in an octahedral FeO_6 environment, has been prepared and its magnetic properties examined in detail. It shows characteristic one-dimensional ferrimagnetic behaviour, with an additional inter-chain antiferromagnetic interaction apparent at low temperatures, and also weak ferromagnetism below 10K [384].

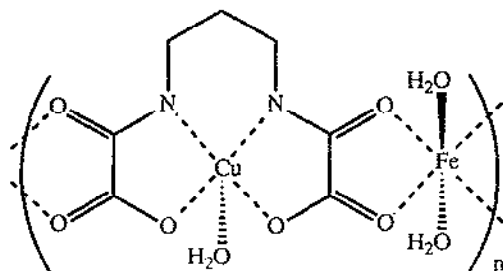
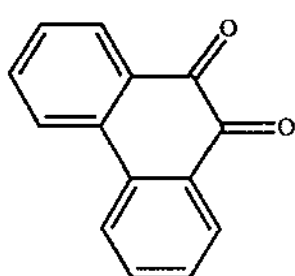


Figure 7 : A linear Fe(II)-Cu(II) chain compound

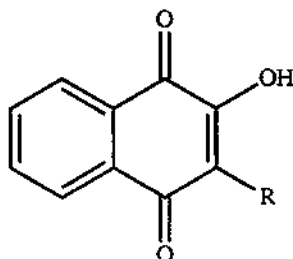
Iron complexes of lawsone (**H118**) and various derivatives have been prepared and studied as possible models for the ferroquinone complex of photosynthetic bacteria and photosystem(II). $\text{Fe}(\text{II})(\text{118})_2(\text{H}_2\text{O})_2$ has been structurally characterised, and is a *trans*-octahedral complex with axial compression and a rhombic distortion. The two lawsonate ligands are in the fully oxidised form and chelating bidentate, through the phenolate oxygen and the adjacent carbonyl oxygen. Each complex molecule has a total of eight hydrogen bonds to its six nearest neighbours, involving the free carbonyl, the phenolate oxygen, and axial water molecules; there is thus a three-dimensional H-bonding network. However, the high-spin Fe(II) centres are magnetically isolated and the magnetic moment of the complex is normal for an $S = 2$ system. By contrast, in the complex of 3-aminolawsone $\text{Fe}(\text{II})(\text{119})_2(\text{CH}_3\text{OH})$, (**119**) coordinates in a chelating bidentate manner through the phenolate and amino groups; both carbonyl groups are free, and the ligand is in the fully oxidised form. The magnetic susceptibility measurements show strong antiferromagnetic coupling, whose temperature-dependence is best explained by magnetically isolated dimers in the solid. Each Fe(II) would have an axial interaction to the phenolate oxygen of the other complex in the dimeric unit, completing the octahedral coordination sphere of each Fe(II) and establishing an Fe_2O_2 bridge. This interaction makes the complex rather insoluble. Mössbauer and electronic spectroscopic studies were also performed [385]. Six other high-spin Fe(II) complexes $\text{FeL}_2(\text{H}_2\text{O})_2$ of lawsone and derivatives all show the same mode of bidentate (phenolate, carbonyl) coordination as the parent complex. The spin-state of the metal, and the oxidation states of the metal and ligands, were determined by magnetic susceptibility, electrochemical, and spectroscopic measurements [386]. Maltol, **H(120)**, behaves as a chelating bidentate O,O donor; the solubility of $\text{Fe}(\text{120})_3$ in methanol-water mixtures has been investigated [387].

The chiral tripodal ligand (**121**), in which each side-chain contains a chiral leucine residue condensed to a β -keto amide binding site, has been prepared and its coordination chemistry investigated. The chirality built into each arm means that the two coordination isomers are

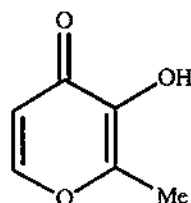
diastereoisomeric, and **121** forms complexes of high configurational purity with Fe(III) and other metals. The three deprotonated β -diketonate binding sites confer an octahedral geometry on the central metal ion. Electronic and CD spectra show transitions that arise from exciton coupling among the three binding sites [388].



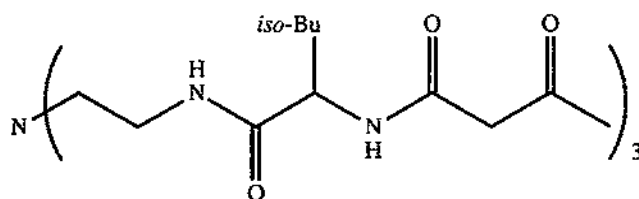
9,10-Phenanthroquinone
(117)



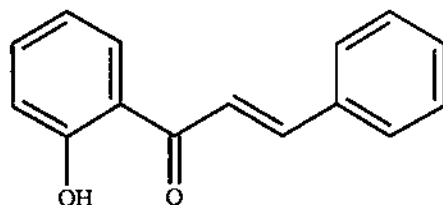
Lawsonone, H(118) (R = H)
Aminolawsonone, H(119) (R = NH₂)



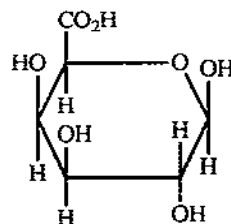
Maltol, H(120)



(121)



2'-hydroxychalcone, (122)



Galacturonic acid, (123)

The oxo-centred hexanuclear Fe(III) complex $[\text{Me}_4\text{N}][\text{O}\{\text{Fe}(\text{OCH}_2)_3\text{CMe}\}_6]$ was isolated from the reaction of $\text{CH}_3\text{C}(\text{CH}_2\text{OH})_3$ with Fe(III) in the presence of $[\text{Me}_4\text{N}][\text{OMe}]$. The crystal structure shows that the six Fe(III) ions are octahedrally disposed around the central oxo-atom. Each tris-alcohol (fully deprotonated) caps three sites at each Fe(III) and has two bridging contacts to adjacent Fe atoms, all of which are in octahedral O_6 environments. The bonds from the Fe atoms to the oxo centre are unusually long. The structure shows that polyhydric alcohols may be as effective as carboxylates in supporting oxo-centred polynuclear structures [389].

Table 5 : Summary of some iron complexes with O donor ligands (N = iron oxidation state)

<u>N</u>	<u>Ligand</u>	<u>Studies performed</u>	<u>Ref</u>
3	1,3-diketones, 3-ketoesters	Bromination of coordinated ligands at positions adjacent to carbonyl groups by $[\text{C}_5\text{H}_5\text{NH}][\text{Br}_3]$	[391]
2	2'-Hydroxychalcone (122)	Monomeric, low-spin, square-planar FeL_2 complexes (HL = 122) prepared and characterised	[392]
3	Oligomaltose	Complexes of $\text{Fe}(\text{OH})_3$ with oligomaltose and its electrochemical oxidation products	[393]
3	Peptidoglycan monomer (PGM)	Complex between PGM and $\text{Fe}(\text{II})$ shown to have stoichiometry $\text{Fe}_5(\text{PGM})_2$ by NMR and IR studies; coordinating atoms are carbonyl oxygens (from peptide chain) and terminal carboxylate	[394]
3	Galacturonic acid (123)	Reduction of $\text{Fe}(\text{III})$ in the presence of <i>D</i> -galacturonic acid is accelerated by the presence of $\text{Cu}(\text{II})$, due to a $\text{Cu}(\text{II})$ -promoted ring-opening reaction which forms reducing aldehyde groups	[395]
2,3	Dinitrosoresorcinol	$\text{Fe}(\text{II})$ and $\text{Fe}(\text{III})$ complexes of dinitrosoresorcinol thought to be octahedral on the basis of electronic spectroscopy; the ligand is chelating bidentate through one OH and one nitroso O atom	[396]
2	(124)-(128)	$\text{Fe}(\text{II})$ complexes of (124)-(128) prepared	[397]
2	2-Methylfuran	$[\text{Fe}(\text{H}_2\text{O})_5(\text{HL})][\text{ClO}_4]_2$ (HL = 2-methylfuran) prepared and spectroscopically characterised; polymerisation to $[\text{L}_2\text{FeH}(\text{ClO}_4)]_x$ and $[(\text{HL})\text{FeL}(\text{ClO}_4)]_x$, in which some 2-methylfuran ligands are cyclometallated, occurs on heating, with a loud cracking noise	[398]
3	H_2O	The alums $\text{CsFe}(\text{SO}_4)_2 \cdot 12\text{H}_2\text{O}$ and $\text{CsFe}(\text{SeO}_4)_2 \cdot 12\text{H}_2\text{O}$ were structurally characterised by neutron diffraction at 15K. Both contain octahedral $\text{Fe}(\text{III})$ -(H_2O) ₆ centres, with slightly different stereochemistries of water coordination related to the alum type	[399]
3	Ph_3PO , Ph_3AsO	$[\text{FeL}_4\text{X}_2][\text{FeX}_4]$ (X = Br, Cl) react with SO_2 in toluene slurries to give $[\text{FeL}_4(\text{OSOX})][\text{FeX}_4]$	[400]
3	$\text{Ph}(\text{PhCH}_2)_2\text{PO}$, $(\text{PhCH}_2)_3\text{PO}$	$[\text{FeL}_4][\text{ClO}_4]_3$, $[\text{FeL}_2(\text{NO}_3)_3]$ and $[\text{FeL}_4][\text{FeCl}_4]$ prepared and characterised. Stereochemistries compared to complexes with Ph_3PO ; only the uncharged nitrate complex has a different structure	[401]
3	Ascorbic acid	The reaction of aqueous $\text{Fe}(\text{III})$ with ascorbic acid is surprisingly fast. The dependence of kinetics on pH indicates the formation of two protonated complexes	[402]

Table 5 continued: Summary of some iron complexes with O donor ligands (**N** = iron oxidation state)

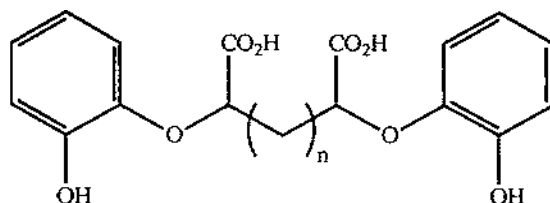
2,3	Water	Kinetic measurements on the $[\text{Fe}(\text{H}_2\text{O})_6]^{3+/2+}$ and $[\text{Fe}(\text{H}_2\text{O})_5(\text{OH})]^{2+}/[\text{Fe}(\text{H}_2\text{O})_6]^{2+}$ exchange reactions as a function of pressure; activation parameters. Implications for reaction mechanisms	[403]
2	Malic acid	Kinetics of oxidation of Fe(II)-malate complex by O_2 ; activation parameters; solvent effects	[404]
2,3	Water	Accurate calculations of free energies of hydration and time-averaged coordination numbers of Fe(II) and Fe(III); good agreement with experimental results	[405]
2	Water	Kinetics of reduction of $[\text{Co}(\text{C}_2\text{O}_4)(\text{NH}_3)_4]^{1+}$ by $[\text{Fe}(\text{H}_2\text{O})_6]^{2+}$; pH dependence	[406]
3	<i>o</i> -hydroxybenzylamine- and <i>o</i> -aminophenol- $\text{N}_1\text{N}_2\text{O}$ -triacetic acid	Kinetics of complexation with Fe(III); pH dependence of kinetics shows that complex formation occurs through two different paths	[407]
3	Hydroquinone	Time-resolved X-ray absorption spectroscopy used to study electron-transfer between $\text{Fe}(\text{NO}_3)_3$ and hydroquinone - detection of intermediate species and measurement of rate constants	[408]
3	Nitrite	$\text{NO}[\text{Fe}(\text{ONO})_4]$ reversibly adds O_2 at 1 atm pressure and 20°C ; adduct formation causes decrease of magnetic moment and a colour change. 40% of O_2 carrying ability retained after 30 cycles	[409]
3	Nitrate, water, hydroxide	Formation in solution of a heteropolynuclear Fe-Cr hydroxy complex between pH = 2.5 and 4.5	[410]
3	Oxide, water, sulphate	Crystal structure of $[\text{Rb}_2.74(\text{NH}_4)_{2.26}][\text{Fe}_3\text{O}(\text{SO}_4)_6] \cdot 7\text{H}_2\text{O}$, contains discrete trinuclear $[\text{Fe}_3(\text{H}_2\text{O})_3\text{O}(\text{SO}_4)_6]^{5-}$ anions - structure analogous to basic Fe(III) acetate	[411]
2	Cytosinium $[\mathbf{81.H}]^+$	$[\text{Fe}(\mathbf{81.H})_2\text{Cl}_2]\text{Cl}_2$ and $[\text{Fe}(\mathbf{81.H})_4\text{Cl}_2]\text{Cl}_4$ have been prepared and characterised; the cytosine acts as a monodentate O-donor and is protonated at one of the ring nitrogen atoms	[412]
3	O	Electrocatalytic reduction of H_2O_2 by $[(\text{H}_2\text{O})\text{FeSiW}_{11}\text{O}_{39}]^{5-}$ in presence of hydroxide	[413]
3	Hydroxide, sulphate	Study of the formation of $\text{K}[\text{Fe}_3(\text{OH})_6(\text{SO}_4)_2]$ (jarosite) from $\text{Fe}_2(\text{SO}_4)_3$ and KOH, depending on mole ratio of reactants and temperature	[414]

PPh₃ is oxidised by O₂ in the presence of Fe(ClO₄)₃ in a stoichiometric reaction. The Fe(III) is irreversibly reduced to Fe(II), resulting in formation of [Fe(Ph₃PO)₄][ClO₄] [390].

Complexes of other O-donor ligands are summarised in Table 5 [391- 414].

Thermogravimetric studies have been performed on the complexes (NH₄)₃[Fe(III)(C₂O₄)₃].3H₂O [415], tris(N-benzoyl-N-phenylhydroxylamine)iron(III) [416], Fe^{II}(C₂O₄)₂.2H₂O [417] and [Fe₄Mn(OAc)₆(OH)₈].12H₂O [418].

The following mixed-metal oxides have been studied: Ba₆Nd₂Fe₄O₁₅, Ba₅SrLa₂Fe₁₄O₁₅ and Ba₅SrNd₂Fe₄O₁₅ [419], Ba₆La₂Fe₄O₁₅ [420], [Fe₃Co₄W₁₇O₇₀H₁₁]¹⁰⁻ [421], BiPbSr₂Fe_{1-x}M_xO_{6+z} (M = Co, Ni) [422], SrFe₁₂O₁₉ [423] and [(CH₃)₄N]₂[Fe(III)₂(H₂O)₆UMo₁₂O₄₂].18H₂O [424].

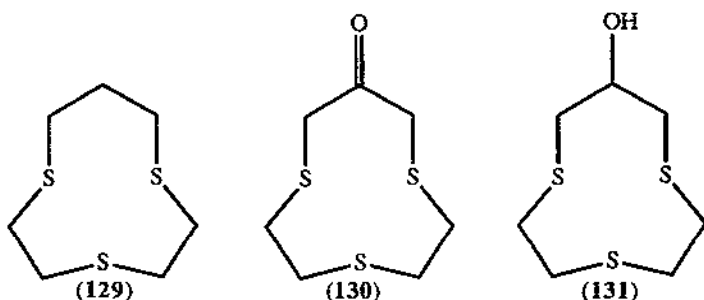


$n = 2-6$; (124) - (128)

1.9 COMPLEXES WITH S DONOR LIGANDS

A variable-energy photoelectron spectroscopic study of [Fe(III)S₄]⁵⁻ has been carried out. The results give detailed information on the electronic structure and orbital energy levels in the complex, and show that it has similarities to [Fe(Cl)₄]⁻ [425]. Single-crystal polarised absorption, MCD and ESR spectroscopy were used to elucidate the electronic structure of [Fe(III)(SR)₄]⁻ (R = 2,3,5,6-Me₄C₆H), which is a model for the oxidised active site of rubredoxin. The extents of σ and π bonding behaviour are discussed, and full assignments of the ligand-field transitions and charge-transfer spectrum are given. The electronic spectrum was found to be strongly dependent on the orientations of the R groups [426].

The coordination behaviour of the crown thioethers (129), (130) and (131) was studied in order to see the effects of structural alterations to the ligand backbone on complex formation. The crystal structure of [Fe(129)₂]²⁺ shows that each ligand coordinates in the expected facial manner, conferring an octahedral geometry on the Fe(II) ion. Surprisingly however the two six-membered rings have a *gauche* rather than an *anti* relationship; the complex is therefore chiral and, unusually, spontaneously resolves on crystallisation. [Fe(130)₂]²⁺ is thought to have the six-membered chelate rings in an *anti* configuration and therefore be optically inactive, by analogy with the Ni(II) complex which has been structurally characterised. [Fe(131)₂]²⁺ did not crystallise, but the electronic spectrum is indicative of octahedral coordination. In terms of ligand-field properties and metal-ligand bond lengths these ligands are intermediate between the known nine- and twelve-membered triithia-crown-ethers [427].



$\text{Fe}(\text{16-ane-S}_4)_2$ and $\text{Fe}(\text{16-ane-S}_4)\text{Br}_2$ (16-ane-S₄ = 1,5,9,13-tetrathiacyclohexadecane) have been prepared, and are high-spin complexes with Mössbauer parameters very characteristic of five coordinate Fe(II). However the crystal structure of $\text{Fe}(\text{16-ane-S}_4)_2$ shows that the Fe(II) is in the S₄ plane with unusually long (2.9 Å) interactions to the axial iodides, and may therefore be regarded either as a square-planar ionic or an octahedral covalent structure [428]. The complex $[\text{Fe}(\text{9-ane-S}_3)]^{2+}$ (9-ane-S₃ = 1,4,7-trithiacyclononane) was oxidised with $[\text{NO}][\text{PF}_6]$ in a strongly acidic medium. Although the resulting Fe(III) complex is unstable and rapidly reduces in air, it could be crystallised from the acidic reaction mixture and is stable in contact with the acid. The crystal structure shows an *elongation* of the Fe-S bonds relative to the Fe(II) complex, which is the first direct evidence for π back-bonding in thioether ligands [429]. The rate constant for electron self-exchange between the low-spin complexes $[\text{Fe}(\text{9-ane-S}_3)]^{2+}$ and $[\text{Fe}(\text{9-ane-S}_3)]^{3+}$ were measured by ^{13}C NMR line-broadening experiments at low temperature. The results are roughly consistent with the predictions of Marcus-Hush theory [430].

A new route to alkyl and aryl thiolate complexes involves protonation of $\text{FeH}_2(\text{dmpe})_2$ by the (acidic) thiol, followed by displacement of the weakly-bound $\eta^2\text{-H}_2$ by the thiolate anion. The products $\text{FeH}(\text{RS})(\text{dmpe})_2$ and $\text{Fe}(\text{RS})_2(\text{dmpe})_2$ (R = aryl, alkyl) exist as an equilibrium mixture of *cis* and *trans* isomers, apart from the complexes with chelating dithiolates which are necessarily *cis*. The coordinated thiolates readily exchange with free thiol in solution. The crystal structure of $\text{Fe}(\text{dmpe})_2(\text{edt})$ (H_2edt = 1,2-ethanedithiol) has been determined [431].

The electrochemical behaviour of $\text{Fe}(\text{sacsac})_2$ and $\text{Fe}(\text{sacsac})_2(\text{CO})_2$ (Hsacsac = pentane-2,4-dithione) has been examined. $\text{Fe}(\text{sacsac})_2$ is reversibly reduced to $[\text{Fe}(\text{sacsac})_2]^-$; $\text{Fe}(\text{sacsac})_2(\text{CO})_2$ undergoes an irreversible reduction with concomitant loss of CO, which becomes reversible under a CO atmosphere. Two-electron oxidation of $\text{Fe}(\text{sacsac})_2(\text{CO})_2$ results in the formation of $[\text{Fe}(\text{sacsac})(\text{CO})_2]^+$, with conversion of the other sacsac ligand to a 3,5-dimethyl-1,2-dithiolium cation [432].

The dimeric complex $\text{K}_4[\text{Fe}(\text{dto})_2(\text{NO})]_2 \cdot 2\text{H}_2\text{O}$ (H_2dto = dithiooxalic acid) has been structurally characterised, and has the structure depicted in Figure 8. The dimer is rather loosely bound (the long Fe-S distance is 3.82 Å), with strong Fe-N bonds; each iron is displaced 0.5 Å out of the S₄ ring towards its nitrosyl ligand. The intramolecular antiferromagnetic interaction is surprisingly strong considering the long Fe-S superexchange pathway, and suggests that sulphur bridges are very efficient at mediating such interactions [433].

The dithiophosphinate anion **132** acts as a chelating bidentate ligand to Fe(II). The complexes *trans*-Fe(**132**)₂X₂ (X = thf, tetrahydrothiophene, methanol) have been prepared and structurally characterised; all are similar, with near-octahedral geometries at the Fe(II) centre [434]. Fe(III)(**133**)₃ has also been prepared and spectroscopically characterised [435].

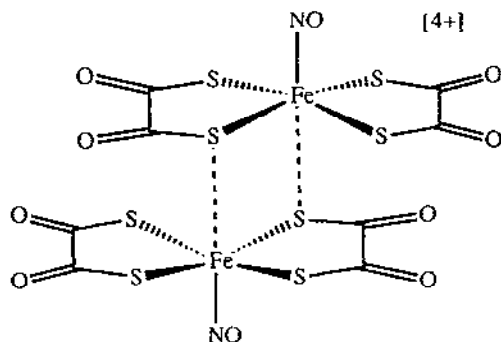
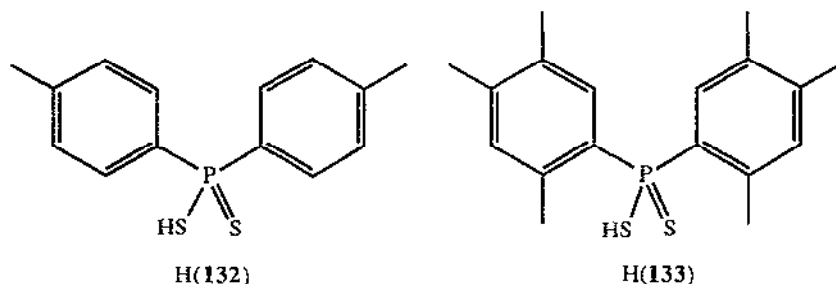


Figure 8 : Structure of the anionic part of $K_4[Fe(dto)_2(NO)]_2 \cdot 2H_2O$



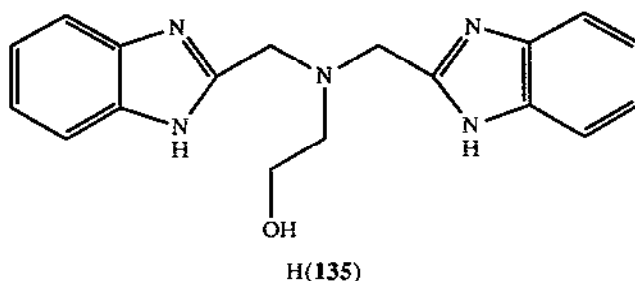
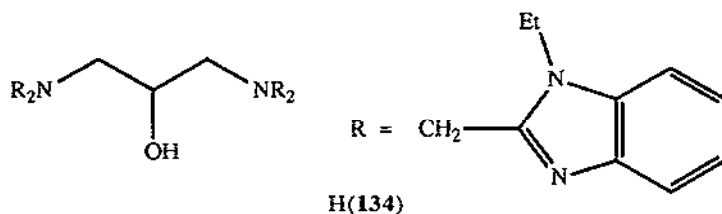
The silicon isothiocyanate compounds $Me_xSi(NCS)_{4-x}$ ($x = 0 - 3$) have been prepared and examined as ligands for Fe(III) [436]. The thermal decomposition of the polymeric complex of Fe(III) with N,N'-bis(dithiocarboxy)piperazine was studied, and follows first-order kinetics [437].

1.10 COMPLEXES WITH MIXED-DONOR LIGANDS

1.10.1 Complexes with mixed N,O donor sets

The popularity of oxo- or carboxylato-bridged binuclear Fe(III) complexes as models for the active sites of many iron-containing proteins has already been mentioned. The following examples are all directed towards the same goal, but in these cases the bridging oxygen atom is provided by, and is an integral part of, the polydentate ligand. In $[Fe_2(\mathbf{134})(PhCO_2)](BF_4)_2$ the two iron(III) centres are in trigonal bipyramidal environments, coordinated by two imidazole and

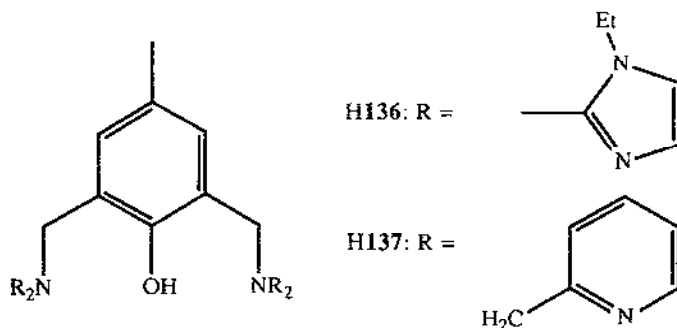
one amine nitrogen atoms and the bridging alkoxide from (134) and the bridging benzoate. The magnetic susceptibility data indicate high-spin ions with a strong antiferromagnetic coupling, which is typical of the $\text{Fe(III)}\text{-O-Fe(III)}$ core. Due to the vacant coordination site on each iron, the complex reacts irreversibly with dioxygen at -60°C to give a symmetrical bis- Fe(III) peroxo-bridged complex [438].



In $[\text{Fe(III)}_2(\text{135})_2(\text{PhCO}_2)_2][\text{ClO}_4]_2$ each iron atom is in a distorted octahedral N_3O_3 coordination environment. Unlike many other tripodal ligands, (135) does not 'face-cap'; instead the two benzimidazole and amino N-donors of each ligand bind in a planar arrangement with the imidazoles *trans* to one another. The alkoxide residues of each ligand both act as bridges, giving an $\text{Fe}_2(\text{OR})_2$ core, and each iron atom rather unusually has a terminally-bound benzoate to complete the coordination sphere. The antiferromagnetic exchange is relatively strong for an alkoxo-bridged complex. The physical and spectroscopic properties of the complex, and the spectroscopic properties of the mixed-valence Fe(II)-Fe(III) species (prepared by reduction with cobaltocene), are similar to those of methane monooxygenase, which may have a μ -alkoxo rather than a μ -oxo bridge [439]. The septadentate binucleating ligand H(136) was used to prepare the mixed-metal complex $[\text{Fe(III)Mn(II)}(\text{136})(\mu\text{-OAc})_2][\text{ClO}_4]_2$ as a model for heterobimetallic centres in purple acid phosphatase and uteroferrin. Each octahedral metal ion is 'capped' by two imidazole and an amine nitrogen atoms, and two μ -acetato bridges and the μ -phenolate bridge complete the N_3O_3 coordination spheres. Both metal centres are high-spin, giving an $S = 5$ spin state with weak antiferromagnetic coupling. The complex is electrochemically active, showing a reversible Fe(III)-Fe(II) reduction and an Mn(II)-Mn(III) oxidation [440].

In order to examine thoroughly the relationship between structural and magnetic properties in these enzyme models, four closely-related Cu(II)-Fe(III) complexes were prepared and characterised. $[\text{Cu(II)Fe(III)}(\text{137})(\text{EtCO}_2)_2][\text{PF}_6]_2$ has the expected structure with a phenolate and two propionate bridges, and each six co-ordinate metal atom face-capped by an amino and two

pyridyl nitrogen atoms. Replacement of a bridging carboxylate by a methoxide in $[\text{Cu}^{\text{II}}\text{Fe}^{\text{III}}(\mathbf{137})(\text{OAc})(\text{OCH}_3)] [\text{BPh}_4]_2$ results in several important structural changes. The

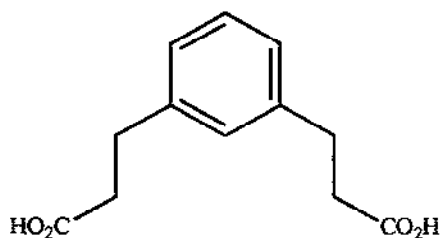
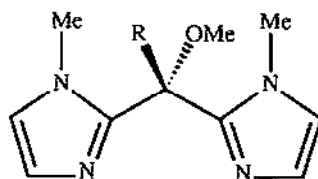


methoxide ion is bound only to the iron atom, leaving a five coordinate copper(II) centre in a square pyramidal environment with the bridging phenolate at the apex. Both metal-phenolate bonds are lengthened, resulting in a considerably increased inter-metal distance. In addition $[\text{Cu}^{\text{II}}\text{Fe}^{\text{III}}(\mathbf{137})(\text{OAc})_2][\text{BPh}_4]_2$ and $[\text{Cu}^{\text{II}}\text{Fe}^{\text{III}}(\mathbf{137})(\text{EtCO}_2)(\text{OCH}_3)][\text{BPh}_4]_2$ were also prepared; the former exhibits weak ferromagnetic coupling, having an $S = 3$ ground state, whereas the latter is antiferromagnetically coupled, with an $S = 2$ ground state [441]. In a similar vein the series of complexes $[\text{Fe}^{\text{II}}\text{M}(\mathbf{137})(\text{RCO}_2)_2][\text{BPh}_4]_x$ ($\text{M} = \text{Fe}^{\text{II}}, \text{Zn}^{\text{II}}; \text{R} = \text{Et}, \text{Ph}; x = 1; \text{M} = \text{Ga}^{\text{III}}, \text{R} = \text{Et}, x = 2$) was synthesised to serve as models for the diferrous forms of Fe-oxo protein centres. The bis-Fe(II) complex with $\text{R} = \text{Et}$ was structurally characterised, and has the expected N_3O_3 environment at each metal with a phenolate and two propionate bridges. Electronic, NMR, ESR and Mössbauer spectroscopy indicate the presence of two high-spin Fe(II) centres with ferromagnetic coupling. Most interestingly, the signal at $g = 16$ in the ESR spectrum is similar to those reported for various binuclear iron proteins in the diferrous state [442]. $[\text{Fe}^{\text{III}}\text{Ni}^{\text{II}}(\mathbf{137})(\text{EtCO}_2)_2][\text{BPh}_4]_2$ is again structurally similar to its related complexes and has been thoroughly characterised. The ground state is $S = 3/2$, from antiferromagnetic coupling between high-spin Fe(III) ($S = 5/2$) and high-spin Ni(II) ($S = 1$) [443].

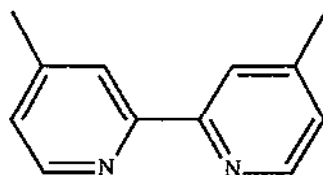
$[\text{Zn}^{\text{II}}\text{Fe}^{\text{III}}(\mathbf{137})(\text{O}_2\text{P}(\text{OPh})_2)_2][\text{ClO}_4]_2$ is a possible model for the active site of purple acid phosphatases. It contains one μ -phenoxo and two μ -diphenylphosphato bridges, and has an inter-metal distance longer than the carboxylato-bridged analogues; the cyclic voltammogram shows one reversible Fe(III)-Fe(II) reduction. The diiron analogue $[\text{Fe}^{\text{II}}\text{Fe}^{\text{III}}(\mathbf{137})(\text{O}_2\text{P}(\text{OPh})_2)][\text{ClO}_4]_2$ shows antiferromagnetic coupling, with a coupling constant similar to that of reduced interoferrin phosphate, and two reversible redox processes. Both complexes were characterised by electronic and Mössbauer spectroscopy [444].

A general method for assembling $(\mu\text{-oxo})\text{-bis-}(\mu\text{-carboxylato})\text{-diiron(III)}$ complexes containing labile, monodentate terminal ligands has been devised, using the bridging ligand $\text{H}_2(\mathbf{138})$ to provide the two carboxylate bridges. The complexes $\text{Fe}_2\text{O}(\mathbf{138})\text{L}_2\text{Cl}_2$ were thus prepared ($\text{L} = (\mathbf{139}), (\mathbf{140}), (\mathbf{141})$). Instead of the more usual face-capping of all three terminal coordination sites of each metal by a single chelating polydentate ligand, each metal is now bound

to a bidentate ligand and a (labile) chloride. These complexes mimic not only the essential structural features of the enzyme active site models, but also the coordinative unsaturation necessary for substrate binding. The crystal structures of two of the complexes ($L = (139), (141)$) show that the chloride ligands are both *cis* to the μ -oxo bond, the position where O_2 binding occurs in hemerythrin, and all complexes undergo ligand exchange reactions at the terminal coordination sites similar to those observed in μ -oxo-diiron proteins. Such complexes could not be prepared with conventional mono-carboxylate ions as bridges [445]. Instead, reaction of (139) with $Fe(OAc)_2$ gives an unusual trinuclear complex $(139)Fe(II)(\mu-OAc)_3Fe(II)(\mu-OAc)_3Fe(II)(139)$ which has been structurally characterised. The terminal $Fe(II)$ ions are in trigonal bipyramidal five coordinate environments, each bound to a bidentate (139) and three carboxylate bridges; the central $Fe(II)$ is in a near-octahedral FeO_6 environment. In each set of three bridging acetate ions two bind in the normal bidentate manner and one, very unusually, is monodentate [446].

H₂(138)

(139), R = Ph; (140), R = N-methylimidazole

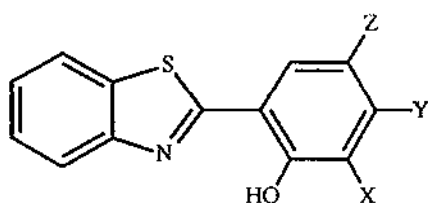


(141)

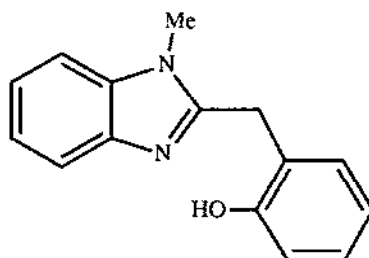
Compounds (142) and (143) are bidentate ligands with one imidazole and one phenolate donor. Their $Fe(III)$ complexes were mostly characterised as oxo-bridged binuclear species $[Fe(L)_2]_2O$ by their magnetic susceptibility and ESR behaviour, which show strong antiferromagnetic coupling. Electron-releasing ligand substituents (methyl, methoxy, or dimethylamino at positions X, Y, or Z) cause the phenolate- $Fe(III)$ charge transfer bands to move to lower energy, and the (irreversible) metal-based reductions to move to more negative potentials [447].

The six ligands (144)-(149) were synthesised as possible iron-chelating pharmaceuticals. Electronic spectroscopy and potentiometry show that at physiological pH the ligands are predominantly neutral, allowing passage through cell membranes and hence access to intracellular iron pools [448]. The stability constants with $Fe(III)$ were measured for (144), (145), (148) and

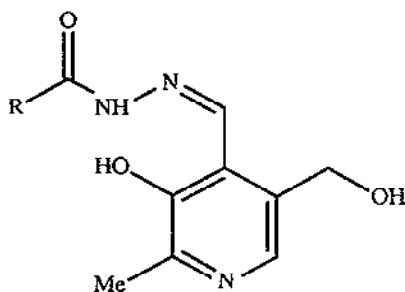
(149); at pH 7.4, all four ligands have $\log\beta$ values between 27.7 and 50. By comparison, transferrin has a $\log\beta$ value of 25.6 and desferrioxamine B, the strongest iron-chelating drug currently in use, has a $\log\beta$ value of 28.6 [449].



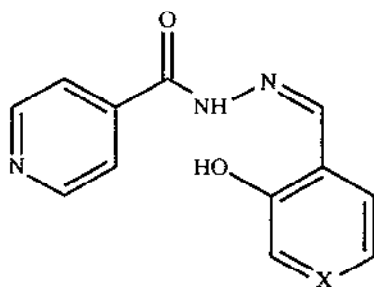
H(142) ; X, Y, Z = electron-releasing groups



H(143)



(144), R = 4-pyridyl; (145), R = phenyl
(146), R = 4-methoxyphenyl
(147), R = 3-fluorophenyl

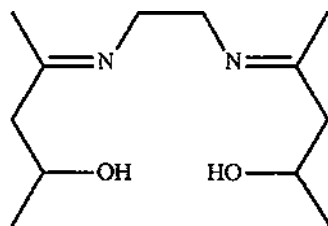
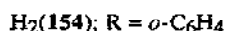
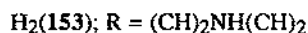
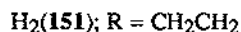
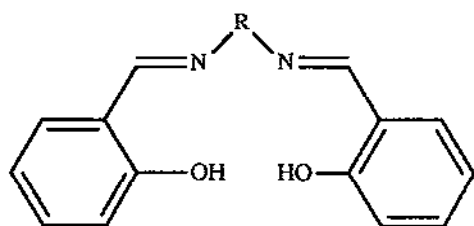
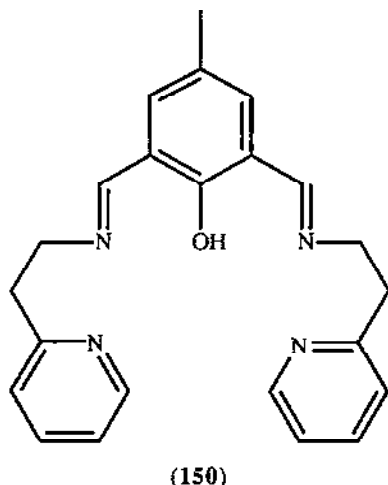


(148), X = CH; (149), X = N

Although (150) can act as a binucleating ligand, the unexpected mononuclear complex Fe(150)Cl_3 has also been isolated. The ligand is terdentate via a phenol oxygen, and imine and pyridyl nitrogen atoms bound in a *mer* configuration; the other two nitrogen atoms do not coordinate. Three chloride ions complete the octahedral coordination sphere [450].

To probe further the effects of multiatom bridges on the magnetic properties of binuclear iron complexes, $[\text{Fe(III)}_2(\text{salen})_2\text{L}]$ (salen = (151); L = oxalate, 2,5-dihydroxy-1,4-benzoquinone dianion, 3,4-dihydroxy-3-cyclobutene-1,2-dione dianion (=squarate)) have been prepared in which L acts as a bridging ligand. The complex with a squarate bridge has been structurally characterised, and contains two $[\text{Fe(III)}(\text{salen})(\text{CH}_3\text{OH})]$ units in which the salen is behaving normally as a planar N_2O_2 donor, bridged by the μ -1,3-squarate dianion. Each Fe(III) is in a distorted octahedral environment; all of the complexes are weakly antiferromagnetically coupled [451]. The mononuclear iron(III) complexes Fe(salen)NO_2 , Fe(salen)(SCN) , $\text{K[Fe(salen)(CN)}_2]$ and the binuclear complexes $[\text{Fe(salen)(NO}_3)]_2$ and $[\text{Fe(salen)}]_2\text{O}$ were prepared and studied by NMR and

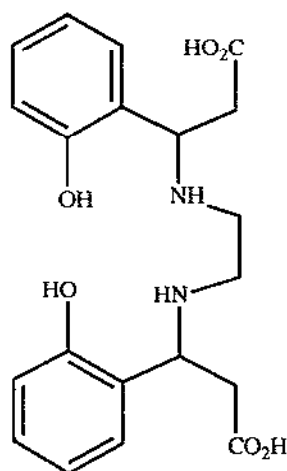
Mössbauer spectroscopy and cyclic voltammetry [452]. The behaviour of iron(III) has also been studied in the heterobinuclear complex $(\text{thf})(\text{TPP})\text{Cr}(\text{III})\cdot\text{O}\cdot\text{Fe}(\text{III})(\text{salmah})$ (salmah = **152**). Salmah is a pentadentate ligand, which effectively restricts solvation to the Cr(III) centre only. The coordinated thf may be displaced by a variety of Lewis bases; equilibrium constants for these reactions were determined. Weak antiferromagnetic coupling was observed [453]. $[\text{Fe}(\text{III})(\text{153})\text{X}]$ and $[(\text{153})\text{Fe}(\text{III})\text{ZFe}(\text{III})(\text{153})][\text{BPh}_4]_2$ ($\text{X} = \text{Cl}, \text{NCS}, \text{NCO}, \text{N}_2$, pyridine; $\text{Z} = \text{pyrazine}, 4,4'$ -bipyridine, 1,2-bis[4-pyridyl]ethene) were characterised by electronic and Mössbauer spectroscopy and magnetic moment measurements; all of the complexes are high-spin ($S = 5/2$) [454].



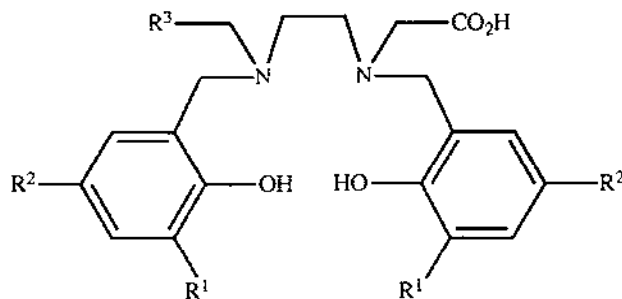
$\text{Fe}(\text{II})$ complexes of (**151**), (**154**) and (**155**) form bimetallic adducts in which the oxygen atoms act as bridges. Thus $\text{Fe}(\text{155})$ reacts with $\text{MCl}_2 \cdot (\text{thf})_n$ ($\text{M} = \text{Fe}, \text{Zn}$) to give $[(\text{thf})\text{Fe}(\text{155})\text{MCl}_2]$. The crystal structure for $\text{M} = \text{Fe}$ shows that the original iron atom is in a square pyramidal geometry coordinated by the planar tetradentate ligand with an axial thf, and the FeO_2Cl_2 centre is tetrahedral. Similarly, the crystal structure of $[\text{ClFe}(\text{154})\text{FeCl}(\text{thf})_2]$ reveals two five coordinate centres; the $\text{Fe}(\text{II})$ bound to (**154**) is in a square pyramidal environment with axial chloride, and the $\text{Fe}(\text{II})\text{O}_2\text{Cl}(\text{thf})_2$ is trigonal bipyramidal. Reaction of these $\text{Fe}(\text{II})$ complexes with

metals in a higher oxidation state results in ligand migration. Fe(155) reacts with $\text{TiCl}_4 \cdot 2\text{thf}$ to give $\text{Ti}(155)\text{Cl}_2$ and FeCl_2 , and TiCl_3 behaves similarly. The ligand migration proceeds via initial formation of a bimetallic complex through the two oxygen bridges [455].

Various iron phenolate chelates are prototype liver-enhancing agents for NMR imaging, and are transported in the blood bound to human serum albumin (HSA). $\text{Na}[\text{Fe}(\text{III})(156)]$ (both meso and racemic forms) and $\text{K}[\text{Fe}(\text{III})(157)]$ were prepared to study the relationship between structure and binding affinity with HSA. All three complexes have a *cis*- N_2O_4 geometry reminiscent of EDTA complexes, with the phenolates mutually *cis* and the carboxylates mutually *trans*; the crystal structure of $\text{K}[\text{Fe}(\text{III})(157)]$ was determined. The structure-affinity relationships were studied by dialysis and proton NMR relaxation measurements. $[\text{Fe}(157)]^-$ and racemic (RR + SS) $[\text{Fe}(156)]^-$ both bind to HSA at the same site; the *cis*-equatorial phenolate rings result in a compact, cylindrical shape which may be complementary with the binding cleft on the protein surface. By contrast the binding of *meso*- $[\text{Fe}(156)]^-$ is much weaker, since the relative orientations of the phenolate rings in this case result in a bulky shape which is less compatible with the binding site. All of the complexes show increased relaxivities for their outer protons on binding to the protein surface [456].



$\text{H}_4(156)$



$\text{H}_4(157)$: $\text{R}^1 = \text{R}^2 = \text{H}$; $\text{R}^3 = \text{CO}_2\text{H}$

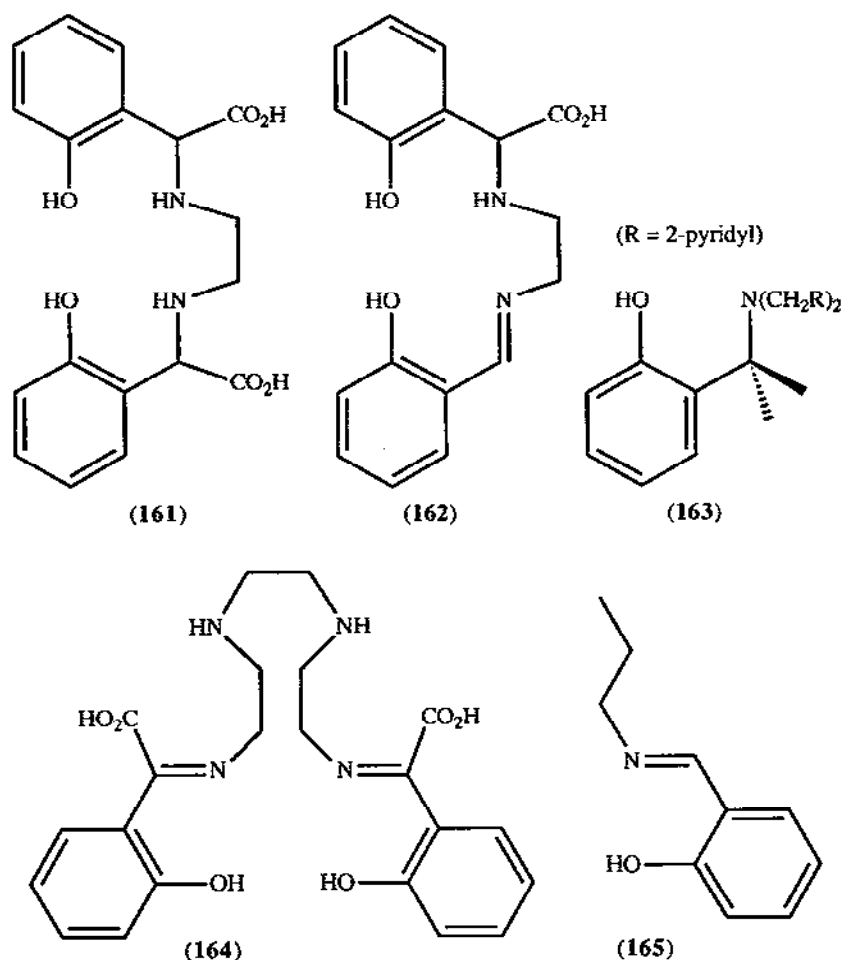
$\text{H}_4(158)$: $\text{R}^1 = \text{R}^2 = \text{CH}_3$; $\text{R}^3 = \text{CO}_2\text{H}$

$\text{H}_4(159)$: $\text{R}^1 = \text{Me}$; $\text{R}^2 = \text{tBu}$; $\text{R}^3 = \text{CO}_2\text{H}$

$\text{H}_4(160)$: $\text{R}^1 = \text{R}^2 = \text{Me}$; $\text{R}^3 = \text{CH}_2\text{OH}$

The stability constants of the complexes of $\text{Fe}(\text{III})$ with (158), (159) and (160) have been measured to determine the suitability of the ligands, which all have an 'EDTA-type' framework, as chelating agents for biological use. The ligand protonation constants and complex bio-distribution have also been examined. It was found that alkylation of the aromatic ring increases ligand basicity (as measured by the protonation constants) at the cost of decreased metal-ion affinity due to steric hindrance. The reduction of one acetate to an alcohol group in (160) decreases the affinity of the

ligand for M(III) ions by 4 to 6 orders of magnitude. The effectiveness of these and other related ligands in binding Fe(III) in aqueous media at physiological pH are compared [457]. Fe(III) complexes with the ligands (161)-(165) were prepared as models for iron proteins containing bound tyrosinate at the active site, and their resonance Raman spectra were recorded during excitation within the phenolate-to-Fe(III) charge transfer band. The spectra are dominated by phenolate vibrations; there is a correlation between the Fe-phenolate oxygen bond length and $\nu(\text{Fe}-\text{O})$. The spectra are also sensitive to the spin state of the Fe(III) [458].



The series of complexes FeL_2 (L = (166) and the derivatives depicted) all have square-planar geometries in which the N atoms are mutually *trans*, and all are low-spin ($S = 1$). Spectroscopic characterisation of the complexes revealed some interesting magnetic behaviour; they have an anomalously high magnetic moment at room temperature, but are antiferromagnetically coupled at low temperatures. Together with the Mössbauer parameters, these results indicate the presence of at least two Fe sites with both ferrimagnetic and antiferromagnetic interactions [459].

The iron complexes of the series of amides depicted in Figure 9 were prepared and characterised by ^1H NMR as simple models of the binding sites in non-heme iron proteins [460].

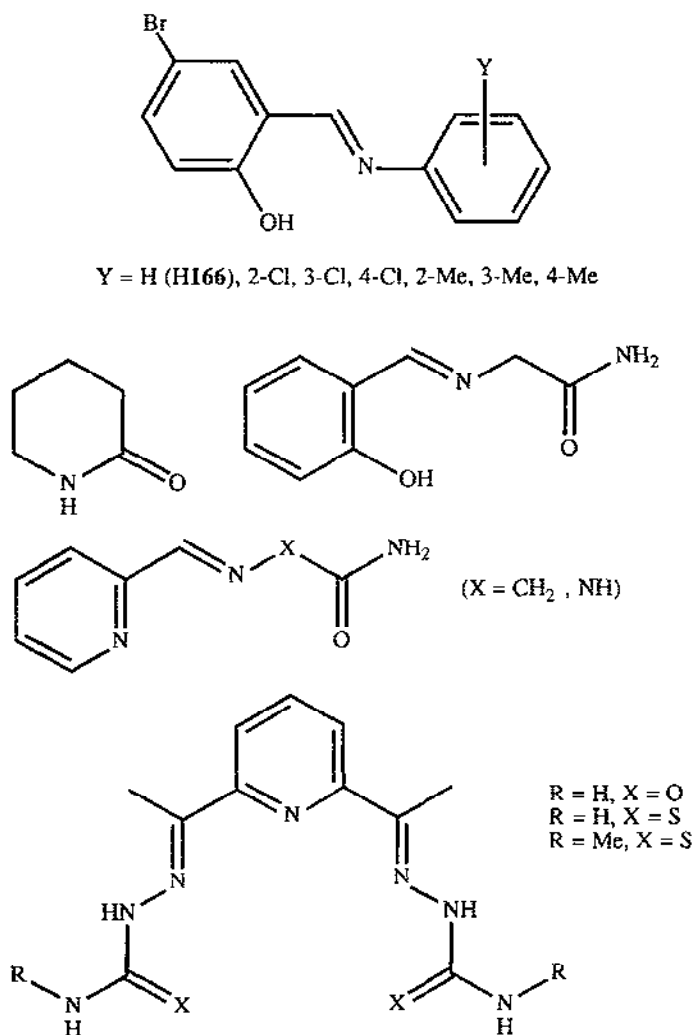
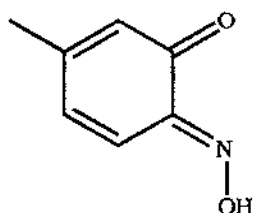
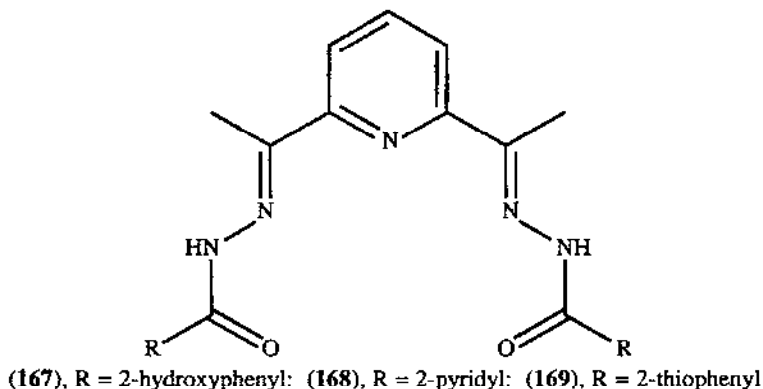


Figure 9 : Series of amides used in models of non-heme iron proteins

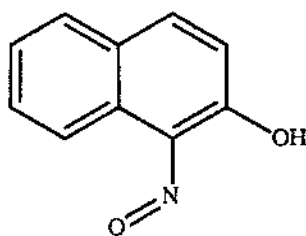
The syntheses of several mono and binuclear $\text{Fe}(\text{II})$ complexes with the bis-acyl hydrazone ligands (167), (168) and (169) have been carried out. The complexes were characterised by infrared, electronic and Mössbauer spectroscopy, and $[\text{Fe}(\text{167})\text{Cl}_2 \cdot \text{H}_2\text{O} \cdot (\text{toluene})_{0.5}]$ was crystallographically characterised. The ligand behaves as a planar pentadentate N_3O_2 donor, with two axial chloride ions giving a pentagonal bipyramidal geometry [461].

Feroverdin is a naturally occurring green pigment which is thought to contain an octahedral $\text{Fe}(\text{II})$ centre with three benzoquinone-oximate ligands (rather than the isomeric nitroso-phenolate

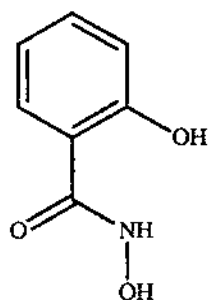
form). It has been modelled by the complex $\text{Na}[\text{Fe}(\mathbf{170})_3]$, which reacts with a variety of dications to give the trinuclear species $\text{M}[\text{Fe}(\mathbf{170})_3]_2$ ($\text{M} = \text{Mg}, \text{Ca}, \text{Mn}, \text{Fe}, \text{Co}, \text{Ni}, \text{Zn}, \text{Cd}$). Both $\text{Fe}(\text{II})$ ions are low-spin; the $\text{M}(\text{II})$ ions are octahedrally coordinated by the six oximate oxygen atoms of two *fac*- $[\text{FeL}_3]^-$ fragments and are, where appropriate, high-spin. The ability of the parent complex to bind additional metal ions in this manner may account for the reported variations in the iron content of ferroverdin [462,463]. The N_3O_3 coordination sphere in $\text{Na}[\text{Fe}(\text{II})(\mathbf{171})]$ (another ferroverdin analogue) and $\text{Fe}(\text{III})(\mathbf{171})_3$ selectively stabilises low-spin $\text{Fe}(\text{II})$ and $\text{Fe}(\text{III})$ in *fac* and *mer* geometries respectively. Mismatched combinations generated by chemical or electrochemical oxidations or reductions undergo spontaneous isomerisation to the more stable forms [463,464].



H(170)

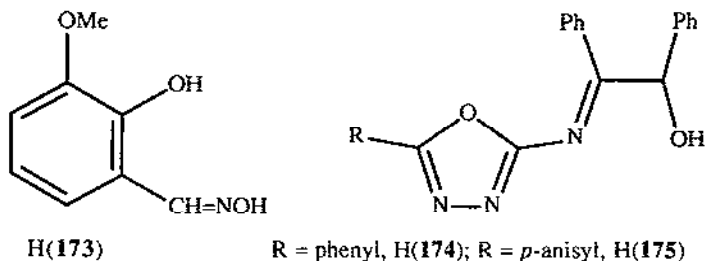


H(171)

H₃(172)

The tetranuclear cluster $\text{Fe}(\text{III})[\text{Fe}(\text{III})(\mathbf{172})(\text{CH}_3\text{OH})(\text{OAc})]_3\cdot 3\text{CH}_3\text{OH}$ has a structure which is described as an analogue of an $\text{M}(\text{III})$ -(9-crown-3) complex. Each salicylhydroximate ligand is trianionic and tetradentate, donating the carbonyl and hydroximate oxygen atoms to one $\text{Fe}(\text{III})$, and the phenolate oxygen and hydroximate nitrogen atoms to another. This results in a cyclic $(\text{Fe}-\text{O}-\text{N})_3$ arrangement of atoms, akin to a 9-crown-3 ring in which the carbon atoms are replaced by Fe and N. Unlike any other metallomacrocycles, the 'ethereal' oxygen atoms are capable of coordination to a central metal ion, in this case the central $\text{Fe}(\text{III})$. The structure is further stabilised by three μ_2 -acetato bridges between the central iron and the ring iron atoms. The

complex exhibits both intra- and inter-cluster antiferromagnetic interactions and has an $S = 5$ ground state [465].



$\text{Fe(II)}(\text{173})_2(\text{H}_2\text{O})_2$ and $[\text{Fe(III)}(\text{173})_2(\text{H}_2\text{O})_2]\text{Cl}$ are octahedral complexes in which the *o*-vanillin oxime behaves as a uninegative bidentate chelating ligand [466]. A series of complexes $\text{Fe(III)}\text{L}_3$ (L = Schiff-base ligand derived from 5-nitro or 5-chlorosalicylaldehyde) were prepared and characterised spectroscopically; they are high-spin, with the L acting as N,O donors, and have mild fungitoxic properties [467]. $\text{Fe(II)}\text{LCl} \cdot 2\text{H}_2\text{O}$ (L = (174) or (175), Schiff bases derived from benzoin and substituted oxadiazoles) are octahedral with the ligands behaving as uninegative tridentate O,N,N- donors [468].

A series of trinuclear complexes in which the dianion of dimethylglyoxime acts as bridging ligand have been prepared (figure 10). The Fe(III) at each end are in a distorted *fac*- N_3O_3 environment, coordinated by a terminal $\text{Me}_3\text{-tacn}$ ligand and three oxygen atoms from bridging dimethylglyoximates. The central M(II) (M = Mn, Fe, Co, Ni, Cu, Zn) is in an N_6 environment, with three chelating dimethylglyoxime ligands. Magnetic moment measurements show that antiferromagnetic exchange occurs between the terminal high-spin Fe(III) ions [469].

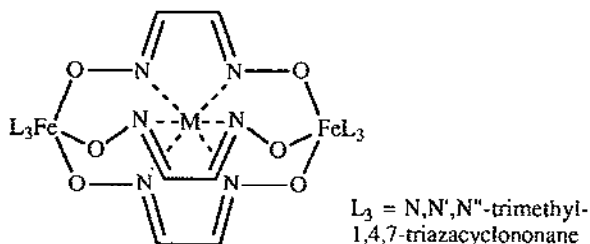
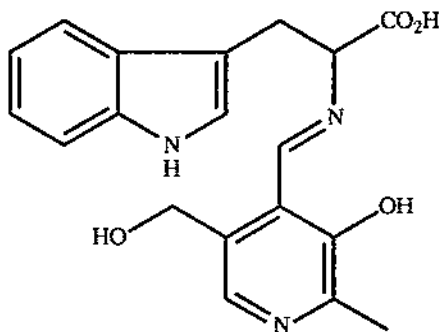


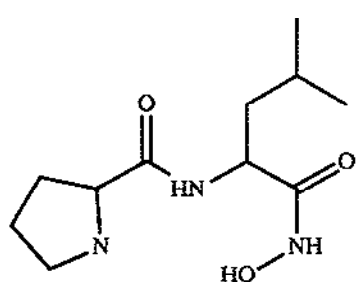
Figure 10 : Series of trinuclear $\text{Fe(III)}\text{-M(II)}\text{-Fe(III)}$ complexes

The coordination chemistry of amino acids and their derivatives is of continuing interest. The Schiff base H(176), formed by condensation of pyridoxal with L-tryptophan, forms the complex $[\text{Fe(III)}(\text{176})_2]^+$ in acidic aqueous solution; such complexes are of interest as possible reaction intermediates in the racemisation and decarboxylation reactions of amino acids in living systems. The kinetics of formation were studied by a stopped-flow circular dichroism method; complexation proceeds through six parallel pathways. Ligand displacement by EDTA was also studied kinetically [470]. The interactions of various metal ions including Fe(III) with L-prolyl-L-

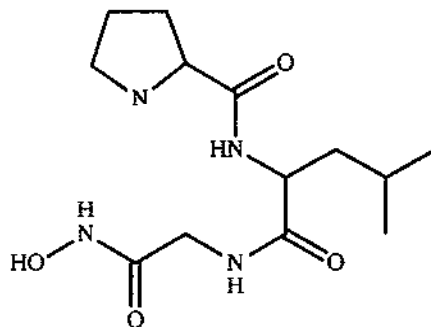
leucinehydroxamic acid and L-prolyl-L-leucyl-glycinehydroxamic acid, (177) and (178) respectively, were studied at a variety of metal:ligand ratios. (177) forms principally a 1:1 complex, and a small amount of a 2:1 ligand:metal complex in which it is assumed that hydroxo ligands are also present ('conventional' hydroxamate coordination would give a 3:1 complex). The bulkier ligand (178) formed only a 1:1 complex with Fe(III) [471]. $[\text{Fe}^{\text{II}}\text{LL}'(\text{OH})(\text{H}_2\text{O})]\text{H}_2\text{O}$ ($\text{L} = (81)$, cytosine; $\text{L}' = \text{glycinate}$) has an octahedral geometry in which both cytosine and glycinate are N,O-bidentate [472]. Cytosine also acts as a bidentate N,O ligand in the octahedral complex $[\text{Fe}^{\text{II}}\text{L}_2(\text{H}_2\text{O})]\text{X}_2$ ($\text{X} = \text{Cl}, 1/2 \text{SO}_4$) [473].



H(176)



(177)

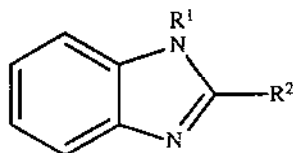
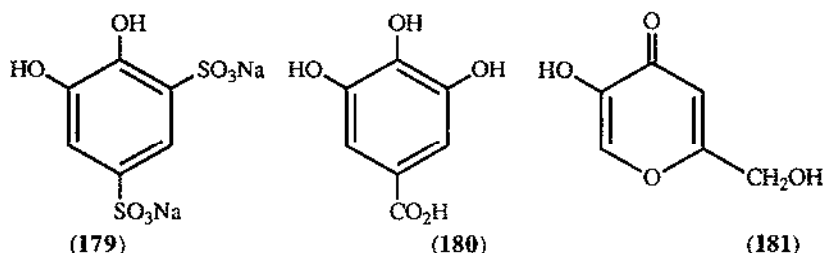


(178)

Kinetic studies have been performed on some ternary complexes of Fe(III) with a variety of N and O-donor ligands by spectrophotometric methods. The ligand systems studied are 1,10-phenanthroline with catechol, Tiron (179) or gallic acid (180) [474], ethylene diamine/catechol/EDTA [475], 1,10-phenanthroline/kojic acid (181) [476] and 1,10-phenanthroline with salicylic acid or 5-sulfosalicylic acid [477].

The ternary complexes $[\text{Fe}^{\text{III}}\text{LL}'(\text{H}_2\text{O})_n]$ ($\text{L} = (182)$ to (185), $\text{H}_2\text{L}' = \text{salicylic acid}, o\text{-hydroxyphenylacetic acid}, 3\text{-methylsalicylic acid}$) were prepared as models for the iron binding site of lactoferrin; the carboxylate donor mimics an aspartate ligand, imidazole mimics histidine and the phenol donor mimics tyrosine. The crystal structure of $[\text{Fe}(183)\text{L}'(\text{MeIm})_2]$ ($\text{H}_2\text{L}' = 3\text{-}$

methylsalicylic acid), MeIm = N-methylimidazole) reveals a *mer*-octahedral N_3O_3 donor set around the Fe(III) in which the two MeIm ligands are *cis* to one another. These model complexes have similar spectroscopic, electrochemical and reactivity properties to the transferrin enzymes [478].



H(182): $R^1 = H$, $R^2 = o\text{-C}_6\text{H}_4\text{OH}$. H(183): $R^1 = H$, $R^2 = \text{CH}_2\text{-}o\text{-(C}_6\text{H}_4\text{OH)}$
 H(184): $R^1 = H$, $R^2 = o\text{-hydroxy-}m\text{-methyl-(C}_6\text{H}_3\text{)}$. H(185): $R^1 = \text{Me}$, $R^2 = \text{CH}_2\text{-}o\text{-(C}_6\text{H}_4\text{OH)}$

The trinuclear, oxo-centred mixed-valence complex $[\text{Fe}^{\text{III}}_2\text{Fe}^{\text{II}}\text{O}(\text{OAc})_6(\text{py})_3](\text{py})$ was doped with $[\text{Fe}^{\text{III}}_2\text{Co}^{\text{II}}\text{O}(\text{OAc})_6(\text{py})_3](\text{py})$ to form $[\text{Fe}^{\text{III}}_2\text{Fe}^{\text{II}}_{0.5}\text{Co}^{\text{II}}_{0.5}\text{O}(\text{OAc})_6(\text{py})_3](\text{py})$, in order to study the effect of 'quenched disorder' in the crystal on the phase transition of the Fe_3O complex from valence-trapped to valence-detrapped. The Fe_3O and Fe_2CoO complexes were both crystallographically characterised; in both cases, the M_3O complex units and pyridine solvate molecules are alternatively stacked along the crystallographic C_3 axis. Adiabatic calorimetry, NMR spectroscopy and Mössbauer spectroscopy were all used to determine the temperature at which valence-detraping occurs in the 'disordered' Fe_3O complex [479]. The temperature-dependence of the behaviour of the mixed-valence state was also examined as a function of alkyl chain length on the bridging carboxylates, since it is known that relatively small structural changes in these trinuclear oxo-centred carboxylates may cause large changes in their delocalisation behaviour. Accordingly $\text{Fe}^{\text{III}}_2\text{Fe}^{\text{II}}\text{OX}_6(\text{py})_3$ (HX = myristic, palmitic, stearic acids) were prepared; X-ray powder diffraction indicated that all three have a layer structure. Mössbauer spectroscopy showed that all three undergo a valence-detraping phase transition. In the absence of lattice solvent molecules therefore, it is the long alkyl chains that communicate the intermolecular interactions associated with the valence delocalisation [480]. The mixed-metal complex $[\text{Fe}^{\text{III}}_2\text{Ni}^{\text{II}}\text{O}(\text{OAc})_6(\text{py})_3](\text{py})$ has been crystallographically characterised and has the expected structure with a planar Fe_2NiO core [481].

Picolinate (PA) and 2,6-pyridinedicarboxylate (DPA) complexes of Fe(II) are known to catalyse the decomposition of superoxide in aqueous media. Accordingly their electron-transfer properties and complexation with O_2 and H_2O_2 have been studied in non-aqueous media. In DMF and pyridine/acetic acid solvents, $Fe(PA)_2$ and $Fe(DPA)_2$ react with H_2O_2 and O_2 to form $L_2FeOFeL_2$, $L_2Fe(OO)$ and $L_2FeOFeL_2 \cdot H_2O_2$ ($L = PA, DPA$). Electrochemical and magnetic measurements and electronic spectroscopy elucidated the mechanism of formation of $(PA)_2FeO(OO)Fe(PA)_2$ from $(PA)_2FeOFe(PA)_2$ and H_2O_2 . This complex will oxidise methylene groups to ketones and converts diphenylacetylene to benzil, and in DMF decomposes to singlet O_2 and $(PA)_2FeOFe(PA)_2$. Kinetic data for the oxidation of $Fe(PA)_2$ and $Fe(DPA)_2$, and for reductions of $(HDP A)_2FeOFe(HDP A)_2$ are reported [482, 483]. $Fe(II)(HDP A)_2$ also reacts with molecular oxygen to give $(HDP A)_2Fe(OO)Fe(HDP A)_2$, which shows the same catalytic oxidative properties as those of the $(DPA)FeOFe(DPA)/H_2O_2$ system; for example, it oxidises cyclohexane to cyclohexanone, but in the absence of a substrate slowly decomposes to the catalytically inert $(HDP A)_2FeOFe(HDP A)_2$. In addition, the dioxygenation of catechol and benzoin parallels the activity of catechol dioxygenase enzymes [484].

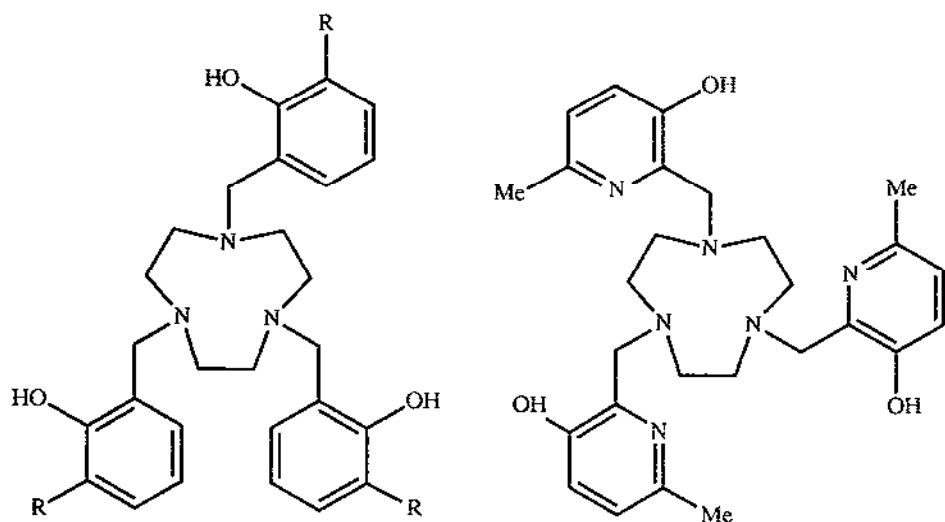
The autoxidation of Fe(II) complexes by O_2 is significantly facilitated by the presence of a chelating ligand. A detailed kinetic study was performed for the oxidation in the presence of EDTA, N-(hydroxyethyl)-ethylenediaminetriacetate, and diethylenetriaminepentaacetate as a function of complex concentration, O_2 concentration, pH, temperature and pressure. All of the observations are consistent with a mechanism in which O_2 reacts rapidly with $Fe(II)L$ to give $Fe(II)L \cdot O_2$ followed by one of three parallel reaction steps [485]. Intermediate Fe(III)-peroxo complexes have been detected by ESR in a study of $[Fe(III)(EDTA)]^-$ as a superoxide dismutase model. The reaction of $[Fe(III)(EDTA)]^-$ with H_2O_2 , $tBu\text{-}OOH$ or $nBu\text{-}OOH$ leads to a side-bound Fe(III)-peroxo complex or an end-bound hydroperoxo complex. These react further to generate an Fe(II)-superoxo species. On the basis of these observations a reaction mechanism is proposed. The existence of the complex $[Fe(III)(EDTA^{4-})(O_2^{2-})]^{3-}$ has been proposed by other workers but the mode of O_2 binding was previously uncertain [486].

An Fe(II)/EDTA complex has been covalently attached to a cysteine residue in bovine serum albumin. In the presence of H_2O_2 the iron chelate cleaves the peptide backbone at a site that is spatially adjacent but remote on the primary sequence; analysis of the fragmentation therefore gives information on the tertiary structure [487]. In a similar vein, Fe(II)/EDTA was covalently attached to a pyrimidine oligodeoxyribonucleotide which binds to the major groove of DNA and allows site-specific cleavage by the iron chelate [488].

EXAFS and XANES spectra of complexes of Fe(III) with EDTA and EDDDA ($H_4EDDDA = \text{ethylenediamine-N,N'-diacetic-N,N'-dipropionic acid}$) in neutral or weakly acidic aqueous media showed that the EDDDA complex is predominantly six coordinate, whereas the EDTA complex is predominantly seven coordinate with an additional H_2O ligand [489]. Similar results were obtained when Raman spectroscopy was used to determine the solution structures of Fe(III)-EDTA complexes at a variety of pH values. In neutral solution, these results also indicated a seven coordinate structure with a hexadentate EDTA and one coordinated water. In acidic solution one of the carboxylate groups protonates and dissociates to give a six coordinate structure with

pentadentate HEDTA and one coordinated water. In alkaline solutions an Fe-O-Fe dimer could be detected, in which each Fe(III) centre is six coordinate with a pentadentate ligand [490]. The crystal structure of $[\text{Fe}(\text{III})(\text{HEDTA})(\text{H}_2\text{O})]$ reveals a pentadentate N_2O_3 ligand with a dangling carboxylic acid group, and a water ligand completing the coordination sphere, as in acidic solution [491]. The crystal structure of $\text{Na}[\text{Fe}(\text{III})(\text{PDTA})]$ (H_4PDTA = propane-1,3-diamine-tetraacetic acid) reveals the expected N_4O_2 octahedral coordination by the hexadentate ligand [492].

The two hexadentate macrocycles $\text{H}_3(\mathbf{186})$ and $\text{H}_3(\mathbf{187})$ give monomeric, pseudo-octahedral complexes with Fe(III) (and other metal ions); $\text{Fe}(\mathbf{186})$, $\text{Fe}(\mathbf{187})$ and $\text{Fe}(\mathbf{187})(\text{Hacac})$ (Hacac = pentane-2,4-dione) were all prepared and characterised; the crystal structure of the last example reveals the expected *fac*- N_3O_3 coordination, with the pendant arms forming six-membered chelate rings. The cyclic voltammogram shows a quasi-reversible metal-based reduction. All of the Fe(III) complexes are high-spin and show phenolate-iron(III) charge-transfer bands in the visible region [493]. A potentiometric study of the interaction between Fe(III) and $\text{H}_3(\mathbf{188})$ showed that the complex has the highest stability constant at physiological pH so far reported for any artificial siderophore ($\log \beta = 49.98$) [494].



$\text{H}_3(\mathbf{186})$: R = H. $\text{H}_3(\mathbf{187})$: R = *tert*-butyl

$\text{H}_3(\mathbf{188})$

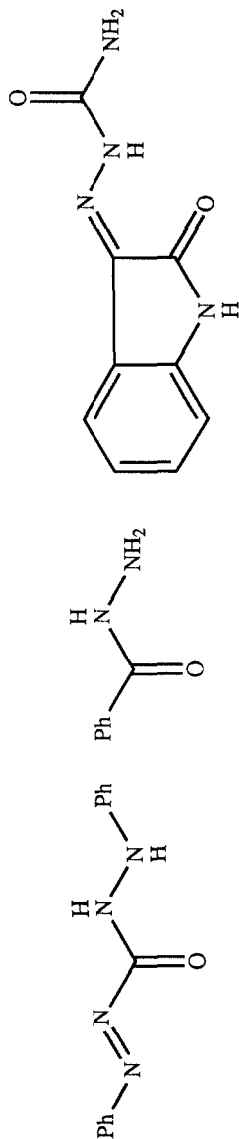
Complexes with other mixed N,O donor ligands are summarised in Table 6 [495 - 509].

Table 6 : Summary of some complexes of mixed N,O-donor ligands (N = iron oxidation state)

<u>N</u>	<u>Ligand</u>	<u>Studies performed</u>	<u>Ref</u>
2	Acetamide	[FeL ₄ (H ₂ O) ₂] ₂ prepared and characterised; the water molecules are mutually <i>trans</i>	[495]
2,3	Diphenylcarbazone (H189)	FeL ₂ and FeL ₃ prepared; IR spectra show that the Fe(II) complex is enolic, whereas the Fe(III) complex is ketonic. Both complexes are six coordinate	[496]
2,3	Benzoylhydrazide (190)	FeLCl ₃ and FeL(SO ₄).6H ₂ O prepared; L is bidentate at the CO and -NH ₂ sites	[497]
2	<i>o</i> -Aminobenzoic acid	FeL ₂ is polymeric; characterised by X-ray diffraction, IR, Messbauer and photoacoustic spectra	[498]
2	Isatin- and 5-bromoisatin-semicarbazone (H191)	FeLCl(py) ₂ .nH ₂ O prepared and characterised; both are octahedral complexes in which the anionic ligand is tridentate (two O and hydrazine N atoms)	[499]
2	Gallacetophenone phenylhydrazone (H192)	FeL ₂ (H ₂ O) ₂ prepared and characterised; IR spectra indicate that L is bidentate, through the <i>o</i> -hydroxy O and azomethine N atoms. Electronic spectroscopy indicates an octahedral geometry	[500]
3	2-[(<i>o</i> -hydroxybenzylidene)amino]phenol	Fe ₂ (μ-O)L ₂ (py) ₄ .2H ₂ O prepared and its crystal structure determined	[501]
3	5-arylazo-barbituric acid derivatives	Complexation of L with Fe(III) to give octahedral complexes (aryl = <i>p</i> -R-C ₆ H ₄ ; R = Me, MeO, CH ₃ CO, Cl, Br, I, O ₂ N, HO ₃ S, HO ₂ C)	[502]
2	Cinchonidine (193)	FeL(H ₂ O) ₂ (SO ₄) prepared and characterised; the complex has a tetragonally distorted octahedral geometry, with L behaving as a bidentate N,O chelating ligand	[503]
3	Various hydrazone -1,3-diketone ligands	Stepwise stability constants of Fe(III) complexes with several hydrazone-1,3-diketone ligands determined by pH titration	[504]
3	4-(2-pyridylazo)resorcinol (194)	Kinetics and mechanism of ligand substitution reactions of Fe(III) complexes of N(CH ₂ CO ₂ H) ₃ and N-(2-hydroxyethyl)ethylendiaminetriacetate with L as function of pH and temperature	[505]
2	Formate, urea	Fe(HCO ₂) ₂ (urea) ₂ prepared and characterised by magnetic susceptibility measurements	[506]

Table 6 continued: Summary of some complexes of mixed N,O-donor ligands (N = iron oxidation state)

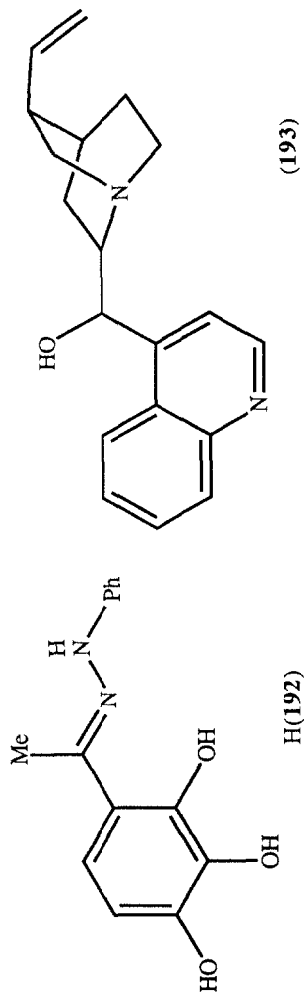
3	n-tetradecylamine	$\text{Fe(III)Mo(V)O}_4\text{Cl}(\text{C}_{14}\text{H}_{29}\text{NH}_2)_{1.7}$ prepared and characterised magnetically; the Fe(III) has $S = 3/2$. The complex is a two-dimensional Heisenberg antiferromagnet	[507]
2	(195)	L complexes to Fe(II) as a dihydroxyazo donor (O-N-O) rather than a hydroxyquinoline donor; complexation studied by electronic spectroscopy and stopped-flow kinetics	[508]
2	(196)	L complexes to Fe(II) as N-N-O terdentate donor; complexation kinetics and electronic spectra	[509]



H(189)

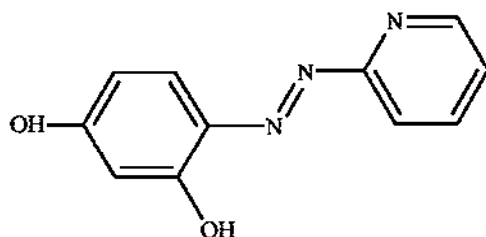
H(190)

(191)

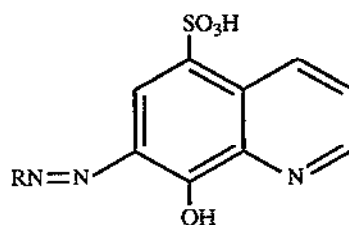


H(192)

(193)



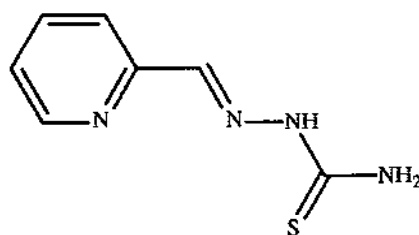
(194)

(195) (R = C₆H₃-2-(OH)-5-(CO₂H))

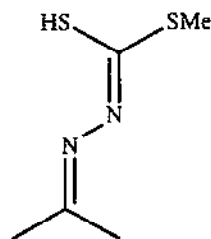
(196) (R = 8-quinolinyl)

1.10.2 Complexes with mixed N,S donor sets

2-Formylpyridinethiosemicarbazone (**H197**) is the simplest member of a series of conjugated, tridentate N,N,S donors which exhibit antitumour activity and inhibit DNA synthesis; the active forms of these drugs are thought to be their iron complexes. Mössbauer studies on [Fe(III)(**H197**)₂]³⁺, [Fe(II)(**H197**)₂]²⁺ and [Fe(II)(**197**)₂] show that all complexes are low-spin. The reducing nature of the ligand is shown by the observation from kinetic studies that either excess free ligand or a coordinated ligand may reduce Fe(III) to Fe(II) [510]. The reagent [Fe(III)(**198**)₃], where (**198**) is an anionic, bidentate N,S-donor, has been studied as a transmetalating reagent for Cu(I) tetranuclear complexes, to produce new mixed-metal clusters. Stoichiometric transmetalation of the cubanes L₄Cu₄X₄ (L = N,N'-diethylnicotinamide; X = Cl, Br) by Fe(**198**)₃ is preceded by electron transfer from Cu(I) to Fe(III) to give L₄Cu^(I)₂Cu^(II)Fe^(II)(**198**)₂X₄. This product may undergo further transmetalations with other transition-metal (Fe, Co, Ni, Cu, Zn) complexes of (**198**) to give a variety of mixed-metal binuclear and trinuclear complexes; alternatively, oxidation by O₂ generates (μ₄-O)(μ-O)L₄Cu₃Fe(OH)X₄ which can in turn undergo further transmetalations [511].

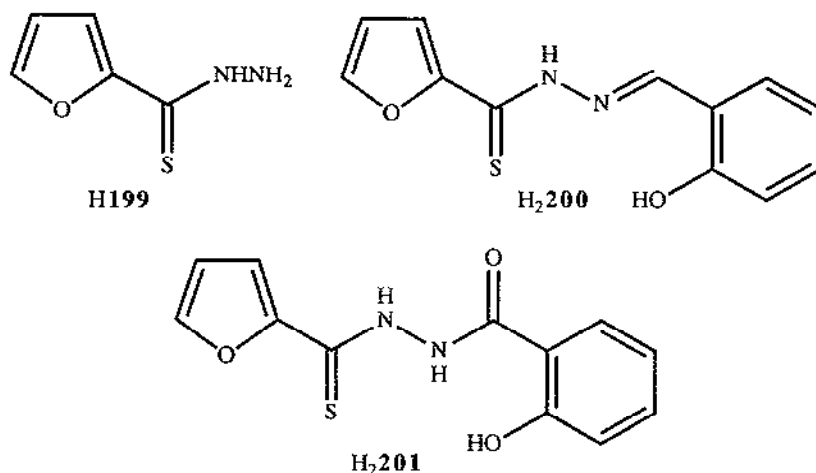


H197



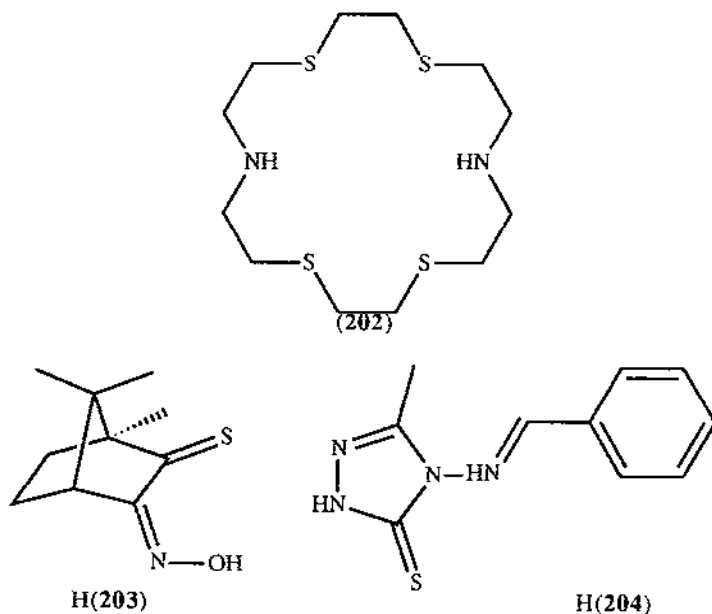
H198

The series of complexes FeL₂(CO)₂ (HL = *o*-NH₂C₆H₄SH, HSCH₂CH₂NH₂ or HSCH₂CH(NH₂)(CO₂Et)) and FeL¹(SPh)₂(CO)₂ (L¹ = ethylene diamine, 2,2'-bipyridine) were prepared. Fe(CO)₂(*o*-SC₆H₄NH₂)₂ and Fe(SPh)₂(CO)₂(en) were both crystallographically characterised and have an octahedral geometry containing two *cis*-CO ligands, two *cis*-N ligands (trans to the CO) and two *trans*-S ligands. All complexes lose CO on heating; this is partly reversible [512].

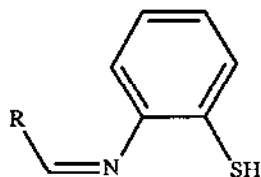


The Fe(III) complexes $[\text{Fe}(\text{H199})_2\text{Cl}_2]\text{Cl}$, $\text{Fe}(\text{H199})_3$, $[\text{Fe}(\text{H2201})_2\text{Cl}_2]\text{Cl}$, $\text{Fe}(\text{H200})\text{Cl}_2$ and $\text{Fe}(\text{H200})(\text{200})$ have been prepared and characterised. The first three all have octahedral geometries in which the ligands are bidentate N,S donors; $\text{Fe}(\text{H200})\text{Cl}_2$ is high-spin tetrahedral; and $\text{Fe}(\text{H200})(\text{200})$ is low-spin octahedral, with each ligand behaving as a tridentate N,S,O donor. $[\text{Fe}(\text{H2201})_2\text{Cl}_2]\text{Cl}$ exists as a mixture of $S = 1/2$ and $S = 5/2$ spin isomers [513].

The crystal structure of $[\text{Fe}(\text{II})(\text{202})][\text{BPh}_4]_2$ reveals a distorted octahedral geometry with the N atoms *trans*. The crystal contains a racemic mixture of stereoisomers [514].



$\text{Fe}(\mathbf{203})_2$ ($\mathbf{H203}$ = isonitrosothiocamphor) has been prepared [515]. In $\text{Fe}(\mathbf{204})_3$ the ligands behave as bidentate N,S donors; the complex is low-spin octahedral [516]. The monoanionic ligands $\mathbf{205}$, $\mathbf{206}$ and $\mathbf{207}$ all behave as bidentate N,S donors in the complexes $\text{Fe}(\text{II})\text{L}_2\text{Cl}$, $[\text{Fe}(\text{III})\text{L}_2(\text{O}^i\text{Pr})_2]$ and $\text{Fe}(\text{III})\text{L}_3$ [517]. *Trans*- $\text{Fe}(\text{dioxH})_2\text{L}_2$ (dioxH_2 - α -benzildioxime, dimethylglyoxime; L = thioacetamide, thiourea, 2-aminothiazole) all exhibit intramolecular H-bonding [518].



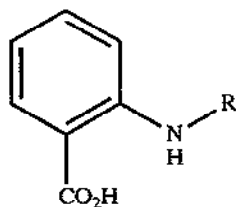
$\mathbf{H205}$: R = 2-pyridinyl

$\mathbf{H206}$: R = 2-furyl

$\mathbf{H207}$: R = 2-thienyl

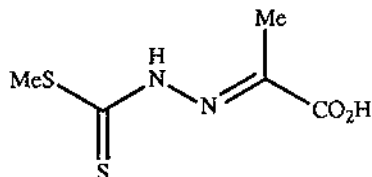
1.10.3 Complexes with other mixed-donor ligands

$\text{M}(\text{II})\text{Fe}(\text{III})_2(\text{SO}_3)_3 \cdot 6\text{N}_2\text{H}_4 \cdot 2\text{H}_2\text{O}$ (M = Mg, Mn, Co, Ni, Zn) were prepared and characterised by IR spectroscopy, and their thermoanalytical properties studied; they undergo autocatalytic decomposition at lower temperatures than the corresponding monometallic complexes [519]. The mixed-valence trinuclear clusters $[\text{Fe}_3\text{OL}_6(\text{H}_2\text{O})_3] \cdot [2\text{HL}]$, HL = the anthranilic acid derivatives $\mathbf{H(208)}$ or $\mathbf{H(209)}$, show antiferromagnetic exchange interactions [520]. $\text{Fe}(\text{II})(\mathbf{210})_2$ is octahedral, with each ligand behaving as a tridentate N,S,O donor [521]. N-(2-pyridyl)furan-2-aldehyde thiosemicarbazone ($\mathbf{211}$) and N-(2-pyridyl)thiophene-2-aldehyde thiosemicarbazone ($\mathbf{212}$) both form complexes $[\text{Fe}(\text{III})\text{LCl}_2]\text{Cl}$. Mössbauer, electronic spectral and IR spectroscopic studies show that both ligands act as tetradentate donors (N,S,N,O and N,S,N,S respectively) in the high-spin, octahedral complexes [522]. $[\text{Fe}(\text{III})(\mathbf{213})\text{Cl}]\text{Cl}$ is high-spin, with a dimeric thiolo-bridged five-coordinate structure with weak antiferromagnetic coupling [523].

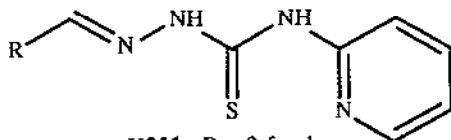


$\mathbf{H208}$: R = 3-difluoromethyl-2-thiophenyl

$\mathbf{H209}$: R = 2,3-dimethylphenyl

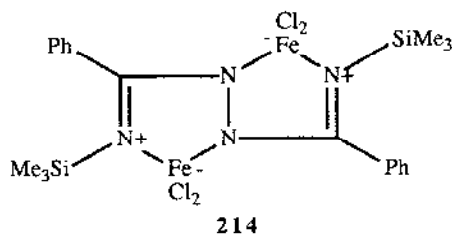
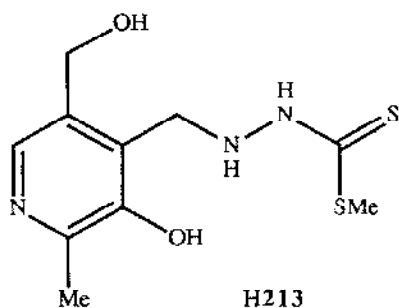


$\mathbf{H210}$

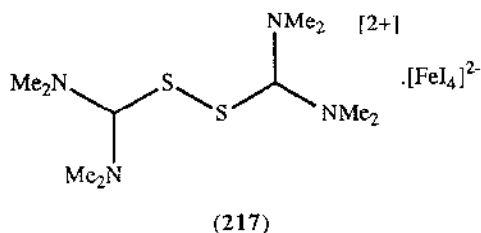
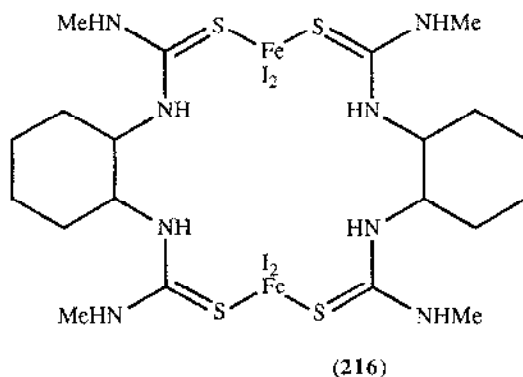
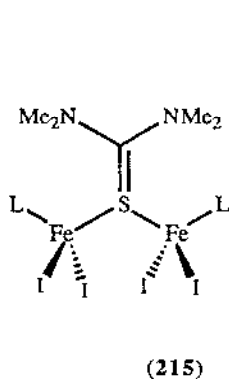


$\mathbf{H211}$: R = 2-furyl

$\mathbf{H212}$: R = 2-thienyl



$\text{Fe}^{\text{III}}(\text{L}_2\text{L}^1) \cdot n\text{H}_2\text{O}$, $\text{Fe}^{\text{III}}(\text{LL}^2) \cdot n\text{H}_2\text{O}$ and $[\text{Fe}^{\text{III}}\text{LL}^2]^+$ ($\text{HL} = \text{vitamin U}$; $\text{HL}^1 = \text{cysteine}$; $\text{HL}^2 = \text{S-methyl cysteine}$) were prepared and characterised by IR, electronic and Mössbauer spectra [524]. In $[(\text{Ph}_3\text{P})_2\text{Cu}(\text{trto})]_3\text{Fe}^{\text{III}}$ ($\text{H}_2\text{trto} = \text{trithiooxalic acid}$) each trithiooxalate ligand bridges the Cu(I) and Fe(III) centres; the precise mode of coordination is unknown [525]. In thf, Grignard reagents or Mg halides react with $\text{Fe}(\text{acac})_2$ (and other transition-metal acac complexes) to give the rather unexpected products $(\text{thf})_2\text{Mg}(\text{acac})_2\text{FeX}_2$ ($\text{X} = \text{Cl}, \text{Br}$). The Fe(II) is tetrahedral, coordinated by two *cis*-positioned oxygen atoms from the octahedral $(\text{thf})_2\text{Mg}(\text{acac})_2$ moiety and two halides [526,527]. The cyclic hydrazido bis-Fe(III) complex **214** was prepared from FeCl_3 and N,N,N'-tris(trimethylsilyl)benzamidine in CH_2Cl_2 solution. The crystal structure shows that the Fe atoms are members of two fused, planar, heterocyclic rings [528].



The ability of thiourea derivatives to stabilise neutral Fe-S clusters has been examined. Reaction of FeI_2 with 1,1,3,3-tetramethylthiourea (L) in thf gives FeI_2L_2 , which is pseudotetrahedral and has C_2 symmetry, and $\text{Fe}_2\text{L}_4\text{L}_4$ (215). 1,2-(Methylthiourea)cyclohexane (L^1) reacts with FeI_2 in acetonitrile to give $\text{Fe}_2\text{L}_4\text{L}^1_2$ (216), in which two bidentate ligands coordinate to two FeI_2 units to form an 18-membered ring, with the metal atoms in pseudotetrahedral environments. FeI_3L and I_2 react in CH_2Cl_2 to give 217, in which two ligands have coupled. All four new compounds have been crystallographically characterised [529].

Iron complexes of $\text{X}_2\text{PN(R)PX}_2$ ($\text{R} = \text{Me, Ph, X} = \text{OCH}_2\text{CF}_3, \text{OPh}$; $\text{R} = \text{Me}_2\text{CH, X} = \text{Ph}$; $\text{R} = \text{Ph, X} = p\text{-OC}_6\text{H}_4\text{Br}$) were characterised by IR and ^1H , ^{31}P and ^{13}C NMR spectra [530]. $[\text{Fe}(\text{NCS})_3(\text{Ph}_3\text{PO})_2]$ and $[\text{Fe}(\text{NCS})_3(p\text{-Tol}_3\text{AsO})_2]$ ($\text{Tol} = \text{tolyl}$) react with HgCl_2 in acetone to form $[\text{Fe}(\text{NCS})_3(\text{Ph}_3\text{PO})_2(\text{HgCl}_2)_3] \cdot 2\text{Me}_2\text{CO}$ and $[\text{Fe}(\text{NCS})_3(p\text{-Tol}_3\text{AsO})_2(\text{HgCl}_2)_3] \cdot \text{H}_2\text{O}$ respectively; all four compounds were studied by IR and ESR spectroscopy [531]. The reaction of FeCl_3 with bulky phosphine ligands PR_3 ($\text{R} = \text{cyclohexyl (Cy), CMe}_3$) afforded stable mononuclear, pseudotetrahedral adducts $\text{FeCl}_3(\text{PR}_3)$ which were characterised by standard spectroscopic and magnetic techniques. Reaction of $\text{FeCl}_3(\text{PCy}_3)$ with ethanol gave only the phosphonium salt $[\text{PHCy}_3][\text{FeCl}_4]$, whereas for $\text{R} = \text{CMe}_3$ the novel dianion $[\text{Fe}_2(\mu\text{-OEt})_2\text{Cl}_6]^{2-}$ was isolated and has been structurally characterised. The dianion exhibits five co-ordination around the two non-bonded Fe atoms, which are antiferromagnetically coupled [532]. $\text{RP}(\text{NCS})_2$ ($\text{R} = \text{Me, Ph}$) are prepared from the reaction of RPNCl_2 with AgSCN in CH_2Cl_2 . They are unstable in the absence of solvent, but form stable complexes with various transition metals; magnetic measurements and reflectance spectra suggest that in $[\text{Fe}(\text{III})\text{LCl}]\text{Cl}_2$ the ligand chelates via the P and S atoms [533].

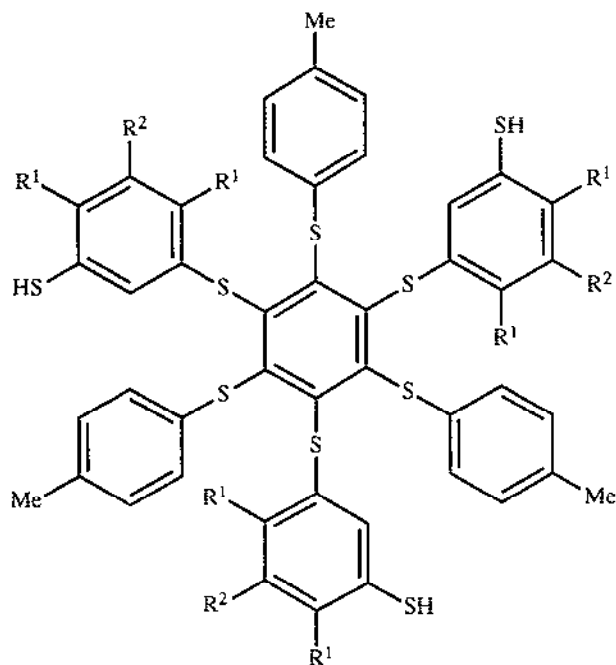
The effects of replacing S atoms by Se in dithiocarbamate complexes of $\text{Fe}(\text{III})$ were examined for FeL_3 ($\text{HL} = \text{R}_2\text{N-CXYH}$; $\text{X} = \text{S, Se}$; $\text{Y} = \text{S, Se}$). The complexes were characterised by Mössbauer and magnetic measurements at room temperature, and the results compared to the analogous complexes with $[\text{R}_2\text{N-CS}_2]^-$ and $[\text{R}_2\text{NCSO}]^-$ ligands. Several distinct trends were observed; the isomer shift values vary with donor set in the order $\text{OS} < \text{S}_2\text{-SeS-Se}_2$, the quadrupole splittings decrease in the order $\text{OS} < \text{S}_2 < \text{SSe} < \text{Se}_2$, and the magnetic moment values increase in the order $\text{OS} > \text{S}_2 > \text{SSe} > \text{Se}_2$ [534].

1.11 IRON-SULPHUR CLUSTERS

1.11.1 Fe-S cubanes

Many properties of 'native' Fe_4S_4 clusters are specific to a particular, uniquely differentiated Fe atom, which raises the problem of how one Fe 'subsite' may be chemically distinct from the other three. In order to model this behaviour, the tridentate ligand H_3 (218) was prepared and shown to bind to three of the four iron sites in $[\text{Fe}_4\text{S}_4(218)\text{Cl}]^{2-}$, thus rendering one subsite distinct. This cluster was reacted with ten different bidentate or tridentate ligands to give the products $[\text{Fe}_4\text{S}_4(218)\text{L}^1]^n$, in order to examine the effects of the high coordination number at the unique subsite, and of cluster charge, on the cluster properties. It was found that the $[\text{Fe}_4\text{S}_4]^{2+/3+}$

oxidation potentials were 300 - 700mV more negative with a polydentate L^1 than in the reference compound $[\text{Fe}_4\text{S}_4(\mathbf{218})(\text{PhS})]^{2-}$. In addition, the electron distributions in the clusters were found to be skewed towards a ferric-like unique subsite (L^1 = pyridine-2-thiolate, $\text{Me}_2\text{NCS}_2^-$, benzene-1,2-dithiolate) or a ferrous-like subsite (L^1 = 1,4,7-triazacyclononane, hydro-trispyrazolylborate) compared to the symmetrical, delocalised reference cubane. These data approximate the intrinsic effect of different ligand sets on unique subsites in native clusters [535].



$\text{H}_3(\mathbf{218})$: $\text{R}^1 = \text{Me}$, $\text{R}^2 = \text{H}$. $\text{H}_3(\mathbf{219})$: $\text{R}^1 = \text{H}$, $\text{R}^2 = \text{}^t\text{Bu}$. $\text{H}_3(\mathbf{220})$: $\text{R}^1 = \text{R}^2 = \text{H}$

The factors affecting the ability of $\text{H}_3(\mathbf{218})$ to act as a tridentate donor to Fe_4S_4 cubanes were explored. The preparation and molecular structure of the selenium analogue $[\text{Fe}_4\text{Se}_4(\mathbf{218})(\text{SEt})]^{2-}$ reveal the flexibility of the ligand, since the $[\text{Fe}_4\text{Se}_4]^{2+}$ core is approximately 10% larger than the $[\text{Fe}_4\text{S}_4]^{2+}$ core. $\text{H}_3(\mathbf{219})$ forms complexes with cubanes similar to those of $\text{H}_3(\mathbf{218})$. ^1H NMR evidence indicates that in these complexes, the steric directing effects of the ring substituents (methyl, tertiary butyl) cause the six peripheral rings to be oriented in such a way that the three thiol groups are all turned inward over the central benzene ring. These ligands are thus predisposed to a 'cavitand' conformation suitable for cubane binding. $\text{H}_3(\mathbf{220})$, which lacks these steric directing effects, gives polymeric complexes when reacted with $[\text{Fe}_4\text{S}_4(\text{SEt})_4]^{2-}$. These results are supported by detailed molecular dynamics calculations and conformational analyses of the cluster structures [536].

$[\text{Fe}_4\text{S}_4(\mathbf{218})\text{Cl}]^{2-}$ undergoes site-specific substitution reactions with a large variety of ligands. The products show trigonal symmetry by NMR spectroscopy, and have an $S = 0$ ground state in common with the starting material. By contrast, reaction with the strongly π -acidic

isonitriles RNC (L) gives $[\text{Fe}_4\text{S}_4(\mathbf{218})\text{L}_3]^-$ ($\text{R} = \text{Me}_3\text{C}, \text{Me}, \text{Et}, \text{C}_6\text{H}_{11}, 2,6\text{-Me}_2\text{C}_6\text{H}_3$). Mössbauer spectroscopy shows that the cluster with $\text{R} = \text{Me}_3\text{C}$ contains a unique, six-coordinate low-spin Fe(II) subsite, and a spin-isolated $[\text{Fe}_3\text{S}_4]^0$ fragment which is electronically very similar to some naturally occurring Fe_3S_4 clusters. This fragment has an $S = 2$ ground state arising from antiferromagnetic exchange between a high-spin Fe(III) ($S = 5/2$) and a delocalised Fe(II)/Fe(III) pair with $S = 9/2$. Localisation within the Fe_3S_4 fragment to a trapped-valence Fe(III) site and a delocalised Fe(II)-Fe(III) pair occurs below 260K. The occurrence of this delocalised pair/Fe(III) ground state in several proteins as well as this model strongly suggests that the state is an intrinsic property of the $[\text{Fe}_3\text{S}_4]^0$ cluster core, and not induced by the protein. By comparison, site-specific substitution of $[\text{Fe}_4\text{S}_4(\mathbf{218})\text{Cl}]^{2-}$ with cyanide gives $[\text{Fe}_4\text{S}_4(\text{LS}_3)(\text{CN})]^{2-}$, with only one extra ligand binding at the unique Fe(II) site [537, 538]. Reaction of the non-site-differentiated analogue $[\text{Fe}_4\text{S}_4\text{Cl}_4]^{2-}$ with Me_3CNC gives $\text{Fe}_4\text{S}_4\text{Cl}_2(\text{Me}_3\text{CNC})_6$, in which two of the Fe sites are in tetrahedral S_3Cl geometries and the other two are in octahedral S_3L_3 environments; each of these latter Fe sites is identical by Mössbauer spectroscopy to the unique FeS_3L_3 site in $[\text{Fe}_4\text{S}_4(\mathbf{218})\text{L}_3]^-$ [538].

In order to examine the factors which stabilise the water-sensitive $[\text{Fe}_4\text{S}_4]^{3+}$ core of the high-potential iron-sulphur proteins in the 3+ oxidation state, a series of Fe_4S_4 clusters with attached dipeptides (containing cysteine and a hydrophobic amino-acid residue) were examined electrochemically. It was found that the resistance to decomposition of the 3+ state correlates with the hydrophobicities of the amino acids in the ligand envelope, and that the redox potentials become more positive as the electron-releasing ability of the coordinated cysteinyl groups decreases [539]. The effects of solvent (in terms of donor number, DN, and acceptor number, AN) on the redox properties of Fe_4S_4 clusters was also examined; the redox potentials correlate well with a linear combination of solvent DN and AN [540]. Also, the redox potential values of a variety of Fe_4S_4 clusters are linearly related [541].

The high-potential iron protein model $[\text{Fe}_4\text{S}_4(\text{S-2,4,6-}(\text{iPr})_3\text{C}_6\text{H}_2)_4]^-$, in which the Fe_4S_4 core is in the +3 oxidation state, was prepared by controlled-potential electrolysis of the +2 analogue and studied by variable temperature magnetic susceptibility. It obeys the Curie-Weiss law between 5 and 15K, but at higher temperatures antiferromagnetic coupling appears. The data could be fitted accurately with a theoretical model. The $J[\text{Fe(III)}-\text{Fe(III)}]$ and $J[\text{Fe(III)}-\text{Fe(II)}]$ coupling constants are somewhat higher than normal, due to the contraction of the Fe_4S_4 core on oxidation [542]. $[\text{Fe}_4\text{Cp}_4\text{S}_4]$ is part of five-member redox series. It was oxidised to the +1, +2 and +3 oxidation states by controlled-potential electrolysis, and the products were characterised by electronic spectroscopy [543]. $[\text{Cp}^*_2(\text{Ph}_2\text{C}_2\text{S}_2)_2\text{Fe}_4\text{S}_4]$, which contains two dithiolene ligands, has been prepared and crystallographically characterised. The Fe_4S_4 core is highly distorted, and has a structure consistent with localisation of Fe-Fe bonds, with three long and three short contacts. It is part of a five-member redox chain comprising the +2, +1, 0, -1 and -2 oxidation states [544].

Fe_4S_4 cubanes have been inserted into a series of macrocyclic surrounds which contain pendant thiol groups (Figure 11); a variety of macrocycle sizes and links between the ligand skeleton and the thiol groups have been employed [545, 546, 547]. This results in a positive shift of the -1/-2 redox couple compared to other cubanes, and stabilises the core towards reactions with

to an extent which depends on the macrocyclic ring size and the 'goodness of fit' of the Fe_4S_4 core within the shielding macrocyclic cavity [546]. Some of the clusters with a 36-membered macrocyclic surround are capable of electrochemical reduction of CO_2 to formate, at a potential 700mV less negative than that normally required for CO_2 reduction [547]. A similar set of encapsulated Fe_4S_4 cubanes contain four phenyl rings in the 38-membered macrocyclic chain, giving a hydrophobic, cyclophane-like exterior to the complexes [548].

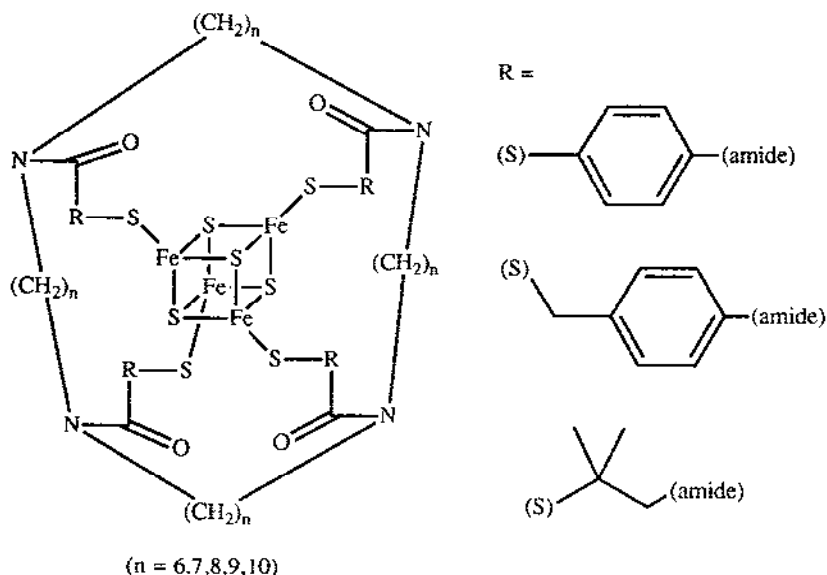


Figure 11 : Fe_4S_4 cubanes encapsulated in macrocycles

$\text{A}_2[\text{Fe}_4\text{S}_4\text{Cl}_4]$ ($\text{A} = \text{Et}_4\text{N}$, Bu_4N) reacts with Li_2S to give $\text{A}_4[(\text{Fe}_4\text{S}_4\text{Cl}_3)_2\text{S}]$, a sulphide-bridged dicubane. The crystal structure ($\text{A}_4 = [\text{Ph}_4\text{P}]_2[\text{Bu}_4\text{N}]_2$) shows that the tetraanion consists of a $(\mu_2\text{-S}^{2-})$ -singly bridged double cubane with C_2 symmetry, and has a structure very similar to that proposed for the active site of some nitrogenase enzymes [549].

The crystal structure of $[\text{Fe}(\text{DMF})_6][\text{Bu}_4\text{N}]_2[\text{Fe}_4\text{S}_4\text{Br}_4]_2$ has been determined; the anion has the expected cubane structure [550]. Reaction of the polymeric species $\{(\text{Ph}_4\text{P})_2[\text{Fe}_4\text{S}_4(\text{tmbdt})_2]\}_n$ ($\text{H}_2\text{tmbdt} = 2,4,6$ -trimethylbenzene-1,3-dithiol) with $\text{Mo}(\text{V})\text{OCl}_3(\text{thf})_2$ gives a molybdenum-oxo-containing agglomerate $\{(\text{Ph}_4\text{P})_2[\text{Fe}_4\text{S}_4(\text{tmbdt})_2(\text{Mo}(\text{V})\text{O})_{0.76}]\}_n$, in which the $[\text{Mo}(\text{V})\text{O}]^{3+}$ cation is coordinated to the sulphur ligands binding the $[\text{Fe}_4\text{S}_4]^{2+}$ core. The agglomerate exhibits catalytic activity for the reduction of azobenzene to hydrazobenzene, and phenylacetylene to phenylethylene, by $[\text{Et}_4\text{N}][\text{BH}_4]$ [551]. $[\text{Et}_4\text{N}]_2[\text{Fe}_4\text{S}_4(\text{S}_2\text{CNEt}_2)_4]$ has been synthesised under anaerobic, anhydrous conditions. The crystal structure shows the cubane-like Fe_4S_4 core, with a disulphide chelate on each Fe atom. The Mössbauer, IR, electronic and X-ray photoelectron spectra are reported, as well as the electrochemical properties [552].

1.11.2 Heterometallic cubanes

$[\text{Mo}_2\text{Fe}_2\text{S}_4(\text{S}_2\text{CNEt}_2)_5]\cdot\text{MeCN}$ contains the cubane-like $\text{Mo}_2\text{Fe}_2\text{S}_4$ core, with each metal atom attached to a bidentate chelating disulphide ligand. In addition, a fifth $[\text{S}_2\text{CNEt}_2]^-$ ligand bridges the two Mo atoms, which are therefore both six coordinate; the Fe atoms are five coordinate. The $\text{Mo}_2\text{Fe}_2\text{S}_4$ core has a formal oxidation level of +5 [553]. X-ray photoelectron and Mössbauer spectroscopy, and comparison of the M-S bond lengths, suggest that both Mo centres have the same oxidation state (formally +4) whereas the Fe centres are different (+2 and +3) [554]. $[\text{MoFe}_3\text{S}_4(\text{S}_2\text{CNMe}_2)_5]\cdot 2\text{CH}_2\text{Cl}_2$ has a similar structure, with the fifth chelating disulphide ligand bridging the Mo atom and an Fe atom. The synthesis is described as a spontaneous self-assembly from $\text{Na}(\text{Me}_2\text{NCS}_2)$, FeCl_2 and $(\text{NH}_4)_2\text{MoS}_4$ in which the coordination behaviour of the bidentate dithiocarbamate ligands is responsible for the formation of the single-cubane structure. In addition a series of clusters $[\text{MFe}_3\text{S}_4(\text{R}_2\text{NCS}_2)_x]^{n-}$ ($\text{M} = \text{Mo}, \text{W}, \text{Fe}$; $x = 4, 5, 6$; $n = 0, 1$; $\text{R}_2 = \text{Me}_2, \text{Et}_2, \text{C}_4\text{H}_8, \text{C}_5\text{H}_{10}$) was prepared, which has allowed the formation of oxidation levels of +4, +5 and +6 for the MoFe_3S_4 core in addition to the previously reported +2 and +3 levels. A comparison of the structural parameters of seven members of the series, whose structures had been previously reported, was performed. The clusters were characterised by Mössbauer and NMR spectroscopy and cyclic voltammetry. In the $[\text{MoFe}_3\text{S}_4]^{5+}$ core, each Fe(III) interacts magnetically with the other metals in the core; in the reduced $[\text{MoFe}_3\text{S}_4]^{4+}$, the extra electron is delocalised over all four metals [555].

$[\text{Mo}_3\text{FeS}_4(\text{H}_2\text{O})_{10}]^{4+}$ has been prepared from Fe metal and $[\text{Mo}_3\text{S}_4(\text{H}_2\text{O})_9]^{4+}$; it has a four coordinate Fe site and six coordinate Mo sites. The solution magnetic susceptibility shows two unpaired electrons, but the complex is ESR silent; the Mössbauer spectrum is consistent with a high-spin Fe(III) centre, antiferromagnetically coupled to the Mo atoms giving an overall spin-state of zero. Reaction with chloride ion produces $[\text{Mo}_3\text{S}_4(\text{H}_2\text{O})_9\text{Cl}]^{3+}$, from ligand substitution at the tetrahedral Fe site. Oxidations with $[\text{NH}_4][\text{Co}(\text{III})(\text{DPA})_2]$ (DPA = dianion of 2,6-dipicolinic acid) and $[\text{Fe}(\text{H}_2\text{O})_6]^{3+}$ were also examined [556]. $[\text{Mo}_3\text{FeS}_4(\text{H}_2\text{O})_{10}]^{4+}$ reacts with O_2 in solution to give $[\text{Mo}_3\text{S}_4(\text{H}_2\text{O})_9]^{4+}$ and Fe(II) in a two-electron redox process. The mechanism was determined by spectrophotometric and kinetic studies [557].

The nature of substrate binding to a double cubane core has been examined. The reaction of $\{[\text{MoFe}_3\text{S}_4\text{Cl}_2(\text{Cl}_4\text{cat})]_2(\mu_2\text{-S})(\mu_2\text{-OH})\}^{5-}$ ($\text{H}_2\text{Cl}_4\text{cat} = \text{tetrachlorocatechol}$) with $\text{N}_2\text{H}_5\text{Cl}$ or R_3SiCN gave $\{[\text{MoFe}_3\text{S}_4\text{Cl}_2(\text{Cl}_4\text{cat})]_2(\mu_2\text{-S})(\mu_2\text{-X})\}^{4-}$ ($\text{X} = \text{N}_2\text{H}_4$ or CN respectively). The basic dicubane structure is flexible enough to be able to accommodate bridging ligands with very different steric requirements between the two Mo binding sites. This illustrates the feasibility of introducing nitrogenase substrates (such as N_2H_4) in an end-to-end bridging mode within two cubane subunits at the enzyme active site [558].

$[\text{Mo}_2\text{Fe}_7\text{S}_8(\mu\text{-SEt})_6(\text{SEt})_6]^{3-}$ contains two MoFe_3S_4 core units with a $\text{Mo}(\mu\text{-SEt})_3\text{Fe}(\mu\text{-SEt})_3\text{Mo}$ bridge; its reaction with ethyl cysteinate hydrochloride was followed by ^1H NMR spectroscopy, since cysteine is the amino acid which most commonly ligates to iron-sulphur clusters in biological systems. The initial product is the terminal chloride-substituted cluster $[\text{Mo}_2\text{Fe}_7\text{S}_8(\mu\text{-SEt})_6\text{Cl}_6]^{3-}$, which reacts further to form a novel terminal cysteinate-substituted

cluster $[\text{Mo}_2\text{Fe}_7\text{S}_8(\mu\text{-SEt})_6\text{L}_6]^{3-}$ (HL = cysteine) [559]. The iron-bridged dicubanes $[\text{Mo}_2\text{Fe}_7\text{S}_8(\text{SR})_{12}]^{4-}$ (R = Ph, *o*-, *m*-, *p*- tolyl) were prepared and spectroscopically, electrochemically and structurally (R = Ph, *m*-tolyl) characterised; different thiolato ligands only cause significant structural variation at the $\text{Fe}(\text{SR})_6$ bridge. ^1H NMR spectroscopy and magnetic susceptibility measurements indicate virtually no magnetic interaction amongst the three magnetic centres, i.e. an $\text{Fe}(\text{SR})_6$ bridge and two isolated $[\text{MoFe}_3\text{S}_4(\text{SR})_3]$ units. Reaction with acyl chloride in acetonitrile yields $[\text{Mo}_2\text{Fe}_6\text{S}_8\text{Cl}_6(\text{SR})_3]^{3-}$, in which the iron bridge has been removed; this is the first example of such a chemical conversion. The compound (R = *o*-tolyl) has been structurally characterised; unlike the variation of thiolate substituents, the presence of terminal chlorides induces structural changes over the whole cluster. In addition, the very similar differences of $E_{p,c}$ for the first and second cubane units in $[\text{Mo}_2\text{Fe}_7\text{S}_8(\text{SR})_{12}]^{4-}$ and $[\text{Mo}_2\text{Fe}_6\text{S}_8(\text{SR})_9]^{3-}$ imply that both structural types show the same degree of synergism between the two core subunits. Synergism in Fe-Mo-S clusters is thus proposed to play an important role in their structure-reactivity relationships [560, 561].

An MoFe_3S_4 core has been inserted into macrocyclic tetrathiol ligands (Figure 12); the bridged Mo-SR group is shown for the first time to be reactive toward nucleophiles [562].

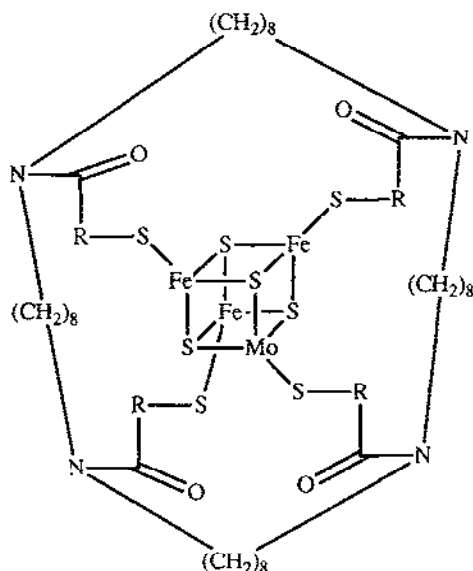


Figure 12 : Macrocycle-encapsulated MoFe_3S_4 cluster (R = CH_2CH_2 , *p*- C_6H_4)

An extension of the heterometal MFe_3S_4 series is provided by synthesis of three rhenium analogues. $[\text{Re}_2\text{Fe}_6\text{S}_8(\text{SEt})_9]^{3-}$ contains two cubane-type ReFe_3S_4 cores, bridged through the Re atoms by three $\mu_2\text{-SEt}$ bridges, and has a 5-member electron transfer series. $[\text{Re}_2\text{Fe}_7\text{S}_8(\text{SEt})_{12}]^{2-}$ and $[\text{Re}_2\text{Fe}_7\text{S}_8(\text{SEt})_{12}]^{4-}$ both contain trigonal $(\mu_2\text{-SEt})_3\text{-Fe(II)}-(\mu_2\text{-SEt})_3$ bridges between the Re atoms of the cubane subunits, which are in oxidation states +4,+4 and +3,+3 respectively. Both clusters are parts of a 4-member redox series. $[\text{Re}_2\text{Fe}_6\text{S}_8(\text{SEt})_3(\text{SPh})_6]^{3-}$ and

$[\text{Re}_2\text{Fe}_7\text{S}_8(\text{SEt})_6(\text{SPh})_6]^{2-}$ were prepared by displacement of terminal $[\text{SEt}]^-$ by $[\text{SPh}]^-$ [563]. Linear $\text{Fe}_3(\mu_2\text{-Q})_4(\text{SET})_4]^{3-}$ ($\text{Q} = \text{S}, \text{Se}$) reacts with $\text{Ni}(\text{PPh}_3)_3$ to give the heterometallic cubane $[\text{Fe}_3\text{Ni}(\mu_3\text{-Q})_4(\text{PPh}_3)_n(\text{SET})_{4-n}]^{(3-n)-}$ ($n = 0, 1$) which were characterised by X-ray crystallography, NMR, ESR and Mössbauer spectroscopy and magnetic susceptibility measurements [564]. Reaction of $(\text{Et}_4\text{N})_2\text{WS}_4$, FeCl_2 and NaS_2CR_2 ($\text{R}_2 = \text{pyrrolidino}$) yields $[\text{WFe}_3\text{S}_4(\text{S}_2\text{CR})_5] \cdot 2\text{DMF}$ which was crystallographically characterised. The Mössbauer spectrum indicates two types of iron atom in a 2:1 ratio [565].

$[\text{Fe}_4\text{Te}_4(\text{SPh})_4]^{3-}$ has been prepared and crystallographically characterised, and has a cubane core structure. The ground state has $S = 3/2$, arising from (formally) three $\text{Fe}(\text{II})$ centres and one $\text{Fe}(\text{III})$; the ESR and NMR properties of the cluster are discussed. The increased Fe-Fe distance in the $[\text{Fe}_4\text{Te}_4]^+$ core compared to $[\text{Fe}_4\text{S}_4]^+$ and $[\text{Fe}_4\text{Se}_4]^+$ result in a smaller antiferromagnetic coupling [566].

1.11.3 Other iron-sulphur clusters

The anion $[\text{Fe}_2(\mu\text{-S}_2\text{O}_3)_2(\text{NO})_4]^{2-}$, in which the two Fe centres are bridged by two $(\mu_2\text{-}\eta^1\text{-S})$ thiosulphates, was prepared and structurally characterised as the $[\text{PPN}]^+$ salt. It adopts a conformation in which the two pendant SO_3 groups lie in a *trans* arrangement on opposite sides of the Fe_2S_2 ring. ^{15}N NMR spectroscopy confirmed that this conformation is maintained in solution. The dianion reacts with RSH to give good yields of $\text{Fe}_2(\mu\text{-SR})_2(\text{NO})_4$ [567, 568]. $\text{Na}_2[\text{Fe}_2(\text{S}_2\text{O}_3)_2(\text{NO})_4]$ reacts with Na_2S in water (i.e. SH^-) to give a mixture of $\text{Na}_2[\text{Fe}_2\text{S}_2(\text{NO})_4]$ (which might be expected by analogy with the thiol reactions) and $\text{Na}[\text{Fe}_4\text{S}_3(\text{NO})_7]$, which are easily separated since only the latter is soluble in ether. These compounds are, respectively, the red and black Roussin salts. $\text{Na}[\text{Fe}_4\text{S}_3(\text{NO})_7]$ reacts with arene diazonium salts $[\text{RN}_2][\text{BF}_4]$ and the alkylating agents $[\text{R}_3\text{O}][\text{BF}_4]$ ($\text{R} = \text{Me}, \text{Et}$) to give $[\text{Fe}_2(\mu\text{-SR})_2(\text{NO})_4]$. However reaction with $[\text{Me}_3\text{S}][\text{BF}_4]$ or $[\text{Me}_3\text{SO}][\text{BF}_4]$ results only in cation metathesis. The crystal structure of $[\text{Me}_3\text{S}][\text{Fe}_4\text{S}_3(\text{NO})_7]$ was determined; there is no incipient cubane formation due to cation/anion interaction. The structural parameters are compared with those from other structural determinations of $[\text{Fe}_4\text{S}_3(\text{NO})_7]^-$ with different cations [568].

The electrochemical behaviour of some of these Fe-S-NO compounds has been examined. $\text{Fe}(\text{SR})_2(\text{NO})_4$ ($\text{R} = \text{alkyl}$) undergoes two reversible, one-electron reductions to the mono and dianion; the monoanion was characterised by ESR spectroscopy, and the reactivity of the dianion with trialkyl phosphites was studied. $[\text{Fe}_2\text{S}_2(\text{NO})_4]^{2-}$ undergoes two, reversible, one-electron reductions; for $[\text{Fe}_2(\text{S}_2\text{O}_3)_2(\text{NO})_4]^{2-}$ only the first reduction is reversible whereas $[\text{Fe}_4\text{S}_3(\text{NO})_7]^-$ undergoes three, reversible one-electron reductions. In all cases the oxidations are complex and irreversible. $[\text{Fe}(\text{NO})(\text{S}_2\text{CNR}_2)_2]$ loses NO after its one-electron reduction [569]. $\text{Fe}(\text{SO}_4) \cdot 7\text{H}_2\text{O}$, NaNO_2 and cysteine react to give $[\text{Fe}_4\text{S}_3(\text{NO})_7]^-$, which can only arise from cleavage of C-S bonds in cysteine; the yield of the reaction is improved if sodium ascorbate is added to the reaction mixture. S is similarly captured from several other molecules such as cysteine derivatives, aminopenicillanic acid and thiourea [570].

Reaction of $(\text{NH}_4)_2\text{MoS}_4$ and FeCl_3 with $\text{HOCH}_2\text{CH}_2\text{ONa}$ in ethylene glycol (L) solution followed by treatment with Bu_4NBr gives the trinuclear heterometallic cluster $[\text{Bu}_4\text{N}]_3[\text{Mo}_2\text{FeS}_8\text{O}] \cdot \text{L}$ which was characterised crystallographically and by the standard spectroscopic methods. The anion consists of an Fe atom bonded to an MoS_4 unit via two S^{2-} bridges, and to a $\text{MoOS}_2(\text{S}_2)$ unit also by two S^{2-} bridges. In addition there are two Fe-Mo bonds. The cluster catalytically reduces C_2H_2 in the presence of KBH_4 [571].

A new model for the interpretation of Mössbauer parameters in reduced $[\text{Fe}_3\text{S}_4]^0$ clusters has been proposed [572].

The 'basket' cluster $\text{Fe}_6\text{S}_5(\mu\text{-SPh})(\text{PBu}_3)_4(\text{SPh})_2$ was prepared by the reaction of $[\text{Bu}_4\text{N}]_2[\text{Fe}_4\text{S}_4(\text{SPh})_4]$ with $\text{Fe}(\text{SPh})_2(\text{PBu}_3)_2$ in acetonitrile/thf. The crystal structure shows the presence of an $[\text{Fe}_6\text{S}_6]^+$ core, consisting of six Fe_2S_2 units fused into the form of an Fe_6S_5 basket by sharing edges with an Fe-S(Ph)-Fe bridge as the handle. All six Fe atoms are tetrahedrally coordinated, with formal oxidation states of five Fe(II) and one Fe(III) [573, 574]. The electrochemical behaviour and NMR and ESR spectra are discussed [574].

The synthesis and characterisation of a series of Fe_6S_6 'prismanes' has been described. $[\text{Fe}_6\text{S}_6(p\text{-R-C}_6\text{H}_4\text{O})_6]^{3-}$ ($\text{R} = \text{OMe}, \text{NMe}_2, \text{COMe}$) have a rhombic dodecahedral core, which may be envisaged as consisting of two Fe_3S_3 puckered 'chairs' sitting one on top of the other, with a *p*-substituted phenolate is attached to each iron atom. The crystal structure of $[\text{Et}_4\text{N}]_3[\text{Fe}_6\text{S}_6(p\text{-MeO-C}_6\text{H}_4\text{O})_6]$ has been determined. The three S atoms in each face of the prism can act as a tridentate, face-capping donor set to other metals. This has allowed synthesis of the adducts $[\text{Fe}_6\text{S}_6(p\text{-R-C}_6\text{H}_4\text{O})_6\{\text{M}(\text{CO})_3\}_2]^{n-}$ ($\text{M} = \text{Mo}, n = 3, \text{R} = \text{Me}, \text{OMe}, \text{NMe}_2$; $\text{M} = \text{W}, n = 3, \text{R} = \text{Me}$; $\text{M} = \text{Mo}, n = 4, \text{R} = \text{Me}, \text{OMe}, \text{COMe}$) in which an $\text{M}(\text{CO})_3$ unit is attached to each face of the Fe_6S_6 core, resulting in an elongation of the core along its six-fold axis; two crystal structures ($\text{M} = \text{Mo}, n = 4, \text{R} = \text{COMe}$; $\text{M} = \text{W}, n = 3, \text{R} = \text{Me}$) have been determined. The Mo adducts are proposed as precursors for synthetic analogues of the Fe/Mo/S site of nitrogenase. The electronic and Mössbauer spectra and electrochemical properties are discussed in detail, and are in general sensitive to the nature of the *para* ring substituents. Strongly electron-releasing groups (e.g. NMe_2) facilitate the dissociation of one $\text{M}(\text{CO})_3$ fragment, leading to heptametallic clusters [575].

The basket-core clusters $\text{Fe}_6\text{S}_6(\text{PET}_3)_4\text{L}_2$ ($\text{L} = \text{halide, thiocyanate}$), which are topological isomers of the prismanes but not isoelectronic, have been known for a while. Since the formation of these polynuclear clusters is generally very dependent on the nature of the terminal ligands L and the reactant stoichiometry, an attempt was made to see if the same core structure would self-assemble in the absence of any ancillary ligands other than PET_3 . A 1:4:1 mixture of $[\text{Fe}(\text{H}_2\text{O})_6][\text{BF}_4]_2 \cdot \text{Et}_3\text{P} \cdot \text{Li}_2\text{S}$ in thf gave a 14% yield of $[\text{Fe}_6\text{S}_6(\text{PET}_3)_6][\text{BF}_4]$ which has been crystallographically characterised. The $[\text{Fe}_6\text{S}_6]^+$ core has a basket-core structure similar to those already known, with a few minor dimensional differences. It has crystallographically imposed C_3 symmetry but is nearly C_{2v} . All Fe atoms are four coordinate, with an S_3P coordination sphere; two Fe atoms are tetrahedral, whilst the others are better described as being trigonal planar with an axial phosphine ligand. The basket-core topology has thus been shown to support the $[\text{Fe}_6\text{S}_6]^+$ oxidation level as well as the known $[\text{Fe}_6\text{S}_6]^{2+}$. Higher oxidation levels (+3, +4) are only found in prismanes. $[\text{Fe}_6\text{S}_6(\text{PET}_3)_6][\text{BF}_4]$ does not show clean electrochemical behaviour, but reacts with

chloride or chlorinated solvents to give $\text{Fe}_6\text{S}_6(\text{PET})_4\text{Cl}_2$ and with O_2 or S to give the known species $[\text{Fe}_6\text{S}_8(\text{PET}_3)_6]^{2+}$ and $[\text{Fe}_6\text{S}_8(\text{PET}_3)_6]^+$ which both have an octahedral Fe_6 core structure with an S cap on every face [576].

$[\text{Pr}_4\text{N}]_6\text{Na}_4\text{Fe}_{18}\text{S}_{30} \cdot 14\text{MeCN}$ was prepared by the reaction of FeCl_3 , $\text{Na}[\text{PhNC}(\text{O})\text{Me}]$ and Li_2S in the ratio 1 : 3.15 : 1.78 in methanol/ethanol followed by recrystallisation of the product from acetonitrile. The crystal structure consists of discrete Pr_4N^+ ions and two Na^+ ions weakly associated with the cluster anion $[\text{Na}_2\text{Fe}_{18}\text{S}_{30}]^{8-}$, which has a quite unprecedented cyclic structure. It is constructed by the fusion of 24 non-planar Fe_2S_2 rhombohedra in edge- and corner-sharing modes such that there are 20 $\mu_2\text{-S}$, 8 $\mu_3\text{-S}$ and 2 $\mu_4\text{-S}$. Every FeS_4 unit is tetrahedral and the 18 Fe atoms are essentially coplanar, leading to a cyclic toroidal structure with no terminal ligands. Two Na^+ ions are bound to the interior S atoms of the cluster. The cluster is mixed-valent (14 Fe(III) and 4 Fe(II)) with a singlet ground state arising from antiferromagnetic coupling; the Mössbauer spectrum indicates substantial delocalisation. Molecular orbital calculations show that the cluster has a quasi-band structure with the orbitals divided into ≥ 4 well separated blocks. The reactivity of the cluster to various thiols is discussed. The cluster size and structural relationships to Fe-S phases means that $[\text{Na}_2\text{Fe}_{18}\text{S}_{30}]^{8-}$ is on the boundary between molecular and solid-state materials. A conceptual model of cluster buildup arising from sequential connection of Fe_2S_2 rhombohedra and FeS_4 tetrahedra is presented, which suggests that many new core topologies which have not yet been observed may be accessible [577].

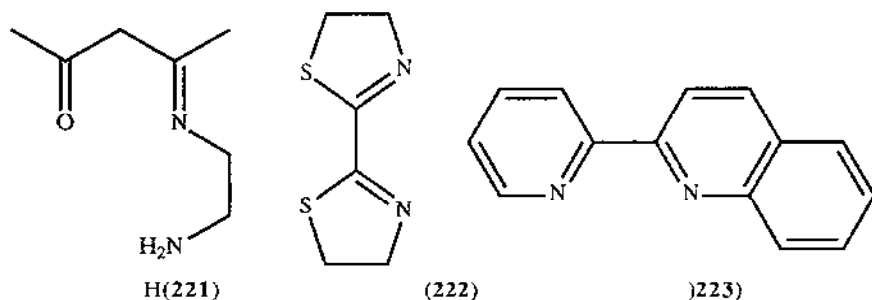
1.12 COMPLEXES EXHIBITING SPIN-EQUILIBRIA

An X-ray structural determination shows that $[\text{Fe}^{\text{III}}(221)_2][\text{BPh}_4]$ has a distorted octahedral N_4O_2 geometry provided by two tridentate ligands binding in a meridional manner, with the O atoms *cis* to one another and the imine nitrogen atoms *trans*. The bond lengths are consistent with the complex being high-spin (HS) at room temperature. Variable temperature magnetic susceptibility measurements show a gradual but complete high-spin to low-spin (HSLS) crossover ($S = 5/2$ to $S = 1/2$) with decreasing temperature; the ESR spectra are consistent with the presence of two HS sites and one LS site. The ΔH and ΔS values for the spin transition are similar to those for related complexes of Schiff-base ligands [578].

$[\text{Fe}(\text{mtz})_6][\text{BF}_4]_2$ (mtz = 1-methyltetrazole) undergoes both thermally induced and light-induced HSLS ($S = 2$ to $S = 0$) transitions which were observed by Mössbauer spectroscopy. Both the crystal structure and the Mössbauer spectrum show two distinct Fe(II) sites (A and B - both HS) below 160K. On cooling from 110K to 60K the A sites undergo a thermal HSLS transition; the B sites remain HS down to 4.2K. At 20K, the A sites (which are now LS) undergo a LIESST (Light-Induced Excited State Spin-Trapping) LSHS transition on irradiation with a Xenon-arc lamp; the light-induced HS state is stable for hours below 40K. By contrast the B sites (which are HS at 20K) undergo a HSLS transition with red light, giving a LS-trapped state which is indefinitely stable below 50K. This is the first example of light-induced formation of a metastable LS state in a HS Fe(II) complex [579].

$\text{Fe}(\mathbf{222})_2(\text{NCS})_2$ and $\text{Fe}(\mathbf{222})_2(\text{NCSe})_2$ both undergo thermally-induced HSLS transitions on cooling. They also give rise to LIESST effects on excitation with a He-Ne laser, Ne-He laser or tungsten-filament lamp at 6K. These spin-trapped excited LS states were studied by variable-temperature FT-IR spectroscopy, and are stable for several hours at 6K [580].

$[\text{FeL}_3]^{2+}$ ($\text{L} = 2\text{-[pyridin-2-yl]quinoline}$ ($\mathbf{223}$) or 6-methyl-bipy), both show anomalous magnetic properties consistent with a temperature-dependent HSLS transition. Two forms of $[\text{Fe}(\mathbf{223})_3][\text{ClO}_4]_2$ were obtained; one is HS between 300K and 89K, whereas the other shows a gradual HSLS transition over the same temperature range. The crystal structure has been determined. $[\text{Fe}(\text{6-Me-bipy})_3][\text{X}_2]$ ($\text{X} = \text{ClO}_4, \text{BF}_4, \text{PF}_6$) show some spin-pairing at low temperatures, but are not completely LS at 89K. Two distinct sites for the HS species at low temperatures were detected by Mössbauer spectroscopy, arising from ordering of the anion sites in the crystal lattice. The structure of the complex cation shows considerable distortion, with the ligand molecules twisted about the interligand bond. These effects are due to the methyl group on the ligand, which induces a steric barrier to coordination and also causes greater inter-ligand repulsions than in complexes of bipyridine, and this is presumably responsible for the accessibility of the HS state. The steric effects of the fused benzene ring in ($\mathbf{223}$) are predicted to be similar [581].



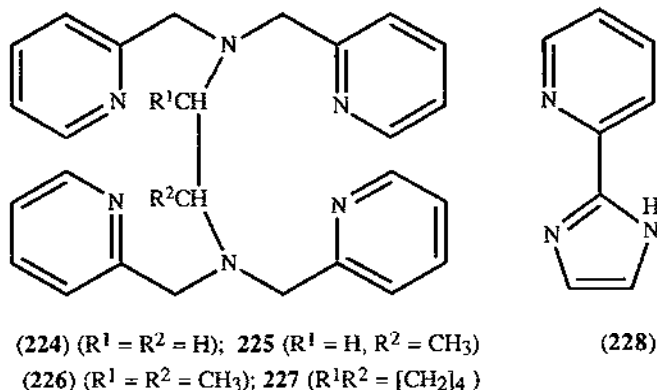
Crystals of $\text{Fe}(\text{amp})_3\text{Cl}_2 \cdot \text{EtOH}$ ($\text{amp} = 2\text{-aminomethyl pyridine}$) were prepared doped with Mn(II). The Mn(II) ESR signal may be used as a probe for spin-crossover in the Fe(II) system. There are three Mn(II) environments in the crystal, each giving a separate ESR signal; the intensities of these signals varies with temperature [582].

The continuous HSLS transitions of $[\text{Fe}(\text{D}_2\text{amp})_3]\text{Cl}_2 \cdot \text{EtOH}$ ($\text{D}_2\text{amp} = 2\text{-aminomethyl-pyridine with } -\text{ND}_2 \text{ rather than } -\text{NH}_2$) and of $[\text{Fe}(\text{amp})_3]\text{Cl}_2 \cdot \text{MeOH}$ are isobaric above their T_c values, but at or below T_c they exhibit a rather complex behaviour due to an elastic interaction between the HS and LS molecules in the crystal. $[\text{Fe}_x\text{Zn}_{1-x}(\text{amp})_3]\text{Cl}_2 \cdot \text{EtOH}$ shows a two-step spin transition below T_c , which has been studied by Mössbauer spectroscopy at several values of x between 0.78 and 1 and at different applied pressures. The unusual transition behaviour is an intrinsic property of the process itself, rather than (as with the other cases) being triggered by lattice properties [583].

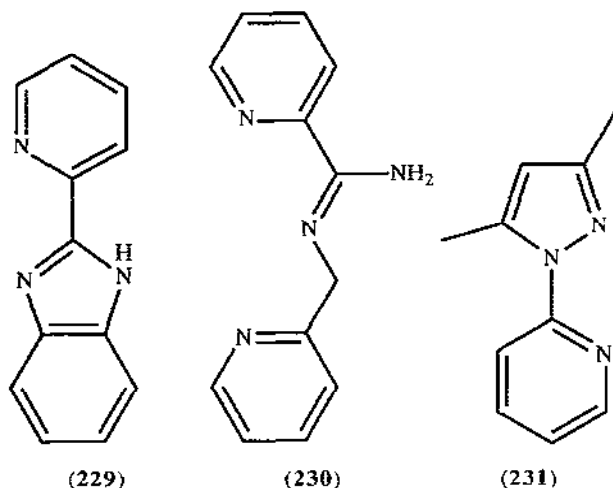
$[\text{Fe}(\text{btz})_2(\text{NCS})_2] \cdot \text{H}_2\text{O}$ ($\text{btz} = 4,4'\text{-bis-1,2,4-triazole}$) has a two-dimensional network structure with bridging btz ligands and *trans* thiocyanates; the crystal structure has been determined.

The hydrated material shows an abrupt HSLS transition at 123.5K on cooling and 144.5K on warming, whereas the dehydrated material is permanently HS. The spin transition was followed by doping Cu(II) into the lattice, and using the Cu(II) signal as a probe for the Fe(II) HSLS transition. When the Fe(II) centres are HS, the Cu(II) signal is poorly resolved due to exchange broadening; when the Fe(II) centres are LS, the Cu(II) signal is well resolved [584].

The crystal structure of $[\text{Fe}(\mathbf{224})][\text{ClO}_4]_2 \cdot 2/3\text{H}_2\text{O}$ reveals two crystallographically distinct Fe sites, of which one has a higher HS content (as evidenced by bond lengths and trigonal distortions). The complex undergoes HSLS transitions at a rate faster than the Mössbauer timescale. The T_c value is 365K both in solution and the solid state, indicating that there are no intermolecular interactions involved in the spin transition. The rapid HSLS interconversion is attributed to a large trigonal distortion induced by the steric constraints of the ligand, which causes an unusually large spin-orbit interaction between the ^1A and $^5\text{T}_2$ states [585].



Relaxation times for HSLS transitions in a variety of Fe(II) complexes have been measured as a function of temperature and pressure in order to determine the activation volumes for the spin transition, since the detailed reaction pathway followed by this process is still obscure. To assess the role of radial and twisting motions in the crossover process, a series of complexes with sterically constraining ligands ($\mathbf{225}$)-($\mathbf{227}$), exhibiting varying degrees of conformational freedom, were examined alongside complexes of smaller ligands with fewer structural constraints ($\mathbf{228}$)-($\mathbf{230}$). The activation volumes for the spin transitions of these complexes in several solvents were determined, together with the corresponding activation enthalpy and entropy values. In the complex $[\text{Fe}(\mathbf{227})][\text{ClO}_4]_2$ the ligand impedes rhomboidal twist motion, and in DMF solution it was found that the relaxation time for HS to LS crossover increased significantly with pressure, and that the activation volume is positive. This is in contrast to all of the other complexes, which have negative activation volumes for their HS to LS transitions. A mechanism for spin crossover is proposed, involving both radial and angular motion. In the case of $[\text{Fe}(\mathbf{227})][\text{ClO}_4]_2$ there is a larger contribution from the radial pathway since twisting is impeded by the cyclohexyl ring; this accounts for the different activation parameters compared to the other complexes [586].



$\text{Fe}(\mathbf{231})_2\text{X}_2$ ($\text{X} = \text{Cl}, \text{Br}, \text{NCS}$), $[\text{Fe}(\mathbf{231})_2(\text{ClO}_4)_2] \cdot 2\text{H}_2\text{O}$ and $[\text{Fe}(\mathbf{231})_3][\text{ClO}_4]_2$ were prepared and characterised by electronic spectroscopy, variable temperature magnetic susceptibility and Mössbauer spectroscopy. Whereas $\text{Fe}(\mathbf{231})_2\text{X}_2$ are HS, the other two complexes show intermediate magnetic moment values which are consistent with a HSLS equilibrium [587].

The formation of local domains within $[\text{Fe}(\text{phenph})_2][\text{ClO}_4]_2$ (phenph = 1,10-phenanthroline-2-carbaldehyde phenylhydrazone) has been studied by magnetic susceptibility and detailed hysteresis measurements. Domain formation within a material results in a distribution of T_c values and is one of the causes of such hysteresis effects. The temperature-dependencies of the Mössbauer parameters, X-ray powder diffraction spectra and magnetic susceptibilities were measured, resulting in ΔH and ΔS values for the HSLS spin transition. The results cannot be accounted for by simple theories of nucleation and domain formation [588].

The crystal structure of $\text{Fe}(\text{phen})_2(\text{NCS})_2$ has been determined at 293K and 130K in order to detect structural changes associated with the HSLS transition. No change in crystal symmetry was found between the two temperatures, but a large reorganisation of the $\text{Fe}(\text{II})$ environment is evident. The transition from HS to LS on cooling results in shortening of all of the Fe-N bonds, and a change in the bond angles giving a more regular octahedral geometry about the $\text{Fe}(\text{II})$ [589].

The abrupt HSLS transitions observed in $[\text{Fe}(\text{py})_2(\text{bpym})(\text{NCS})_2] \cdot 1/4\text{py}$ (bpym = 2,2'-bipyrimidine) and the phenanthroline analogue $[\text{Fe}(\text{py})_2(\text{phen})(\text{NCS})_2] \cdot 1/2\text{py}$ were studied by variable-temperature magnetic susceptibility, Mössbauer spectroscopy and calorimetry. The crystal structure of the HS form of $[\text{Fe}(\text{py})_2(\text{bpym})(\text{NCS})_2] \cdot 1/4\text{py}$ was determined at 293K; the py ligands are *trans* to one another and the NCS⁻ groups are *cis*. The occluded pyridines have high thermal motion and/or a positional disorder. $[\text{Fe}(\text{py})_2(\text{bpym})(\text{NCS})_2] \cdot 1/4\text{py}$ has a very sharp HSLS transition, with the T_c values being 113.5K (temperature decreasing) and 116.5K (temperature increasing). $[\text{Fe}(\text{py})_2(\text{phen})(\text{NCS})_2] \cdot 1/2\text{py}$ also has an abrupt HSLS transition centred at $T_c = 106\text{K}$; the temperature dependence of the Mössbauer spectra provides evidence for the structural change in the lattice associated with the transition (c.f. crystallographic observation of the same effect in ref. 589), and also shows that the bpym complex is more nearly octahedral than the phen

complex. The enthalpy and entropy changes associated with the spin transition were determined from calorimetric measurements. It is suggested that previous reports of the magnetic behaviour of $\text{Fe}(\text{py})_2(\text{phen})(\text{NCS})_2$ were erroneous, and are consistent with the samples used containing considerable amounts of $\text{Fe}(\text{phen})_2(\text{NCS})_2$ and $\text{Fe}(\text{py})_4(\text{NCS})_2$ [590].

The $\text{Fe}(\text{III})$ complexes of a series of bulky thioselenocarbamates FeL_3 ($\text{L} = \text{SSeCNR}_2$ monoanions; $\text{NR}_2 = \text{N}(\text{benzyl})_2$, pyrrolidino, piperidino, morpholino, dicyclohexylamino) were examined by variable-temperature magnetic susceptibility measurements between 8 and 310K. The dibenzylamino, piperidyl and morpholyl derivatives show a HSLS crossover starting at room temperature, with complete conversion to LS at 77K. The dicyclohexylamino derivative is LS at all temperatures, whereas the pyrrolidyl derivative shows crossover behaviour at 8K. The ESR spectra of these complexes diluted (1:99) in a diamagnetic host lattice of $\text{Co}(\text{III})$ or $\text{In}(\text{III})$ were recorded between 120K and room temperature. These spectra may be used as fingerprints to study the effects of temperature and matrix on the HSLS transitions. All of the ESR spectra show two broad signals at $g \approx 2$ and $g \approx 4$ from the $S = 5/2$ species, and a sharp signal at $g \approx 2$ from the $S = 1/2$ species [591].

REFERENCES

- 1 B. F. G. Johnson and A. Bott, *J. Chem. Soc., Dalton Trans.*, (1990) 2437
- 2 D. Braga, F. Grepioni and P. Sabatino, *J. Chem. Soc., Dalton Trans.*, (1990) 3137
- 3 C. Mealli and D. M. Proserpio, *J. Organometal. Chem.*, 386 (1990) 203
- 4 R. H. Hooker and A. J. Rest, *Appl. Organomet. Chem.*, 4 (1990) 141
- 5 E. S. Kirkor, D. E. David and J. Michl, *J. Am. Chem. Soc.*, 112 (1990) 139
- 6 E. L. Kirley and D. H. Russell, *J. Am. Chem. Soc.*, 112 (1990) 5959
- 7 S. R. Horning, M. Vincenti and R. G. Cooks, *J. Am. Chem. Soc.*, 112 (1990) 119
- 8 K. Norwood, A. Ali, G. D. Flesch and C. Y. Ng, *J. Am. Chem. Soc.*, 112 (1990) 7502
- 9 S. W. Lee, W. D. Tucker and M. G. Richmond, *Inorg. Chem.*, 29 (1990) 3053
- 10 Y. K. Chung, *Chayon Kwahak Taehak Nonmunjip (Soul Taehakkyo)*, 13 (1988) 27 [*Chem. Abstr.* 112: 21122n]
- 11 S. Sato and T. Ohmari, *J. Chem. Soc., Chem. Commun.*, (1990) 1032
- 12 J.-J. Brunet and M. Taillefer, *J. Organometal. Chem.*, 384 (1990) 193
- 13 Y. Wada, Y. Toshiyawa and A. Morikawa, *J. Chem. Soc., Chem. Commun.*, (1990) 319
- 14 M. O. Albers, E. Singleton and N. J. Coville, *Inorg. Synth.*, 26 (1989) 52
- 15 D. Lentz, *J. Organometal. Chem.*, 377 (1989) 305
- 16 J. B. Murray, B. K. Nicholson and A. J. Whetton, *J. Organometal. Chem.*, 385 (1990) 91
- 17 J. W. Connolly, A. H. Cowley and C. M. Nunn, *Polyhedron*, 9 (1990) 1337
- 18 J. Barrau, N. Ben Hamida and J. Satge, *J. Organometal. Chem.*, 387 (1990) 65
- 19 J. Barrau, N. Ben Hamida, H. Agrebi and J. Satge, *Inorg. Chem.*, 29 (1990) 1674
- 20 S. G. Anema, K. M. Mackay, B. K. Nicholson and M. Van Tiel, *Organometallics*, 9 (1990) 2436
- 21 D. Lei, M. J. Hampden-Smith and E. N. Duesler, *Polyhedron*, 9 (1990) 1127
- 22 M. Veith, S. Becker and V. Huch, *Angew. Chem.*, 102 (1990) 186
- 23 D. Lei, M. J. Hampden-Smith, E. N. Duesler and J. C. Huffman, *Inorg. Chem.*, 29 (1990) 795
- 24 S. G. Anema, K. M. Mackay and B. K. Nicholson, *J. Organometal. Chem.*, 372 (1989) 25
- 25 W. Petz, B. Wrackmeyer and W. Storch, *Chem. Ber.*, 122 (1989) 2261
- 26 M. Ferrer, O. Rossell, M. Seco, X. Solans and M. Gomez, *J. Organometal. Chem.*, 381 (1990) 183
- 27 M. Knorr, H. Piana, S. Gilbert and U. Schubert, *J. Organometal. Chem.*, 388 (1990) 327
- 28 M. Ferrer, A. Perales, O. Rossell and M. Seco, *J. Chem. Soc., Chem. Commun.*, (1990) 1447
- 29 T. P. Fehlner, M. M. Amini, W. F. Stickle, O. A. Pringle, G. J. Long and F. P. Fehlner, *Chem. Mater.*, 2 (1990) 263

- 30 A. S. Katugin, A. A. Pasynskii, I. L. Eremenko, E. A. Vas'utinskaya, Y. T. Struchkov and A. I. Yanovskii, *J. Organometal. Chem.*, 386 (1990) 225
- 31 W. Weigand, U. Nagel and W. Beck, *Chem. Ber.*, 123 (1990) 439
- 32 M. O. Albers, E. Singleton and N. J. Colville, *Inorg. Synth.*, 26 (1989) 59
- 33 H. G. Ang, W. L. Kwik and P. T. Lau, *Polyhedron*, 9 (1990) 1479
- 34 G. Bellachioma, G. Cardaci, A. Macchioni and G. Reichenbach, *J. Organometal. Chem.*, 391 (1990) 367
- 35 D. L. Allen, M. L. H. Green and J. A. Bandy, *J. Chem. Soc., Dalton Trans.*, (1990), 541
- 36 H. R. Allcock, I. Manners, M. N. Mang and M. Parvez, *Inorg. Chem.*, 29 (1990) 522
- 37 J. Takacs, L. Marko, P. Kiprof, E. Herdtweck and W. A. Herrmann, *Polyhedron*, 8 (1989) 1503
- 38 J. T. Lin, Y. F. Lin, S. Y. Wang, J. S. Sun and S. K. Yeh, *Bull. Inst. Chem., Acad. Sin.*, 36 (1989) 63 [*Chem. Abstr.* 112:170917c]
- 39 C. P. Casey, G. T. Whiteker, C. F. Campana and D. R. Powell, *Inorg. Chem.*, 29 (1990) 3376
- 40 T. S. A. Hor and L. T. Phang, *J. Organometal. Chem.*, 381 (1990) 121
- 41 T. S. A. Hor and L. T. Phang, *J. Organometal. Chem.*, 390 (1990) 345
- 42 M. S. Balakrishna, T. K. Prakasha, S. S. Krishnamurthy, U. Siriwardane and N. S. Hosmane, *J. Organometal. Chem.*, 390 (1990) 203
- 43 R. B. King, F. J. Wu and E. M. Holt, *J. Organometal. Chem.*, 383 (1990) 295
- 44 R. B. King, N. K. Bhattacharya and E. M. Holt, *J. Organometal. Chem.*, 394 (1990) 305
- 45 H. Adams, N. A. Bailey, G. W. Bentley and B. E. Mann, *J. Chem. Soc., Dalton Trans.*, (1989) 1831
- 46 D. Buchholz, G. Huttner and W. Imhof, *J. Organometal. Chem.*, 388 (1990) 307
- 47 D. Buchholz, G. Huttner, W. Imhof and O. Orama, *J. Organometal. Chem.*, 388 (1990) 321
- 48 F. Bitterer, D. J. Brauer, F. Dorrenbach and O. Stelzer, *J. Organometal. Chem.*, 399 (1990) C4
- 49 A. Gourdon and Y. Jeannin, *J. Organometal. Chem.*, 388 (1990) 195
- 50 L. J. Arnold, K. M. Mackay and B. K. Nicholson, *J. Organometal. Chem.*, 387 (1990) 197
- 51 S. Luo and K. H. Whitmire, *J. Organometal. Chem.*, 376 (1989) 297
- 52 A.-M. Caminade, M. Veith, V. Huch and W. Malisch, *Organometallics*, 9 (1990) 1798
- 53 L. Song, R. Wang, Y. Li, H. Wang and J. Wang, *Youji Huaxue*, 9 (1989) 512 [*Chem. Abstr.* 113: 16848v]
- 54 M. Mavlonov and A. I. Nekhaev, *Koord. Khim.*, 15 (1989) 861 [*Chem. Abstr.* 112: 15520z]
- 55 M.-J. Don and M. G. Richmond, *Inorg. Chim. Acta*, 173 (1990) 61
- 56 A. Kramer and I. P. Lorenz, *J. Organometal. Chem.*, 388 (1990) 187
- 57 A. Kramer, R. Lingnau, I. P. Lorenz and H. A. Mayer, *Chem. Ber.*, 123 (1990) 1821
- 58 L. Song, M. Kadiata, J. Wang, R. Wang and H. Wang, *J. Organometal. Chem.*, 391 (1990) 387
- 59 M. B. Hall and A. A. Low, *Polyhedron*, 8 (1989) 1885
- 60 C. Diaz, *Polyhedron*, 9 (1990) 1045
- 61 A. J. Banister, I. B. Gorrell, W. Clegg and K. A. Joergensen, *J. Chem. Soc., Dalton Trans.*, (1989) 2229
- 62 A. I. Nekhaev, B. I. Kolobkov, M. T. Toshev, K. B. Dustov and G. G. Aleksandrov, *Izv. Akad. Nauk SSSR, Ser. Khim.*, (1989) 1705 [*Chem. Abstr.* 112:47537b]
- 63 L. Song, Q. Hu and J. Wang, *Gaodeng Xuexiao Huaxue Xuebao*, 10 (1989) 1251 [*Chem. Abstr.* 113:107970v]
- 64 M.-H. Desbois, C. M. Nunn, A. H. Cowley and D. Astruc, *Organometallics*, 9 (1990) 640
- 65 M.-H. Desbois and D. Astruc, *J. Chem. Soc., Chem. Commun.*, (1990) 943
- 66 D. Sellmann, R. Weiss and F. Knoch, *Angew. Chem.*, 101 (1989) 1719
- 67 D. Sellmann, R. Weiss, F. Knoch, G. Ritter and J. Dengler, *Inorg. Chem.*, 29 (1990) 4107
- 68 D. Sellman, R. Weiss, F. Knoch and M. Moll, *J. Organometal. Chem.*, 391 (1990) 327
- 69 D. Buchholz, G. Huttner, L. Zsolnai and W. Imhof, *J. Organometal. Chem.*, 377 (1989) 25
- 70 P. Mathur and V. D. Reddy, *J. Organometal. Chem.*, 387 (1990) 193
- 71 D. Chakrabarty, P. Mathur, I. J. Mavunkal, R. V. Pannikar, V. D. Reddy and B. H. S. Thimmappa, *Proc. Indian Natl. Sci. Acad., Part A*, 55 (1989) 342
- 72 P. Mathur, D. Chakrabarty, I. J. Mavunkal, V. D. Reddy, V. Rugmini and B. H. S. Thimmappa, *Metalloorg. Khim.*, 3 (1990) 768 [*Chem. Abstr.* 113: 243556s]
- 73 P. Mathur and V. D. Reddy, *J. Organometal. Chem.*, 385 (1990) 363
- 74 P. Mathur, I. J. Mavunkal, B. H. S. Thimmappa, V. Rugmini and B. B. S. Shastri, *Proc. Indian Acad. Sci., Chem. Sci.*, 102 (1990) 395
- 75 P. Mathur, I. J. Mavunkal, V. Rugmini and M. F. Mahon, *Inorg. Chem.*, 29 (1990) 4838

- 76 B. W. Eichhorn, R. C. Haushalter and J. S. Merola, *Inorg. Chem.*, 29 (1990) 728
- 77 R. Jund, J. Rimmelin and M. Gross, *J. Organometal. Chem.*, 381 (1990) 239
- 78 R. S. Armstrong, T. Bell, A. F. Masters, M. A. Williams and A. L. Chaffee, *Polyhedron*, 9 (1990) 2815
- 79 H. Vahrenkamp, *Inorg. Synth.*, 26 (1989) 351
- 80 A. S. Katugin, A. A. Pasyinskii, I. L. Eremenko, B. Orazsakhmatov, A. S. Aliev, Y. T. Struchkov and A. I. Yanovsky, *J. Organometal. Chem.*, 382 (1990) 423
- 81 P. Braunstein, J.-L. Richert and Y. Dusauso, *J. Chem. Soc., Dalton Trans.*, (1990) 3801
- 82 P. Braunstein, C. De Meric de Bellefon and M. Ries, *Inorg. Chem.*, 29 (1990) 1181
- 83 R. Bender, P. Braunstein, J.-L. Richert and Y. Dusauso, *New. J. Chem.*, 14 (1990) 569
- 84 R. Della Pergola, L. Garlaschelli, F. Demartin, M. Manassero, N. Masciocchi and M. Sansoni, *J. Chem. Soc., Dalton Trans.*, (1990) 127
- 85 N. K. Bhattacharyya, T. J. Coffy, W. Quintana, T. A. Salupo, J. C. Bricker, T. B. Shay, M. Payne and S. G. Shore, *Organometallics*, 9 (1990) 2368
- 86 M. R. Churchill and J. C. Fetting, *Organometallics*, 9 (1990) 446
- 87 R. D. Adams, G. Chen and J. G. Wang, *Polyhedron*, 8 (1989) 2521
- 88 R. D. Adams, I. Arafat, G. Chen, J.-C. Lii and I.-G. Wang, *Organometallics*, 9 (1990) 2350
- 89 A. E. Mauro and M. N. G. Mancini, *Eclectica Quim.*, 13 (1988) 63 [*Chem. Abstr.* 112: 15544k]
- 90 P. Braunstein, M. Knorr, A. Tiripicchio and M. T. Camellini, *Angew. Chem.*, 101 (1989) 1414
- 91 P. Braunstein, M. Knorr, B. E. Villarroja and J. Fischer, *New. J. Chem.*, 14 (1990) 583
- 92 S. Alvarez, M. Ferrer, R. Reina, O. Rossell, M. Seco and X. Solans, *J. Organometal. Chem.*, 377 (1989) 291
- 93 R. Reina, O. Rossell and M. Seco, *J. Organometal. Chem.*, 398 (1990) 285
- 94 O. Rossell, M. Seco and P. G. Jones, *Inorg. Chem.*, 29 (1990) 348
- 95 L. W. Arndt, C. E. Ash, M. Y. Darensbourg, Y. M. Hsiao, C. M. Kim, J. Reibenspies and K. A. Youngdahl, *J. Organometal. Chem.*, 394 (1990) 733
- 96 V. Riera, J. Ruiz, X. Solans and E. Tauler, *J. Chem. Soc., Dalton Trans.*, (1990) 1607
- 97 B. E. Hanson and K. H. Whitmire, *J. Am. Chem. Soc.*, 112 (1990) 974
- 98 E. P. Cappellani, P. A. Maltby, R. H. Morris, C. T. Schweitzer and M. R. Steele, *Inorg. Chem.*, 28 (1989) 4437
- 99 A. Hills, D. L. Hughes, M. Jimenez-Tenorio and G. J. Leigh, *J. Organometal. Chem.*, 391 (1990) C41
- 100 P. Amendola, S. Antoniutti, G. Albertin and E. Bordignon, *Inorg. Chem.*, 29 (1990) 318
- 101 N. Bampas and L. D. Field, *Inorg. Chem.*, 29 (1990) 587
- 102 C. Bianchini, F. Laschi, M. Peruzzini, F. M. Ottaviani, A. Vacca and P. Zanello, *Inorg. Chem.*, 29 (1990) 3394
- 103 C. Bianchini, M. Peruzzini and F. Zanobini, *J. Organometal. Chem.*, 390 (1990) C16
- 104 L. S. Van der Sluis, J. Eckert, O. Eisenstein, J. H. Hall, J. C. Huffman, S. A. Jackson, T. F. Koetzle, G. J. Kubas, P. J. Vergamini and K. G. Caulton, *J. Am. Chem. Soc.*, 112 (1990) 4831
- 105 J. Eckert, H. Blank, M. T. Bautists and R. H. Morris, *Inorg. Chem.*, 29 (1990) 747
- 106 D. R. Schaad and C. R. Landis, *J. Am. Chem. Soc.*, 112 (1990) 1628
- 107 L. D. Field, A. V. George and T. W. Hambley, *Polyhedron*, 9 (1990) 2139
- 108 J.-J. Brunet, F. B. Kindela, D. Labroue and D. Neibecker, *Inorg. Chem.*, 29 (1990), 4152
- 109 H. A. Jenkins, S. J. Loeb, D. G. Dick and D. W. Stephan, *Can. J. Chem.*, 68 (1990) 869
- 110 R. G. Bhattacharyya, M. Malik and P. N. Ghosh, *Inorg. Chim. Acta*, 168 (1990) 141
- 111 H. Tom Dieck, H. Bruder, E. Kuchl, D. Junghans and K. Hellfeldt, *New J. Chem.*, 13 (1989) 259
- 112 H. Li Kam Wah, M. Postel and M. Pierrot, *Inorg. Chim. Acta*, 165 (1989) 215
- 113 J. L. Rouston, N. Ansari, J. P. Charland and Y. Le Page, *Can. J. Chem.*, 67 (1989) 2016
- 114 D. Sellman, *J. Organometal. Chem.*, 372 (1989) 99
- 115 S. A. Yousif-Ross and A. Wojcicki, *Inorg. Chim. Acta*, 171 (1990) 115
- 116 C.-N. Chau, A. Wojcicki, M. Calligaris and G. Nardin, *Inorg. Chim. Acta*, 168 (1990) 105
- 117 L. I. Kuznetsova, L. G. Detusheva, M. A. Fedotov, T. P. Lazorenko, A. Z. Golovin and E. N. Yurchenko, *Zh. Neorg. Khim.*, 35 (1990) 1498 [*Chem. Abstr.* 113: 243493u]
- 118 J. C. Barnes, C. Glidewell, A. Lees and R. A. Howie, *Acta Cryst., Sect. C*, C46 (1990) 2051
- 119 M. Postel, F. Tomi, H. Li Kam Wah, L. Mordenti and P. Guillaume, *Phosphorus, Sulfur Silicon Relat. Elem.*, 49-50 (1990) 453 [*Chem. Abstr.* 113: 231618a]
- 120 G. Benner and R. Hoppe, *J. Fluorine Chem.*, 46 (1990) 283
- 121 R. Hoppe and G. Benner, *Z. Anorg. Allg. Chem.*, 580 (1990) 50

- 122 A. Le Bail, A. Desert and J. L. Fourquet, *J. Solid State Chem.*, 84 (1990) 408
- 123 J. L. Fourquet and H. Duroy, *Eur. J. Solid State Inorg. Chem.*, 26 (1989) 413 [*Chem. Abstr.* 112:149368q]
- 124 E. Herdtweck, J. Graulich and D. Babel, *Z. Naturforsch., B: Chem. Sci.*, 45 (1990) 161
- 125 E. Herdtweck and W. Massa, *Z. Anorg. Allg. Chem.*, 579 (1989) 191
- 126 M. Leblanc and G. Feret, *Acta Cryst., Sect. C*, C46 (1990) 13
- 127 A. LeBail, *J. Solid State Chem.*, 83 (1989) 267
- 128 F. A. Cotton, R. L. Luck and K. A. Son, *Acta Cryst., Sect. C*, C46 (1990) 1424
- 129 J. H. So and P. Boudjouk, *Inorg. Chem.*, 29 (1990) 1592
- 130 K. D. Butcher, S. V. Didziulis, B. Briat and E. I. Solomon, *Inorg. Chem.*, 29 (1990) 1626
- 131 K. D. Butcher, S. V. Didziulis, B. Briat and E. I. Solomon, *J. Am. Chem. Soc.*, 112 (1990) 2231
- 132 J. A. Zora, K. R. Seddon, P. B. Hitchcock, C. B. Lowe, D. P. Shum and R. L. Carlin, *Inorg. Chem.*, 29 (1990) 3302
- 133 C. B. Lowe, R. L. Carlin, A. J. Schultz and C. K. Loong, *Inorg. Chem.*, 29 (1990) 3308
- 134 R. E. Greeney, C. P. Landee, J. H. Zhang and W. M. Reiff, *Inorg. Chem.*, 29 (1990) 3119
- 135 K. B. Yoon and J. K. Kochi, *Inorg. Chem.*, 29 (1990) 869
- 136 V. V. Zhilinskaya, Y. G. Gol'tsov, A. M. Glukhoi and E. N. Korol, *Teor. Eksp. Khim.*, 25 (1989) 733 [*Chem. Abstr.* 112:241093u]
- 137 R. Benedix and H. Hennig, *Z. Anorg. Allg. Chem.*, 577 (1989) 23
- 138 H. E. Toma and M. M. Takayasu, *An. Acad. Bras. Cienc.*, 61 (1989) 131 [*Chem. Abstr.* 113:66195a]
- 139 H. Zhu, R. Cong, X. Xin, A. Dai, H. Zhang and Y. Han, *Wuji Huaxue Xuebao*, 5 (1989) 54 [*Chem. Abstr.* 113:47276m]
- 140 D. H. Macartney and L. J. Warrack, *Can. J. Chem.*, 67 (1989) 1774
- 141 F. H. Chao, B. K. Sun, P. C. Juang and A. Yeh, *J. Chin. Chem. Soc.*, 37 (1990) 327
- 142 A. M. Alonso, P. A. M. Williams and P. J. Aymonino, *An. Asoc. Quim. Argent.*, 76 (1988) 151 [*Chem. Abstr.* 112:131033s]
- 143 S. Huang, Y. Xie, X. Xin, A. Dai and Y. Zhang, *Huaxue Xuebao*, 47 (1989) 846 [*Chem. Abstr.* 113:51487y]
- 144 C. H. Hung, H. Y. Huang, J. Y. Liao and A. Yeh, *Inorg. Chem.*, 29 (1990) 2940
- 145 A. Doubila, J. L. Brisset and J. Amouroux, *J. Chim. Phys. Phys.-Chim. Biol.*, 87 (1990) 599
- 146 V. Lopez, J. Catalan, R. M. Claramunt, C. Lopez, E. Cayon and J. Elguero, *Can. J. Chem.*, 68 (1990) 958
- 147 A. Rodriguez, M. L. Moya, P. Lopez and E. Munoz, *Int. J. Chem. Kinet.*, 22 (1990) 1017
- 148 P. Guardado and R. Van Eldik, *Inorg. Chem.*, 29 (1990) 3474
- 149 W. Brune, J. D. Fabris and S. Jose, *An. Acad. Bras. Cienc.*, 60 (1988) 355 [*Chem. Abstr.* 112:179773k]
- 150 E. L. Varetto, M. M. Vergara, G. Rigotti and A. Navaza, *J. Phys. Chem. Solids*, 51 (1990) 381
- 151 D. F. Mullica, E. L. Sappenfield, D. B. Tippin and D. H. Leschnitzer, *Inorg. Chim. Acta*, 164 (1989) 99
- 152 N. Burger, V. Hankonyi and Z. Smeric, *Inorg. Chim. Acta*, 165 (1989) 83
- 153 C. Hidalgo-Luandilok and A. B. Bocarsly, *Inorg. Chem.*, 29 (1990) 2894
- 154 M. M. Monzyk and R. A. Holwerda, *Polyhedron*, 9 (1990) 2433
- 155 K. C. Cho, P. M. Cham and C. M. Che, *Chem. Phys. Lett.*, 168 (1990) 361
- 156 W. U. Malik, S. P. Srivastava, K. K. Thallam and R. Gupta, *Proc. Indian Natl. Sci. Acad., Part A*, 55 (1989) 864
- 157 I. Krack and R. Van Eldik, *Inorg. Chem.*, 29 (1990) 1700
- 158 T. Taura, *Inorg. Chim. Acta*, 163 (1989) 13
- 159 S. Idemura, E. Suzuki and Y. Ono, *Clays Clay Miner.*, 37 (1989) 553 [*Chem. Abstr.* 113:16815g]
- 160 C. Glidewell and V. A. J. Musgrave, *Inorg. Chim. Acta*, 167 (1990) 253
- 161 G. Stochel and R. Van Eldik, *Inorg. Chim. Acta*, 174 (1990) 217
- 162 S. Eller, M. Adam and D. R. Fischer, *Angew. Chem.*, 102 (1990) 1157
- 163 S. Eller, S. Duelsen and D. R. Fischer, *J. Organometal. Chem.*, 390 (1990) 309
- 164 M. Adam, A. K. Brimah, D. R. Fischer and X. Li, *Inorg. Chem.*, 29 (1990) 1595
- 165 M. Zhou, B. W. Pfennig, J. Steiger, D. Van Engen and A. B. Bocarsly, *Inorg. Chem.*, 29 (1990) 2456
- 166 M. K. Carpenter, R. S. Conell and S. J. Simko, *Inorg. Chem.*, 29 (1990) 845
- 167 Y. Kuroda, M. Goto and T. Sakai, *Bull. Chem. Soc. Jpn.*, 62 (1989) 3614
- 168 Y. Kuroda, M. Goto and T. Sakai, *Bull. Chem. Soc. Jpn.*, 62 (1989) 3437

- 169 E. Hejmo, E. Porcel-Ortega, T. Senkowski and Z. Stasicka, *Bull. Pol. Acad. Sci., Chem.*, 36 (1989) 351 [*Chem. Abstr.* 112:131173n]
- 170 S. Prasad, P. C. Nigam and R. M. Naik, *Transition Met. Chem.* (London), 15 (1990) 58
- 171 D. Laloo and M. K. Mahanti, *J. Chem. Soc., Dalton Trans.*, (1990) 311
- 172 M. Kamaluddin, S. Nath and W. D. Sushama, *Bull. Chem. Soc. Jpn.*, 62 (1989) 3291
- 173 D. M. Wang and E. De Boer, *J. Chem. Phys.*, 92 (1990) 4698
- 174 B. N. Figgis, E. S. Kucharski, J. M. Raynes and P. A. Reynolds, *J. Chem. Soc., Dalton Trans.*, (1990) 3597
- 175 W. Petter, V. Gramlich, A. Dommann, H. Vetsch and F. Hulliger, *Inorg. Chim. Acta*, 170 (1990) 5
- 176 D. Rieger, F. E. Hahn and W. P. Fehlhammer, *J. Chem. Soc., Chem. Commun.*, (1990) 285
- 177 B. K. Kanungo, *Inorg. Chim. Acta*, 167 (1990) 239
- 178 M. J. Capitan, E. Munoz, M. M. Graciani, R. Jimenez, I. Tejera and F. Sanchez, *J. Chem. Soc., Faraday Trans. 1*, 85 (1989) 4193
- 179 K. Winkler and T. Krogulec, *J. Electroanal. Chem. Interfacial Electrochem.*, 273 (1989) 257
- 180 D. M. Eichhorn and W. H. Armstrong, *Inorg. Chem.*, 29 (1990) 3607
- 181 I. B. Gorrell and G. Parkin, *Inorg. Chem.*, 29 (1990) 2452
- 182 H. Fukui, M. Ito, Y. Morooka and N. Kitajima, *Inorg. Chem.*, 29 (1990) 2868
- 183 N. Kitajima, H. Fukui, Y. Morooka, Y. Mizutani and T. Kitagawa, *J. Am. Chem. Soc.*, 112 (1990) 6402
- 184 P. Gomez-Romero, E. H. Witten, W. M. Reiff and G. B. Jameson, *Inorg. Chem.* 29 (1990) 5211
- 185 H. Adams, N. A. Bailey, J. D. Crane, D. E. Fenton, J. M. Latour and J. M. Williams, *J. Chem. Soc., Dalton Trans.*, (1990) 1727
- 186 J. D. Crane and D. E. Fenton, *J. Chem. Soc., Dalton Trans.*, (1990) 3647
- 187 Y. Nishida, M. Nasu and T. Tokii, *Inorg. Chim. Acta*, 169 (1990) 143
- 188 F.-J. Wu, D. M. Kurtz, Jr., K. S. Hagen, P. D. Nyman, P. G. Debrunner and V. A. Vankai, *Inorg. Chem.*, 29 (1990) 5174
- 189 R. E. Norman, S. Yan, L. Que, Jr., G. Backes, J. Ling, J. Sanders-Loehr, J. H. Zhang and C. J. O'Connor, *J. Am. Chem. Soc.*, 112 (1990) 1554
- 190 R. E. Norman, R. C. Holz, S. Menage, L. Que, Jr., J. H. Zhang and C. J. O'Connor, *Inorg. Chem.*, 29 (1990) 4629
- 191 P. N. Turowski, W. H. Armstrong, M. E. Roth and S. J. Lippard, *J. Am. Chem. Soc.*, 112 (1990) 681
- 192 R. A. Leising, R. E. Norman and L. Que, Jr., *Inorg. Chem.*, 29 (1990) 2553
- 193 D. Boinnard, P. Cassoux, V. Petrouleas, J. M. Savariault and J. P. Tuchagues, *Inorg. Chem.*, 29 (1990) 4114
- 194 G. Guillot, E. Mulliez, P. Leduc and J. C. Chottard, *Inorg. Chem.*, 29 (1990) 577
- 195 A. Natrajan, S. M. Hecht, G. A. van der Marel and J. H. van Boom, *J. Am. Chem. Soc.*, 112 (1990) 3997
- 196 J. R. Barr, R. B. van Atta, A. Natrajan, S. M. Hecht, G. A. van der Marel and J. H. van Boom, *J. Am. Chem. Soc.*, 112 (1990) 4058
- 197 A. Natrajan, S. M. Hecht, G. A. van der Marel and J. H. van Boom, *J. Am. Chem. Soc.*, 112 (1990) 4532
- 198 S. J. Brown, M. M. Olmstead and P. K. Mascharak, *Inorg. Chem.*, 29 (1990) 3229
- 199 R. Hage, J. G. Haasnoot and J. Reedijk, *Inorg. Chim. Acta*, 172 (1990) 19
- 200 D. Onggo, A. D. Rae and H. A. Goodwin, *Inorg. Chim. Acta*, 178 (1990) 151
- 201 J. Lipkowski, *J. Inclusion Phenom. Mol. Recognit. Chem.*, 8 (1990) 439
- 202 R. R. Rumsini and J. L. Kiplinger, *Inorg. Chem.*, 29 (1990) 4581
- 203 R. M. Berger and D. R. McMillin, *Inorg. Chim. Acta*, 177 (1990) 65
- 204 K. Arora, A. P. Bhargava and Y. K. Gupta, *J. Chem. Soc., Dalton Trans.*, (1990) 1257
- 205 H. Kobayashi, M. Fujioka, T. Ohno and S. Mizusawa, *Nippon Kagaku Kaishi*, (1990) 163 [*Chem. Abstr.* 112:241096x]
- 206 M. J. Blandamer, J. Burgess, H. J. Cowles, I. M. Horn, J. B. F. N. Engberts, S. A. Galema and C. D. Hubbard, *J. Chem. Soc., Faraday Trans. 1*, 85 (1989) 3733
- 207 F. J. Berry, M. H. B. Hayes and S. L. Jones, *Inorg. Chim. Acta*, 178 (1990) 203
- 208 R. Ziessel and J.-M. Lehn, *Helv. Chim. Acta*, 73 (1990) 1149
- 209 A. C. Maliyakkal, W. L. Waltz, J. Lilie and R. J. Woods, *Inorg. Chem.*, 29 (1990) 340
- 210 A. Horvath and Z. Uzonyi, *Inorg. Chim. Acta*, 170 (1990) 1
- 211 A. Al-Aousy and J. Burgess, *Inorg. Chim. Acta*, 169 (1990) 167
- 212 C. M. Mikulski, G. Borges Jr., A. Renn and N. M. Karayannis, *J. Coord. Chem.*, 21 (1990) 89

- 213 C. M. Mikulski, G. Borges Jr., D. Kanach, K. Udell and N. M. Karayannis, *Transition Met. Chem. (London)*, 15 (1990) 328
- 214 A. R. Sarkar and R. K. Bandyopadhyay, *J. Indian Chem. Soc.*, 66 (1989) 409
- 215 C. M. Mikulski, S. Grossman, M. L. Bayne, M. Gaul, D. Kanach, K. Udell and N. M. Karayannis, *Inorg. Chim. Acta*, 173 (1990) 31
- 216 C. M. Mikulski, M. L. Bayne, S. Grossman, M. Gaul, A. Renn and D. L. Staley, *J. Coord. Chem.*, 20 (1989) 185
- 217 P. D. Verweij, F. J. Rietmeijer, R. A. G. DeGraaff, A. Erdonmez and J. Reedijk, *Inorg. Chim. Acta*, 163 (1989) 223
- 218 N. Hadjiladis, A. Yannopoulos, E. De Grave and R. Bau, *Bull. Soc. Chim. Belg.*, 98 (1989) 223
- 219 C. Engelter, G. E. Jackson, C. L. Knight and D. A. Thornton, *J. Coord. Chem.*, 20 (1989) 289
- 220 C. Engelter, G. E. Jackson, C. L. Knight and D. A. Thornton, *J. Coord. Chem.*, 20 (1989) 297
- 221 D. M. L. Goodgame, D. J. Williams and R. E. P. Winpenny, *Inorg. Chim. Acta*, 166 (1989) 159
- 222 S. Fukuzumi, S. Mochizuki and T. Tanaka, *J. Chem. Soc., Dalton Trans.*, (1990) 695
- 223 H. E. Toma and L. A. Morino, *Transition Met. Chem. (London)*, 15 (1990) 66
- 224 S. Gangopadhyay, A. Das and D. Banerjee, *J. Indian Chem. Soc.*, 66 (1989) 517
- 225 I. V. Khoroshun, N. M. Samus, S. P. Yuschenko and K. I. Turte, *Zh. Neorg. Khim.*, 34 (1989) 3053 [*Chem. Abstr.* 112:228575h]
- 226 I. I. Bulgak, V. E. Zubareva, K. I. Turte, V. N. Shafranskii and V. T. Balan, *Koord. Khim.*, 16 (1990) 650 [*Chem. Abstr.* 113:125254u]
- 227 M. J. Blandamer, N. J. Blundell, J. Burgess, H. J. Cowles, J. B. F. N. Engberts, I. M. Horn and P. Warrick, Jr., *J. Am. Chem. Soc.*, 112 (1990) 6854
- 228 D. W. Thompson and D. V. Stynes, *Inorg. Chem.*, 29 (1990) 3815
- 229 Y. Z. Voloshin, N. A. Kostromina and A. Y. Nazarenko, *Inorg. Chim. Acta*, 170 (1990) 181
- 230 R. A. Marusak, C. Sharp and G. A. Lappin, *Inorg. Chem.*, 29 (1990) 2298
- 231 M. M. Aly, *Transition Met. Chem. (London)*, 15 (1990) 99
- 232 M. Jacob, P. K. Bhattacharya, P. A. Ganeshpure, S. Satish and S. Sivaram, *Bull. Chem. Soc. Jpn.*, 62 (1989) 1325
- 233 A. V. Sokolov, R. P. Smirnov, M. I. Bazanov, M. K. Islyaikin and E. A. Danilova, *Izv. Vyssh. Uchebn. Zaved., Khim. Khim. Tekhnol.*, 32 (1989) 38 [*Chem. Abstr.* 112:158216r]
- 234 A. V. Sokolov, R. P. Smirnov, M. I. Bazanov, N. A. Kolesnikov and M. K. Islyaikin, *Izv. Vyssh. Uchebn. Zaved., Khim. Khim. Tekhnol.*, 32 (1989) 102 [*Chem. Abstr.* 113:164297e]
- 235 G. De M. Norante, M. Di Vaira, F. Mani, S. Mazzi and P. Stoppioni, *Inorg. Chem.*, 29 (1990) 2822
- 236 R. M. Izatt, R. L. Bruening, B. J. Tarbet, L. D. Griffin, M. L. Bruening, K. E. Krakowiak and J. E. Bradshaw, *Pure Appl. Chem.*, 62 (1990) 1115
- 237 K. Wiegardt, S. Drueke, P. Chaudhuri, U. Floerke, H. J. Haupt, B. Nuber and J. Weiss, *Z. Naturforsch., B: Chem. Sci.*, 44 (1989) 1093
- 238 R. Hotzelmann, K. Wiegardt, U. Floerke and H. J. Haupt, *Angew. Chem.*, 102 (1990) 720
- 239 A. Geilenkirchen, K. Wiegardt, B. Nuber and J. Weiss, *Z. Naturforsch., B: Chem. Sci.*, 44 (1989) 1333
- 240 J. L. Sessler, J. W. Sibert and V. Lynch, *Inorg. Chem.*, 29 (1990) 4143
- 241 E. G. Jaeger, J. Liehr, E. Morich and A. Dix., *Proc. Conf. Coord. Chem.*, 12th, (1989) 123
- 242 T. J. Collins, K. L. Kostka, E. Munck and E. S. Uffelman, *J. Am. Chem. Soc.*, 112 (1990) 5637
- 243 C. Harding, D. McDowell, J. Nelson, S. Raghunathan, C. Stevenson, M. G. B. Drew and P. C. Yates, *J. Chem. Soc., Dalton Trans.*, (1990) 2521
- 244 J. Hunter, J. Nelson, C. Harding, M. McCann and V. McKee, *J. Chem. Soc., Chem. Commun.*, (1990) 1148
- 245 L. L. Martin, R. L. Martin, K. S. Murray and A. M. Sargeson, *Inorg. Chem.*, 29 (1990) 1387
- 246 H. Chen, R. A. Bartlett, M. M. Olmstead, P. P. Power and S. C. Shoner, *J. Am. Chem. Soc.*, 112 (1990) 1048
- 247 S. P. Perlepes, D. Kovala-Demertzi, S. Skaribas, D. Nicholls and S. Paraskevas, *Thermochim. Acta*, 147 (1989) 153
- 248 D. X. West, C. S. Carlson, A. C. White and A. E. Liberta, *Transition Met. Chem. (London)*, 15 (1990) 43
- 249 C. T. Chen, D. S. Liaw, G. H. Lee and S. M. Peng, *Transition Met. Chem. (London)*, 14 (1989) 76

- 250 A. M. A. Hassaan, E. M. Soliman and M. El-Shabasy, *Synth. React. Inorg. Met.-Org. Chem.*, 19 (1989) 773 [*Chem. Abstr.* 112:171005r]
- 251 G. Yuksel, M. Pekin and E. Dolen, *Marmara Univ. Eczacilik Derg.*, 5 (1989) 19 [*Chem. Abstr.* 113:230894a]
- 252 K. Bodek and S. Petri, *Acta Pol. Pharm.*, 46 (1989) 146 [*Chem. Abstr.* 112: 166010j]
- 253 K. Micskei and I. Nagypal, *J. Chem. Soc., Dalton Trans.*, (1990) 743
- 254 K. Bayo, G. V. Ouedraogo, G. Terzian and D. Benlian, *Polyhedron*, 9 (1990) 1087
- 255 S. Zhao, Q. Zheng and J. Xie, *Huaxue Xuebao*, 47 (1989) 842 [*Chem. Abstr.* 113:50446x]
- 256 M. Hanack, A. Hirsch and H. Lehmann, *Angew. Chem.*, 102 (1990) 1499
- 257 P. Ascenzi, M. Brunori, G. Pennesi, C. Ercolani and F. Monacelli, *J. Chem. Soc., Dalton Trans.*, (1990) 105
- 258 M. N. Golovin, P. Seymour, K. Jayaraj, Y. S. Fu and A. B. P. Lever, *Inorg. Chem.*, 29 (1990) 1719
- 259 M. Ostropolska, *Polyhedron*, 9 (1990) 1021
- 260 N. Kobayashi, K. Sudo and T. Osa, *Bull. Chem. Soc. Jpn.*, 63 (1990) 571
- 261 B. Moubarak, M. Ley, D. Benlian and J. P. Sorbier, *Acta Cryst., Sect. C*, C46 (1990) 379
- 262 M. Tanaka, Y. Sakai, T. Torninaga, A. Fukuoaka, T. Kimura and M. Ichikawa, *J. Radioanal. Nucl. Chem.*, 137 (1989) 287
- 263 M. Hanack and G. Renz, *Chem. Ber.*, 123 (1990) 1105
- 264 T. Ohya, J. Takeda, N. Kobayashi and M. Sato, *Inorg. Chem.*, 29 (1990) 3734
- 265 G. P. Gupta, G. Lang, C. A. Koch, B. Wang, W. R. Scheidt and C. A. Reed, *Inorg. Chem.*, 29 (1990) 4234
- 266 C. T. Brewer and G. Brewer, *J. Chem. Soc., Dalton Trans.*, (1990) 843
- 267 M. K. Safo, W. R. Scheidt and G. P. Gupta, *Inorg. Chem.*, 29 (1990) 626
- 268 O. K. Medhi and J. Silver, *J. Chem. Soc., Dalton Trans.*, (1990) 555
- 269 O. K. Medhi and J. Silver, *Inorg. Chim. Acta*, 168 (1990) 271
- 270 T. B. Higgins, M. K. Safo and W. R. Scheidt, *Inorg. Chim. Acta*, 178 (1990) 261
- 271 O. K. Medhi and J. Silver, *Inorg. Chim. Acta*, 171 (1990) 247
- 272 Y.-T. Chen, Z. Zhu and Y. Ma, *Inorg. Chim. Acta*, 177 (1990) 75
- 273 G. Al-Jaff, J. Silver and M. T. Wilson, *Inorg. Chim. Acta*, 176 (1990) 307
- 274 D. Mandon, F. Ott-Woelfel, J. Fischer, R. Weiss, E. Bill and A. X. Trautwein, *Inorg. Chem.*, 29 (1990) 2442
- 275 H. Nasri, J. A. Goodwin and W. R. Scheidt, *Inorg. Chem.*, 29 (1990) 185
- 276 M. G. Finnegan, A. G. Lappin and W. R. Scheidt, *Inorg. Chem.*, 29 (1990) 181
- 277 T. Komatsu, E. Hasegawa, H. Nishide and E. Tsuchida, *J. Chem. Soc., Chem. Commun.*, (1990) 66
- 278 E. Tsuchida, E. Hasegawa, T. Komatsu, K. Nakao and H. Nishide, *Chem. Lett.*, (1990) 1071
- 279 C. Tetreau, M. Momenteau and D. Lavalette, *Inorg. Chem.*, 29 (1990) 1727
- 280 Y. Uemori and E. Kyuno, *Inorg. Chim. Acta*, 165 (1989) 115
- 281 H. R. Jimenez, J. M. Moratal, J. Faus and M. Momenteau, *New J. Chem.*, 14 (1990) 13
- 282 S. Matile and W.-D. Woggon, *J. Chem. Soc., Chem. Commun.*, (1990) 774
- 283 A. L. Balch, C. R. Cornman, L. Latos-Grazyński and M. M. Olmstead, *J. Am. Chem. Soc.*, 112 (1990) 7552
- 284 T. J. Bartczak, L. Latos-Grazyński and A. Wyslouch, *Inorg. Chim. Acta*, 171 (1990) 205
- 285 H. Zhang, U. Simonis and F. A. Walker, *J. Am. Chem. Soc.*, 112 (1990) 6124
- 286 A. L. Balch, R. L. Hart, L. Latos-Grazyński and T. G. Traylor, *J. Am. Chem. Soc.*, 112 (1990) 7382
- 287 R. D. Arasasingham, A. L. Balch, C. R. Cornman, J. S. de Ropp, K. Eguchi and G. N. LaMar, *Inorg. Chem.*, 29 (1990) 1847
- 288 T. Uno, K. Hatano, Y. Nishimura and Y. Arata, *Inorg. Chem.*, 29 (1990) 2803
- 289 R. D. Arasasingham, A. L. Balch, R. L. Hart and L. Latos-Grazyński, *J. Am. Chem. Soc.*, 112 (1990) 7566
- 290 K. Shin, B.-S. Yu and H. M. Goff, *Inorg. Chem.*, 29 (1990) 889
- 291 A. L. Balch, C. R. Cornman, N. Safari and L. Latos-Grazyński, *Organometallics*, 9 (1990) 2420
- 292 C. Guetin, D. Lexa, M. Momenteau and J.-M. Saveant, *J. Am. Chem. Soc.*, 112 (1990) 1874
- 293 H. M. Abu-Soud and J. Silver, *Inorg. Chim. Acta*, 164 (1989) 105
- 294 Y. O. Kim and H. M. Goff, *Inorg. Chem.*, 29 (1990) 3907
- 295 H. Hori, K. Kadono, K. Fukuda, H. Inoue, T. Shirai and E. Fluck, *Radiochim. Acta*, 49 (1990) 77
- 296 X. H. Mu and K. M. Kadish, *Inorg. Chem.*, 29 (1990) 1031
- 297 T. Shi, D. Zhao and X. Cao, *Huaxue Xuebao*, 48 (1990) 459 [*Chem. Abstr.* 113:164397n]

- 298 X. Cao, Q. Wang and S. Zhang, *Gaodeng Xuexiao Huaxue Xuebao*, 11 (1990) 36 [*Chem. Abstr.* 113:48483p]
- 299 R. A. Reed, K. R. Rodgers, K. Kushmeider, T. G. Spiro and Y. O. Su, *Inorg. Chem.*, 29 (1990) 2881
- 300 H. Otake, A. Miyata and H. Tomiyasu, *Inorg. Chim. Acta*, 168 (1990) 153
- 301 M. Nakamura, *Inorg. Chim. Acta*, 161 (1989) 73
- 302 M. Nakamura and N. Nakamura, *Chem. Lett.*, (1990) 181
- 303 Y. Zhang, J. G. Jones and D. A. Sweigert, *Inorg. Chim. Acta*, 166 (1989) 85
- 304 B. R. Serr, C. E. L. Headford, C. M. Elliott and O. P. Anderson, *Acta. Cryst., Sect. C*, C46 (1990) 500
- 305 O. K. Medhi and J. Silver, *J. Chem. Soc., Dalton Trans.*, (1990) 263
- 306 K. Hatano and T. Uno, *Bull. Chem. Soc. Jpn.*, 63 (1990) 1825
- 307 L. N. Ji, M. Liu, S. H. Huang, G. Z. Hu, Z. Y. Zhou, L. L. Koh and A. K. Hsieh, *Inorg. Chim. Acta*, 174 (1990) 21
- 308 H. M. Abu-Soud and J. Silver, *Inorg. Chim. Acta*, 161 (1989) 139
- 309 C. Brewer, *J. Chem. Soc., Chem. Commun.*, (1990) 344
- 310 M. Massoudipour, S. K. Tewari and K. K. Pandey, *Polyhedron*, 8 (1989) 1447
- 311 L. Toupet, P. Sodano and G. Simonneaux, *Acta Cryst., Sect. C*, C46 (1990) 1631
- 312 T. S. Kurtikyan, G. G. Martirosyan, A. V. Gasparyan, M. E. Akopyan and G. A. Zhamkochyan, *Zh. Prikl. Spektrosk.*, 53 (1990) 67 [*Chem. Abstr.* 113:243520a]
- 313 S. Zhu, M. Gui and C. Guo, *Gaodeng Xuexiao Huaxue Xuebao*, 10 (1989) 1100 [*Chem. Abstr.* 112:186647a]
- 314 A. Nanthakumar and H. M. Goff, *Inorg. Chem.*, 29 (1990) 4559
- 315 T. Zeng, J. Huang, T. Cheng and L. Ji, *Huaxue Xuebao*, 47 (1989) 128 [*Chem. Abstr.* 112:68555w]
- 316 L. Ohlhausen, D. Cockrum, J. Register, K. Roberts, G. J. Long, G. L. Powell and B. B. Hutchinson, *Inorg. Chem.*, 29 (1990) 4886
- 317 T. Higuchi, S. Uzu and M. Hirobe, *J. Am. Chem. Soc.*, 112 (1990) 7051
- 318 F. S. Woo, M. Cahiwat-Alquiza and H. C. Kelly, *Inorg. Chem.*, 29 (1990) 4718
- 319 R. E. Rodriguez, F. S. Woo, D. A. Huckaby and H. C. Kelly, *Inorg. Chem.*, 29 (1990) 1434
- 320 B. R. Serr, C. E. L. Headford, O. P. Anderson, C. M. Elliott, C. K. Schauer, K. Akabori, K. Spartalian, W. E. Hatfield and B. R. Rolfs, *Inorg. Chem.*, 29 (1990) 2663
- 321 R. Panicucci and T. C. Bruice, *J. Am. Chem. Soc.*, 112 (1990) 6063
- 322 K. Murata, R. Panicucci, E. Gopinath and T. C. Bruice, *J. Am. Chem. Soc.*, 112 (1990) 6072
- 323 T. G. Traylor and F. Xu., *J. Am. Chem. Soc.*, 112 (1990) 178
- 324 P. K. S. Tsang and D. T. Sawyer, *Inorg. Chem.*, 29 (1990) 2848
- 325 I. R. Paeng and K. Nakamoto, *J. Am. Chem. Soc.*, 112 (1990) 3289
- 326 Y. Mizutani, S. Hashimoto, Y. Tatsuno and T. Kitagawa, *J. Am. Chem. Soc.*, 112 (1990) 6809
- 327 K. Tajima, *Inorg. Chim. Acta*, 163 (1989) 115
- 328 K. Tajima, M. Shigematsu, J. Jinno, K. Ishizu, H. Ohya-Nishiguchi, *J. Chem. Soc., Chem. Commun.*, (1990) 144
- 329 K. Tajima, M. Yoshino, K. Mikami, T. Edo, K. Ishizu and H. Ohya-Nishiguchi, *Inorg. Chim. Acta*, 172 (1990) 83
- 330 D. Mandon, R. Weiss, M. Franke, E. Bill and A. X. Trautwein, *Angew. Chem.*, 101 (1989) 1747
- 331 E. Tsuchida, T. Komatsu, E. Hasegawa and H. Nishide, *J. Chem. Soc., Dalton Trans.*, (1990) 2713
- 332 S.-M. Chen and Y. O. Su, *J. Chem. Soc., Chem. Commun.*, (1990) 491
- 333 Y. Watanabe, K. Tekchira, M. Shimizu, T. Hayakawa, H. Orita and M. Kaise, *J. Chem. Soc., Chem. Commun.*, (1990) 1262
- 334 E. Tsuchida, E. Hasegawa, T. Komatsu, T. Nakata and H. Nishide, *Chem. Lett.*, (1990) 389
- 335 L. Ding, C. Casas, G. Etemad-Moghadam, B. Meunier and S. Cros, *New. J. Chem.*, 14 (1990) 421
- 336 L. Baltzer and M. Landergren, *J. Am. Chem. Soc.*, 112 (1990) 2804
- 337 T. Yoshimura, *Bull. Chem. Soc. Jpn.*, 63 (1990) 3689
- 338 N. Li, Z. Su., P. Coppens and J. Landrum, *J. Am. Chem. Soc.*, 112 (1990) 7294
- 339 J. P. Collman, P. D. Hampton and J. I. Brauman, *J. Am. Chem. Soc.*, 112 (1990) 2977
- 340 J. P. Collman, P. D. Hampton and J. I. Brauman, *J. Am. Chem. Soc.*, 112 (1990) 2986
- 341 I. Artaud, N. Gregoire, P. Leduc and D. Mansuy, *J. Am. Chem. Soc.*, 112 (1990) 6899
- 342 Y. Watanabe, K. Takehira, M. Shimizu, T. Hayakawa and H. Orita, *J. Chem. Soc., Chem. Commun.*, (1990) 927

- 343 E. Baciocchi, M. Crescenzi and O. Lanzalunga, *J. Chem. Soc., Chem. Commun.*, (1990) 687
- 344 S. Nakashima, H. Ohya-Nishiguchi, N. Hirota, H. Fujii and I. Morishima, *Inorg. Chem.*, 29 (1990) 5207
- 345 K. Shin and H. M. Goff, *J. Chem. Soc., Chem. Commun.*, (1990) 461
- 346 A. G. Cochran and P. G. Schultz, *J. Am. Chem. Soc.*, 112 (1990) 9414
- 347 J. P. Mahy, G. Bedi, P. Battioni and D. Mansuy, *New. J. Chem.*, 13 (1989) 651
- 348 A. Nanthakumar and H. M. Goff, *J. Am. Chem. Soc.*, 112 (1990) 4047
- 349 A. Gismelseed, E. L. Bominaar, E. Bill, A. X. Trautwein, H. Winkler, H. Nasri, P. Doppelt, D. Mandon, J. Fischer and R. Weiss, *Inorg. Chem.*, 29 (1990) 2741
- 350 A. Gold, K. Jayaraj, P. Doppelt, R. Weiss, E. Bill, X. Q. Ding, E. L. Bominaar, A. X. Trautwein and H. Winkler, *New. J. Chem.*, 13 (1989) 169
- 351 A. L. Balch, R. L. Hart and L. Latos-Grazyinski, *Inorg. Chem.*, 29 (1990) 3253
- 352 M. Landergren and L. Baltzer, *Inorg. Chem.*, 29 (1990) 556
- 353 W. Beck, W. Knauer and C. Robl, *Angew. Chem.*, 102 (1990) 331
- 354 T. Wijesekera, A. Matsumoto, D. Dolphin and D. Lexa, *Angew. Chem.*, 102 (1990) 1073
- 355 J. C. Huang, *Proc. Electrochem. Soc.*, 89 (1989) 268
- 356 H. Orita, M. Shimizu, C. Nishihara, T. Hayakawa and K. Takehira, *Can. J. Chem.*, 68 (1990) 787
- 357 O. K. Medhi and J. Silver, *Inorg. Chim. Acta*, 164 (1989) 231
- 358 O. A. Chamaeva and A. N. Kitaigorodskii, *Izv. Akad. Nauk. SSSR, Ser. Khim.*, (1989) 1269 [*Chem. Abstr.* 112:35522e]
- 359 H. E. Toma and K. Araki, *J. Chem. Res., Synop.*, (1990) 82
- 360 A. J. Thompson and P. M. A. Gadsby, *J. Chem. Soc., Dalton Trans.*, (1990) 1921
- 361 A. M. Bond, T. F. Mann, G. A. Tondreau and D. A. Sweigart, *Inorg. Chim. Acta*, 169 (1990) 181
- 362 S. Modi, V. P. Shedbalkar and D. V. Behere, *Inorg. Chim. Acta*, 173 (1990) 9
- 363 S. Mazumdar, O. K. Medhi and S. Mitra, *J. Chem. Soc., Dalton Trans.*, (1990) 1057
- 364 S. Mazumdar and O. K. Medhi, *J. Chem. Soc., Dalton Trans.*, (1990) 2633
- 365 H. Langbein and P. Eichhorn, *Z. Chem.*, 30 (1990) 142
- 366 G. V. Shilov, V. I. Ponomarev and L. O. Atovmyan, *Koord. Khim.*, 16 (1990) 230 [*Chem. Abstr.* 112: 189396d]
- 367 K. L. Taft and S. J. Lippard, *J. Am. Chem. Soc.*, 112 (1990) 9629
- 368 D. Hanzel, D. Hanzel, H. Bilinski, T. A. Himdan, M. Miljak and V. Vancina, *Hyperfine Interact.*, 53 (1990) 339
- 369 M. Tonkovic, S. Horvat, J. Horvat, S. Music and O. Hadzija, *Polyhedron*, 9 (1990) 2895
- 370 J. K. Puri, A. Miglani, M. Malhotra and V. K. Sharma, *Inorg. Chim. Acta*, 170 (1990) 103
- 371 D. Collison and A. K. Powell, *Inorg. Chem.*, 29 (1990) 4735
- 372 G. Albertin, D. Baldan and E. Bordignon, *J. Organometal. Chem.*, 377 (1989) 145
- 373 R. Demuth and W. Heuermann, *Prax. Naturwiss. Chem.*, 39 (1990) 41
- 374 A. N. Glebov, E. V. Kirillova and Y. I. Saifnikov, *Koord. Khim.*, 15 (1989) 1683 [*Chem. Abstr.* 112: 106167f]
- 375 M. Akiyama, A. Katoh and T. Ogawa, *J. Chem. Soc., Perkin Trans. 2*, (1989) 1213
- 376 Y. Sun and A. E. Martell, *Tetrahedron*, 46 (1990) 2725
- 377 E. Farkas, J. Szoke, T. Kiss, H. Kozlowski and W. Bal, *J. Chem. Soc., Dalton Trans.*, (1989) 2247
- 378 E. Farkas and P. Buglyo, *J. Chem. Soc., Dalton Trans.*, (1990) 1549
- 379 S. N. Kane, S. M. Ali, A. Gupta and P. V. Khadikar, *Bull. Chem. Soc. Belg.*, 99 (1990) 293
- 380 S. N. Kane, S. M. Ali, A. Gupta and P. V. Khadikar, *Hyperfine Interact.*, 53 (1990) 345
- 381 M. R. Jan, Imdadullah and J. Shah, *J. Chem. Soc. Pak.*, 11 (1989) 330
- 382 C. Natarajan and P. R. Athappan, *Indian J. Chem., Sect. A*, 29A (1990) 599
- 383 M. Doering and T. Waldbach, *Z. Anorg. Allg. Chem.*, 577 (1989) 93
- 384 P. J. Van Koningsbruggen, O. Khan, K. Nakatani, Y. Pei, J. P. Renard, M. Drillon and P. Legoll, *Inorg. Chem.*, 29 (1990) 3325
- 385 P. Garge, R. Chikate, S. Padhye, J. M. Savariault, P. Le Doth and J. P. Tuchagues, *Inorg. Chem.*, 29 (1990) 3315
- 386 P. Garge, S. Padhye and J. P. Tuchagues, *Inorg. Chim. Acta*, 157 (1989) 239
- 387 J. Burgess and M. S. Patel, *Inorg. Chim. Acta*, 170 (1990) 241
- 388 Y. Tor, A. Shanzer and A. Scherz, *Inorg. Chem.*, 29 (1990) 4069
- 389 K. Hegetschweiler, H. Schmalte, H. M. Streit and W. Schneider, *Inorg. Chem.*, 29 (1990) 3625
- 390 I. Ondrejovicova, V. Vancova and G. Ondrejovic, *Proc. Conf. Coord. Chem.*, 12th, (1989) 263 [*Chem. Abstr.* 112:150751r]

- 391 S. K. Ramalingham and S. A. Samath, *Indian J. Chem., Sect. A*, 29A (1990) 818
- 392 M. Irudayasamy and S. Nagarajan, *Asian J. Chem.*, 1 (1989) 214 [*Chem. Abstr.* 112:150558h]
- 393 B. Jankiewicz, R. Soloniewicz and M. Teodorczyk, *Acta Pol. Pharm.*, 45 (1988) 517
- 394 M. Tonkovic, O. Hadzija, B. Ladesic, B. Klaić and S. Music, *Inorg. Chim. Acta*, 161 (1989) 81
- 395 S. Deiana, C. Gessa, B. Manunza, P. Piu and R. Seeber, *J. Inorg. Biochem.*, 39 (1990) 25
- 396 R. M. Awadallah, A. E. Mohamed, M. A. El Maghraby, A. M. M. Ramadan, *Transition Met. Chem. (London)*, 15 (1990) 273
- 397 F. Mhenni, A. Bouraoui, Z. Mighri and R. Gallo, *Bull. Soc. Chim. Fr.*, (1989) 824
- 398 N. M. Karayannis and C. M. Mikulski, *Transition Met. Chem. (London)*, 14 (1989) 478
- 399 S. P. Best and J. B. Forsyth, *J. Chem. Soc., Dalton Trans.*, (1990) 395
- 400 B. Beagley, D. G. Kelly, P. P. MacRory, C. A. McAuliffe and R. G. Pritchard, *J. Chem. Soc., Dalton Trans.*, (1990) 2657
- 401 S. I. Klein, A. C. Massabni, J. C. Moreira and A. Tancredo, *Eclectica Quim.*, 13 (1988) 7 [*Chem. Abstr.* 112:15543j]
- 402 J. Xu and R. B. Jordan, *Inorg. Chem.*, 29 (1990) 4180
- 403 W. H. Jolley, D. R. Stranks and T. W. Swaddle, *Inorg. Chem.*, 29 (1990) 1948
- 404 S. S. Atkaabi and E. M. Nour, *Orient. J. Chem.*, 6 (1990) 90 [*Chem. Abstr.* 113:198935b]
- 405 J. H. Urban and J. R. Damewood, Jr., *J. Chem. Soc., Chem. Commun.*, (1990) 1636
- 406 J. S. Lim, J. W. Lee, S. G. Kang and B. K. Park, *Bull. Korean Chem. Soc.*, 11 (1990) 303 [*Chem. Abstr.* 113:198940z]
- 407 L. Peiyi and Z. Hualin, *Inorg. Chim. Acta*, 173 (1990) 255
- 408 N. Yoshida, T. Matsushita, S. Saigo, H. Oyanagi, H. Hashimoto and M. Fujimoto, *J. Chem. Soc., Chem. Commun.*, (1990) 354
- 409 D. K. Sanyal, *S. Afr. J. Chem.*, 43 (1990) 23 [*Chem. Abstr.* 113:90324n]
- 410 T. L. Zalevskaya, E. V. Radion and A. K. Baev, *Vestsi Akad. Navuk BSSR, Ser. Khim. Navuk*, (1989) 3 [*Chem. Abstr.* 112:90301g]
- 411 K. Mereiter, *Acta Cryst., Sect. C*, C46 (1990) 972
- 412 A. R. Sarkar and R. K. Bandyopadhyay, *Indian J. Chem., Sect. A*, 28A (1989) 998
- 413 J. E. Toth, J. D. Melton, D. Cabelli, B. H. J. Bielski and F. C. Anson, *Inorg. Chem.*, 29 (1990) 1952
- 414 A. Martin and A. Feltz, *Z. Anorg. Allg. Chem.*, 575 (1989) 115
- 415 E. H. Merrachi, R. Cohen-Adad, F. Chassagneux, J. Paris, B. F. Mentzen and J. Bouix, *Thermochim. Acta*, 152 (1989) 77
- 416 J. C. Machado, M. M. Braga and B. F. Rodrigues, *Thermochim. Acta*, 158 (1990) 283
- 417 Y. N. Makurin, E. A. Nikonenko, G. G. Kasimov and N. A. Zhelonkin, *Zh. Neorg. Khim.*, 34 (1989) 2754 [*Chem. Abstr.* 112:190727u]
- 418 V. Bujoreanu, D. Sahleanu, M. Brezeanu and E. Segal, *Thermochim. Acta*, 161 (1990) 357
- 419 H. Mevs and H. Mueller-Buschbaum, *J. Less-Common Met.*, 158 (1990) 147
- 420 H. Mevs and H. Mueller-Buschbaum, *J. Less-Common Met.*, 157 (1990) 173
- 421 S. H. Wasfi and C. E. Costello, *Synth. React. Inorg. Met.-Org. Chem.*, 19 (1989) 1059
- 422 T. Fries, G. Mayer-Von Kuerthy, A. Ehmann, W. Wischert and S. Kemmler-Sack, *J. Less-Common Met.*, 159 (1990) 337
- 423 K. Kimura, M. Ohgaki, K. Tanaka, H. Morikawa and F. Marumo, *J. Solid State Chem.*, 87 (1990) 186
- 424 M. A. Petrukhnina, V. N. Molchanov, I. V. Tat'yana and E. A. Torchenkova, *Kristallografiya*, 35 (1990) 386 [*Chem. Abstr.* 113:201817x]
- 425 K. D. Butcher, M. S. Gebhard and E. I. Solomon, *Inorg. Chem.*, 29 (1990) 2067
- 426 M. S. Gebhard, J. C. Deaton, S. A. Koch, M. Millar and E. I. Solomon, *J. Am. Chem. Soc.*, 112 (1990) 2217
- 427 W. N. Setzer, E. L. Cacioppo, Q. Guo, G. J. Grant, D. D. Kim, J. L. Hubbard and D. G. Van Derveer, *Inorg. Chem.*, 29 (1990) 2672
- 428 A. Hills, D. L. Hughes, M. Jimenez-Tenorio, G. J. Leigh, A. Houlton and J. Silver, *J. Chem. Soc., Chem. Commun.*, (1989) 1774
- 429 A. J. Blake, A. J. Holder, T. I. Hyde and M. Schröder, *J. Chem. Soc., Chem. Commun.*, (1989) 1433
- 430 H. Doine and T. W. Swaddle, *Can. J. Chem.*, 68 (1990) 2228
- 431 S. E. Boyd, L. D. Field, T. W. Hambley and D. J. Young, *Inorg. Chem.*, 29 (1990) 1496
- 432 S. J. Brown, S. K. C. Kok, P. A. Lay and A. F. Masters, *Aust. J. Chem.*, 42 (1989) 1839
- 433 L. Qian, P. Singh, H. Ro and W. E. Hatfield, *Inorg. Chem.*, 29 (1990) 761

- 434 K. Kirschbaum, K. Griewe, K. Mueller, H. Strasdeit, B. Krebs and G. Henkel, *Z. Naturforsch., B: Chem. Sci.*, 45 (1990) 497
- 435 R. N. Mukherjee and B. S. Shastri, *Indian J. Chem., Sect. A*, 29A (1990) 809
- 436 A. Syngolliou-Kourakou and I. Tossidis, *J. Therm. Anal.*, 35 (1989) 1433
- 437 K. K. Aravindakshan and K. Muralidharan, *Thermochim. Acta*, 159 (1990) 101
- 438 S. Menage, B. A. Brennan, C. Juarez-Garcia, E. Munck and L. Que, Jr., *J. Am. Chem. Soc.*, 112 (1990) 6423
- 439 S. Menage and L. Que, Jr., *Inorg. Chem.*, 29 (1990) 4293
- 440 R. M. Buchanan, M. S. Mashuta, J. F. Richardson, R. J. Webb, K. J. Oberhausen, M. A. Nanny and D. N. Hendrickson, *Inorg. Chem.*, 29 (1990) 1299
- 441 T. R. Holman, K. A. Andersen, O. P. Anderson, M. P. Hendrich, C. Juarez-Garcia, E. Munck and L. Que, Jr., *Angew. Chem.*, 102 (1990) 933
- 442 A. S. Borovik, M. P. Hendrich, T. R. Holman, E. Munck, V. Papaefthymiou and L. Que, Jr., *J. Am. Chem. Soc.*, 112 (1990) 6031
- 443 T. R. Holman, C. Juarez-Garcia, M. P. Hendrich, L. Que, Jr. and E. Munck, *J. Am. Chem. Soc.*, 112 (1990) 7611
- 444 K. Schepers, B. Bremer, B. Krebs, G. Henkel, E. Althaus, B. Mosel and W. Mueller-Warmuth, *Angew. Chem.*, 102 (1990) 582
- 445 R. H. Beer, W. B. Tolman, S. G. Bott and S. J. Lippard, *Inorg. Chem.*, 28 (1989) 4557
- 446 R. L. Rardin, A. Bino, P. Poganiuch, W. B. Tolman, S. Liu and S. J. Lippard, *Angew. Chem.*, 102 (1990) 842
- 447 C. G. Wahlgren, A. W. Addison, S. Burman, L. K. Thompson, E. Sinn and T. M. Rowe, *Inorg. Chim. Acta*, 166 (1989) 59
- 448 D. R. Richardson, L. M. Wis Votolo, G. T. Hefter, P. M. May, B. W. Clare, J. Webb and P. Wilairat, *Inorg. Chim. Acta*, 170 (1990) 165
- 449 L. M. Wis Votolo, G. T. Hefter, B. W. Clare and J. Webb, *Inorg. Chim. Acta*, 170 (1990) 171
- 450 M. Mikuriya, K. Kushida, H. Nakayama, W. Mori and M. Kishita, *Inorg. Chim. Acta*, 165 (1989) 35
- 451 F. Lloret, M. Julve, J. Faus, X. Solans and Y. Journaux, *Inorg. Chem.*, 29 (1990) 2232
- 452 X. Wang, M. E. Kotun and J. C. Fanning, *Huaxue Xuebao*, 48 (1990) 204 [*Chem. Abstr.* 113:143810b]
- 453 E. N. Bakshi, R. L. Elliott, K. S. Murray, P. J. Nichols and B. O. West, *Aust. J. Chem.*, 43 (1990) 707
- 454 J. F. Sheu and H. H. Wei, *J. Chin. Chem. Soc. (Taipei)*, 36 (1989) 539 [*Chem. Abstr.* 112:244808s]
- 455 E. Solari, F. Corazza, C. Floriani, A. Chiesi-Villa and C. Guastini, *J. Chem. Soc., Dalton Trans.*, (1990) 1345
- 456 S. K. Larsen, B. G. Jenkins, N. G. Memon and R. B. Lauffer, *Inorg. Chem.*, 29 (1990) 1147
- 457 R. J. Motekaitis, A. E. Martell and M. J. Welch, *Inorg. Chem.*, 29 (1990) 1463
- 458 C. J. Carrano, M. W. Carrano, K. Sharma, G. Backes and J. Sanders-Loehr, *Inorg. Chem.*, 29 (1990) 1865
- 459 J. Costamanga, L. Araya and R. Latorre, *Pure. Appl. Chem.*, 61 (1989) 829
- 460 L.-J. Ming, R. B. Lauffer and L. Que, Jr., *Inorg. Chem.*, 29 (1990) 3060
- 461 A. Bonardi, C. Carini, C. Merlo, C. Pelizzi, G. Pelizzi, P. Tarasconi, F. Vitali and F. Cavatorta, *J. Chem. Soc., Dalton Trans.*, (1990) 2771
- 462 P. Basu, S. Pal and A. Chakravorty, *J. Chem. Soc., Dalton Trans.*, (1990) 9
- 463 S. Chattopadhyay, P. Basu, D. Ray, S. Pal and A. Chakravorty, *Proc. Indian Acad. Sci., Chem. Sci.*, 102 (1990) 195
- 464 P. Basu, S. Pal and A. Chakravorty, *J. Chem. Soc., Chem. Commun.*, (1989) 977
- 465 M. S. Lah, M. L. Kirk, W. Hatfield and V. L. Pecoraro, *J. Chem. Soc., Chem. Commun.*, (1989) 1606
- 466 K. H. Reddy, *Indian J. Chem., Sect. A*, 29A (1990) 497
- 467 S. Goyal and K. Lal, *J. Indian Chem. Soc.*, 66 (1989) 477
- 468 B. B. Mahapatra, M. K. Raval and B. K. Patel, *Indian J. Chem., Sect. A*, 28A (1989) 434
- 469 P. Chaudhuri, M. Winter, P. Fleischhauer, W. Haase, U. Florke and H.-J. Haupt, *J. Chem. Soc., Chem. Commun.*, (1990) 1728
- 470 H. Kuno, K. Okamoto, J. Hidaka and H. Einaga, *Bull. Chem. Soc. Jpn.*, 62 (1989) 2824
- 471 E. Farkas and I. Kiss, *J. Chem. Soc., Dalton Trans.*, (1990) 749
- 472 A. R. Sarkar and R. K. Bandyopadhyay, *Synth. React. Inorg. Met.-Org. Chem.*, 20 (1990) 167

- 473 A. R. Sarkar and R. K. Bandyopadhyay, *Synth. React. Inorg. Met.-Org. Chem.*, 19 (1989) 761
- 474 S. Koch and G. Ackermann, *Z. Chem.*, 29 (1989) 297
- 475 S. Koch and G. Ackermann, *Z. Chem.*, 29 (1989) 219
- 476 S. Koch and G. Ackermann, *Z. Chem.*, 30 (1990) 33
- 477 S. Koch and G. Ackermann, *Z. Chem.*, 30 (1990) 32
- 478 M. R. McDevitt, A. W. Addison, E. Sinn and L. K. Thompson, *Inorg. Chem.*, 29 (1990) 3425
- 479 H. G. Jang, K. Kaji, M. Sorai, R. J. Wittebort, S. J. Geib, A. L. Rheingold and D. N. Hendrickson, *Inorg. Chem.*, 29 (1990) 3547
- 480 T. Nakamoto, M. Katada and H. Sano, *Chem. Lett.*, (1990) 225
- 481 Z. Wang and X. Yu, *Jiegou Huaxue*, 9 (1990) 10 [*Chem. Abstr.* 113:181962k]
- 482 P. Cofre, S. A. Richert, A. Sobkowiak and D. T. Sawyer, *Inorg. Chem.*, 29 (1990) 2645
- 483 C. Sheu, S. A. Richert, P. Cofre, B. Ross, Jr., A. Sobkowiak, D. T. Sawyer and J. R. Kanofsky, *J. Am. Chem. Soc.*, 112 (1990) 1936
- 484 C. Sheu, A. Sobkowiak, S. Jeon and D. T. Sawyer, *J. Am. Chem. Soc.*, 112 (1990) 879
- 485 V. Zang and R. Van Eldik, *Inorg. Chem.*, 29 (1990) 1705
- 486 S. Fujii, H. Ohya-Nishiguchi and H. Hirota, *Inorg. Chim. Acta*, 175 (1990) 27
- 487 T. M. Rana and C. F. Mearns, *J. Am. Chem. Soc.*, 112 (1990) 2457
- 488 D. A. Horne and P. B. Dervan, *J. Am. Chem. Soc.*, 112 (1990) 2435
- 489 H. Sakane, I. Watanabe, K. Ono, S. Ikeda, S. Kaizaki and Y. Kushi, *Inorg. Chim. Acta*, 178 (1990) 67
- 490 K. Kanamori, H. Dohniwa, N. Ukita, I. Kanesaka and K. Kawai, *Bull. Chem. Soc. Jpn.*, 63 (1990) 1447
- 491 T. Mizuta, T. Yamamoto, K. Miyoshi and Y. Kushi, *Inorg. Chim. Acta*, 175 (1990) 121
- 492 K. Okamoto, K. Kanamori and J. Hidaka, *Acta Cryst., Sect. C*, C46 (1990) 1640
- 493 U. Auerbach, U. Eckert, K. Wiegardt, B. Nuber and J. Weiss, *Inorg. Chem.*, 29 (1990) 938
- 494 A. E. Martell, R. J. Motekaitis and M. J. Welch, *J. Chem. Soc., Chem. Commun.*, (1990) 1748
- 495 V. V. Kravchenko, G. G. Sadikov, N. S. Rukk, E. V. Savinkina, M. G. Zaitseva, L. A. Butman, L. Y. Alkberova and B. D. Stepin, *Zh. Neorg. Khim.*, 34 (1989) 1492 [*Chem. Abstr.* 112:90249w]
- 496 M. F. R. Fouda, R. S. Amin and M. Hassanein, *Thermochim. Acta*, 145 (1989) 281
- 497 G. M. Iskander, S. B. Salama, R. H. Osman, E. L. Gulta and E. O. Schlemper, *J. Prakt. Chem.*, 332 (1990) 293
- 498 M. Vithal, T. G. N. Babu and B. N. Murthy, *Indian J. Chem., Sect. A*, 28A (1989) 689
- 499 D. Phung and N. M. Samus, *Tap Chi Hoa Hoc*, 26 (1988) 25 [*Chem. Abstr.* 112:110765s]
- 500 K. R. Reddy, K. L. Reddy and K. A. Reddy, *Indian J. Chem., Sect. A*, 28A (1989) 916
- 501 D. Liu, X. Cui, F. Geng, F. Li and Q. Kong, *Gaodeng Xuexiao Huaxue Xuebao*, 10 (1989) 787 [*Chem. Abstr.* 112:170989c]
- 502 M. S. Masoud, E. A. Khalil and A. R. Youssef, *Synth. React. Inorg. Met.-Org. Chem.*, 20 (1990) 793
- 503 M. Dudeja, J. Singh, N. K. Sangwan and K. S. Dhindsa, *Vijnana Parishad Anusandhan Patrika*, 32 (1989) 1 [*Chem. Abstr.* 112:244781c]
- 504 M. S. Abdel-Moez, S. L. Stefan, M. M. El-Beairy, M. M. Mashely and B. A. El-Shetary, *Can. J. Chem.*, 68 (1990) 774
- 505 N. Gupta and P. C. Nigam, *Wuji Huaxue Xuebao*, 5 (1989) 61 [*Chem. Abstr.* 112:146487s]
- 506 K. Yamagata, Y. Saito, T. Abe and M. Hashimoto, *J. Phys. Soc. Jpn.*, 58 (1989) 3865
- 507 J. H. Choy and D. Y. Noh, *Bull. Korean Chem. Soc.*, 10 (1989) 472 [*Chem. Abstr.* 112:29484c]
- 508 Z. P. Bai, H. Einaga and J. Hidaka, *Bull. Chem. Soc. Jpn.*, 63 (1990) 929
- 509 M. Noritake, K. Okamoto, J. Hidaka and H. Einaga, *Bull. Chem. Soc. Jpn.*, 63 (1990) 353
- 510 A. Abras, H. Beraldo, E. O. Fantini, R. H. U. Borges, M. A. Da Rocha and L. Tosi, *Inorg. Chim. Acta*, 172 (1990) 113
- 511 G. Davies, M. A. El-Sayed, A. El-Toukhy and M. Henary, *Inorg. Chim. Acta*, 168 (1990) 65
- 512 J. Takacs, E. Soos, Z. Nagy-Magos, L. Marko, G. Gervasio and T. Hoffmann, *Inorg. Chim. Acta*, 166 (1989) 39
- 513 N. K. Singh, U. Sharma, S. Agrawal and M. J. M. Campbell, *Polyhedron*, 9 (1990) 1065
- 514 N. Atkinson, A. D. Lavery, A. J. Blake, G. Reid and M. Schröder, *Polyhedron*, 9 (1990) 2641
- 515 S. P. Malve, N. V. Thakkar and B. C. Halder, *Indian J. Chem., Sect. A*, 29A (1990) 356

- 516 S. Sharma, V. Chowdhary, M. Parihar, R. Goyal, S. Guar and R. K. Mehta, *Indian J. Chem., Sect. A*, 28A (1989) 809
- 517 A. Garg and J. P. Tandon, *Proc. Indian Acad. Sci., Chem. Sci.*, 100 (1988), 463
- 518 I. I. Bulgak, I. E. Rychagova, V. E. Zubareva, K. I. Turte and V. N. Shafranskii, *Zh. Neorg. Khim.*, 35 (1990) 1737 [*Chem. Abstr.* 113:243529k]
- 519 J. S. Budkuley and K. C. Patil, *Synth. React. Inorg. Met.-Org. Chem.*, 19 (1989) 909
- 520 A. S. Grigor'eva, N. F. Konakhovich and V. V. Zelentsov, *Koord. Khim.*, 16 (1990) 646 [*Chem. Abstr.* 113:203757b]
- 521 P. Thomas, A. Seidel, U. Leibnitz, R. Szargan, I. Uhlig and H. Hennig, *Z. Chem.*, 29 (1989) 248
- 522 C. L. Jain, P. N. Mundley, Y. Kumar and P. D. Sethi, *J. Indian Chem. Soc.*, 66 (1989) 431
- 523 M. Kumar, A. Kumar, P. H. Madhuranath, N. S. Gupta, N. K. Jha and M. Mohan, *Synth. React. Inorg. Met.-Org. Chem.*, 20 (1990) 599
- 524 A. B. Akbarov, *Zh. Neorg. Khim.*, 35 (1990) 660 [*Chem. Abstr.* 113:90248r]
- 525 W. Dietzsch, L. Golic, A. Mewes and E. Hoyer, *Proc. Conf. Coord. Chem.*, 12th, (1989) 85
- 526 M. Doering, E. Uhlig and L. Dahlenburg, *Z. Anorg. Allg. Chem.*, 578 (1989) 58
- 527 E. Uhlig and M. Dering, *Proc. Conf. Coord. Chem.*, 12th, (1989) 391
- 528 W. Hiller, E. Hartmann and K. Dehnicke, *Z. Naturforsch., B: Chem. Sci.*, 44 (1989) 495
- 529 U. Bierbach, W. Saak, D. Haase and S. Pohl, *Z. Naturforsch., B: Chem. Sci.*, 45 (1990) 45
- 530 M. S. Nalakraishna, T. K. Prakasha and S. S. Krishnamurthy, *Proc. Indian Natl. Sci. Acad., Part A*, 55 (1989) 335
- 531 T. S. Lobana and A. Sharma, *Transition Met. Chem. (London)*, 14 (1989) 13
- 532 J. D. Walker and R. Poli, *Inorg. Chem.*, 29 (1990) 756
- 533 Z. A. Siddiqi, S. N. Qidwai and M. Shakir, *Bull. Soc. Chim. Fr.*, (1990) 193
- 534 W. Dietzsch, N. V. Duffy, D. Boyd, D. L. Uhrich and E. Sinn, *Inorg. Chim. Acta*, 169 (1990) 157
- 535 S. Ciarli, M. Carrie, J. A. Wiegel, M. J. Carney, T. D. P. Stack, G. C. Papaefthymiou and R. H. Holm, *J. Am. Chem. Soc.*, 112 (1990) 2654
- 536 T. D. P. Stack, J. A. Wiegel and R. H. Holm, *Inorg. Chem.*, 29 (1990) 3745
- 537 J. A. Wiegel, R. H. Holm, K. K. Surerus and E. Munck, *J. Am. Chem. Soc.*, 111 (1989) 9246
- 538 J. A. Wiegel, K. K. P. Srivastava, E. P. Day, E. Munck and R. H. Holm, *J. Am. Chem. Soc.*, 112 (1990) 8015
- 539 R. Ohno, N. Ueyama and A. Nakamura, *Inorg. Chim. Acta*, 169 (1990) 253
- 540 M. Kodaka, T. Tomohiro and H. Okuno, *Chem. Express*, 5 (1990) 97
- 541 M. Kodaka, T. Tomohiro and H. Okuno, *Chem. Express*, 5 (1990) 117
- 542 J. Jordanov, E. K. H. Roit, P. H. Fries and L. Noodelman, *Inorg. Chem.*, 29 (1990) 4288
- 543 H. Ogino, A. Satoh and M. Shimoi, *Bull. Chem. Soc. Jpn.*, 63 (1990) 2314
- 544 S. Inomata, H. Tobita and H. Ogino, *J. Am. Chem. Soc.*, 112 (1990) 6145
- 545 H. Okuno, K. Uoto, T. Tomohiro and M.-T. Youinou, *J. Chem. Soc., Dalton Trans.*, (1990) 3375
- 546 T. Tomohiro, K. Uoto and H. Okuno, *J. Chem. Soc., Dalton Trans.*, (1990) 2459
- 547 T. Tomohiro, K. Uoto and K. Ukono, *J. Chem. Soc., Chem. Commun.*, (1990) 194
- 548 K. Uoto, T. Tomohiro and H. Okuno, *Inorg. Chim. Acta*, 170 (1990) 123
- 549 P. R. Challen, S. M. Koo, W. R. Dunham and D. Coucouvanis, *J. Am. Chem. Soc.*, 112 (1990) 2455
- 550 A. C. M. Young, M. A. Walters and J. C. Dewan, *Acta Cryst., Sect. C*, C45 (1989) 1733
- 551 N. Ueyama, T. Sugawara, T. Okamura and A. Nakamura, *Makromol. Chem.*, 191 (1990) 1807
- 552 J. Xu, J. Qian, Q. Wei, C. Guo and G. Yang, *Sci. China, Ser. B*, 32 (1989) 927 [*Chem. Abstr.* 113:51362d]
- 553 J. Xu, J. Qian, Q. Wei, N. Hu, Z. Jin and G. Wei, *Inorg. Chim. Acta*, 164 (1989) 55
- 554 J. Xu, J. Qian, Q. Wei, N. Hu, Z. Jin and G. Wei, *Huaxue Xuebao*, 47 (1989) 853 [*Chem. Abstr.* 112: 209704h]
- 555 Q. Liu, L. Huang, H. Liu, X. Lei, D. Wu, B. Kang and J. Lu, *Inorg. Chem.*, 29 (1990) 4131
- 556 P. W. Dimmock, D. P. E. Dickson and A. G. Sykes, *Inorg. Chem.*, 29 (1990) 5120
- 557 P. W. Dimmock and A. G. Sykes, *J. Chem. Soc., Dalton Trans.*, (1990) 3101
- 558 P. R. Challen, S. M. Koo, C. G. Kim, W. R. Dunham and D. Coucouvanis, *J. Am. Chem. Soc.*, 112 (1990) 8606
- 559 D. J. Evans, G. J. Leigh and J. B. Parra-Soto, *Polyhedron*, 8 (1989) 1865
- 560 B. Kang, H. Liu, J. Cai, L. Huang, Q. Liu, D. Wu, L. Weng and J. Lu, *Transition Met. Chem. (London)*, 14 (1989) 427

- 561 B. Kang, J. Cai, D. Wu, H. Liu, Q. Liu, L. Weng and J. Lu, *Huaxue Xuebao*, 47 (1989) 744
- 562 T. Tomohiro, K. Uoto and H. Okuno, *Chem. Express*, 4 (1989) 697
- 563 S. Ciurli, M. Carri and R. H. Holm, *Inorg. Chem.*, 29 (1990) 3493
- 564 S. Ciurli, S. B. Yu, R. H. Holm, K. K. P. Srivastava and E. Munck, *J. Am. Chem. Soc.*, 112 (1990) 8169
- 565 X. Lei, Z. Huang, M. Hong, Q. Liu, H. Liu, *Jiegou Huaxue*, 8 (1989) 152 [*Chem. Abstr.* 112:170914z]
- 566 P. Barbaro, A. Bencini, I. Bertini, F. Briganti and S. Midollini, *J. Am. Chem. Soc.*, 112 (1990) 7238
- 567 C. Glidewell, R. J. Lambert, M. B. Hursthouse and M. Motevalli, *J. Chem. Soc., Dalton Trans.*, (1989) 2061
- 568 C. Glidewell, R. J. Lambert, M. E. Harman and M. B. Hursthouse, *J. Chem. Soc., Dalton Trans.*, (1990) 2685
- 569 J. A. Crayston, C. Glidewell and R. J. Lambert, *Polyhedron*, 9 (1990) 1741
- 570 A. R. Butler, C. Glidewell and S. M. Glidewell, *Polyhedron*, 9 (1990) 2399
- 571 Z. Zhang, W. Sun, S. Niu, S. Li and G. Yang, *Huaxue Xuebao*, 47 (1989) 1061 [*Chem. Abstr.* 112:190663v]
- 572 I. Bertini, F. Briganti and C. Luchinat, *Inorg. Chim. Acta*, 175 (1990) 9
- 573 J. Cai, C. Chen, Q. Liu, B. Zhuang, B. Kang and J. Lu, *Jiegou Huaxue*, 8 (1989) 220 [*Chem. Abstr.* 112:170996c]
- 574 C. Chen, J. Cai, Q. Liu, D. Wu, X. Lei, K. Zhao, B. Kang and J. Lu, *Inorg. Chem.*, 29 (1990) 4878
- 575 S. A. Al-Ahmad, A. Salifoglou, M. G. Kanatzidis, W. R. Dunham and D. Coucouvanis, *Inorg. Chem.*, 29 (1990) 927
- 576 B. S. Snyder and R. H. Holm, *Inorg. Chem.*, 29 (1990) 274
- 577 J. F. You, B. S. Snyder, G. C. Papaefthymiou and R. H. Holm, *J. Am. Chem. Soc.*, 112 (1990) 1067
- 578 J. P. Costes, F. Dahan and J. P. Laurent, *Inorg. Chem.*, 29 (1990) 2448
- 579 P. Poganiuch, S. Decurtins and P. Guetlich, *J. Am. Chem. Soc.*, 112 (1990) 3270
- 580 D. C. Figg and R. H. Herber, *Inorg. Chem.*, 29 (1990) 2170
- 581 D. Onggo, J. M. Hook, A. D. Rae and H. A. Goodwin, *Inorg. Chim. Acta*, 173 (1990) 19
- 582 P. E. Doan and B. R. McGarvey, *Inorg. Chem.*, 29 (1990) 874
- 583 C. P. Koehler, R. Jakobi, E. Meissner, L. Wiehl, H. Spiering and P. Guetlich, *J. Phys. Chem. Solids*, 51 (1990) 239
- 584 W. Vreugdenhil, J. H. van Diemen, R. A. G. de Graaf, J. G. Haasnoot, J. Reedijk, A. M. van der Kraan, O. Kahn and J. Zarembowitch, *Polyhedron*, 9 (1990) 2971
- 585 H.-R. Chang, J. K. McKusker, H. Toftlund, S. R. Wilson, A. X. Trautwein, H. Winkler and D. N. Hendrickson, *J. Am. Chem. Soc.*, 112 (1990) 6814
- 586 J. J. McGarvey, I. Lawthers, K. Heremans and H. Toftlund, *Inorg. Chem.*, 29 (1990) 252
- 587 N. Saha and S. K. Kar, *J. Indian Chem. Soc.*, 66 (1989) 521
- 588 E. Konig, B. Kanellakopoulos, B. Pourietzka and H. A. Goodwin, *Inorg. Chem.*, 29 (1990) 4944
- 589 B. Gallois, J.-A. Real, C. Hauw and J. Zarembowitch, *Inorg. Chem.*, 29 (1990) 1152
- 590 R. Claude, J. A. Real, J. Zarembowitch, O. Kahn, L. Ouahab, D. Grandjean, K. Boukheddaden, F. Varret and A. Dworkin, *Inorg. Chem.*, 29 (1990) 4442
- 591 E. Gelerinter, N. V. Duffy, W. Dietzsch, T. Thanyasiri and E. Sinn, *Inorg. Chim. Acta*, 177 (1990) 185